BIOMECHANICAL ANALYSIS OF REVERSE ANATOMY SHOULDER PROSTHESIS

This thesis is submitted in fulfilment of the requirements for the Degree of

Doctor of Philosophy

Andreas Kontaxis

Centre for Rehabilitation and Engineering Studies

School of Mechanical and Systems Engineering

Newcastle Upon Tyne 2009

Declaration

This Thesis describes work carried out by the author in the School of Mechanical and Systems Engineering of the Newcastle University, United Kingdom and under the supervision of Professor G. R. Johnson.

This Thesis describes original work, which has not been submitted for a higher degree at any other University and is the work solely of the undersigned author, except where acknowledged in the text.

Andreas Kontaxis

Acknowledgments

There are many people who have been influential in the writing of this Thesis, but one of the most is Professor Garth Johnson who gave me the opportunity to take this new direction, has guided me well throughout the work and shared with me many special experiences in research as well as in personal life.

It is difficult to acknowledge all the people that supported me all those years, but I could not have reached this point without the influence and support of my family.

I would also like to say a big thanks to all the other members of CREST and close friends who have also been supportive and inspirational throughout the research. Many thanks to Vassilis, Stuart, Farshid, Jose, Germano, Emmanuel, Ruth who except all the help often encouraged activities of a less academic nature making life more enjoyable. Very special thanks also to Emma who even if I only met recently she gave me all the support and help to overcome all the strains that a PhD thesis writing up can cause.

Abstract

This study uses adaptation of an established 3-D biomechanical shoulder model (Newcastle Shoulder Model) to investigate the biomechanical properties of reverse shoulder replacements that have become popular for severe rotator cuff arthropathy.

The prosthetic model describes the DELTA® III geometry and can predict muscle and joint contact forces for given motion. A custom contact detection algorithm was developed to investigate the impingement problem.

Results showed that the reverse design increases deltoid function by providing sufficient moment arm (42% increase compared to normal anatomy) and restores joint stability by reversing the envelope of joint contact forces. The data showed a good agreement with other biomechanical models.

Further in this study scapula and arm kinematics of a group of DELTA III prosthetic subjects were recorded and compared with normal shoulder activity. The scapula kinematics showed increased lateral rotation and even if it is highly variable within the subjects (range:1.2–1.8 times the normal), there is a trend showing that good recovery shoulders have small change in their scapula rhythm and vice versa. The arm kinematics showed that even if the prosthetic subjects were able to complete most activities there was a variable range of humeral movement. Compared to the normal group the average elevation values were high but the internal/external humeral rotation was significantly smaller.

The kinematic data were further used and analysed with the model and the results showed large differences in glenoid loading compared to normal shoulders, where there is an increase in superior (range:12%-52% bodyweight) and antero-posterior shear forces (range:8%-39% bodyweight). Impingement results predicted scapula bone notches similar in shape and volume with the literature which was impossible to eliminate without design modifications.

The adapted prosthetic model was successfully used to analyse the biomechanics of a reverse design and provide a useful dataset that can be further used for design optimisation

Table of Contents

Chapter 1. Introduction and objectives of the study

1.1. Foreword

The function of the upper extremity is far more complex than the lower limb and gives people control and interaction with the environment. Arguably a disability of the upper limb can demote quality of life as much as (if not more) a disability in the lower limb. Yet the upper extremity is not as heavily researched area in human biomechanics like the joints of hip or knee. Correction of walking disabilities through rehabilitation, corrective surgery and assistive devices, receives much more attention nowadays, with the orthopaedic market being the strongest in that area.

The complexity of the upper limb and especially of the shoulder joint poses many challenges to understand its function. The motion of the shoulder girdle is a coordinated movement of multiple bony segments that are driven from a complex set of muscles in order to give mobility and motion precision. As a mechanism the upper limb seems to be highly balanced and optimised and as such an injury or any kind of muscular or joint malfunction can unstable its mobility and in general its function.

The analysis of the kinematics, dynamics and internal forces in the upper limb differs from the more commonly studied lower limb in a number of ways. Firstly, the range of motion of the upper limb and shoulder girdle is much greater and the motions are much less cyclic and predictable. Secondly, the loading involved is much lower and also less unidirectional due to the variable nature of upper limb function.

The study of upper limb biomechanics started many years ago, with the mechanical simulation of a cadaveric specimen by Mollier (1899), to be considered one of the first biomechanical models. Since then, *in vitro* biomechanical modelling became more popular with the example of the early analytical work by Inman *et al.* (1944) who studied the so-called scapulohumeral rhythm of the shoulder girdle; a topic that continues to be investigated even nowadays and it will be exploited and analysed even in this thesis. Later studies like the one of Poppen and Walker (1978) who presented a multiple muscle model of the glenohumeral joint and estimated the forces involved in the joint and surrounding muscles became the gold standard in upper limb biomechanics and has been referenced in most of the recent studies of upper limb biomechanics.

The complexity of the recent upper limb models has been significantly increased, with a number of studies providing data of location of muscle attachments, the relative sizes and strengths of muscles and their detailed anatomy. Hogfors *et al.* (1987), van der Helm *et al.* (1992), Johnson *et al.* (1996) and Veeger *et al.* (1997) all produced reference

data sets for the morphology of the upper limb and shoulder girdle, each has been used in a number of interactive biomechanical models like the Strathclyde shoulder model (Runciman and Nicol, 1994), the Swedish shoulder model (Karlson and Pederson, 1992), the Dutch shoulder model (van der Helm 1994a,b) and the Newcastle Shoulder model (Charlton and Johnson, 2006).

Up to date, most of the biomechanical models have been heavily used to investigate the function of the normal shoulder and understand its complexity. Application of the models have also been applied to investigate shoulder injuries and disorders which are commonplace especially in the elderly population, where arthritis, stroke and fractures result in a much compromised function of the upper extremity.

Shoulder joint replacement is a common solution to overcome pain and restore function to a pathological shoulder. However the shoulder implant market is much smaller in orthopaedic industry compared to hip and knee. The market was valued at $145 million during the period of 2006/2005 selling 70,000 units worldwide (personal communication, JointsSolutions^{TM}). The shoulder replacement is a specialised area of orthopaedic practice and as such there is a considerably smaller number of surgeons performing the joint replacement compared to the popular hip replacement.

However, the recent development on the upper limb biomechanics and modelling have increased the research investments in the area and as a result the shoulder market has one of the larger annual growth factors within the joint replacement industry (Figure 1.1)

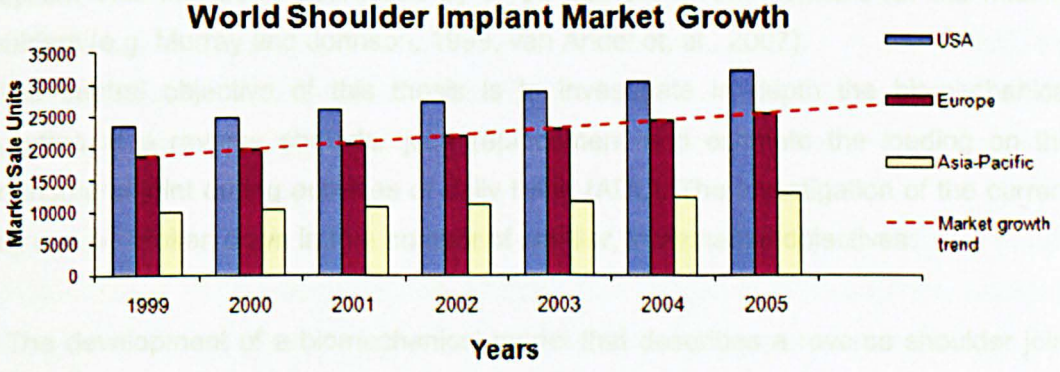

Figure 1.1: The shoulder joint replacement market

The reverse anatomy shoulder prosthesis is a specialised product within the shoulder product range and is used primarily to patients that suffer from rotator cuff arthropathy. Recently the reverse prostheses were estimated to have the larger annual growth of 17% within the shoulder implant market, since clinical studies showed promising results.

Despite the clear potential of the specific product, the understanding of the function of the reverse designs is based mostly on clinical data. There are only limited biomechanical modelling studies in the literature (Nyffeler *et. al.*, 2005, Terrier *et. al.*, 2007) that are investigating the biomechanical properties of the reverse prosthesis. Therefore the main hypothesis (H_0) tested in this study was that *'the reverse design can improve joint function in subjects with rotator cuff arthropathy'*, which is the main indication of use according to surgical guidelines (Grammont et al., 1993, Baulot et al., 1999). However the literature also shows that current reverse prostheses on the market can cause problems (e.g. impingement – Sirveaux et al., 2004, Simovitch et al., 2007), which means that the designs may not be fully optimised. As a result, the second main hypothesis that is tested in this study is that *'there are design parameters that when optimised can increase the function of the prosthesis'*. The two hypotheses are leading to the objectives of the study as they are described in the section below.

1.2. The objectives of this study

Despite the advances in modelling techniques, most studies of the upper limb have been limited mostly to simple, cyclic motions, like abduction and forward flexion of the shoulder and elbow. Even if this method is sufficient for the lower limbs, it is not representative of the true nature of upper limb activity.

In order to examine the kinematics and dynamics of the upper limb, a set of tasks representative of the average "activities of daily living" of the shoulder is needed to be analysed. This has been addressed by a few authors in the literature for the healthy shoulders (e.g. Murray and Johnson, 1999, van Andel et. al., 2007).

The central objective of this thesis is to investigate in depth the biomechanical properties of a reverse shoulder joint replacement and estimate the loading on the glenohumeral joint during activities of daily living (ADL). The investigation of the current study can be broken down in to a number of smaller, incremental objectives:

- The development of a biomechanical model that describes a reverse shoulder joint replacement which will be based on an adaptation of the established *Newcastle Shoulder Model.*
- The deep biomechanical analysis of the reverse prosthesis designs.
- Collection and analysis of kinematics data of subjects with reverse joint replacement based on established motion analysis techniques.

- Estimate glenohumeral range of loading on the reverse prosthesis during representative ADL.
- Analyse joint stability and potential problems and suggest implantation and design solutions for optimum use of the reverse prosthesis.

This study is the next step after the works of Barnett (1996), Murray (1999) and Charlton (2006) who all developed several biomechanical tools. In this study all the previous techniques are used and developed further towards a clinical application: to understand the function of a real product (the reverse prosthesis), for which despite its wide use there is limited biomechanical understanding of its properties.

1.3. Thesis Layout

There are 9 further chapters included in this thesis, which begins with the necessary introduction to the functional anatomy of the upper limb and the relevant kinematic and dynamic techniques. Analytically:

Chapter 2 is on the functional anatomy of the upper limb and includes the terminology used in this thesis and a broad overview of the gross biomechanics of the upper limb and shoulder girdle.

Chapter 3 has an overview of the shoulder pathologies that lead to joint dysfunction and to potential joint replacement. Further in this chapter a historical review of shoulder prostheses is presented together with the current trend of the implant designs. A first introduction to the reverse prosthesis will also be presented in this chapter.

Chapter 4 is presenting the fundamental tool that was used in this study; the Newcastle Shoulder Model. All the methodology of the necessary modifications that are followed to adapt the model to describe the reverse joint replacement are also described in this chapter.

Chapter 5 analyses in depth the biomechanical properties of the reverse prosthesis and explains the change of the muscle function, joint loading and the potential problems of the prosthesis (impingement) by presenting some preliminary results, which are also used to validate the model with other published data in the literature[1].

Chapter 6 is presenting the first set of the kinematics data which describes the scapulohumeral rhythm in subjects with reverse joint replacement[1]

[1] The materials of the chapter is published in scientific journal

Chapter 7 is analysing kinematics data of activities of daily living between healthy and reverse joint replacement subjects which were captured with specific motion analysis techniques that are also analysed in the chapter.

Chapter 8 is presenting the range of the glenohumeral loads that are predicted using the biomechanical model and the kinematic dataset that was summarised in chapter 7 and explains how muscle activity changes under different type of rotator cuff tears.

Chapter 9 analyses in depth the impingement problem of the reverse prosthesis using the new feature of the shoulder model (contact detection) that is developed in this study. The chapter also analyses the importance of the implantation and design parameters and highlights the optimum solutions to minimise the problem.

Chapter 10 finally iterates the conclusions of this study. This includes a brief summary of the study, the major achievements, the most interesting results and importantly, the limitations of the data presented. Finally, the open challenges in this area and the future direction of this research project are suggested.

Chapter 2. Skeletal and functional anatomy of the Upper Limb

2.1. Introduction

The human upper limb is extremely versatile, commanding a considerable workspace around the body and the shoulder joint can be seen as a perfect compromise between mobility and stability. The joint complex allows for a large range of motion, well beyond that of the hip. The particular compromise in the human shoulder is different from other animals and is believed to have played an important role in evolution (Veeger et al., 2007).

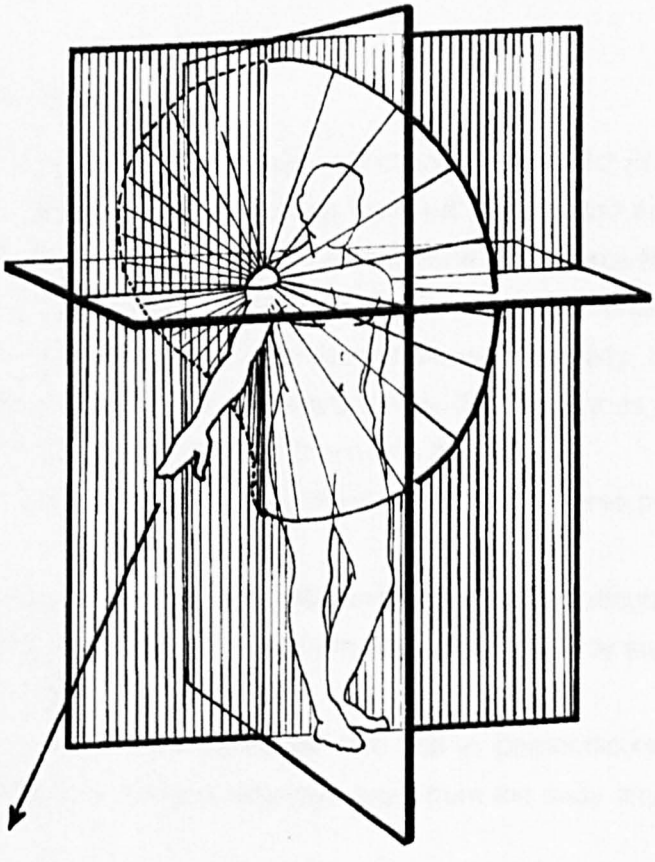

Figure 2.1: Humeral workspace (Kapandji's cone of Circumduction, adapted from Kapandji, 1982).

The extremely wide cone of circumduction (Figure 2.1) is made possible by the synchronous motion of the bones of the clavicle and scapula -the shoulder girdle-, (Figure 2.3) allowing a moveable base on which the humerus can articulate.

The goal of this chapter is to give an overview on the current knowledge about the role of morphological structures, muscle properties and function in the shoulder mechanism that enabling its large mobility and strength while maintaining stability. More specific information will be presented about:

- Skeletal structure of the upper limb
- Details about their joint and the ligament connection,
- Morphological data of the muscles of the shoulder joint and
- Their function in the mobility and stability.

Before that it is important to introduce the terminology used by clinicians to describe physical directions, spatial relationships and gross movements of the body parts.

2.2. *Spatial Terminology*

Three fixed planes within the human body are defined (Figure 2.2 a) as follows: i)*The coronal plane*: the vertical plane that passes from left to right and from head to foot through the body, ii) *The sagittal plane*: the vertical plane that passes from front to back and from head to foot through the body, (perpendicular to the coronal plane)., iii) *The transverse plane*: the horizontal plane that passes through the body, (perpendicular to the coronal and sagittal planes). It is important to note that the planes described above are embedded in the torso and hence they move with the body.

The three main axes of the body are defined in relation to these planes as (Figure 2.2b):

i) *The antero-posterior axis:* the horizontal axis that is perpendicular to the coronal plane. Anterior is defined as directed away from the front of the body and posterior away from the rear of the body.

ii) *The Medio-lateral axis*: the horizontal axis that is perpendicular to the sagittal plane. Lateral is defined as directed sideways away from the body and medial towards the body.

iii) The superio-inferior axis: the vertical axis that is perpendicular to the transverse plane. Superior is defined as directed upwards and inferior as downwards.

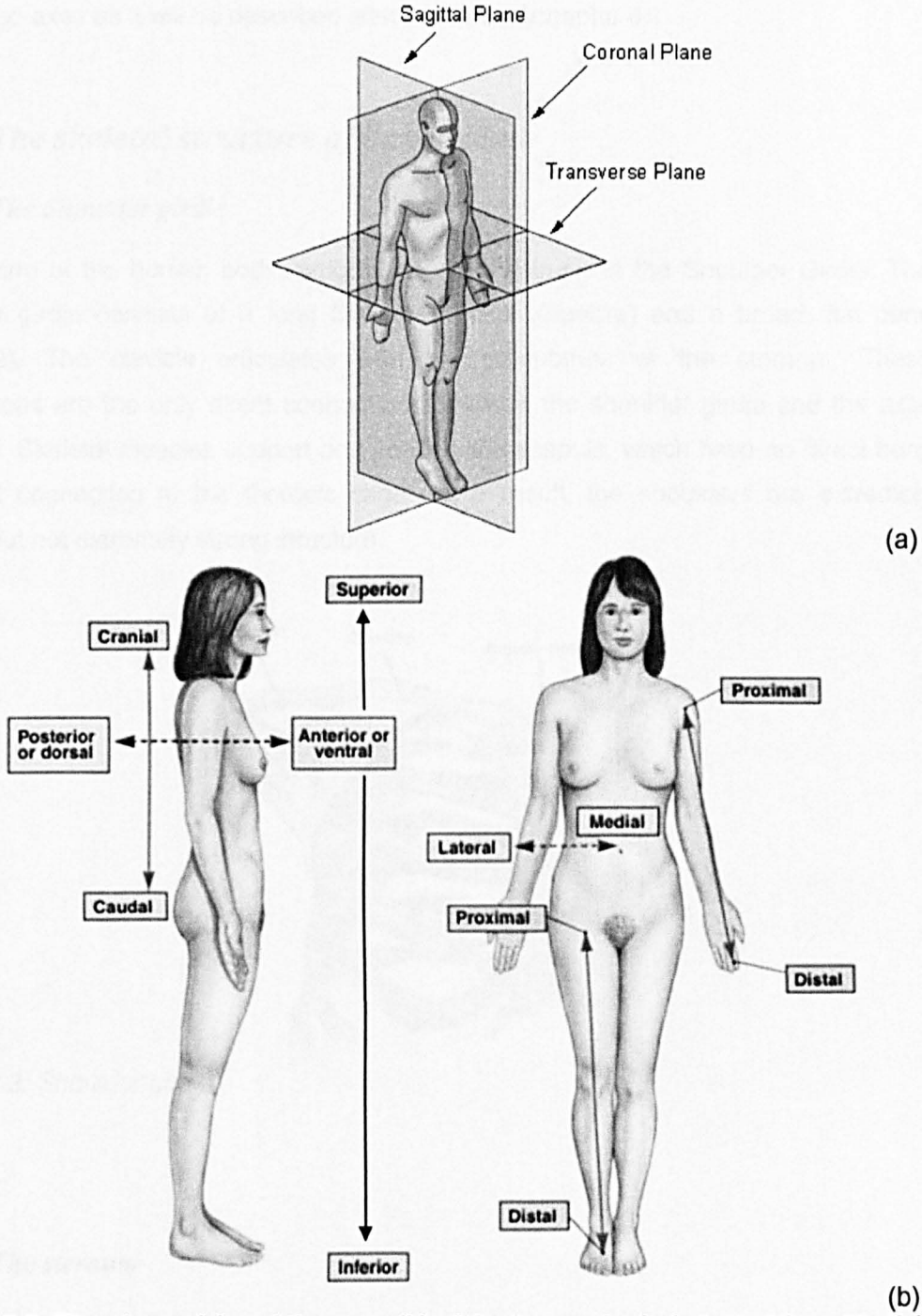

Figure 2.2: The planes (a) and the axes (b) of the human body (adapted from Martini 2001)

These plane and axis definitions allow us to describe locations and relative displacements of regions of the body. However, as movements within any joint result in the rotation of body segments in relation to each other, clinical terminology is used to

describe the rotation of body segments with respect to each other about the various body fixed axes as it will be described later in this and chapter 4.

2.3. The skeletal structure of Upper-Limb

2.3.1. The Shoulder girdle

The arm of the human body, articulates with the trunk at the Shoulder Girdle. The shoulder girdle consists of a long S-shaped bone (Clavicle) and a broad, flat bone (Scapula). The clavicle articulates with the manubrium of the sternum. These articulations are the only direct connections between the shoulder girdle and the axial skeleton. Skeletal muscles support and position the scapula, which have no direct bony ligament connection to the thoracic cage. As a result, the shoulders are extremely mobile but not extremely strong structure.

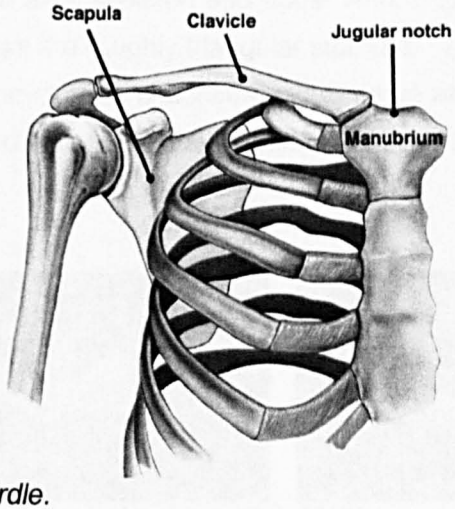

Figure 2.3: Shoulder girdle.

2.3.2. The sternum

The sternum is a flat bone that forms the anterior midline of the thoracic wall. It acts as the base on the trunk for the hard tissues of the upper extremity and has three components. The broad triangular manubrium, the widest and most superior portion of the sternum, articulates with the clavicle at the sternoclavicular joint and also with the first pair of ribs.

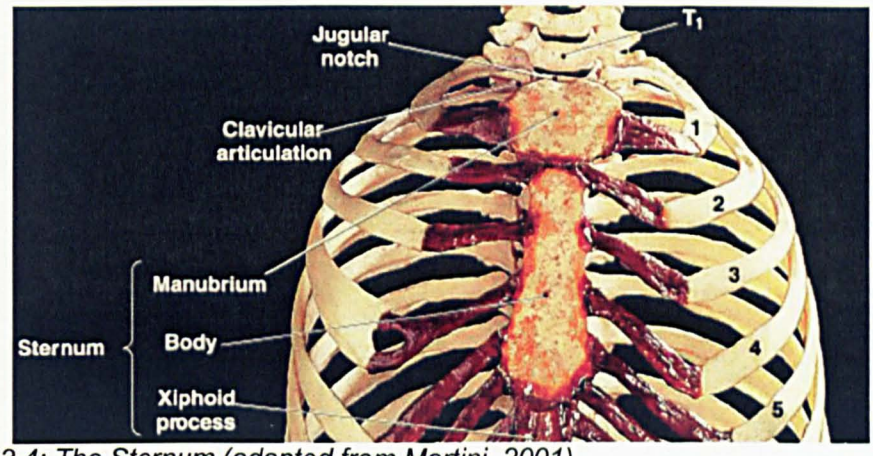

Figure 2.4: The Sternum (adapted from Martini, 2001).

2.3.3. The clavicle

The clavicle lies almost horizontally in the upper thorax and is the only direct connection between the axial skeleton and upper limb. It is an S-shaped bone, curving laterally and dorsally from the roughly triangular sternum.

The lateral end of the clavicle is constrained to move about the surface of a sphere defined by its length and thus holds the scapula laterally and enables the arm to be clear of the trunk.

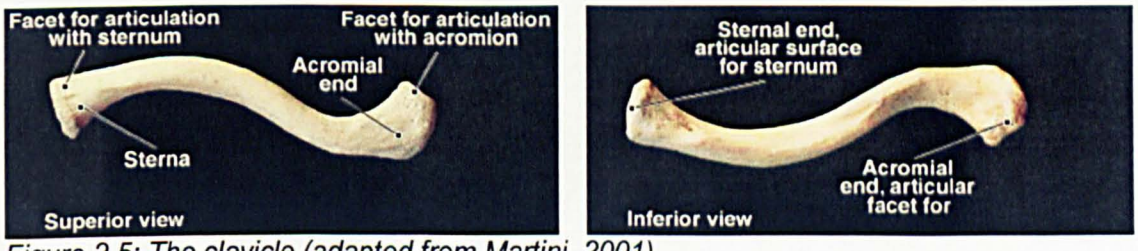

Figure 2.5: The clavicle (adapted from Martini, 2001).

The clavicle articulates at the sternoclavicular joint with the superior and lateral border of the manubrium of the sternum, lateral to the jugular notch and at the acromioclavicular joint with the acromion of the scapula.

2.3.4. The scapula

The scapula is a broad, flat bone having a triangular shape to its anterior aspect and is positioned posterior to the shoulder over ribs 2 to 7. The scapula is dynamically positioned on the axial skeleton by muscles and there is no direct bony or ligament

connection linking to the thoracic cage. It is allowed to glide over the fascia-covered thorax during upper limb movement, giving rise to the scapulothoracic articulation described later and provides the humerus with a stable but mobile base.

The three sides of the triangular shaped scapula are named the superior, medial and lateral borders with the corners being termed the medial, inferior and lateral angels (Figure 2.6).

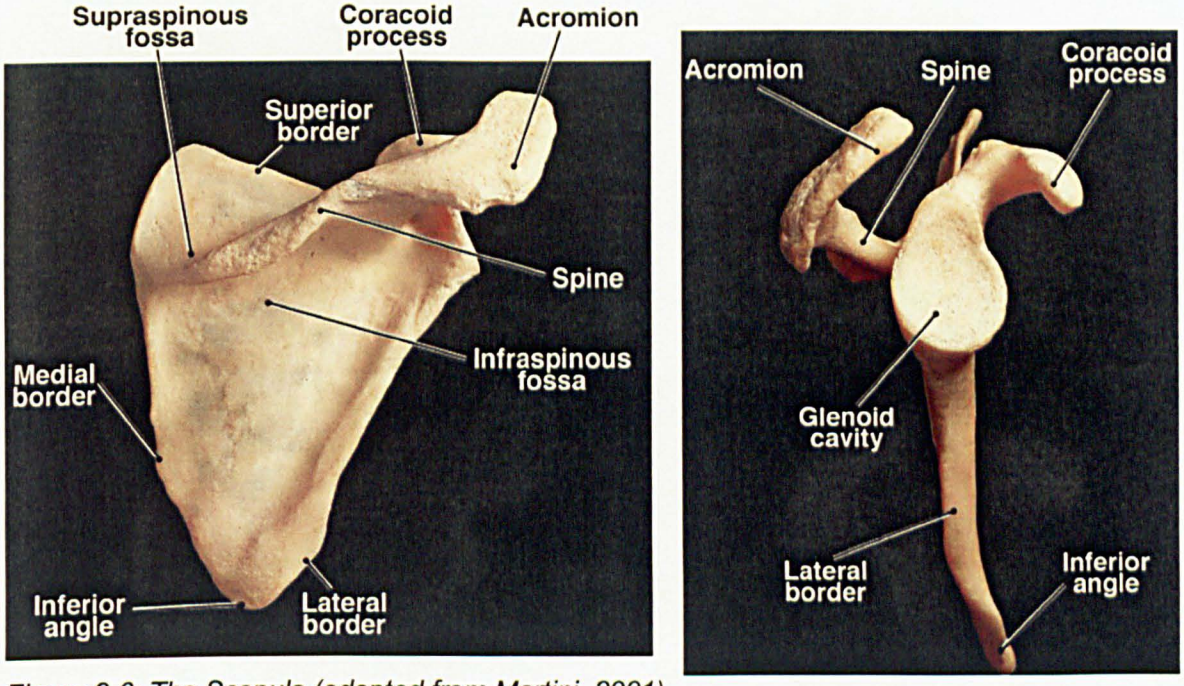

Figure 2.6: The Scapula (adapted from Martini, 2001).

Adjacent to the lateral angle the scapula thickens and becomes rounded to form a neck which supports the shallow pear-shaped glenoid fossa, which is tilted slightly upwards at an angle of approximately 15 degrees to the vertical, providing some support to the humeral head.

2.3.5. The Humerus

The humerus extends proximally, where the hemispherical head articulates with the glenoid fossa. At its distal end is the elbow, where the humerus articulates with the two bones of the forearm, the radius and the ulna.

The prominent greater tubercle of the humerus is a rounded projection near the lateral surface of the humeral head. The articulating surface of the head is large, covering 1/3 of the sphere fitted to the humeral head (Kapandji, 1982) and is retroverted

with an angle that ranges from 16 deg (Inman et al., 1944) to 20 – 30 deg (Saha, 1973). The greater tubercle establishes the lateral contour of the shoulder. The lesser tubercle is a smaller projection that lies on the anterior, medial surface of the epiphysis, separated from the greater tubercle by the intertubercular groove, or intertubercular sulcus. Both tubercles are important sites for muscle attachment; a large tendon (long Biceps tendon) runs along the groove. The anatomical neck marks the extent of the joint capsule and lies between the tubercles and the articular surface of the head. The narrower surgical neck corresponds to the metaphysis of the growing bone.

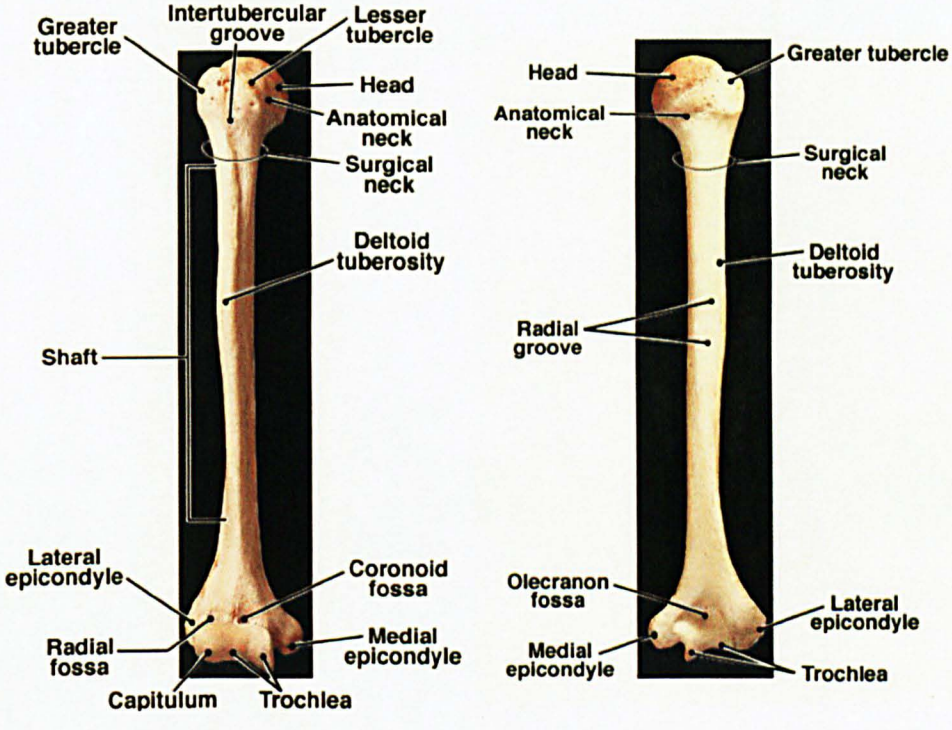

Figure 2.7: The Humerus (adapted from Martini, 2001).

The lower end of the humerus is expanded laterally, flattened anteroposteriorly and bent slightly forwards. It presents two articular surfaces, the capitulum being the lateral of these, providing a rounded, convex surface for articulation with the proximal end of radius.

Medial to the capitulum is the trochlea which articulates with the proximal end of the ulna. This presents a grooved surface with an anterolateral projection on its medial edge, which causes a lateral deviation between the long axis of the ulna in relation to that of the humerus. The lateral and medial epicondyles of the humerus lie lateral to the capitulum and medial to the trochlea respectively.

2.3.6. Ulna and Radius – The forearm

The ulna and the radius are parallel bones that support the forearm. The ulna is the longer of the two bones, lying medial to the radius in the anatomical position and articulating laterally with it at each end. The proximal end of the bone is larger than the distal end and has two projecting processes enclosing a cavity.

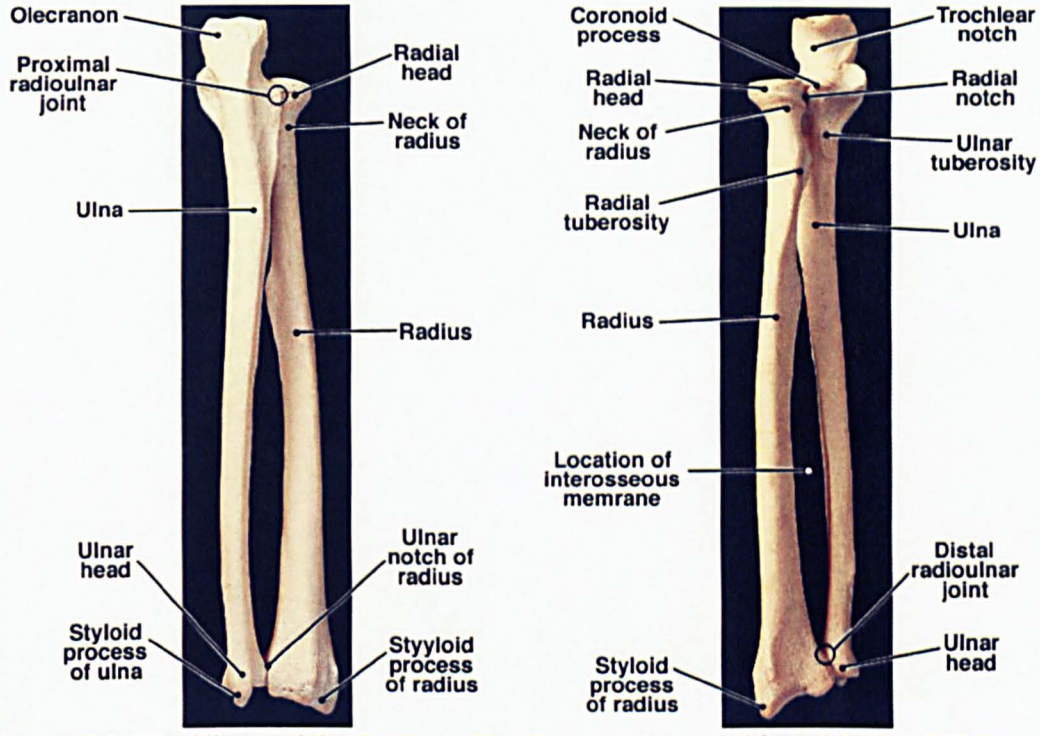

Figure 2.8: The Ulna and the Radius - The Forearm (adapted from Martini, 2001).

When viewed in cross section, the shaft of the ulna is roughly triangular. Near the wrist, the shaft of the ulna narrows before ending at a disc-shaped ulnar head. The posterior, lateral surface of the ulnar head bears a short styloid process. A triangular articular disc attaches to the styloid process; this cartilage separates the ulnar head from the bones of the wrist. The lateral surface of the ulnar head articulates with the distal end of the radius to form the distal radioulnar joint.

The radius is shorter than the ulna and lies laterally to it in the anatomical position. During flexion, the radial head swings into the radial fossa of the humerus. A narrow neck extends from the radial head to the radial tuberosity. The shaft of the radius curves along its length. It also enlarges, and the distal portion of the radius is considerably larger than the distal portion of the ulna. The ulnar notch on the medial surface of the distal end of the radius marks the site of articulation with the head of the ulna. The distal

end of the radius articulates with the bones of the wrist. The styloid process on the lateral surface of the radius helps stabilise this joint.

2.4. Articulations of the shoulder girdle and the passive stabilisers (ligaments)

2.4.1. The sternoclavicular (SC) joint

The sternoclavicular (SC) joint links the medial end of the clavicle with the manubrium of the sternum. This joint has three degrees of freedom allowing the clavicle to i)elevate and depress, ii) retract and protract and iii) axially rotate.

The articulating surfaces of the clavicle and sternum do not have similar radius of curvature and therefore they do not form a particularly stable joint. Some degree of stability is provided by an intra-articular fibrocartilaginous disc, which also provides cushioning as well as contributing to the stability of the joint (Moseley et al., 1968, Kapandji, 1982).

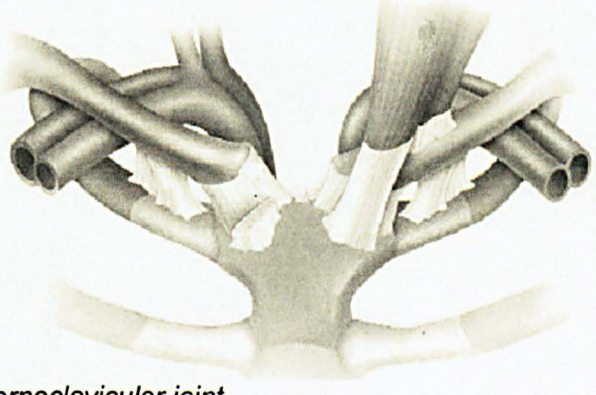

Figure 2.9: The sternoclavicular joint

A fibrous joint capsule surrounds the entire joint attaching to the articular margins of the sternum and clavicle. This capsule is relatively strong gaining reinforcement anteriorly, posteriorly and medially by thickenings of the capsule, the anterior and posterior sternoclavicular ligaments and the interclavicular ligament respectively. The SC joint affords a large range of elevation of the clavicle and moderate protraction – retraction. Axial rotation of the clavicle is observed when the arm is elevated (Hogfors et al., 1991, Marchese, 2000) and is due mainly to the action of the conoid ligament (Pronk et al., 1993).

2.4.2. The acromioclavicular (AC) joint

The acromioclavicular (AC) joint is a synovial joint linking the clavicle and scapula. All the movements in this joint are passive. The shape of the lateral end of the clavicle is that of an oval flat or slightly convex facet and this articulates with a flat or slightly concave facet of a similar shape on the anterior and medial border of the acromial process. A fibrocartilaginous articular disc is present, compensating the different surface shape between the articular surfaces. There is an attached capsule between the articulation which is strongest at the top where it is thickened and reinforced by the muscular fibres of the trapezius. Additional strength is supplied by the superior and inferior acromioclavicular ligaments.

The acromioclavicular ligament is mainly responsible for maintaining the integrity of the AC joint, preventing anterior – posterior displacement and axial rotation within the joint. These stabilising effects and combined observations of very limited translations within the AC joint make it a suitable candidate for modelling as a 3 degree of freedom (DOF) joint (Pronk, 1991, van der Helm, 1994a). Further strength is supplied by the coracoclavicular ligament, anchoring the lateral end of the clavicle to the coracoid process of the scapula. The function of this ligament is to stabilise the clavicle with respect to the acromion. It has two parts, the anterolateral trapezoid and the posteromedial conoid ligaments, restraining movements of the scapula with respect to the clavicle in the backwards and forwards directions respectively.

The most important function of the acromioclavicular joint is to provide an additional range of movement for the shoulder girdle after the limits of the range of motion of the sternoclavicular joint have been reached. Movement with three degrees of freedom is allowed about the superior, anterior and lateral axes.

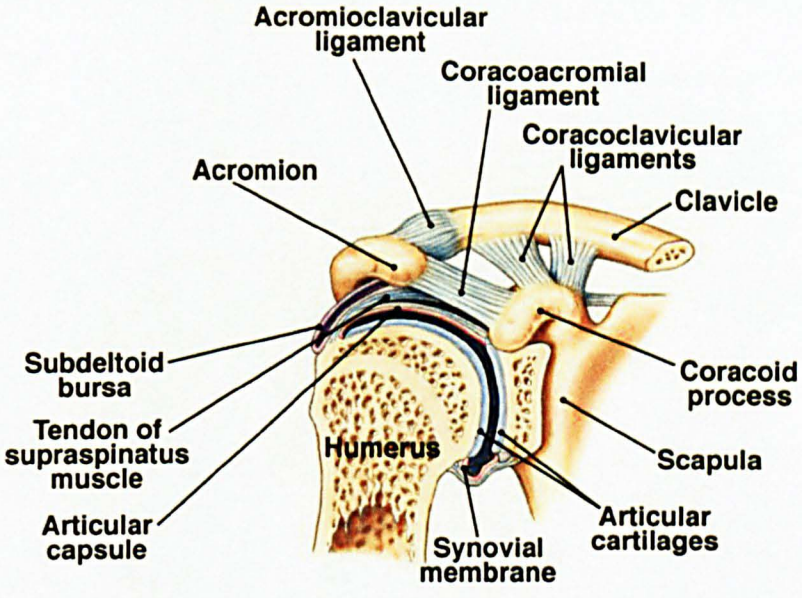

Figure 2.10: Posterior View of the right shoulder joint (adapted from Martini, 2001).

2.4.3. The Glenohumeral (GH) joint

The glenohumeral (GH) joint, permits the greatest range of motion of any joint. Because it is also the most frequently dislocated joint, it provides an excellent demonstration of the principle that stability must be sacrificed to obtain mobility. The GH joint is a ball-and-socket joint formed by the articulation of the head of the humerus with the glenoid cavity of the scapula. The surface of the glenoid cavity is covered by a fibrocartilaginous glenoid labrum, which extends past the bony rim and deepens the socket. The relatively loose articular capsule extends from the scapula, proximal to the glenoid labrum, to the anatomical neck of the humerus. It is a somewhat oversized capsule that permits an extensive range of motion. The bones of the pectoral girdle provide some stability to the superior surface, because the acromion and coracoid process project laterally superior to the head of the humerus. However, most of the stability at this joint is provided by the surrounding skeletal muscles, with help from their associated tendons and various ligaments.

In general, the function of the labrum is not well understood and it is often assumed that its role is mechanical. Results of studies on the effect of labral defects on glenohumeral stability are mixed (Lazarus et al., 1996; McMahon and Lee, 2002), which is not surprising, taking into account that the labrum is easily deformable (Carey et al.,

2000). It is more likely that an important function of the labrum lies in its role in joint lubrication.

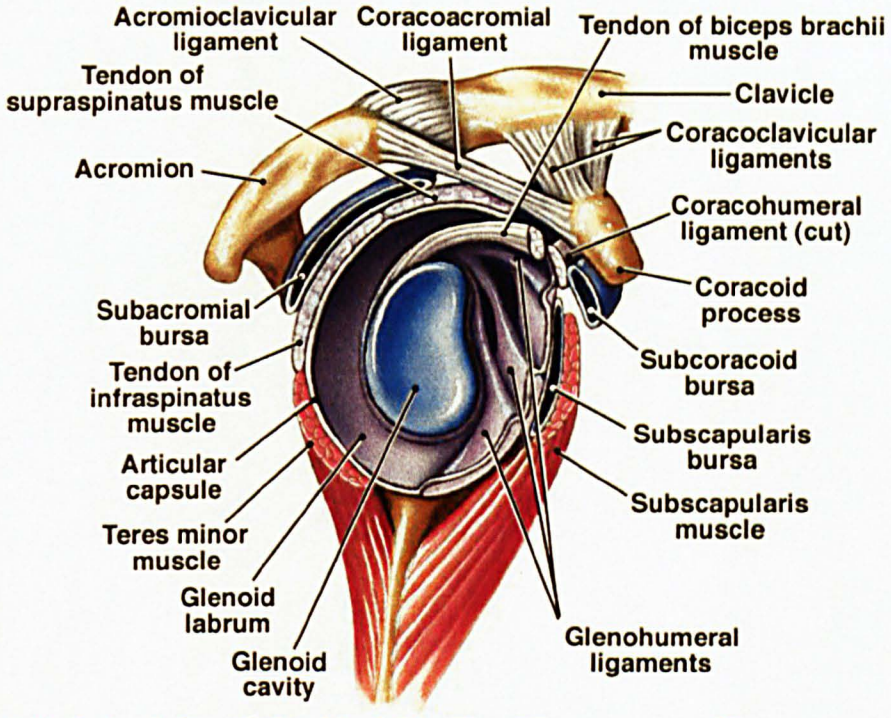

Figure 2.11: Lateral view of shoulder joint without the presence of humerus

The muscles that move the humerus do more to stabilize the shoulder joint than do all the ligaments and capsular fibres combined. Muscles originating on the trunk, pectoral girdle, and humerus cover the anterior, superior, and posterior surfaces of the capsule. The tendons of the supraspinatus, infraspinatus, subscapularis, and teres minor muscles reinforce the joint capsule and limit the range of movement. These muscles, known as the muscles of the rotator cuff, are the primary mechanism for supporting the shoulder joint and limiting the range of movement and they will be discussed further down in this chapter.

Even if the anterior, superior, and posterior surfaces of the GH joint are reinforced by ligaments, muscles, and tendons, the inferior capsule is poorly reinforced. As a result, a dislocation caused by an impact or violent muscle contraction is most likely to occur at this site. Such a dislocation can tear the inferior capsular wall and the glenoid labrum. The healing process typically leaves a weakness that increases the chances for future dislocations.

As at other joints, bursae at the shoulder reduce friction where large muscles and tendons pass across the joint capsule. The shoulder has a relatively large number of

important bursae, such as the subacromial bursa, the subcoracoid bursa, the subdeltoid bursa, and the subscapular bursa.

2.5. *Functional Anatomy of the shoulder girdle – The muscles.*

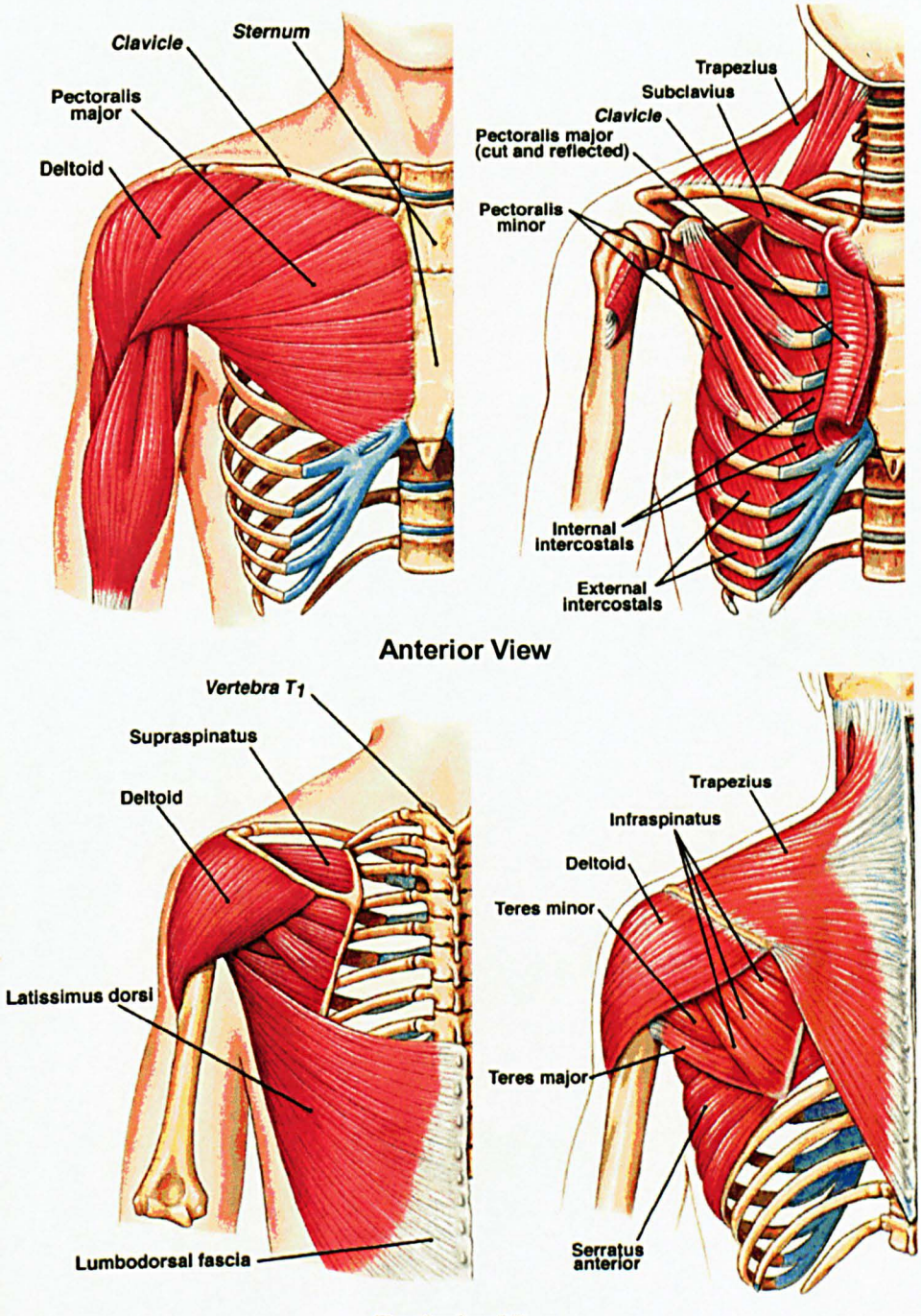

Figure 2.12: Muscle in the Shoulder girdle and upper arm (adapted from Martini,2001)

The muscles that contribute in the movement of the arm can be divided into three groups and as follows:

2.5.1. The scapulohumeral group:

They are the muscles that move the glenohumeral joint and are the main contributors to the motion of the upper limb. These muscles can be grouped by their actions at the shoulder joint. The deltoid muscle is the major abductor, but the supraspinatus muscle assists at the start of this movement as well (Charlton, 2006, VanDerHelm, 1994). The subscapularis and teres major muscles produce medial rotation at the shoulder, whereas the infraspinatus and the teres minor muscles produce lateral rotation. All these muscles originate on the scapula. The small coracobrachialis muscle is the only muscle attached to the scapula that produces flexion and adduction at the shoulder.

Collectively, the supraspinatus, infraspinatus, subscapularis, and teres minor muscles and their associated tendons form the rotator cuff (RC). The RC muscles act mainly as compressors of the humeral head to the glenoid cavity enhancing joint stability. The joint can only dislocate if the resulting joint reaction force (JRF) vector (summation of muscle, ligamentous, gravitational and other external forces) at the centre of the humeral head points outside the glenoid. The rotator cuff muscles are especially suitable to direct the JRF into the glenoid, since these muscles will pull the humerus into the glenoid, mainly based on their force direction and not on the exerted moment. It is advantageous to use muscles with a small antagonistic moment arm to reduce the contraproductive moment. Based on mechanical analysis one might conclude that the rotator cuff musculature, arranged in a half-circle around the GH joint, is very effective in directing the JRF (Blasier et al., 1997). Prime movers with a large moment arm, like the m. Deltoideus, m. Pectoralis Major and m. Latissimus Dorsi, can also pull the humeral head into the glenoid, but action of these muscles will also result in large, possibly antagonistic moments.

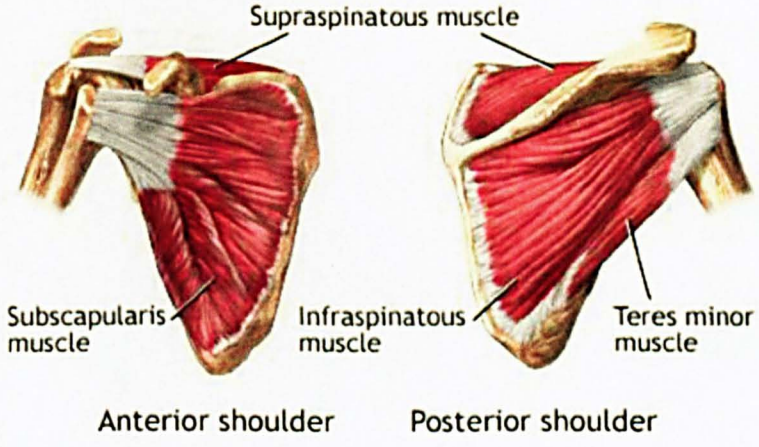

Figure 2.13: The Rotator Cuff muscles

2.5.2. The axioscapular group:

They are the muscles concerned with the manipulation of the scapula. These muscles chiefly span the scapulothoracic gliding plane. This group includes Serratus Anterior, Levator Scapulae, the Rhomboids and Trapezius muscles.

The large, superficial trapezius muscles cover the back and portions of the neck, reaching to the base of the skull. These muscles originate along the midline of the neck and back and insert on the clavicles and the scapular spines. The trapezius muscles are innervated by more than one nerve, and specific regions can be made to contract independently (Martini, 2001). As a result, their actions are quite varied.

Removing the trapezius muscle reveals the rhomboideus and levator scapulae muscles. These muscles are attached to the dorsal surfaces of the cervical and thoracic vertebrae. They insert along the vertebral border of each scapula, between the superior and inferior angles. Contraction of a rhomboideus muscle adducts (retracts) the scapula on that side. The levator scapulae muscle, as its name implies, elevates the scapula.

On the chest, the serratus anterior muscle originates along the anterior surfaces of several ribs. This fan-shaped muscle inserts along the anterior margin of the vertebral border of the scapula. When the serratus anterior muscle contracts, it protracts the scapula and swings the shoulder anteriorly.

2.5.3. The axiohumeral group:

They are the muscles that originate on the thorax and insert on the humerus. The Latissimus Dorsi and Pectoralis Major muscles make up this group and provide further assistance to the motion of the scapula and humerus.

The pectoralis major muscle extends between the anterior portion of the chest and the crest of the greater tubercle of the humerus. The latissimus dorsi muscle extends between the thoracic vertebrae at the posterior midline and the intertubercolar groove of the humerus. The pectoralis major muscle produces flexion at the shoulder joint, and the latissimus dorsi muscle produces extension. These two muscles can also work together to produce adduction and medial rotation of the humerus at the shoulder (Veeger & Van der Helm, 2004)

2.5.4. Other muscles of the shoulder girdle:

The three groups described above do not account for the entire collection of muscles that influence the shoulder girdle. The biceps brachii and the long head of triceps span the glenohumeral joint, but are not limited to insertions on the humerus since they are biarticular muscles. The Biceps brachii inserts on the radius. The triceps possesses a further two origins on the humerus (the medial head and lateral head) and inserts on the ulna.

Two other deep chest muscles arise along the ventral surfaces of the ribs on either side. The subclavius muscle inserts on the inferior border of the clavicle. When it contracts, it depresses and protracts the scapular end of the clavicle. Because ligaments connect this end to the shoulder joint and scapula, those structures move as well. The pectoralis minor muscle attaches to the coracoid process of the scapula. The contraction of this muscle generally complements that of the subclavius muscle.

2.6. *Clinical Description of the Motion of the Upper Limb*

Where the upper limb is concerned, a number of gross movements of the upper arm, forearm and hand can be described by the clinical terminology seen in Figure 2.14.

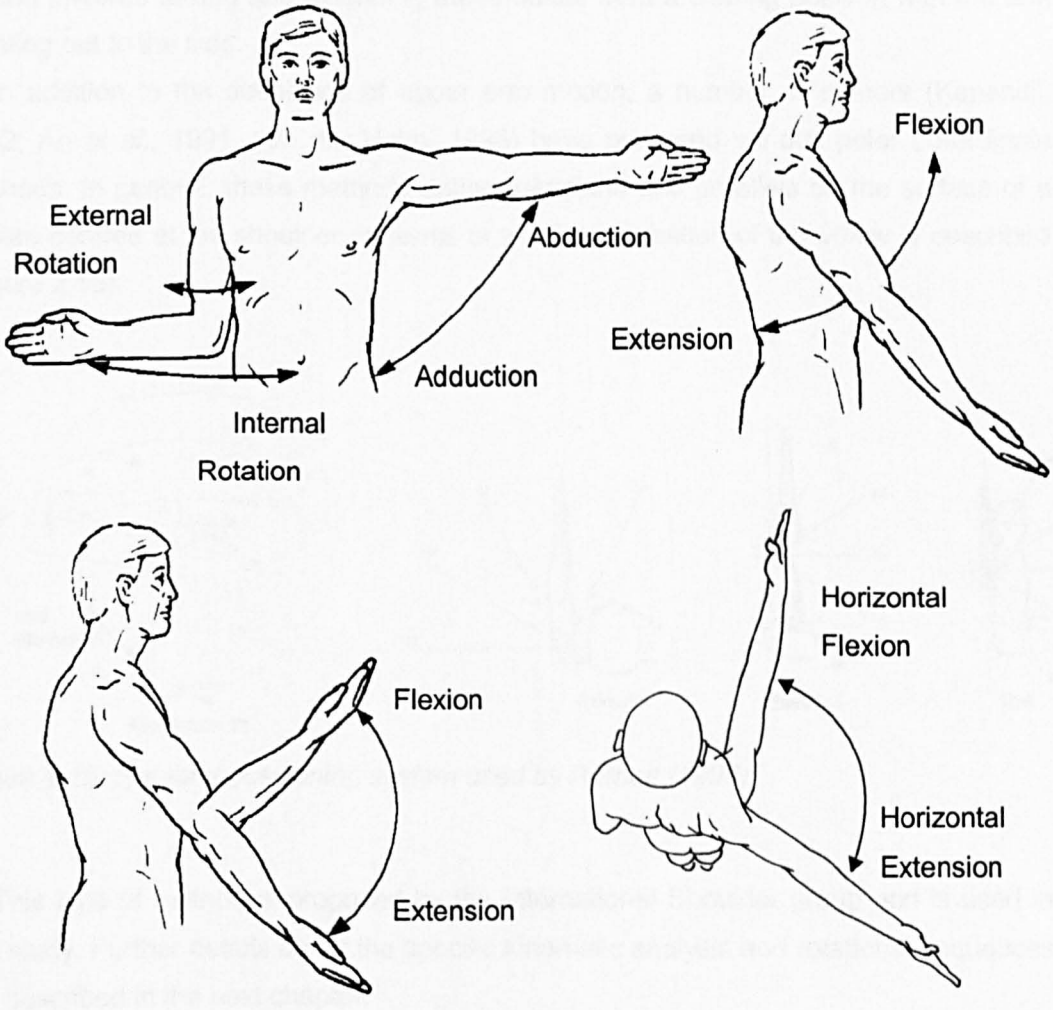

Figure 2.14: Motion of the Upper Limb.

Abduction and adduction of the arm takes place in the coronal plane, abduction meaning to move the arm away from the body. Flexion and extension are similar movements that take place in the sagittal plane. Flexing the arm (taking the hand in the anterior direction) is sometimes also referred to as anteflexion and in this scheme, extension becomes retroflexion. In general, all of these movements can be referred to as *elevation* of the upper limb when they are carrying the arm in an upward direction.

Internal and external rotation of the arm describes the axial twist in the shoulder, internal meaning to carry the hand toward the body. For this reason, this movement is occasionally referred to as medial rotation (external rotation thus becomes lateral rotation).

One further type of movement of the upper limb often used in the clinical context is horizontal flexion – extension (also often reffered to as protraction and retraction). This motion involves flexing and extending the shoulder from a starting position with the arm pointing out to the side.

In addition to the definitions of upper arm motion, a number of authors (Kapandji, 1982; An *et al.*, 1991, van der Helm, 1996) have proposed various polar co-ordinate methods. In general, these methods define meridians and parallels on the surface of a sphere centred at the shoulder, in terms of which the location of the elbow is described (Figure 2.15).

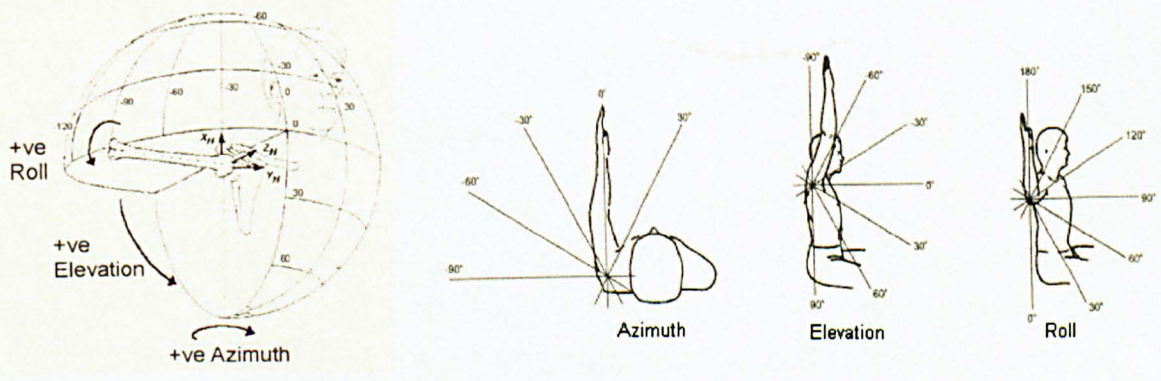

Figure 2.15: Humeral positioning system used by Barnett (1996)

This type of method is proposed by the International Shoulder group and is used in this study. Further details about the specific kinematic analysis and rotational sequences are described in the next chapter.

The forearm is capable of two primary movements, that of flexion – extension (described in the same sense as for the upper arm) and pronation – supination. Supination is that motion which turns the palm upwards: the motion required of a right-handed person to tighten a right-handed screw. Some abduction – adduction also occurs at the elbow, although this is mainly a passive property of the joints. The forearm appears to adduct as the elbow is flexed due to the elbow flexion axis not being perpendicular to the centre-line of the upper limb (Morrey and Chao,1976).

Finally, at the wrist, we are capable of flexion and extension again and in addition, medial – lateral deviation and inversion – eversion. Medial deviation is the movement of

the hand towards the body, made in a plane parallel to the palm of the hand and eversion of the palm carries it in the same sense as elbow supination.

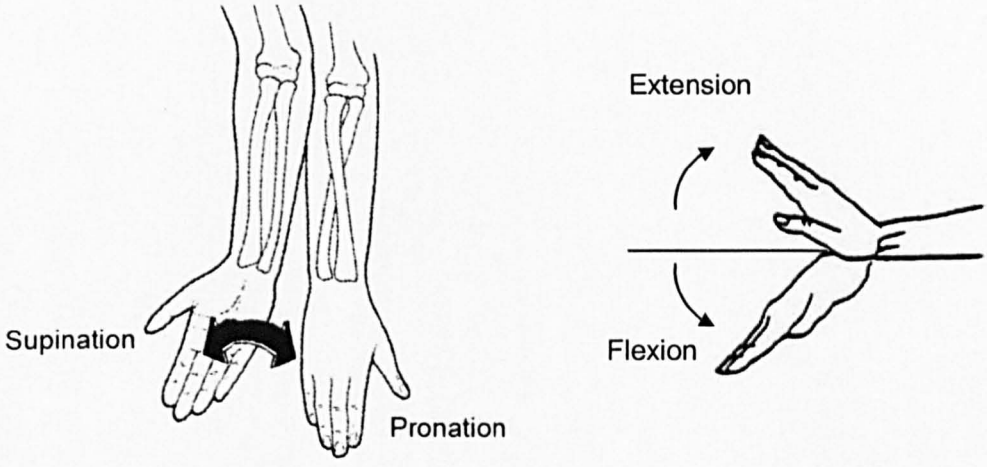

Figure 2.16: Rotational movement of the forearm

Chapter 3. Review of pathologies and joint replacement of the shoulder

3.1. *Introduction*

The normal shoulder is required to have basic mechanical characteristics such as motion, stability and strength. However, each of these characteristics is commonly compromised in the arthritic shoulder. Shoulder arthoplasty is one of the most optimal solutions so far, for immediate pain relief and to restore to a large degree, the functional mechanical characteristics of the natural shoulder.

The objective of this chapter is to introduce the types of shoulder arthroplasties as well as the arthropathies and the indications for shoulder replacements.

A historical review of the joint replacement designs will follow and both anatomical and reverse will be described.

3.2. *Types of shoulder arthroplasty*

Three levels of glenohumeral arthroplasty are commonly used:

Non-prosthetic arthroplasty: Surgical arthroplasty is considered when osteophytes and capsular contractures block motion and function in the presence of congruent glenohumeral contact and reasonable cartilaginous space on radiographs.

Prosthetic humeral hemiarthoplasty in which prosthetic implants are inserted only to the humerus. It is considered when joint surface is rough, but the cartilaginous surface of the glenoid is intact, or there is insufficient bone to support a glenoid component.

Total glenohumeral arthroplasty is desirable when both joint surfaces are damaged and when both are reconstructable.

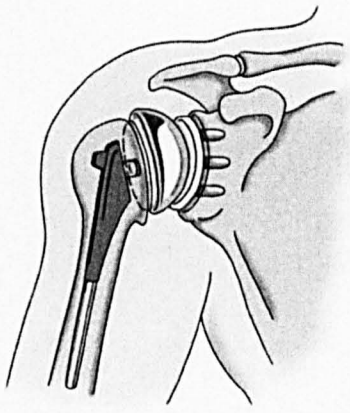

Figure 3.1: Total Shoulder Arthroplasty

Some studies have attempted to compare hemiarthroplasty and total shoulder arthroplasty. Boyd et al., 1990 found in a similar but unmatched series comparison that at 44 month follow-up, hemi-arthroplasty and total shoulder arthroplasty produced similar results in terms of functional improvement. Pain relief, range of motion, and patient satisfaction were better with total shoulder arthroplasty than hemi-arthroplasty in the rheumatoid population. Progressive glenoid loosening was found in 12% of total shoulder arthroplasties but no correlation with pain relief or range of motion was noted.

There is much literature comparing mostly hemi-arthroplasty and total shoulder arthroplasty which seems to favour the former when arthritis and cuff deficiency are concurrent and the later in osteoarthitis and rheumatoid arthritis when the cuff is intact (Rowe, 1984). It is recognized that badly eroded glenoid bone cannot support a glenoid prosthesis (Kelly et al., 1987)

3.3. Shoulder pathologies and indications for joint replacement

3.3.1. Osteoarthritis

Symptomatic osteoarthritis of the glenohumeral joint is relatively uncommon; about one shoulder arthroplasty is performed for every ten hip arthroplasties. The exact cause and mechanism of primary osteoarthritis, which results from a breakdown of the articular cartilage, are unknown. Patients develop cartilage erosions, flattening of the joint surface, osteophytes and asymmetric wear usually of the posterior glenoid (De Wilde L. 2008). There are often soft tissue changes that can include small tears of the anterior capsule and subscapularis. Rotator cuff tears are uncommon except for cuff tear arthropathy, which is defined as a separate clinical entity (described below). According to the work of Walch et al. (1999) defining the amount and the type of posterior glenoid

wear has therapeutic consequences, where moderate and severe posterior wear can compromise anatomical reconstruction with a total shoulder arthroplasty.

3.3.2. Cuff Tear Arthropathy (CTA).

Large and irreparable tears of the rotator cuff (at least two retracted tendons) can result in superior migration of the humeral head. Subsequent erosion of the glenohumeral joint, acromioclavicular joint and undersurface of the acromion, as well as an acetabularisation of the humeral head can be seen on radiographs, indicating cuff tear arthropathy.

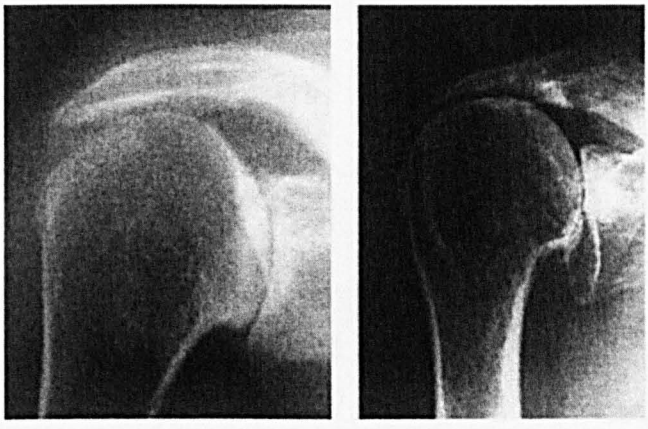

Figure 3.2: Radiographs showing superior glenoid erosion in RC arthropathies (adapted from, Sirveaux F. et al., 2004)

This superior migration of the humeral head and the glenoid erosion can be explained from the chronic loss of the compressive/stabilising action of the rotator cuff muscles on the humeral head in the glenoid face. Further analysis of the CTA and the result of the lack of the rotator cuff muscles is provided later in the thesis (chapter 5).

When the superior glenoid wear is large and anatomical reconstruction is no longer feasible, a reverse total arthroplasty is strongly advised (Grammont & Baulot 1993).

3.3.3. Rheumatoid arthritis

Rheumatoid arthritis can affect the shoulder joint as part of a systemic synovial-based polyarticular disorder. The disease can cause severe pain and disability. Modern medical treatment has reduced the progression of the disease (Ellman MH & Curran JJ 1988).

In rheumatoid arthritis, patients undergo shoulder arthroplasty first in the most symptomatic joint. If multiple joints are involved, a staged plan has to be developed. In the arm the proximal joint must be addressed first. In the case of a shoulder arthroplasty determination of the length of the stem must take into account that an elbow arthroplasty will probably be performed at a later date (De Wilde L. 2008).

A resurfacing arthroplasty is often suggested as it is less invasive from stem prosthesis and can be revised later if the resurfacing is failed. However, if glenoid wear, which is mainly central and superior, is too excessive, resurfacing of the glenoid is not an option.

The results of hemi-arthroplasty are satisfactory, but in an appropriately selected patient with rheumatoid arthritis a total shoulder arthroplasty may be considered (Hedtmann & Werner 2007).

A careful preoperative examination of the rotator cuff is important as in rheumatoid patients with advanced arthritis rotator cuff tears can be very often. If these tears are irreparable, a reverse prosthesis can be considered (Rittmeinster M. & Kerschbaumer F. 2001).

3.3.4. Osteonecrosis

Chronic systemic corticosteroid use and trauma are the main causes of osteo-necrosis of the humeral head. Even if there is small difference in performance between hemi- and total shoulder arthroplasty, primary replacement of the glenoid is preferred to hemi- arthroplasty, because glenoid wear predictably progresses over time and produces pain (De Wilde L. 2008).

Because managing severe glenoid articular wear in young patients is challenging (loosening of the glenoid, polyethylene disease) it is probably wise to treat these patients early with a partial resurfacing prosthesis before glenoid wear occurs.

3.3.5. Acute and Sequelae proximal humeral fractures

Prosthetic replacement has become a well accepted method of treatment for selected three- and four-part (acute) fractures of the proximal humerus (Porcellini et al. 1999) with hemi-arthroplasty and specialised long stems to be popular solution (Antuna et al. 2008). Although the hemi-arthroplasty has usually a favourable outcome in terms of pain relief, function can often be not satisfactory with the key to success to be a functional rotator cuff mechanism.

Boileau et al. (2001) identified four types of fracture (Figure 3.3).

- Type 1 are sequelae of impacted fractures with humeral head collapse or necrosis,
- Type 2 are irreducible dislocations or fracture-dislocations,
- Type 3 are non-unions of the surgical neck, and
- Type 4 are severe tuberosity malunions.

Boileau also report that the results of unconstrained shoulder arthroplasty for Types 1 and 2 sequelae are good, but total shoulder arthroplasty yielded better results than hemi-arthroplasty. Type 3 and 4 are more difficult to reconstruct and low-profile fracture prosthesis are needed (for preservation of bone graft) where reverse prosthesis is also suggested in Type 4 fracture sequelae.

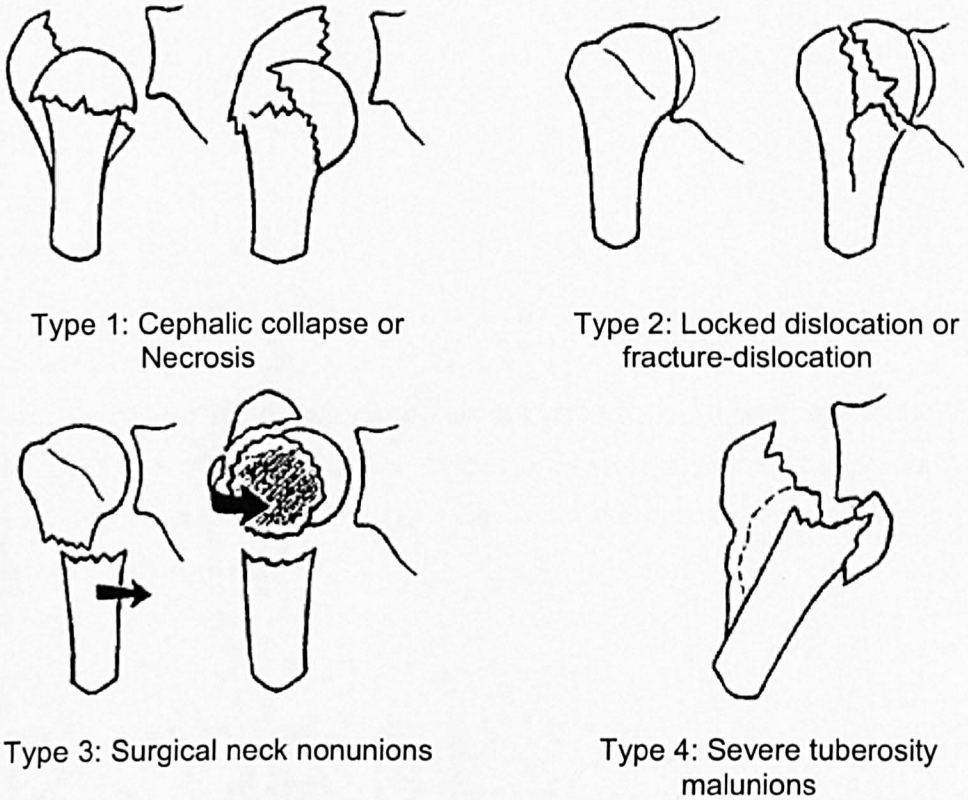

Figure 3.3: Types of sequelae proximal humeral fractures (adopted by Boileau et al. 2001)

3.4. *History of shoulder arthroplasty implants*

In 1893, one of the first prosthetic shoulder replacements was performed by the French surgeon Pean. A platinum and rubber total joint and proximal humeral implant (Figure 3.4) inserted by Pean in a 37 year old baker after his tuberculous arthritis had been debrided. The patient gained increased strength and range of the arm. However the infection recurred. After one of the first X-Ray machines documented an overwhelming reactive process, the prosthesis was removed two years after implantation.

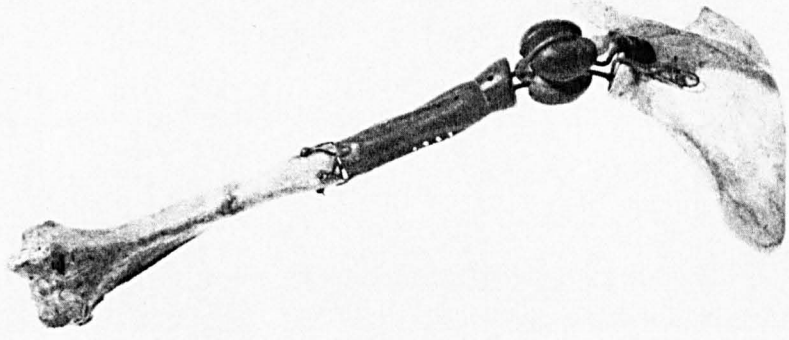

Figure 3.4: Pean design for total shoulder arthroplasty. The first ever shoulder arthroplasty is an artificial joint, composed of platinum and rubber. Inserted in the late 1800s (adapted from Khazzam and Fealy, 2008)

Shoulder joint arthroplasty and shoulder implant designs can be largely credited to Charles S. Neer. His contribution to present day understandings of the shoulder go far beyond the skeletal anatomy and indeed, it has been his teachings on the physiology of the shoulder and its relationships to shoulder replacement which have led to such successful reconstructive surgery.

In 1953, Neer presented the option of replacement of a fractured humeral head with a Vitallium prosthesis. Use of this prosthesis was next applied to patients with irregular articular surfaces as a result of fracturing and osteonecrosis. (Neer, 1955).

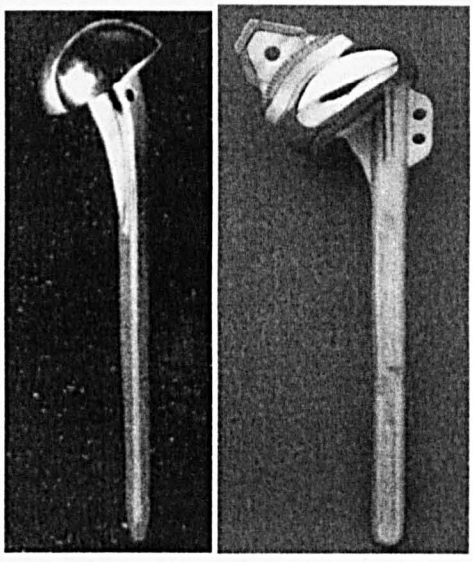

Figure 3.5: The Neer and Neer II designs

The initial Neer prosthesis had three sizes, and two more were added. In the early 1970s, the implant was redesigned to better use the alternative of cement fixation, and the articular portion was made spherical (Neer, 1974). This implant proved its versatility over time. It was initially used for acute fractures but subsequently has been shown to be effective for the care of patients with chronic fracture problems, (Hawkins and Neer, 1989; Rowe and Zarins, 1982; Tanner and Cofield, 1983) osteoarthritis, (Neer, 1974) rheumatoid arthritis, osteonecrosis, (Cruess, 1985) and a variety of the more rare forms of disease affecting the shoulder joint.

Also in 1974, there is development of a polyethylene glenoid component for use with a Neer humeral replacement in the treatment of degenerative joint disease of the shoulder. (Kenmore et al. 1974; Neer et al., 1982)

Other early designs of shoulder arthroplasty components include prostheses of Vitallium as reported by Krueger (1951) and acrylic as reported by Richard etal. (1952).

Figure 3.6: An acrylic prosthesis developed for the treatment of severe fracture-dislocations of the proximal humerus 1952 (adapted by Khazzam and Fealy, 2008)

Some authors suggested a cup arthroplasty might be a satisfactory alternative for prosthetic shoulder surgery, following various examples from hip replacement. (Jonsson, et al., 1986). Initially, hip cups were used, but soon cups were manufactured specifically for the shoulder for surface replacement of the humeral head (Steffee and Moore, 1984). The most frequent problem reported in the literature is cup loosening and some central glenoid wear.

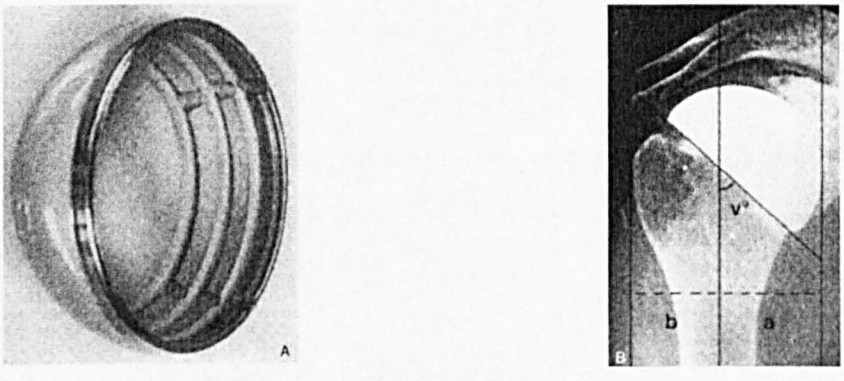

Figure 3.7: Cup Arthroplasty of the Shoulder. (A) The Cup implant (B) Radiographic image after the implantation (adapted from Jonsson et al., 1986)

The 1980's saw the advent of a number of modular humeral component designs, trying to accommodate the variations in humeral anatomy and space available for the joint and humeral medullary canal diameters. On the glenoid side, some designs offered cementless fixation using screws and porous coatings on metal backing to the polyethylene. In the 1990's, increased emphasis was being placed on restoring normal

kinematics with anatomical location and orientation of the humeral and glenoid joint surfaces, advanced soft tissue balancing methods, and physiological stabilization of the joint.

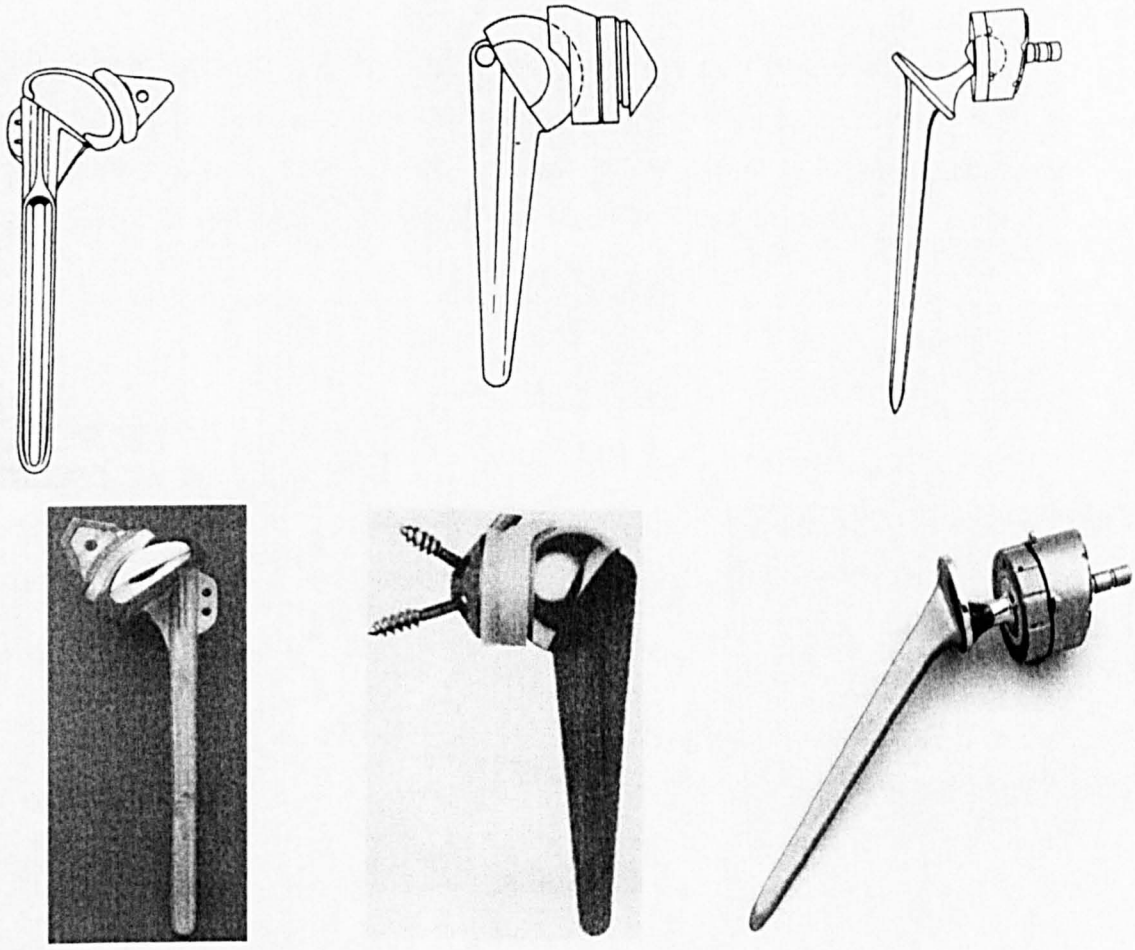

The Neer II design – Unconstraint prosthesis | Partially constrained prosthesis with cup-shaped socket | Constrained Design | Prosthesis

Figure 3.8:Normal anatomy designs of shoulder prosthesis

After all these pioneering efforts, especially from Neer, many additional shoulder prostheses were constructed. During the 1970s total shoulder replacement design developed along two lines, the **unconstrained**, which were focused improving Neer designs and the **constrained,** which developed to overcome stability problems coming from the original designs.

3.5. *Constrained prosthetic designs:*

The advantage of a constrained prosthesis was considered to be stability against dislocation, compensating for **absent rotator cuff function**. Problems though, of endoprosthetic loosening and the desire to achieve a full range of movement motivated the unconstrained designs.

Many of them were developed with total or partial constraint function (Figure 3.8). Partially constrained designs came after many years of experience with unconstrained implants, which were unable to prevent the translation and subluxation of the humeral head. The better understanding of the biomechanical function of the shoulder girdle drove the constraint design factor to be developed. In many cases a glenoid component (something like a hooded or cup-shaped socket) was designed to prevent the humeral head from dislocating without constraining unduly the range of motion. One of the earliest designs in total constrained prosthesis, was the one of Zippel in 1975 (Figure 3.9).

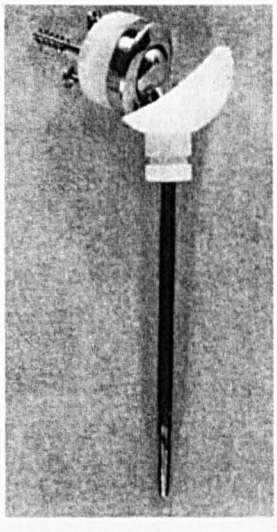

Figure 3.9: Model BME total shoulder arthroplasty designed by Zippel of Hamburg, Germany.

One of the major problems of these designs was also the limited range of movement of the glenohumeral joint since impingement of the implanted components with the bones (and especially with the scapula) was very often. Many attempts have been made to overcome the problem by designing different sizes of neck and ball in the humeral stem.

One of the most popular designs and very similar to Zippel was the design of Michael Reese 1979 (Kelly, 1993). The socket this time was from polyethylene, which fits into a

truncated conical metal cup attached to the scapula by means of a metal post. Both the components are fixed using cement.

More pioneer prostheses were designed in terms of the configuration to allow the prosthesis to have motion in excess of normal anatomic limits. The trispherical total shoulder prosthesis was designed by Gristina (1987). Two spheres are held captive within a third larger component. The design thus allows an extremely large range of motion in a captive ball in socket constrained implant system (Figure 3.10).

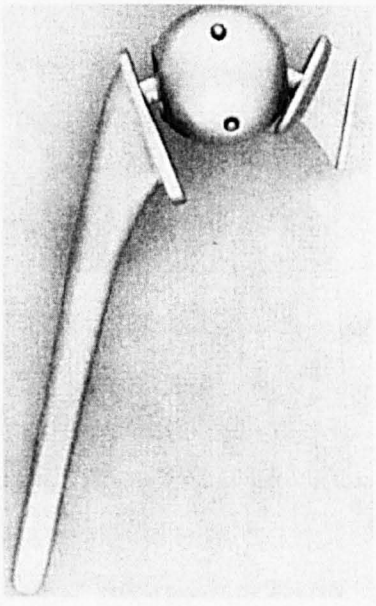

Figure 3.10:Constrained design prosthesis. The trispherical shoulder prosthesis by Gristina and co-workers. Two spheres are held captive within a third larger sphere (adapted by Gristina et al., 1987).

3.6. *Reverse anatomy designs:*

There is a special category of shoulder total arthroplasty. There are some designs that reversed the ball and socket configuration and have attached the ball part of the implant to the glenoid. Reverse anatomy prosthesis can be considered as constrained prosthetic designs as all the humeral component designs up to date, constrain totally or partially the kinematics of the implant. It has been widely reported that they permit a large range of joint movement.

These kind of prosthetic designs are not widely used and this is the reason that there are only few compared with the anatomical prosthesis. One of the most common problems of the reverse anatomy prosthesis, was the loosening of the glenoid

component. The shape and the thickness of the glenoid provide limited bone stock which means that a rigid fixation of the implant can be difficult.

The design variability is mostly due to the different fixation of the humeral and glenoid component. One of the first designs belongs to Fenlin (1975) and is a reverse ball-in-socket. A wedge is driven into the bone of the scapula for fixation and a column is placed down the inferior border of the scapula.

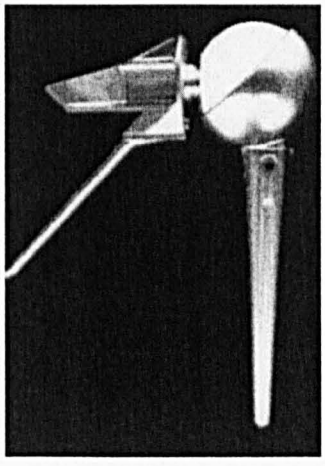

Figure 3.11: Typical reverse anatomy design (adapted by Khazzam and Fealy, 2008)

One of the most popular reverse anatomy prosthesis was developed by Kessel and presented in 1979. (Kessel and Bayley 1979). This prosthesis has a reversed design with the head set on a threaded post that screws into the scapula and a high density polyethylene cup with a stem that in cemented into the humerus. The two parts lock together with a press fit mechanism. The centre of rotation is displaced distally to the glenoid and more into the resected humeral head simulating the location of the centre of rotation of the normal shoulder. As a result the prosthesis can avoid impingement of the humeral component with the scapula and provide a range of motion (free of impingement) that compares to the normal shoulder. This prosthesis was redesigned recently by Bayley and Walker, making changes to the central glenoid peg in order to reduce the rate of loosening and is produced up to date from Stanmore Implants™

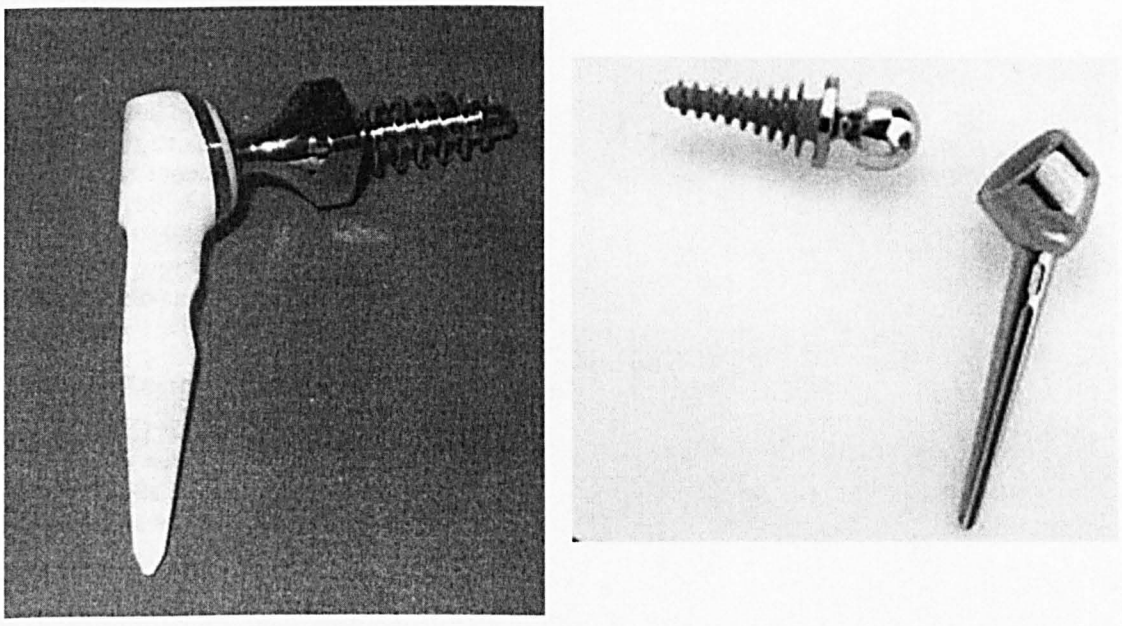

Figure 3.12: The Kessel total shoulder and the updated design in its current form as it was redesigned by Bayley and Walker (Stanmore Implants™)

More recent reverse anatomy prostheses are the designs of the "Liverpool total arthroplasty – 1982-" and that of Kolbel –1987. Both of these are ball in socket designs. In the Liverpool design the glenoid component has a stem that is inserted into the medullary cavity of the axillary border of the scapula to a depth of approximately 50 mm. In Kolbel's design the scapular component fixation includes a flange bolted to the base of the spine of the scapula in order to increase fixation stability. In both prosthetic designs the humeral cup has not an extensive stem.

Figure 3.13: Reverse total shoulder arthroplasty: a)Kobel design b)Liverpool design. Similar "Ball in socket" reverse anatomy designs with a scapular glenoid component and humeral cup. In both cases the humeral cup design does not include stem component. The shoulder centre of rotation resembles the anatomical one, being almost in the centre of the humeral head (adapted by Kobel et al., 1983)

3.7. The Delta Prosthesis

This study is focusing in DELTA prosthesis, which is one of the most recent reverse anatomy designs. The design is a result of Dr. P.M.Grammont. The experience of Paul Grammont's team in Dijon with the reversed system began in 1986, firstly with the so-called "Trumpet" prosthesis, cemented on its two aspects, polyethylene humeral and ceramic glenoid, until 1990. Based on this experience, the concept was further developed with the creation of the first DELTA prosthesis prototype in 1989, which was implanted for the first time in 1991 and was used until 1996 (uncemented prosthesis). (E.Baulot, P.M. Grammont, 2000).

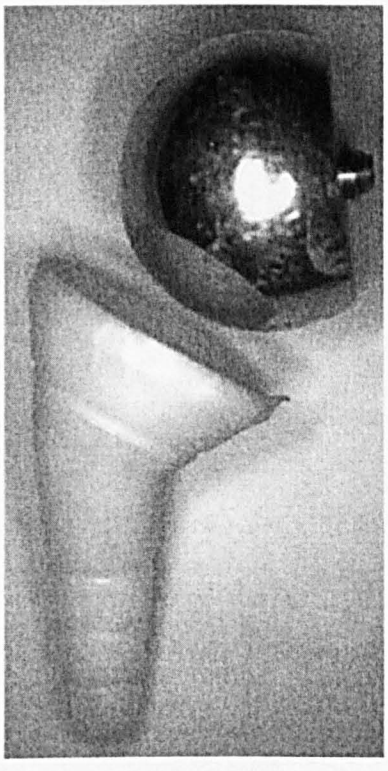

Figure 3.14

The first model of the Grammont reverse prosthesis, designed by Grammont in 1985, had only 2 components: the humeral component was all-polyethylene and trumpet-shaped and the glenoid component was a metallic or ceramic ball, initially two thirds of a sphere and 42 mm in diameter (Adopted from Boileau et al., 2005).

The idea of designing a prosthesis that could permit surgeons to restore a stable, pain free joint with sufficient strength and movement for patient without rotator cuff muscles led Grammont to use a reversed constrained design having both a glenoid and a humeral component.

3.7.1. The glenoid component

The glenoid part, the so-called "Glenosphere", is a steel hemisphere available in two sizes - 36mm and 42mm diameter. The sizes were originally chosen to fit every

anatomical scapula size, but over the years, extensive clinical reports have claimed that the size of the Glenosphere affects the stability and the kinematics of the joint.

The inferior part of the Glenosphere is cavernous having a screw to allow fixation in the scapula.

Figure 3.15: The Glenosphere

A second component (the Metaglen) is used to achieve rigid fixation of the Glenosphere in the glenoid cavity. This is a flat disk, 3 mm thick with an extruded internal cylinder attached in the middle and four holes around the periphery (Figure 3.16).

Figure 3.16:The Metaglen

The Metaglen has a standardised size to fit into the interior of any Glenosphere, and is implanted without cement. Initially, primary stability is provided by screwing the metaglen with four screws (peripherally in the four holes). The inferior is the longest screw and is fixed in an inferior direction to follow the inferior scapula border, where the superior has an apposing direction. The anterior and posterior screws are much smaller

as the bone stock of the glenoid is limited. Biological fixation is later achieved also by bony ingrowth to the Hydroxyapatite (HA) coating. The Glenosphere is attached to the Metaglen by a screw through the centre hole.

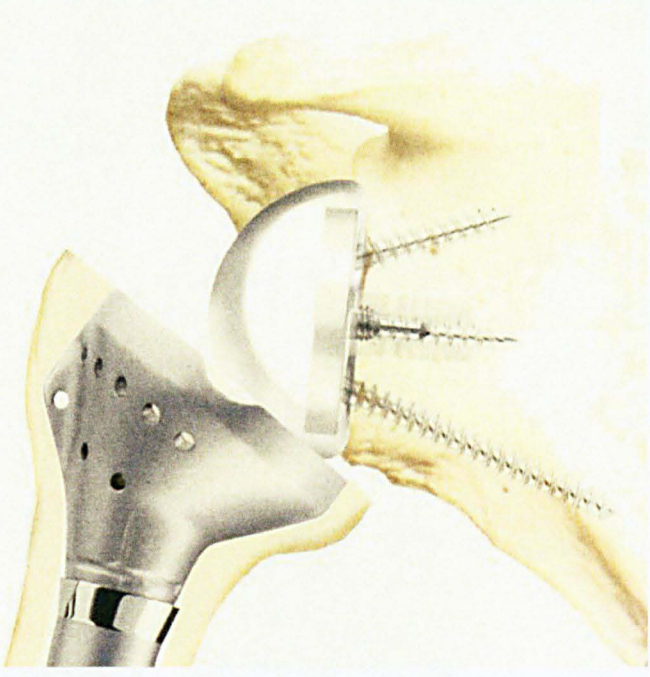

Figure 3.17: DELTA fixation.

3.7.2. The Humeral Component

The humeral component is divided into 3 parts (Figure 3.18):

- The stainless steel Diaphysis, which is the first part of the stem, is inserted along the longitudinal axis of humerus (into the humeral canal) to achieve rigid fixation.
- The metallic Epiphysis (made by stainless steel 316GL – ASTM F138) is designed to fit on to the Diaphysis and to host the humeral cup. Its proximal end protrudes out of the resected humeral head.
- The Humeral cup is made of Ultra High Molecular Weight Polyethylene (UHMPE PUR-1020 Medical grade). The interior part of the cup is moulded to fit in the Epiphysis while the inferior part has an inverted sphere shape with a radius equal to that of the Glenosphere.

There are different sizes for all the humeral components in order to fit in the anatomical sizes. Surgeons have extra option of choices for the cup (thickness, depth, diameter), in order to achieve the optimum mobility and stability of the joint. It is often the

surgeon to choose a thicker cup in order to stretch the joint (thus stretching the muscles and especially the Deltoid) and increase the passive tension for better stability.

Despite the high modularity of the DELTA prosthesis, there are insufficient data to document the importance of implant size to the stability and mobility of the shoulder joint

Diaphysis Epiphysis Humeral cup

Figure 3.18: Humeral components of DELTA system

Figure 3.19: There are cemented and uncemented options for the DELTA shoulder prosthesis

3.7.3. The impingement problem

The design of DELTA has been shown over the last years to provide a high degree of stability and clinical reports indicate that the prosthesis is particularly successful in patients having severe damage to the rotator cuff muscles (Boileau et al. 2006,Valenti P et al. 2001,Wall B.T. & Walch G. 2008). Because of the encouraging results the DELTA has pushed the envelope of its use into severe humeral fracture etc.

However, the long term use of the prosthesis has also revealed some problems which caused a debate about its use (Rockwood, Jr. 2007). Clinical data showed that there are high rates of implications, with impingement and the development of bone notches in the inferior scapula border to be significant. First Boileau et al. (2005) have categorised the

stages of the notching development and showed that it can be catastrophic for the glenoid fixation (Figure 3.20). The causes of the bone notches is not fully understood, but it has been suggested that they may be caused either by the contact of the humeral cup into the scapula border, or by osteolysis.

Extensive investigation of the impingement and notching problem will be provided first in chapter 5 and then in chapter 9.

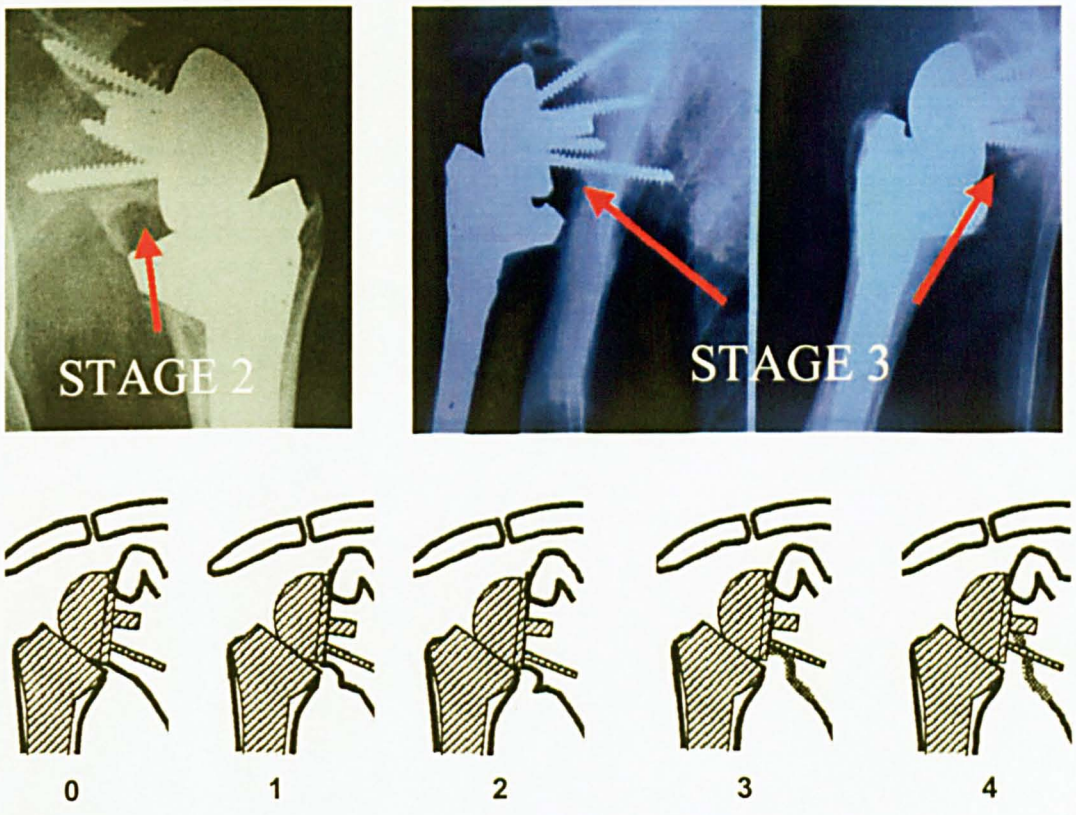

Figure 3.20: Five stages of impingement as they have clinically reported (Boileau et al., 2005)

3.8. The trend of the current joint replacement designs

3.8.1. Anatomical designs – high modularity and adjustability

High modularity of the shoulder prosthesis, where many sizes of stems can be assembled with a variety of head sizes, is a key feature to all of the current designs in the market today. The modularity is providing the surgeon the flexibility to match the large variability on the humeral medullary canal diameters (small to large).

For an anatomical prosthesis it is for critical the design to be able to replicate as accurately as possible the natural anatomy of the replaced joint. Thus clever adjustable designs are introduced in order to fit the variability of the head version and neck angle that is observed amongst the population (Jeong et al. 2009,Kapandji 1982).

One of the first adjustable features that is common to most of the current anatomical design, is the offset connection of the head to the neck of the prosthesis. A rotation of the head of the prosthesis changes its version and can offer the best possible coverage of the resected bone (Roberts et al. 1991) (Figure 3.21). This is critical in avoiding inferior impingement, even if the problem in anatomical prosthesis is not as big concern as in the reverse (Favre et al. 2008).

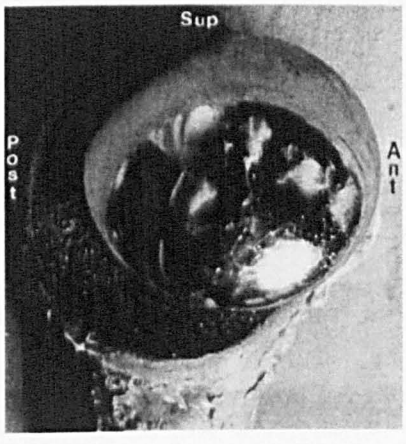

Figure 3.21:

A standard (non adjustable) head is difficult to cover the resected area of the head (adapted from Roberts et al. 1991)

Anatomical Shoulder (Zimmer) Aequalis® (Tornier)

Figure 3.22: Offset head adjustability in order to cover the humeral resected area

Recently, more highly adjustable designs were introduced to the market, where an interconnection mechanism allow infinite adjustments not only on the version, but also in the neck shaft angle and neck length of the prosthesis. These designs have trial parts and specialised jigs which allow the surgeons first to match the natural geometry of the resected head and then assemble the prosthesis accordingly before implanting it to the humerus (Figure 3.23)

Figure 3.23: The PROMOS® (Smith&Nephew) highly adjustable design

3.8.2. Mobile designs

Mobile prostheses were introduced first to hips and have also expanded to knees in order to increase the mobility of the joint. As it was mentioned above, shoulder prosthesis designs with mobile parts are not a new concept, since the Trispherical constraint design can fall into this category. The evolution of the mobile design concept was also expanded to the more traditional anatomical designs, as well as to the reverse.

Current prostheses from Stryker and Biomet (Figure 3.24) offer similar design concepts, where a large head connects with the neck of the prosthesis through a smaller ball and socket joint, providing three degrees of freedom mobility. The large head articulates with the glenoid which is not resurfaced. The basic idea of the mobile mechanism is to provide mobility to the joint when the large head is immobilised due to impingement.

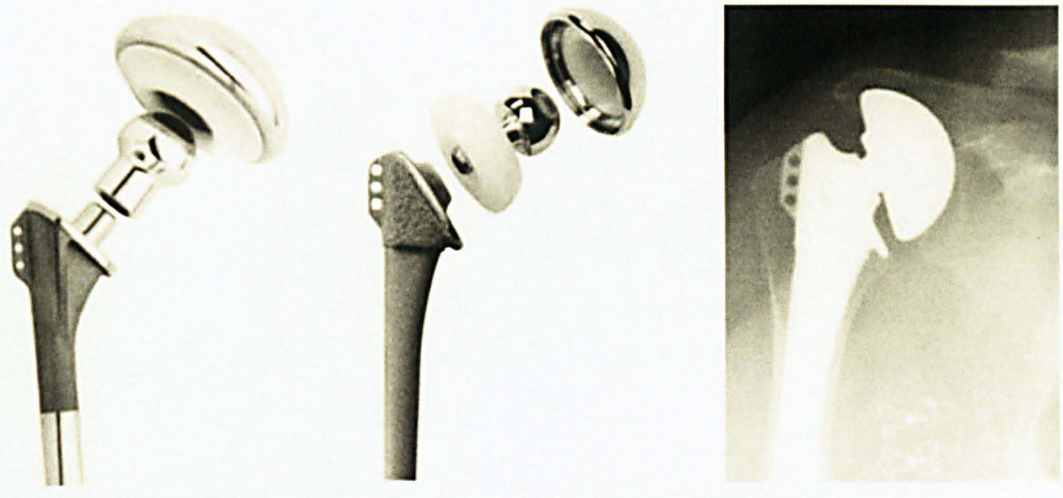

Bipolar Head, Stryker Bipolar, Biomet

Figure 3.24: The Bipolar shoulder systems provide a 3 degree of freedom mobile head that is articulating with the glenoid

The only mobile concept in the reverse prosthesis was introduced by Wright Medical (NGR® prosthesis) where the humeral cup was able to rotate around the long axis of the stem, providing a dynamic change of the version of the prosthesis. The basic idea of the design was again to provide extra internal/external rotation on the humerus when the cup impinges on the scapula inferior border. The influence of the version of the fixation on a reverse prosthesis will be discussed in the biomechanical analysis of the DELTA® III prosthesis in chapter 5.

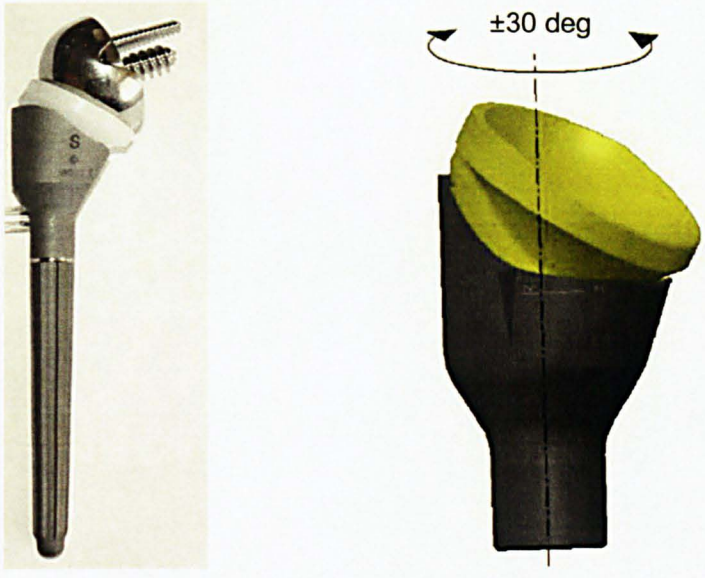

Figure 3.25: The NGR single degree of freedom mobile cup design

3.8.3. Current reverse anatomy prosthesis – following the Grammont design

After the extended use of the DELTA® prosthesis from DePuy, there are many other designs developed by other manufacturers over the recent years. Most of these designs simply replicate the basic geometrical characteristics of DELTA (e.g. half glenoid sphere, neck/shaft angle, cup depth), but introduce slightly different stem designs or glenoid plates with adjustable screw direction to fix the sphere on the glenoid.

Aequalis Reverse (Tornier)

SMR System (Lima-Lto)

Promos Reverse (Smith&Nephew)

Duocentric® (ASTON medical)

Figure 3.26: Current reverse anatomy designs that follow the original Grammont (DELTA) geometry

However, reports of the high rates of complications of the DELTA prosthesis and especially the indication of impingement and notching problem have driven some of the designs to differentiate some of the geometrical features in order to improve survivorship and reduce the problem.

As typical examples of the latter designs are the Encore® reverse (DJO Surgical) and the ARROW® total reverse (Implants Industry-Prothese). The Encore system introduces a glenoid sphere that is a larger portion of the half spherical portion of the DELTA Glenospher (Figure 3.27). As such, the centre of rotation is not as medialised as in the DELTA and the humeral cup is further away from the scapula inferior border (impingement site).

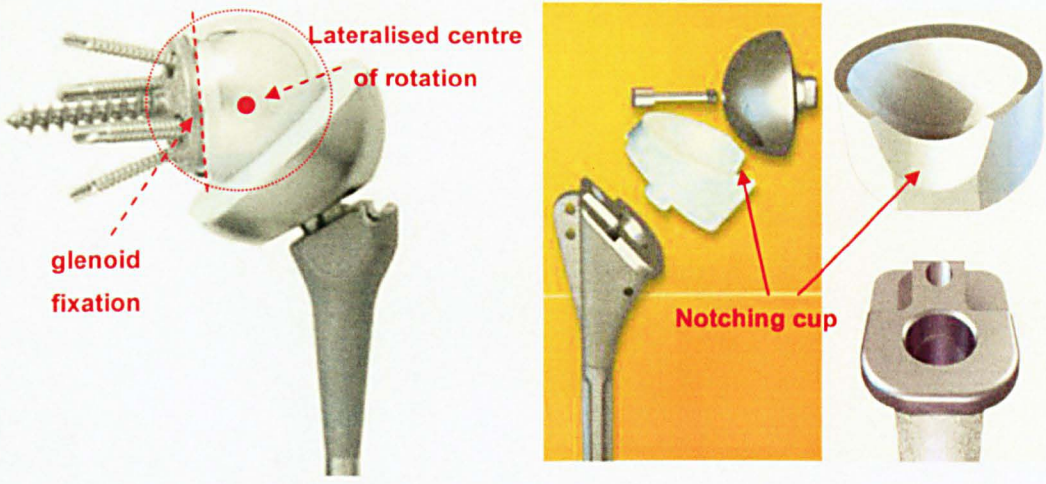

Encore Reverse ® ARROW reverse®

Figure 3.27: Some reverse prostheses are adopting slightly different approach from the original DELTA design in order to reduce the impingement problem

The Arrow reverse system has a different design on the cup, where an artificial notch is introduced in order to avoid contact with the scapula border. The shape and size of the notch is derived from clinical data that show DELTA cups with similar shape notches.

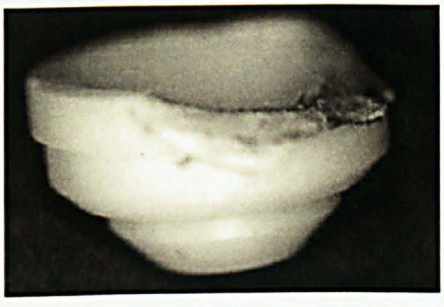

Figure 3.28:

Notches on an explanted DELTA cup (adopted by Boileau et al. 2005)

The importance of the design parameters and how they can affect the stability and the impingement problem will be analysed in detail later in the thesis.

3.8.4. Adaptable reverse to anatomical prosthesis

In an effort to minimise the cost and increase the flexibility of the shoulder prostheses, some designs recently have adopted an approach where they share common parts between the anatomical and the reverse versions. Most commonly the designs introduce universal humeral stems and glenoid fixation plates, where the humeral head/cup and glenoid cup/sphere can be interchangeable in order to revert the geometry from anatomical to reverse or wise versa. This reduces the inventory of the parts of the

prosthesis and provides flexibility in the decision making during the operation (anatomical or reverse) or in revision cases where the common parts like stem does not need to be removed.

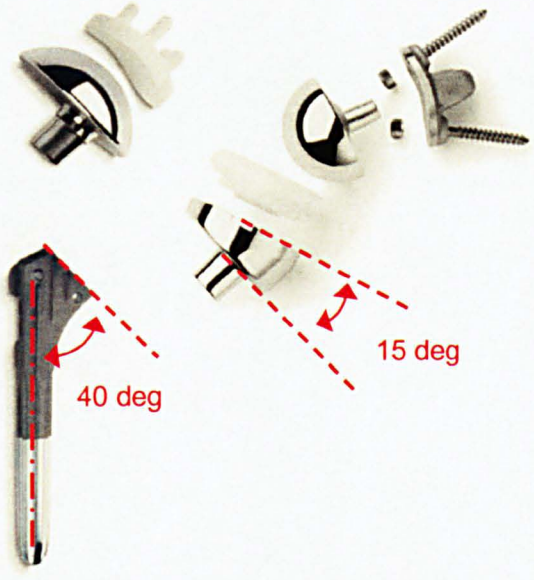

Figure 3.29:

The Zimmer shoulder system that converts from anatomical to reverse reducing the overall parts of the shoulder system

Usually the main challenge on adaptable anatomical/reverse systems is to balance the humeral head resection plane (and thus neck of the prosthesis), where naturally in an anatomical prosthesis is more aggressive. As it will be explained in the biomechanical analysis of DELTA, the neck/shaft angle of the prosthesis in a reverse prosthesis can affect the stability of the joint. Thus the conversion of the anatomical to reverse is usually provided with a correction angle in the proximal support of the cup (Figure 3.29).

Chapter 4. Creating a shoulder reverse joint replacement biomechanical model

4.1. Introduction

The shoulder biomechanical models were not as popular as the hip. One of the earliest examples is probably that of Fick and Weber (1877) who produced a physical model on which loads could be applied to the tendons of a shoulder cadaver. Although this mechanical approach has been also examined by other studies (Guihard & Gorce 2000,Mollier 1899) the majority of studies of the shoulder have centred on the use of theoretical or computer models of varying complexity.

The first of these was the classic study by Inman (1944) who studied the mechanics of the deltoid muscle and more recently the two-dimensional model described by Poppen and Walker (1978) has been referenced extensively in many recent upper limb biomechanics studies. Since then, more sophisticated three dimensional models of the shoulder and elbow have been developed to investigate glenohumeral loads during more complex movements (Charlton 2003,Karlsson & Peterson 1992,Runciman & Nicol 1994,van der Helm 1994).

The validation of biomechanical models is always problematic because of the difficulties of obtaining experimental measurements of internal forces. Even if there are good indications that biomechanical models can predict valid joint loads on the hip (Heller et al. 2001), it is only recently that GH loads were measured in vivo (Westerhoff et al. 2009a) through an instrumented shoulder implant (Westerhoff et al. 2009b) and model validation is still in preliminary stage (Rasmussen et al. 2007).

Charlton (2003) has recently developed a biomechanical model that describes the normal shoulder and elbow (the Newcastle Shoulder Model –NSM), which was validated by comparison to the other published models and showed good agreement. This chapter will provide a detailed description of the NSM and all the methodology that was followed in order to adapt the shoulder model to describe a reverse anatomy joint replacement and more specifically the DELTA® III prosthesis.

4.2. The Newcastle Shoulder Model

4.2.1. Skeletal geometry and embedded coordinate systems

The skeletal models used for visualisation and model parameterisation were extracted from the Visible Human data set (National Library of Medicine, USA, (Spitzer et al. 1996,Spitzer & Whitlock 1998)) and especially the anatomical transverse cryo-sections. The original dataset includes cryo-sections at 1mm intervals, but each bone structure was digitised individually at an interval of 2mm cryo-sections

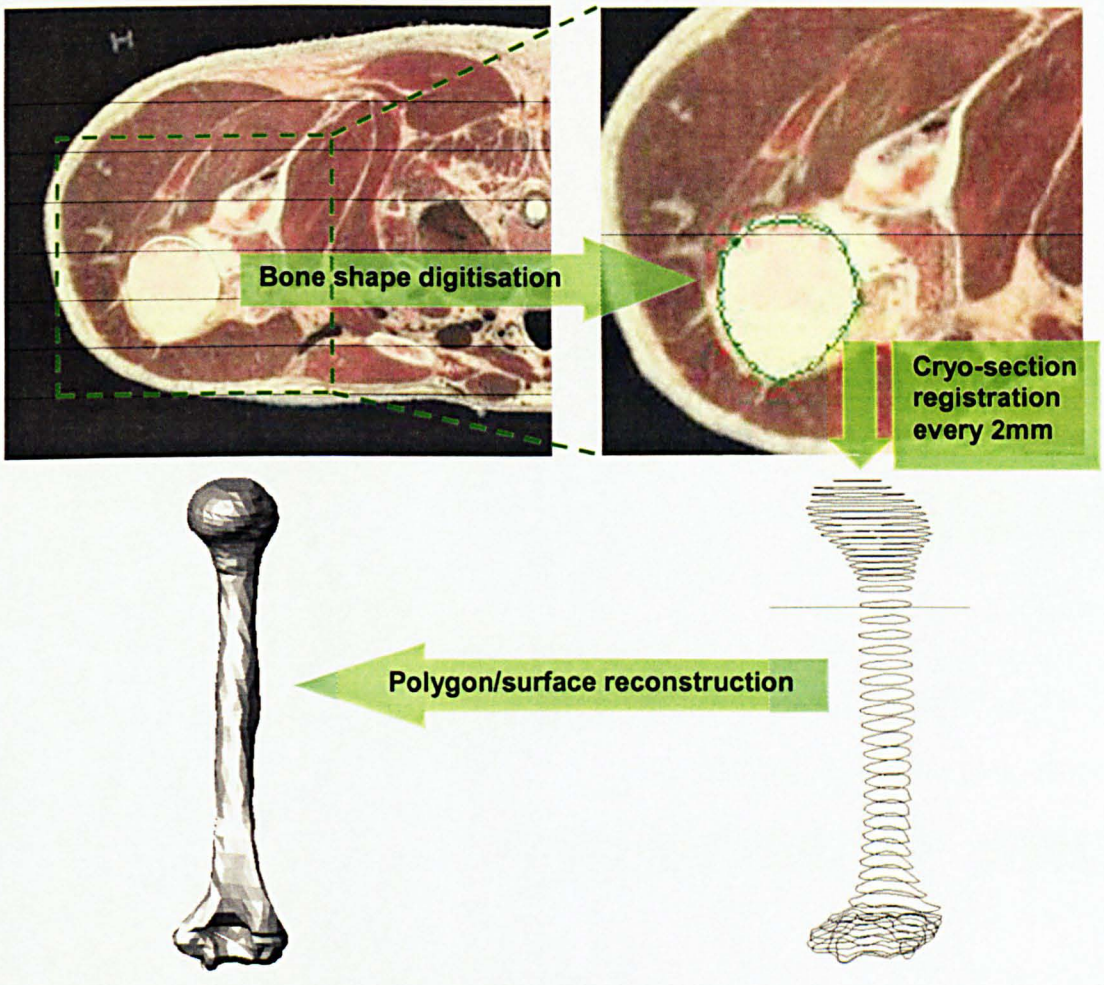

Figure 4.1: Bone digitisation procedure from the Visible human database

The model consists of six rigid bone segments: the thorax, clavicle, scapula, humerus, radius and ulna. These are connected by three spherical joints, the sternoclavicular (SC), acromioclavicular (AC) and glenohumeral (GH), and two single degree-of-freedom (DOF) hinge joints at the elbow. In addition, the scapulothoracic gliding plane (STGP) forms a closed loop between the clavicle, scapula and thorax and

this joint is described as a pair of prismatic joints at the superior and inferior angles of the scapula on ellipsoidal surface (approximating the rib cage).

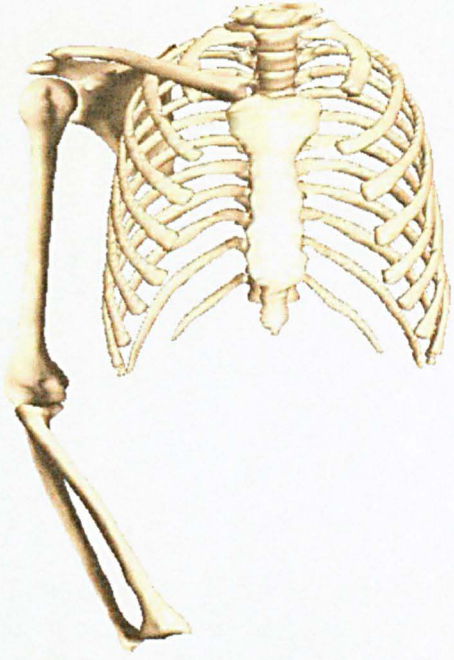

Figure 4.2: The reconstructed 2mm skeleton of NSM

Each bone segment has an associated embedded coordinate system that can be, to a large degree, defined from well-palpable bony landmarks. These systems and other embedded axes are based on the systems recommended by the International Shoulder Group (ISG, (van der Helm, 1996))

The thorax embedded coordinate system uses the anatomical landmarks of Jugular notch (***IJ***) and Xiphoid process (***PX***) as well as the vertebrae of 7th cervical ***C7*** and 8th thoracic (***T8***) as shown in Figure 4.3

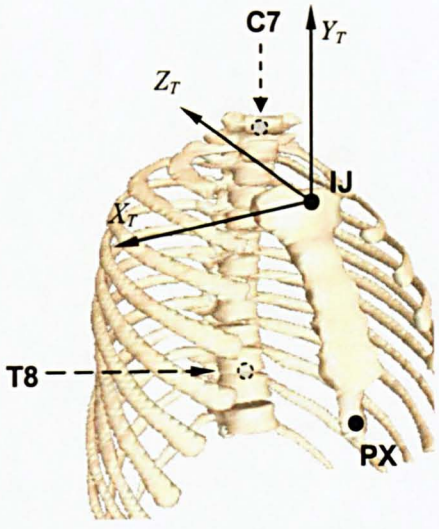

$$\overline{Y}_T = \frac{\left(\overline{IJ} + \overline{C7}\right)/2 - \left(\overline{PX} + \overline{T8}\right)/2}{\left|\left(\overline{IJ} + \overline{C7}\right)/2 - \left(\overline{PX} + \overline{T8}\right)/2\right|}$$

$$\overline{X}_T = \frac{\overline{Y}_T \times \left(\overline{PX} - \overline{T8}\right)}{\left|\overline{Y}_T \times \left(\overline{PX} - \overline{T8}\right)\right|}$$

$$\overline{Z}_T = \overline{X}_T \times \overline{Y}_T$$

Origin = IJ

Figure 4.3: The Thorax embedded coordinate system

Due to the long anatomical shape of the clavicle the embedded coordinate system needs to be defined by the superior thoracic axis and the anatomical landmarks of the sternoclavicular (***SC***) and acromioclavicular (***AC***) joint Figure 4.4.

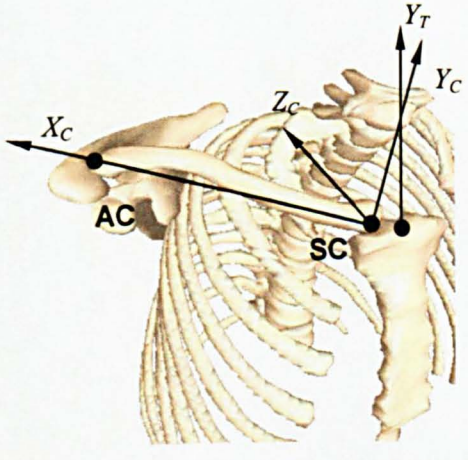

$$\overline{X}_C = \frac{\overline{AC} - \overline{SC}}{\left|\overline{AC} - \overline{SC}\right|}$$

$$\overline{Z}_C = \overline{X}_C \times \overline{Y}_T$$

$$\overline{Y}_C = \overline{Z}_C \times \overline{X}_C$$

Origin = SC

Figure 4.4: The clavicle embedded co-ordinate system

The scapula anatomical embedded coordinate system uses the anatomical landmarks of the tip of the acromion (***AA***), the root of the scapula spine (***TS***) and of the Inferior angle (***AI***) (Figure 4.5).

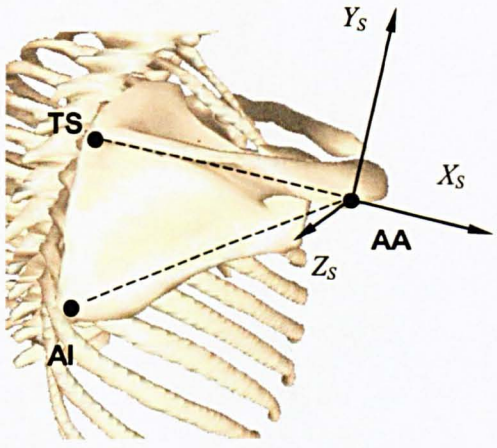

$$\overline{X}_S = \frac{\overline{AA} - \overline{TS}}{\left|\overline{AA} - \overline{TS}\right|}$$

$$\overline{Z}_S = \frac{\overline{X}_S \times \left(\overline{AA} - \overline{AI}\right)}{\left|\overline{X}_S \times \left(\overline{AA} - \overline{AI}\right)\right|}$$

$$\overline{Y}_S = \overline{Z}_S \times \overline{X}_S$$

Origin = AA

Figure 4.5: The scapula embedded coordinate system

For the humeral system the centre of rotation of the ***GH*** centre is used. For the anatomical shoulder this is shown to be the centre of the sphere that fits the humeral head (van der Helm et al. 1989,van der Helm et al. 1992). The lateral (***EL***) and medial (***EM***) epicondyles are also used to define the anatomical embedded coordinate frame of the humerus (Figure 4.6).

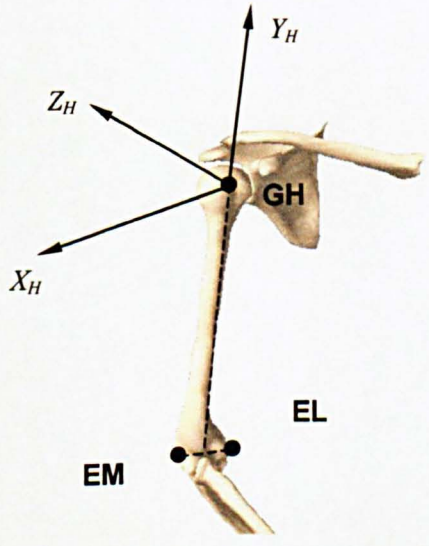

$$\overline{Y}_H = \frac{\overline{GH} - \left(\overline{EM} + \overline{EL}\right)/2}{\left|\overline{GH} - \left(\overline{EM} + \overline{EL}\right)/2\right|}$$

$$\overline{Z}_H = \frac{\overline{Y}_H \times \left(\overline{EM} - \overline{EL}\right)}{\left|\overline{Y}_H \times \left(\overline{EM} - \overline{EL}\right)\right|}$$

$$\overline{X}_H = \overline{Y}_H \times \overline{Z}_H$$

Origin = GH

Figure 4.6: The humerus embedded coordinate system

The forearm, radius and ulna embedded systems share similar landmarks to that proposed by Wu and Cavanagh (1995) in that they have similar longitudinal, lateral and

antero-posterior axes. For the forearm frame the same landmarks of ***EM*** and ***EL*** are used as well as the landmarks of the ulnar and radial styloids (Figure 4.7)

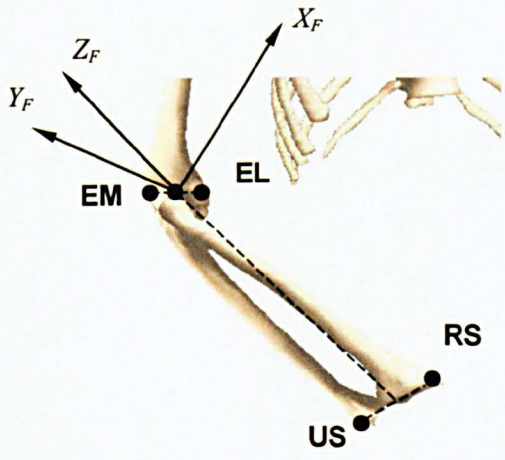

$$\bar{Y}_F = \frac{\left(\overline{EM} + \overline{EL}\right)/2 - \left(\overline{US} + \overline{RS}\right)/2}{\left|\left(\overline{EM} + \overline{EL}\right)/2 - \left(\overline{US} + \overline{RS}\right)/2\right|}$$

$$\bar{Z}_F = \frac{\bar{Y}_F \times \left(\overline{US} - \overline{RS}\right)}{\left|\bar{Y}_F \times \left(\overline{US} - \overline{RS}\right)\right|}$$

$$\bar{X}_F = \bar{Y}_F \times \bar{Z}_F$$

Origin = $\left(\overline{EM} + \overline{EL}\right)/2$

Figure 4.7: The forearm embedded coordinate system

The location of the origin for the forearm system (the midpoint of the vector joining the epicondyles) will hereafter be referred to as **ELB** and the midpoint of the vector connecting the styloids of the wrist as **WR**.

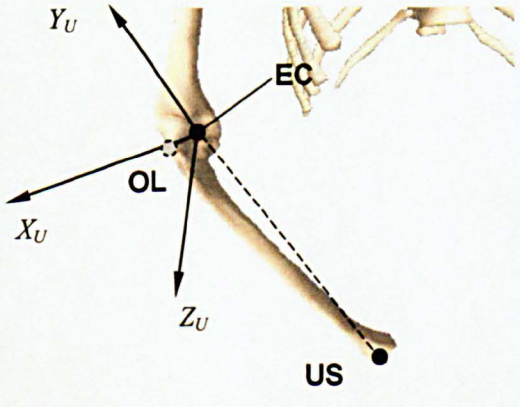

$$\bar{Y}_U = \frac{\overline{EC} - \overline{US}}{\left|\overline{EC} - \overline{US}\right|}$$

$$\bar{X}_U = \frac{\bar{Y}_U \times \left(\overline{OL} - \overline{EC}\right)}{\left|\bar{Y}_U \times \left(\overline{OL} - \overline{EC}\right)\right|}$$

$$\bar{Z}_U = \bar{X}_U \times \bar{Y}_U$$

Origin = EC

Figure 4.8: The ulnar embedded coordinate system

In Figure 4.8, ***EC*** refers to the centre of the humero-ulnar joint and this is located on the flexion axis, $\bar{V}_F$, at the closest point to the vector connecting ***US*** and ***OL*** (Charlton, 2000). Thus, the co-ordinate system of the ulna is coincident with the humero-ulnar joint.

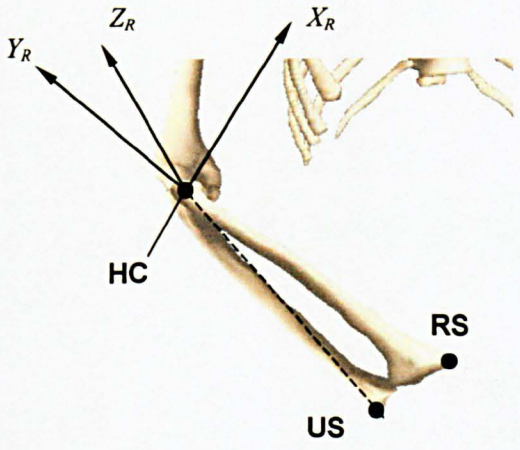

$$\overline{Y}_R = \frac{\overline{HC} - \overline{US}}{\left|\overline{HC} - \overline{US}\right|}$$

$$\overline{Z}_R = \frac{\overline{Y}_R \times \left(\overline{US} - \overline{RS}\right)}{\left|\overline{Y}_R \times \left(\overline{US} - \overline{RS}\right)\right|}$$

$$\overline{X}_R = \overline{Y}_R \times \overline{Z}_R$$

Origin = HC

Figure 4.9: The radius embedded coordinate system

In Figure 4.9, ***HC*** is located at the geometric centre of the radial head, which is placed on the pro-supination axis, $\overline{V}_P$ (Charlton, 2000). Again, this has advantages, as it places the origin of the radial co-ordinate system on the axis about which it rotates.

4.2.2. Muscles and ligaments

The studies carried out by van der Helm et al. (1992), Johnson et al. (1996) and Veeger et al. (1997) were chosen for establishing a complete upper limb morphology set for the NSM. The majority of the selected data are from Johnson et al., but missing data of the larger thoracic muscles of pectoralis major and trapezius as well as ligamentus attachment sites were taken from van der Helm *et. al.* Morphology parameters for the muscles crossing the elbow were extracted from the study of Veeger *et al.*

Muscles in the NSM are modelled as elastic strings that have origin and insertion in the corresponding segments. Muscles with large attachment sites were modelled with more than one string and the division of the muscles into smaller elements is based on the natural division of the muscles into fascicles (Johnson et al., 1996) except for the m.Latissimus dorsi and greater pectoral muscles where the number of strings elements were derived from van der Helm et al. (1992) with methods based on robotic principles (van der Helm & Veebaas 1991).

The finalised muscle and ligament data set (31 muscles, 3 ligaments), the number of elements that are divided (90) and their reference is summarised in Table 4.1.

Muscle	No. Fascicles	Muscle	No. Fascicles
m.Trapezius(clavicular)[1]	3	m.Biceps breve[3]	1
m.Trapezius(scapular)[1]	13	m.Biceps long[3]	1
m.Llevator scapulae[1]	4	m.Triceps long[3]	2
m.Rhomboid minor[1]	2	m.Triceps med[3]	2
m.Rhomboid major[1]	5	m.Triceps lat[3]	2
m.Serratus anterior[1]	9	m.Bracjialis [3]	2
m.Pectoralis minor[1]	3	m.Anconeus[3]	2
m.Latissimus dorsi[2]	5	m.Brachioradialis[3]	2
m.Pectoralis major(thoracic)[2]	5	m.Supinator (humeral)[3]	1
m.Pectoralis major(clavicular)[2]	5	m.Supinators (ulnar)[3]	2
m.Deltoideus (clavicular)[1]	2	m.Pronatior teres(humreral)[3]	2
m.Delttoideus (scapular)[1]	3	m.Pronator teres(ulnar)[3]	2
m.Supraspinatus[1]	1	m.Pronator quadratus[3]	2
m.Infraspinatus[1]	3		
m.Subscapularis[1]	3	**Ligaments**	
m.Teres minor[1]	1	l.Costoclavicular[2]	1
m.Teres major[1]	1	l.Conoid[2]	1
m.Coracobrachialis	2	l.Trapezoideus[2]	1

1 Johnson *et. al.* (1996)
2 Van der Helm *et. al.* (1992)
3 Veeger *et. al.* (1997)

Table 4.1: Complete muscle set used in NSM

The musculoskeletal part of the model was implemented using SIMM software (Musculographics Inc., Illinois). This is a commercially available software package allowing realistic graphical display of the skeleton together with ligaments and muscle fascicles that are wrapping around the relevant structures (Figure 4.10).

The importance of wrapping of the muscle elements around the bones in a biomechanical model has been highlighted in various studies (Charlton et al. 2000,Marsden et al. 2008,Marsden & Swailes 2008). SIMM calculates muscle wrapping by minimising the length of the elastic string around simple geometrical shapes that fit the bone geometry. The NSM includes several wrapping objects that are described in Table 4.2.

Wrapping object that fit relevant bone geometry	Shape of wrapping object
Scapulothoracic Gliding Plane (STGP)	Ellipsoid
Anterolateral rib cage	Ellipsoid
Humeral head	Sphere
Humeral column	Cylinder
Radial column	Cylinder
Olecranon	Cylinder

Table 4.2: Wrapping objects used in NSM

The SIMM software is used only for graphical representation and muscle wrapping by the NSM. All the necessary computation of muscle and joint contact forces is implemented using custom routines in MATLAM software (Mathworks).

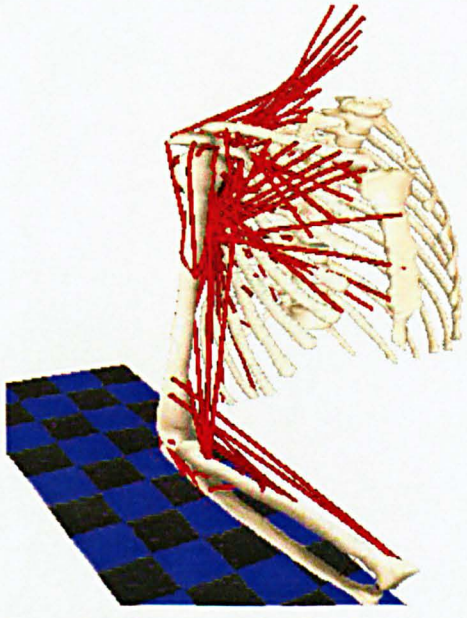

Figure 4.10: The NSM as implemented in SIMM

4.2.3. Model kinematics

Measuring and prescribing the kinematics of the upper limb linkage system involves defining the embedded co-ordinate frames of each rigid segment and describing the relationship between each joint proximal and distal segment in terms of a set of joint angles.

The model follows the ISG recommendations (van der Helm, 1996) where each of the SC and AC joints are described as Cardanic Euler angles and the 3 DOF of the GH joint are described as non-Cardanic Euler angles.

Compounded by the fact that the elbow flexion axes of the individual subjects are not known, the kinematic model includes only flexion and pronation about the axes derived from the Visible Human skeleton. The dynamic model includes all three rotations at the elbow to include the dynamic effect of the presence of the forearm carrying angle.

For the dynamic model, however, the orientation of the humerus relative to the scapula is required.

The sequence of Euler angles describing the rotations of each segment about its local axes are summarised in Table 4.3, as is the terminology relating to each of these rotations.

Segment	**Rotation Sequence**	**Rotation Terminology (in order specified)**		
Clavicle	Y, Z', X''	Clavicle Protraction	Clavicle Elevation	Clavicle Axial Rotation
Scapula	Y, Z', X''	Scapula Protraction	Scapula Lateral Rotation	Scapula Backward Tip
Humerus	Y, Z', Y''	Humeral Azimuth	Humeral Elevation	Humeral Internal Rotation
Ulna	V_F	Elbow Flexion	-	-
Radius	V_P	Forearm Pronation	-	-

Table 4.3: The rotation sequence of each segment and the terminology relating to each of those rotations

The rotation sequence where you choose the plane of elevation (azimuth), the degree of elevation and then the humeral internal rotation in order to describe the humeral position (Figure 4.11), has been popular in kinematics studies of upper extremity which investigate activities of daily living.

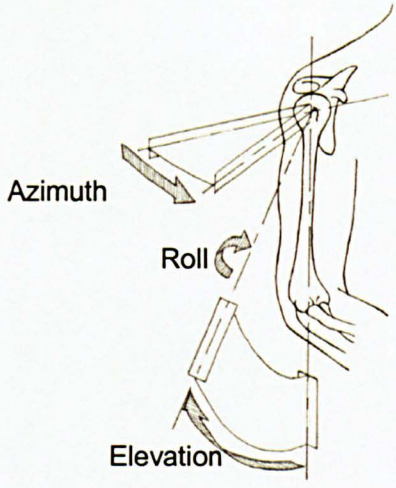

Figure 4.11: Humeral rotations (adapted from Charlton 2003)

However, this sequence presents a gimbal lock when the humerus is on the side where azimuth, elevation and rotation equals to 0 (for this position the azimuth and the humeral rotations are coincident around the same humeral axis - Y_h). Even when the humerus is close to the gimbal lock (small elevation values<20 deg) small arm motion can result in large deviations of the azimuth or the rotation value (Figure 4.12). For example, a 5 deg of abduction is equal of 5 deg of elevation in 0 degrees of azimuth, where 5 deg of forward flexion mean 5 deg of elevation in azimuth 90.

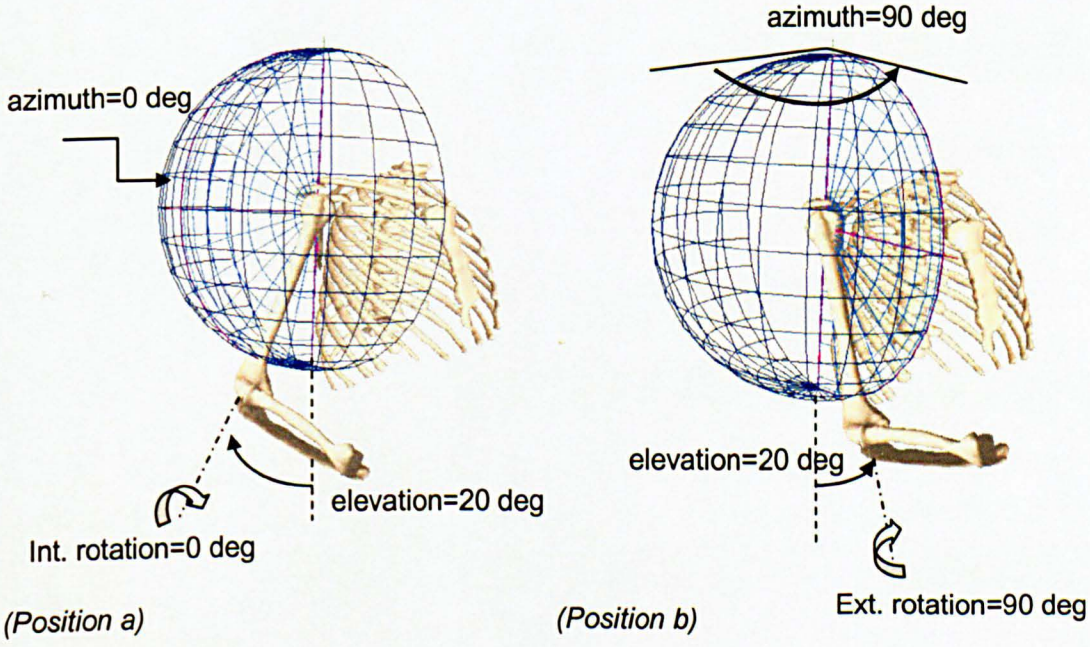

(Position a) *(Position b)*

Figure 4.12: When the arm is close to gimbal lock position, even a small motion of the arm (from the position a to b) can result in large change of azimuth and humeral rotation

4.2.4. Dynamics - Loadsharing

Given the kinematics model consisting of rigid links that was described above, the dynamics engine of NSM includes a description of the upper arm as a robotic linkage that it was first described by Murray (1999) and then further extended by Charlton to include the clavicle and scapula as rigid links (Figure 4.13).

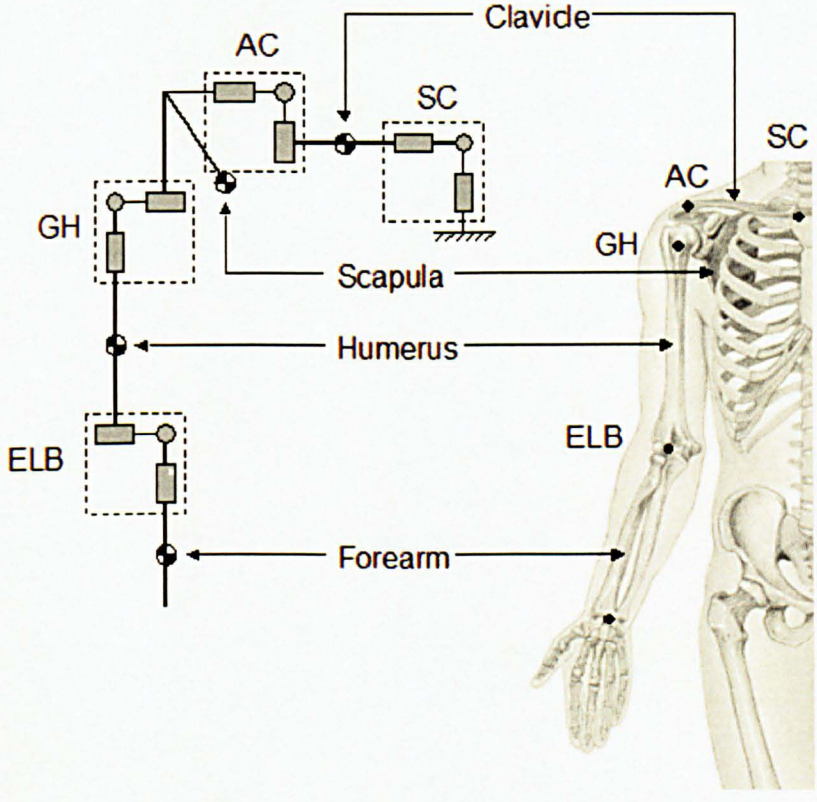

Figure 4.13: The complete upper limb linkage model of NSM (Murray 1999, Charlton 2003).

The robotic linkage can calculate the net forces and net moments at each joint for any given kinematic profile by using the popular recursive Newton-Euler technique (inverse dynamics). The body segment parameters (mass, mass centre, inertia properties) are derived using the equations of de Leva (1996).

The net forces and moments that are mentioned above formulate the equations of motion. In other words, the combination of the action (forces) of each muscle should produce these moments and forces (which result in the predefined kinematic profile).

The formulation of the equations of motion results in a system of equations with many unknowns (which are the muscle forces that should produce the joint net moment and forces). For solving the loadsharing problem and calculating a unique set of muscle forces, a minimisation of a 'physiological cost function' that describes the square muscle stresses (Hogfors et al. 1995) is used by the NSM:

$$V(Fi) = \sum_i \left(\frac{Fi}{PCSAi}\right)^2 \qquad \textit{eq. 4-1}$$

Where: Fi is the muscle force for each individual muscle
$PCSAi$ is the physiological cross-sectional area for the corresponding muscle i

The solution of muscle forces that is calculated from the above minimisation is constrained such as to provide stability to the joints of the upper limb. This is feasible only if the joint contact forces (that are considered to always cross the joint rotation centre) are constrained within the articulation surface of the joint. A technique for constraining the GH force vector within the glenoid is used by the NSM similar to the one first proposed by van der Helm (1994). More analytical description of the GH constraints will be presented later in this chapter.

4.2.5. Anthropometric Scaling and Subject Specific Models

The NSM model is truly representative only of the Visible Human and other subjects cannot be assumed to be a simple linearly scaled copy of the same. Given the limited number of well palpable bony landmarks on the upper limb and torso, each of the bone segments, muscular and ligamentous attachment sites and joint centre locations can be scaled to match other subjects according to measurements of the Visible Human skeleton:

i) clavicle length $l_C = \left|\overline{SC} - \overline{AC}\right|$,

ii) scapula length $l_S = \left|\overline{AC} - \overline{AI}\right|$,

iii) humerus length $l_H = \left|\overline{GH} - \left(\overline{EL} + \overline{EM}\right)/2\right|$,

iv) forearm length (for both radius and ulna) $l_F = \left|\left(\overline{EL} + \overline{EM}\right)/2 - \left(\overline{US} + \overline{RS}\right)/2\right|$

However, the scaling of the thorax by a single length factor can be unreliable (Pronk 1991) and Charlton 2003 used instead three different lengths for the thoracic scaling of

the NSM: i) vertical distance between the C7 and T8 vertebrae Ht, ii) the width of the thoracic cage on T8 height Wt, iii) the depth of the thoracic cage on T8 height Dt

4.3. Model modifications to describe the shoulder reverse joint replacement

4.3.1. Bone model refinements

All the bone files that are digitised in NSM, are represented by a finite number of triangle surface faces. The number of these 3-D faces is a result of the digitisation process and the number of the finite digitised points on every slice of the reconstruction (Figure 4.1). Because of the manual digitisation process, Charlton used an interval of 2mm of the cryo-sections in order to minimise 'cell skewing' problems during the reconstruction (Figure 4.14).

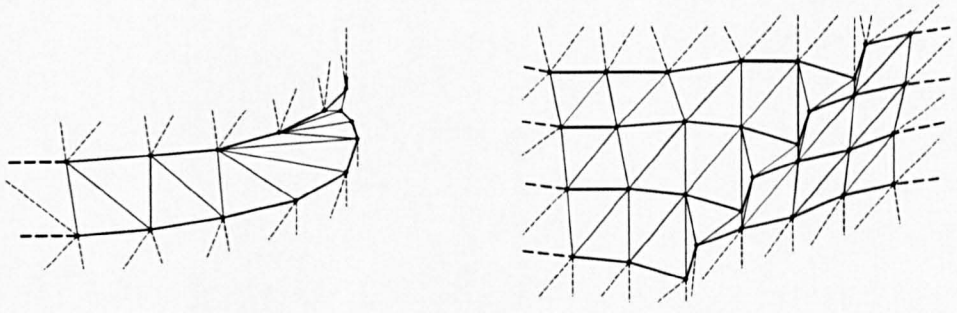

Figure 4.14: Cell skewing problems of the bone reconstruction

The original reconstruction of the bones was detailed enough to identify all the landmarks that are necessary to model the embedded coordinate systems and scaling parameters of the models.

For accurate implantation of the prosthesis and investigation of impingement (presented later in this thesis), there was a need for a higher definition of the glenoid and humeral head reconstruction (larger number of polygons).

The original cryo-section of the Visible human was retrieved, and a specialised software for reconstruction (AMIRA®, Visage Imaging™) was used in order to achieve maximum polygon resolution. For the reconstruction 1mm cryo-sections were used with a minimum density of 10 points digitisation/mm^2. The final result increased the number of digitised vertices from 923 to 27642 for scapula and from 907 to 5355 for humerus with the number of the triangle faces to rise from 3688 to 55280 for scapula and from 1810 to 21400 for the humerus (15 times more triangular surfaces –Figure 4.15)

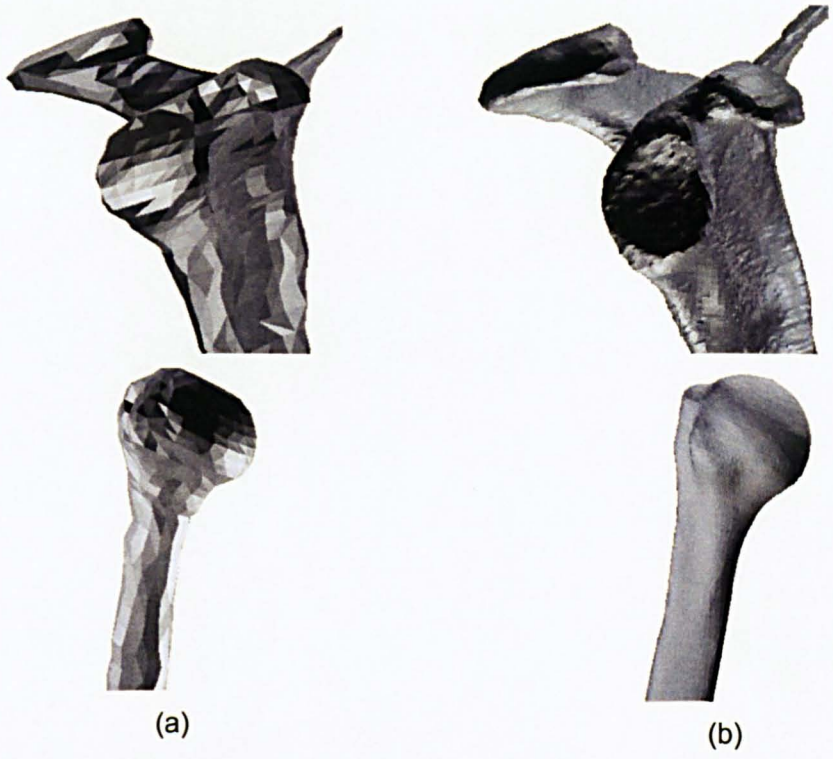

Figure 4.15: (a)Original scapula and humerus resolution, (b) high resolution scapula and humerus after AMIRA® reconstruction

4.3.2. Virtual implantation

In order to investigate the biomechanical properties of the reverse anatomy prosthesis, there is a need for an accurate and realistic representation of the geometry and the alignment of the prosthesis into the NSM.

There are clinical studies and a few biomechanical studies to suggest that positioning of the implant can significantly affect its performance and in general the functionality of the joint (Nyffeler et al. 2005,Simovitch et al. 2007). To address the issue of a realistic implantation, a standardised virtual surgical procedure has been followed, where the skeletal structure of the NSM will be adapted to describe a reverse anatomy joint replacement.

A set of 3-D models of the instrumentation tools as well the full set of the DELTA® III prosthesis was kindly provided by DePuy orthopaedics. All the 3-D virtual models are accurate representations of the real parts that are used by the surgeons. Two prosthesis sizes were used throughout the thesis: DELTA 36 and 42. The names of the different parts as well as their key dimensions are listed on Table 4.4.

Parts of DELTA® III reverse prosthesis	
part name: Metaglen sizes : one fixed size description: Glenoid fixation plate	
part name: Glenosphere, Cup description: GH articulation between the sphere (glenoid) and the cup (humerus) *Sizes:* DELTA 36: R=18mm, h=8mm DELTA 42: R=21mm, h=11mm	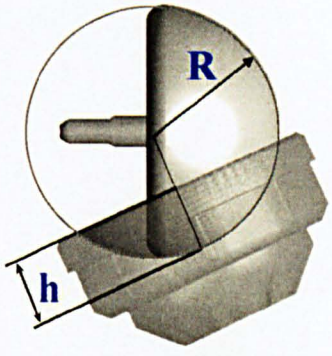
part name: Epiphysis description: proximal support of the cup (neck of the stem) neck/shaft angle β_2 = 115 deg (fixed for DELTA 42 and 36)	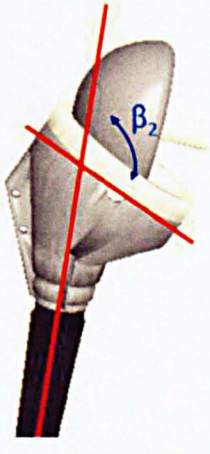

Table 4.4: The parts of the DELTA® III prosthesis and the dimensions of the different sizes (DELTA 36 and DELTA 42)

All the 3-D models of the instrumentation, prosthesis and the bones were converted to standard CAD data graphics format (DXF - Drawing Exchange Format) and loaded to a CAD software (AutoCAD®, Autodesk™) for graphics handling and manipulation.

4.3.2.1. Glenoid implantation

According to the standard description of the surgical procedures of the DELTA® III, the glenoid preparation starts with the marking of the 'Glenoid Centering Hole' and the insertion of the 2.5mm guide pin (Figure 4.16). This position is very critical for the fixation

of the prosthesis, since the guide pin also defines the glenoid ream and the fixation of the Metaglen and thus the Glenosphere on the glenoid. Some studies also suggest that this position can also affect the impingement problem of the reverse prosthesis (Nyffeler et al. 2005,Simovitch et al. 2007). Analytical positioning and other implantation parameters will be investigated in the next chapter of this thesis.

According to the surgical guidelines, the entry of the guide pin should be just posterior and inferior to the intersection of the major (supero/inferior) and minor (postero/anterior) glenoid axis (Figure 4.16). The pin position is identified either empirically by the surgeon (after marking the major and minor glenoid axis) or by the insertion of a marking guide which is fitted along the major axis of the glenoid

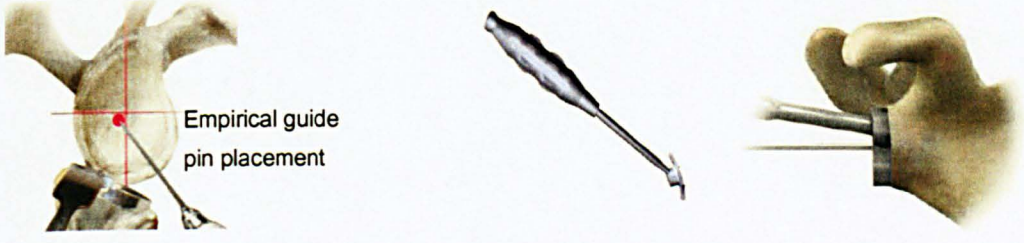

Figure 4.16: The position of the guide pin defines the fixation of the Metaglen and thus the Glenosphere.

Based on the guide pin, the glenoid resurfacing reamer trims away some of the glenoid bone (with a specific depth=3mm) and prepares a smooth surface for the Metaglen fixation. The Metaglen is fixed on the bone with four fixation screws from which the inferior and the superior are longer than the anterior and posterior. The inferior screw is fixed in a direction that follows the inferior scapula border where the superior is fixed in an apposing direction in order to resist the increased superior loading (Figure 4.17).

The placement of the Glenosphere is achieved with a central peg that secures a rigid fixation on the Metaglen.

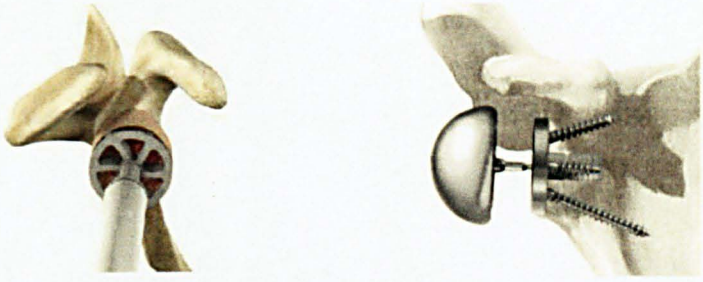

Figure 4.17: (a) Glenoid reaming is performed by a specialised instrument that defines reaming depth to 3mm (b) The Glenosphere is attached to the metaglen, which is also fixed to the glenoid by four fixation screws

The same implantation technique was also followed for the virtual implantation. The major and minor axis of the glenoid of the Visible Human scapula were defined and the marker guide was used to define the insertion point of the guide pin. The insertion point was found to be 0.6 mm posterior and 1.4mm inferior to the intersection of the major and minor glenoid axis. Interestingly, this point also found to match the position of the centre of the circle that fit the inferior half of the glenoid rim, as it is suggested in the surgical guidlines.

The application of the resurfacing glenoid reamer on the vector of the pin guide defined the depth and the shape of the new glenoid. The bone model had to be resurfaced with new polygons to describe the reamed glenoid surface and the increased number of triangle faces on the new high resolution scapula model secured a bone resurfacing that matched the reaming plane.

The fixation of the Metaglen and the Glenosphere on the new bone model was a simple alignment of the two along the direction of the pin guide and with the inferior fixation screw to follow the glenoid border (Figure 4.18)

From the graphical implantation of the sphere it was clear that only the large size Glenosphere (DELTA 42, R=21 mm) was overlapping the inferior border of the reamed glenoid, as it is suggested in the guidelines. Thus the large prosthesis size was considered as the primary fixation, even if the DELTA 36 was also simulated and presented in the biomechanical analysis of chapter 5.

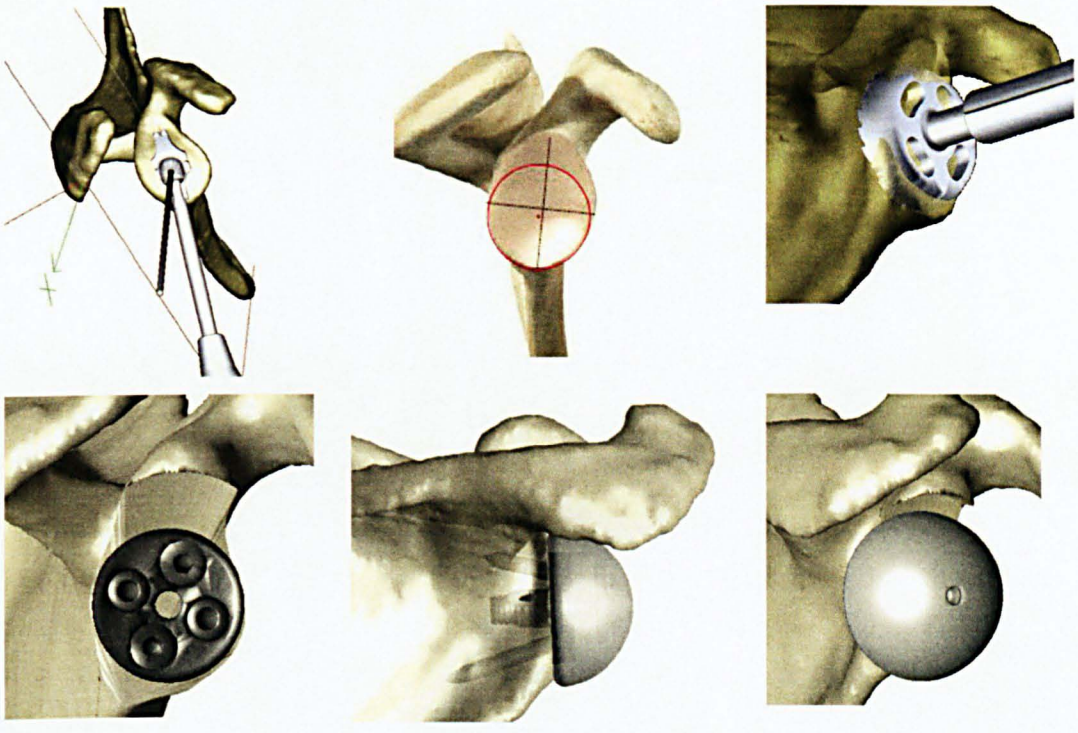

Figure 4.18: The virtual glenoid implantation to the model

4.3.2.2. Humeral implantation

For the humeral implantation there are two different surgical approaches: i) the Superior-Lateral approach, where the middle Deltoid is split to unveil the humeral head ii) Delto-pectoral approach, where the humeral head is exposed through a split of the anterior deltoid and the pectoralis major (clavicular). There is a different assembly set-up of the humeral cutting tool for each of the approaches. For the virtual implantation the Delto-pectoral approach was followed and is described below.

According to the surgical guidelines, a drill/guide is inserted from the top of the humeral head to identify the humeral canal. This provides an alignment for the placement of the humeral head cutting tool, which is placed also along the humeral canal. The cutting tool provides the resection plane of the humeral head which is 65 degrees with respect to the long humeral axis (Figure 4.19b).

The version of the resection needs also to be defined before the cut. The humeral head of a normal shoulder is retroverted around the humeral superior axis Y_h (Figure 4.19a) by an angle that is usually varying from 16 - 20 deg (Inman et al. 1944). According to the surgical guidelines a neutral (0 deg) humeral resection is advised, even if there is a choice of adjustment (of the version) with a guiding pin on the cutting tool

(Figure 4.19b,c). The effect of the retroversion on the biomechanics of the reverse prosthesis will be explained in chapter 5.

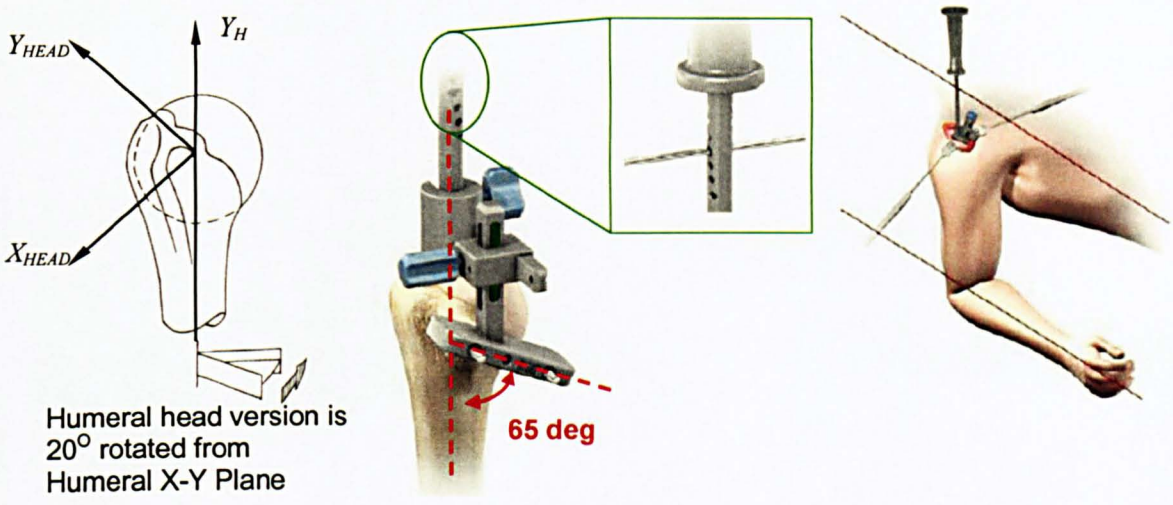

(a)
The anatomical humeral head version is 20 deg rotated from Humeral X-Y Plane

(b)
The cutting tool defines the resection plane on 65 deg in respect to the long axis. The version of the resection is adjusted by a pin on the cutting tool

(c)
The pin guide of the cutting tool is aligned with the forearm, in order to provide the version of the resection

Figure 4.19: Version of the humeral head resection

For the final fixation of the implant the stem is following the humeral canal and the alignment of the neck of the prosthesis (Epiphysis) is following the alignment of the resection plane. The depth of the stem is defined by the 'Proximal Humeral Reaming' tool (Figure 4.20).

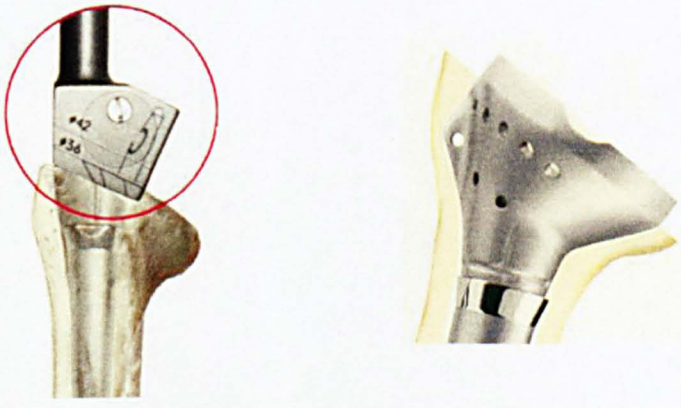

Figure 4.20: The stem of the prosthesis is fixed along the humeral canal in a depth that is defined by the humeral reamer while the alignment of the Epiphysis follows the alignment of the resection plane.

For the virtual implantation only the 3-D model of the humeral cutting tool was used to define the plane of the resection and the alignment of the fixation of the prosthesis. However, in order to guide the cutting tool and later the stem of the prosthesis into the correct palce, the axis of the humeral canal had to be defined from the original Visible human cryo-sections.

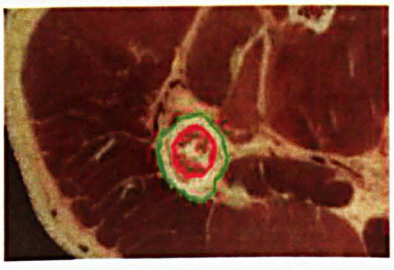

Figure 4.21:

The humeral canal was also reconstructed from the original Visible Human cryo-sections

As expected the axis of the humeral canal was found to be offset laterally in comparison to the superior Y axis of the embedded humeral coordinate system. The humeral cutting tool was assembled for a Delto-pectoral approach and its long axis was aligned with the axis of the humeral canal. Neutral version (0deg) was chosen for the resection plane as advised in the surgical guidelines (Figure 4.21).

The reconstruction of the triangle faces of the bone model (after the resection) was performed in AutoCAD and the placement of the assembled implant (stem and epiphysis) followed the alignment of the resection plane. There was no need to use the humeral reamer to define the depth of the stem fixation, since it was easier to define (according to DePuy's technical drawings) a 6mm spacer for the epiphysis above the plane of the resection (Figure 4.22)

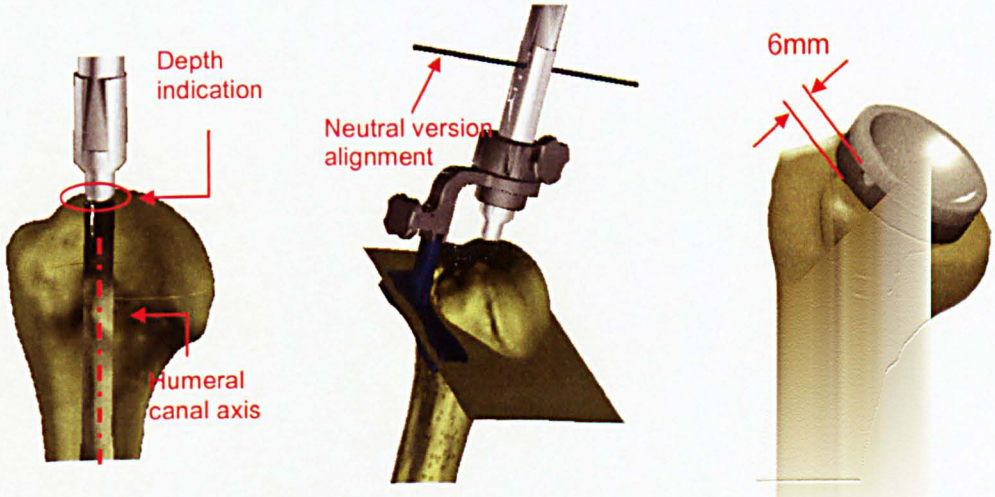

Figure 4.22:Only the humeral cutting tool was needed for the virtual implantation of the stem and neck of the prosthesis, after defining the humeral canal axis

4.3.2.3. Definitions of the new humerus and implant frames.

As described above, the embedded coordinate frame of the humerus uses the landmarks of lateral and medial epicondyles and the GH centre of rotation. Even if the latter point (GH) is not a palpable landmark, van der Helm (1996) and Veeger (2000) showed that it is the centre of the sphere that fits the humeral head, while other studies have developed techniques to estimate the GH through functional movements or from other anatomical landmarks (Murray & Johnson 1999,Veeger 2000).

The reverse anatomy prosthesis changes the kinematics of the GH joint. The rotational centre is not based on the humerus, but is the centre of the glenoid sphere. Thus one of the kinematics constraints of the new joint is that the centre of the cup and the centre of the glenoid sphere have to be coincident.

After the joint replacement the humeral head is removed and it cannot be used to define the embedded coordinate frame like in the normal shoulder. However it makes sense to define the new humerus frame by using the new centre of rotation, since it can be calculated with the same techniques that were used to calculate the rotation centre in normal shoulders (e.g helical axis method, Veeger, 2000).

Before the humerus, the frame of the cup of the implant can be easily calculated, by defining superior axis (Yc) of the frame the vector that is normal to the face of the cup and crosses the new GH centre (Figure 4.23). The kinematic constraint of the new joint (where the cup and the sphere centres coincide) means that the new GH is always located in the Yc axis in a distance equal to the radius of the glenoid sphere.

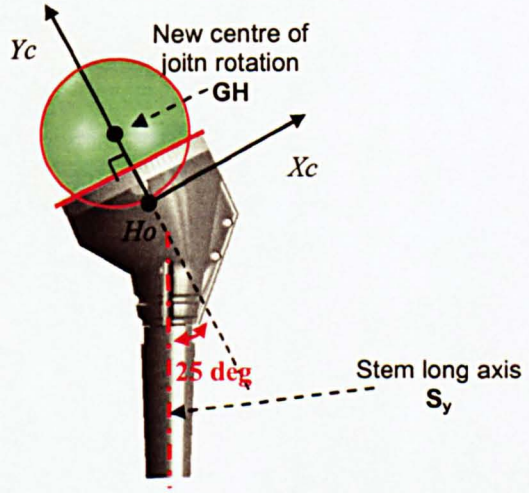

$$\overline{Yc} = \frac{\overline{GH} - \overline{Ho}}{|\overline{GH} - \overline{Ho}|}$$

$$\overline{Xc} = \frac{\overline{Sy} - \overline{Yc}}{|\overline{Sy} - \overline{Yc}|}$$

$$\overline{Zc} = \overline{Xc} \times \overline{Yc}$$

Origin Ho

Figure 4.23: Definition of the Cup embendded coordinate system. The Y axis always crosses the centre of rotation (glenoid sphere) at the same point

As in the definitions for the normal anatomy the embedded coordinate system for the humerus can be defined by the palpable landmarks of lateral and medial epicondyles and the new GH joint rotation (Figure 4.24)

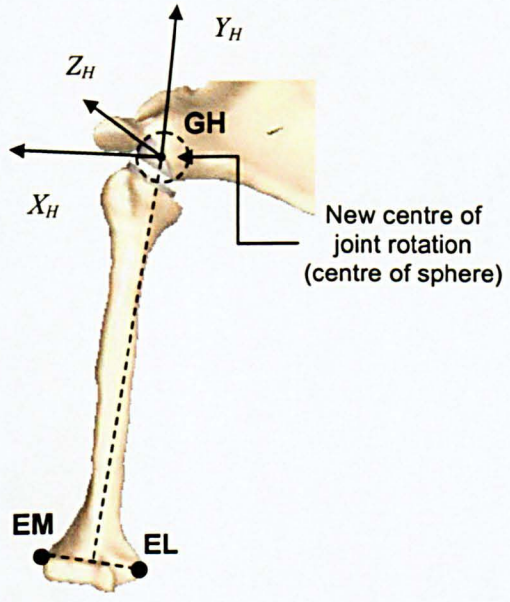

$$\bar{Y}_H = \frac{\overline{GH} - \left(\overline{EM} + \overline{EL}\right)/2}{\left|\overline{GH} - \left(\overline{EM} + \overline{EL}\right)/2\right|}$$

$$\bar{Z}_H = \frac{\bar{Y}_H \times \left(\overline{EM} - \overline{EL}\right)}{\left|\bar{Y}_H \times \left(\overline{EM} - \overline{EL}\right)\right|}$$

$$\bar{X}_H = \bar{Y}_H \times \bar{Z}_H$$

Figure 4.24: The humeral embedded coordinate system in the reverse prosthesis

As mentioned before, all the coordinate frames are based on bony landmarks and are based on the recommendations of the International Shoulder Group. All these frames approximate anatomical planes of the bones (frontal, transverse and sagital) and in the literature they are often referred to as anatomical embedded coordinate frames.

In the case of the new reverse humeral coordinate frame the superior axis (Y_H) deviates slightly from the long anatomical axis of the humerus. However, because of the well defined geometry, a second humeral frame can be defined, which can be based on the origin of the implant frame *Ho* (Figure 4.23) and the axis that connects the *Ho* with the epicondyles centre. This axis approximates closely to the humeral anatomical axis (humeral canal) and is fixed in respect to the new reverse humeral frame described in Figure 4.24.

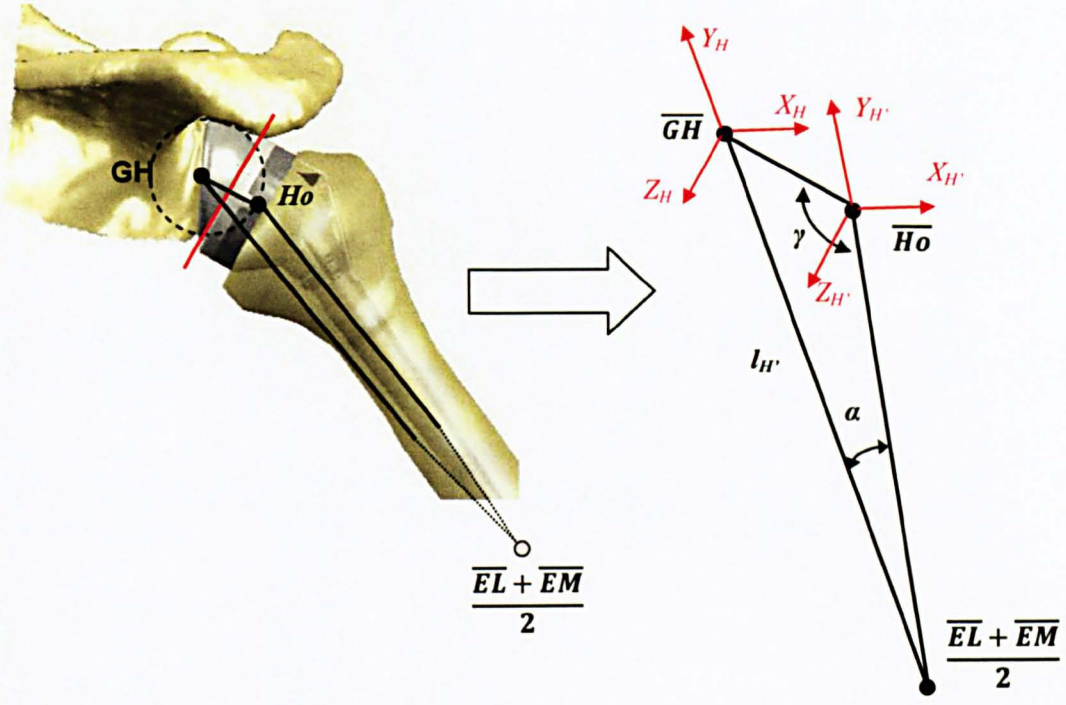

Where:

GH, Ho, $\overline{EL}+\overline{EM}/_2$ are the new centre of rotation, the origin of the implant frame and the centre of the epicondyles

$l_{H'}$ = the distance from the centre of the epicondyles to the new GH centre

γ = the angle of the neck of the prosthesis with the stem

α = the correction angle between the 2 humeral frames

Figure 4.25: Correction angle for the alignment of the humeral frame with the real long anatomical axis of the humerus.

From the above Figure 4.25 the vectors of the centre of the epicondyles and of the GH, as well as the angle of the implant neck γ, are known quantities.

Based on the law of sines the correction angle α between the two frames is:

$$\frac{sin\alpha}{\left|\overline{Ho}-\overline{GH}\right|}=\frac{sin\gamma}{\left|\left(\overline{EL}+\overline{EM}/_2\right)-\overline{GH}\right|} \qquad \textit{eq. 4-2}$$

Where:

$\left|\overline{Ho}-\overline{GH}\right|=R$ is the radius of the glenoid sphere

$\left|\left(\overline{EL}+\overline{EM}/_2\right)-\overline{GH}\right|=l_{h'}$ is the distance from the centre of the epicondyles to the new centre of rotation

From the equation 4-1, the correction angle α for the humeral superior axis is:

$$a=\arcsin\left(\frac{R}{l_{h'}}*sin\gamma\right) \qquad \textit{eq. 4-3}$$

From the above equation it becomes clear that the correction angle is very small; for the geometry of the Visible Human ($l_{H'}$ = 0.34m) and the DELTA III design (R=0.021m, γ=155 deg) the correction is: α = 1.34 deg.

For this study the definition of the second humeral frame was important as the accurate analysis of the contact forces into the joint was necessary for the dynamic constraints of the model (joint stability). However, for a kinematics study where only the humero-thoracic angle decomposition is necessary, the simplified (first) humeral frame can be used.

4.3.2.4. Definition of distal humeral frame for elbow kinematics

The definition of the coordinate frames according to the ISB standards (anatomical frames) creates a problem with the calculation of the elbow flexion extension.

In general the relative orientation of the anatomical frames of the proximal and distal segment can be only indicative of the actual joint rotations because the anatomical axes forming these frames are generally only a rough approximation of the real joint axes of rotations. The consequence of the approximation is that joint kinematics can be affected by kinematic cross-talk (Piazza and Cavanagh, 2000).

This is clear at the elbow joint where the anatomical humeral and forearm frames (by definition) are misaligned, due to the elbow carrying angle. Thus, a simple flexion of the simple hinge elbow joint results in three angle decomposition, instead of just a simple rotation around one axis.

Recommendations of a distal humeral frame, based on functional frame definitions (Cutti et. al., 2008) have been proposed recently in order to overcome the problem (Kontaxis et. al., 2008).

Following the study of Cutti *et. al.* (2008) a distal humeral frame can be defined based on the flexion extension axis V_f, and the superior axis of the anatomical humeral frame (Y_H) (Figure 4.26).

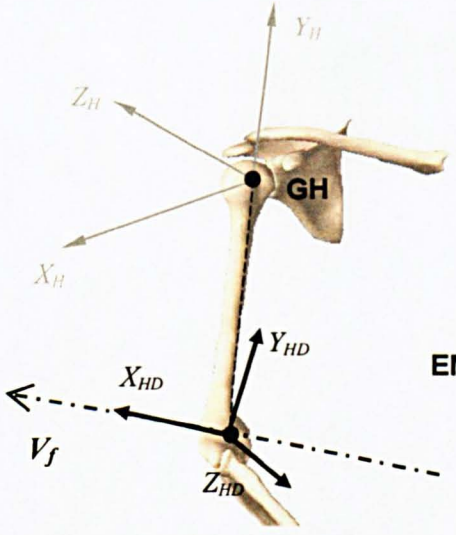

$$\overline{X_{HD}} = \frac{\overline{V_f}}{|V_f|}$$

$$\overline{Z_{HD}} = \overline{X_{HD}} \times \overline{Y_H}$$

$$\overline{Y_{HD}} = \overline{X_{HD}} \times \overline{Z_{HD}}$$

Figure 4.26: Definition of the distal humeral (HD) embedded coordinate system

4.3.3. Model input optimisation – Scapula and clavicle kinematics

The kinematics of the scapula and clavicle for the original NSM are derived from two sets of regression models that predict scapula and clavicle rotations as an input of the humerus position. Both regression models derived from a moderate sized population (10) and describe all three rotations of the scapula (retraction/protraction, lateral rotation, backward tip - Barnet, 1996) and clavicle (retraction/protraction, elevation/depression and axial rotation - Marchese, 2000). However, both models have been only validated for normal (asymptomatic) shoulders.

The shoulder is a closed chain mechanism in which the humeral head is positioned by a closed chain formed by thorax, scapula and clavicle (Veeger and van der Helm, 2006). Based on the latter assumption, Charlton developed an algorithm for the NSM in order to optimise the scapula and clavicle position (as calculated by the regression models) and maintain a closed chain mechanism on the shoulder girdle (Model Input

Optimisation – MIO). A similar algorithm of closed chain mechanism was first proposed by Pronk et. al. (1993) and further developed by de Groot (1998) and used in the Dutch and the Swedish shoulder model.

In this study it was assumed that scapula rhythm in reverse joint replacement subjects may present different kinematic patterns from the normal shoulders. Thus scapula kinematics were measured (and analysed later in chapter 6) and individual regression equations were formulated for each individual subject and integrated to the model. In addition, clavicle kinematics was also assumed to be different, but even if tracking the elevation/depression and the retraction/protraction of the clavicle is relatively easy (by tracking the position of the AC joint), measuring the clavicle axial rotation is very challenging and special equipment is needed (Marchese, 2000, Ludewig, P.M. 2000).

As a result the MIO had to be slightly changed compared to the original algorithm of Charlton (2003) where clavicle position is calculated by the regression equations of Marchese (2000): The first estimation of the clavicle position is based on the position of the AC joint (where only the elevation/depression and the retraction/protraction of the clavicle can be calculated) and then the axial rotation can be derived by the minimisation of the rotation on the ac joint between scapula and clavicle. This method follows the original optimisation algorithm that was proposed by de Groot, where the rigid conoid ligament minimises the rotations at the AC joint.

The algorithm involves the minimisation of the sum of square errors between the predicted (scapula angles from regression model – clavicle angles from AC position) and the constrained angles. The constraints imposed on the optimisation are contact between the landmarks of AI and AS of the scapula on the scapulothoracic gliding plane (STGP) maintaining a maximum conoid ligament length that is calculated in the resting position (Charlton, 2003).

Mathematically, this is represented as:

Minimise: $$J = \sum_{\theta} \left(\theta - \hat{\theta}\right)^2 \qquad \textit{eq. 4-4}$$

with: $\theta = \alpha_C, \beta_C, \gamma_C$, elev./depress., retrac./protract., axial rotation of clavicle

$\theta = \alpha_S, \beta_S, \gamma_S$ backward tip, retrac./protract., lateral rotation of scapula

subject to: $\left|\overline{AS} - \overline{AS}_{ELLIPSOID}\right| \leq 1 \cdot 10^{-6}$ *eq. 4-5*

$\left|\overline{AI} - \overline{AI}_{ELLIPSOID}\right| \leq 1 \cdot 10^{-6}$ *eq. 4-6*

and: $\left|\overline{CON}_{SCAPULA} - \overline{CON}_{CLAVICLE}\right| - L_{CONOID} \leq 1 \cdot 10^{-6}$ *eq. 4-7*

Where:

$\overline{CON}$ is the conoid ligament attachment site

L_{CONOID} is the measured rest length of the conoid ligament. This length is calculated by performing the model input optimisation with the humerus in rest position

$\overline{AS}_{ELLIPSOID}$, $\overline{AI}_{ELLIPSOID}$, the normal projection of the AS and AI landmarks to the ellipsoid that describes the STGP

4.3.4. Force constraints at the GH joint

Most of the joints of the upper limb only have a limited region of stability due to the shape of their articular surface. All of the joint contact forces modelled are considered to pass through the joint rotation centre and, if stability is to be maintained, the proximal and distal articulating surfaces.

In the normal shoulder the glenoid covers roughly one third of the articular surface of the humeral head and provides only limited range for the direction of the GH contact force. The technique for constraining the GH force vector was first proposed by van der Helm (1994a) and similarly in the MSN the GH contact force vector is constrained to pass inside an ellipse that is approximately describing the glenoid surface (Charlton, 2003).

For the reverse prosthesis model, stability of the GH joint is satisfied when the vector of the GH force is constrained within the rim of the polyethylene cup. Considering that contact force is crossing the centre of the glenoid sphere, then the angle φ_{GH} between the force and the superior axis Yc of the cup frame should be smaller than the maximum angle φ_{cup} between the axis Yc and the rim of the cup (Figure 4.27]

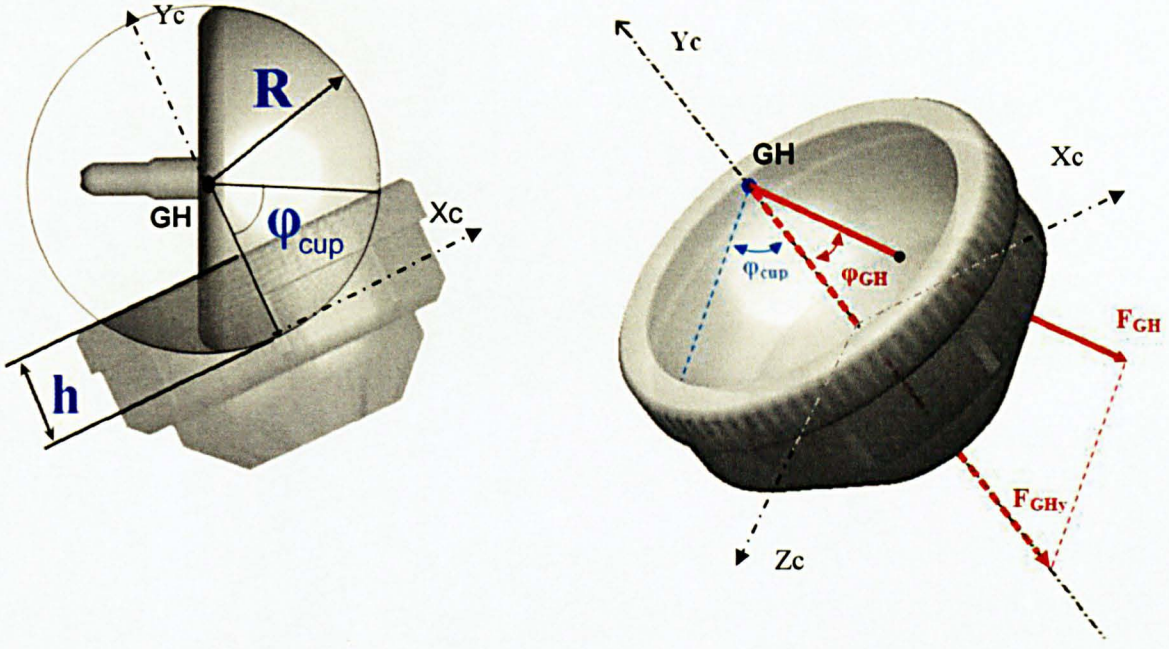

Figure 4.27: GH joint stability is maintained when the vector of the contact force is crossing the articulating surface of the polyethylene cup

By expressing the GH contact force into the cup frame the angle φ_{GH} can be defined:

$$\varphi_{GH} = \arcsin\left(\frac{\left|{}^{cup}\bar{F}_{GH}\right|}{\left|{}^{cup}\bar{F}_{GH_Y}\right|}\right) = \arcsin\left(\frac{\sqrt{\left({}^{cup}F_{GH_X}\right)^2 + \left({}^{cup}F_{GH_Y}\right)^2 + \left({}^{cup}F_{GH_Z}\right)^2}}{{}^{cup}F_{GH_Y}}\right) \quad \textit{eq. 4-8}$$

Where :

${}^{cup}\bar{F}_{GH}$ is the GH contact force vector expressed in the cup frame

${}^{cup}F_{GH_X}$ and ${}^{cup}F_{GH_Z}$ are the shear components of the GH force in the cup frame

${}^{cup}F_{GH_Y}$ is the compressive component of the GH contact force in the cup frame

Thus the constraint equation can be written as:

$$\varphi_{GH} \leq \varphi_{cup} \quad \textit{eq. 4-9}$$

Where the φ_{cup} is a function of the radius ***R*** (of the glenoid sphere) and cup depth ***h*** (Figure 4.27), as it will be shown more analytically in the next chapter (where the biomechanics of the reverse design is analysed in depth).

4.3.5. Contact detection algorithm

As mentioned before, one of the common problems that is often reported on most of the clinical reviews of the reverse prosthesis, is the impingement problem and the creation of notches at the inferior scapula border and the polyethylene cup.

The notch creation is believed to be a result of many factors, but the contact of the polyethylene cup with scapula is considered to be one of the main mechanisms of the bone notching. Based on this assumption an extra algorithm was developed in NSM in order to detect any possible contact of the scapula bone with the prosthesis (contact detection algorithm).

4.3.5.1. Format of the files of the 3-D models

As described above, all the 3-D models that are used in the NSM (bones models and all parts of the prosthesis), are described by small triangular surfaces. Each of these triangular surfaces is defined by three points in the space that are connected to each other.

There is a specific format of the 3-D surface files that are used in SIMM and in general by any CAD software. The files are in ASCII (text) format that contain large matrixes that include information about the coordinates of each point and the order in which they are interconnected in order to build the surfaces (Figure 4.28).

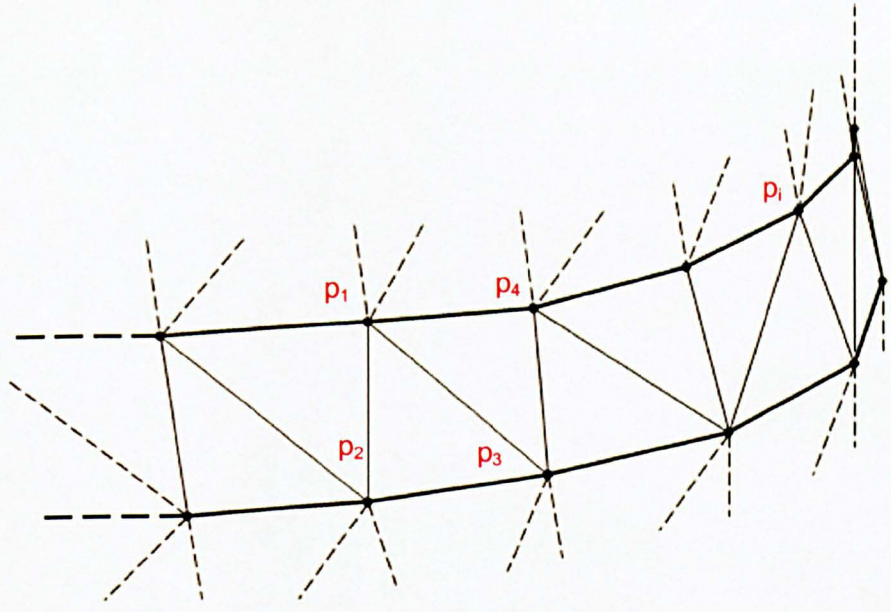

Description of 3-D surface files

Matrix of points

Point No	*Coordinates*		
1st (p_1)	x_1	y_1	z_1
2nd (p_2)	x_2	y_2	z_2
3rd (p_3)	x_3	y_3	z_3
4th (p_4)	x_4	y_4	z_4
.			
.			
.			
ith (p_i)	x_i	y_i	z_i
.			

Matrix of surface reconstruction

Surface No	*no of points/surface*	*surface registration*
1	3	1,2,3
2	3	1,3,4
.		
.		
.		
ith	3	(i-1),(i),(i+1)
.		

Figure 4.28: The structure of the 3-D files that describe the bone models and the parts of the prosthesis.

4.3.5.2. Contact detection

The contact detection algorithm is based on finding all the points that their coordinates are penetrating the cup. First, a custom made routine was developed to extract all the coordinates of the points of the scapula bone. All these coordinates are

originally described in the embedded coordinate frame of the scapula and were stored in a matrix (${}^{S}P$ matrix of coordinates of the points in scapula frame).

For every single frame of any motion, the relative position of the scapula on the humeral frame (${}^{H}_{S}R$) is calculated by the NSM. First, this transformation was applied to all the points of the scapula matrix and then the points were transformed to the frame of the cup (for each frame of the motion):

$$ {}^{cup}P = {}^{cup}_{H}R * {}^{H}_{S}R * {}^{S}P \qquad \textit{eq. 4-10} $$

Where:

${}^{cup}P$ is the matrix that contains all the coordinates of the points of the scapula in the cup frame

${}^{cup}_{H}R$ is the fixed transformation of the humeral frame to the cup frame (defined by the neck/shaft angle of the prosthesis)

Knowing all the points of the scapula in the cup frame, the points of interest can be detected by checking the coordinates to satisfy the geometrical boundaries of the cup (Figure 4.29)

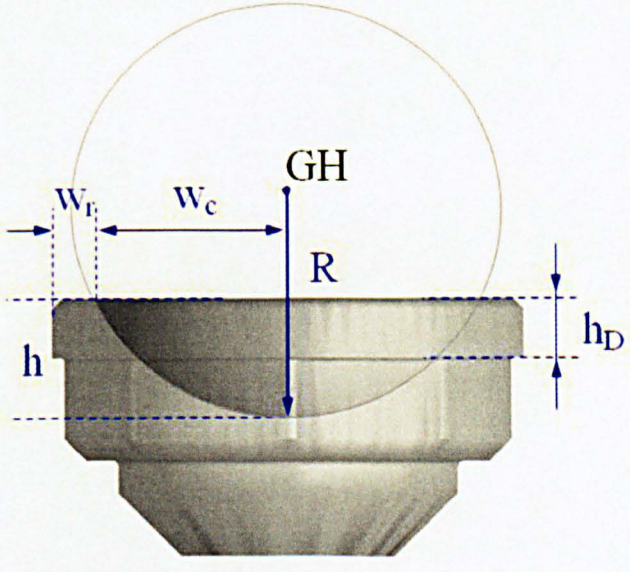

Figure 4.29: Geometrical characteristics of the cup

The algorithm can detect all the coordinates of the points in the matrix such as:

$$h_D \leq y \leq h \qquad \textit{eq. 4-11}$$

$$x^2 + z^2 \leq (w_c + w_r)^2 \qquad \textit{eq. 4-12}$$

$$x^2 + y^2 + z^2 \geq R^2 \qquad \textit{eq. 4-13}$$

Where:

h is the depth of the cup

h_D is the depth of the cup rim

w_c is the cup width which is a function of the radius R of the sphere and the cup depth: $w_c = \sqrt{R^2 - (R - h)^2}$

w_r is the width of the cup rim

The identified points then can be registered in the cup frame, in order to mark their trace on the cup. The same points can be transformed back to the original scapula frame and be excluded from the original 3-D model. The bone model can then be rebuilt excluding all the triangle faces simulating a notch (Figure 4.30).

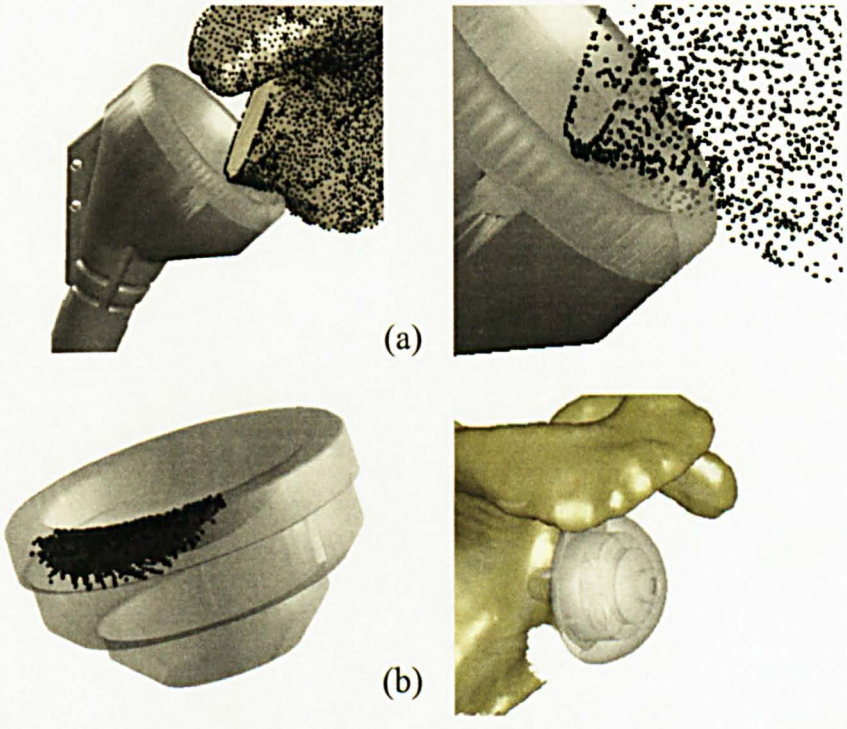

Figure 4.30: (a) The contact detection algorithm registers any point that penetrates the cup in every frame of a motion (b) sum of contact traces after a completed motion

Chapter 5. Understanding the Biomechanics of a Reverse Anatomical Design. Preliminary results[2]

5.1. Introduction

Many prostheses are used to address many different shoulder pathologies and the designs vary in shape and dimensions and in some cases try to address stability issues by fully constraining the joint (Brostrom et al. 1992,Post et al. 1980). As has been indicated in previous chapters, reverse anatomy prostheses are introduced as a solution in challenging pathologies such as an arthritic shoulder with massive rotator cuff (RC) tears (Kessel & Bayley 1979).

The DELTA® prosthesis (produced by DePuy) has been extensively used in RC tear arthropathies. There are many clinical reviews reporting stability and good performance of this design (Sirveaux et al. 2004,Woodruff et al. 2003), but also indicating problems of impingement and glenoid loosening after long term use (Nyffeler et al. 2004). There are now a number of competing prostheses in the United States (e.g. from Encore, and Zimmer) and in Europe (e.g. Lima, Aston, Tornier, Implants Industrie) following the same basic design but with modifications intended to address the above problems.

Despite the long-term use and the popularity of the Grammont type prosthesis, there are only few two dimensional (De Wilde et al. 2004) or three dimensional biomechanical studies (Terrier et al. 2008,Van der Helm F.C. 1998) focusing either on muscle and joint contact analysis or impingement (Nyffeler et al. 2005) without examining how different aspects of the reverse designs can affect the general joint performance.

The aim of this chapter is to analyse in depth the biomechanical properties of the DELTA® (and, in general, the reverse) design using the prosthetic biomechanical model that was described in Chapter 4.

One of the principal difficulties in the development and validation of musculoskeletal models is in obtaining direct *in-vivo* measurements of the forces in muscles, tendons and joints. The first verification studies of musculoskeletal models have been made in the area of gait analysis in measured hip contact force data with the development of an instrumented hip prosthesis (Graichen et al. 1999,Graichen & Bergmann 1991). Instrumented hip joint replacement devices have been used in a number of studies to

[2] Most of the material of this chapter is published in the Journal of Clinical Biomechanics, 2009, March; 24(3): 254-60, "The biomechanics of reverse anatomy shoulder replacement--a modelling study." Extra material has been added for better understanding of the biomechanics of the reverse prosthesis

examine hip contact forces in walking and running (Bergmann et al. 1993), load carrying (Bergmann et al. 1997), routine daily activities (Bergmann et al. 2001) and stair climbing (Heller et al. 2001).

Unfortunately, experimental validation for shoulder models is still limited. The first instrumented shoulder prosthesis was developed at the Free University of Berlin and the prosthesis uses a normal anatomy design (Biomet anatomical (Westerhoff et al. 2009). There are some initial data sets published for GH loading for a preliminary validation of shoulder biomechanical models, but those sets represent only a small overall set of shoulder tasks and, as a result, only a limited range of loading. In addition, the data are valid only for normal anatomy shoulder replacements. Attempts to compare normal anatomy joint contact loads with predictions of reverse anatomical models can be inaccurate, since the reverse design can change the direction of GH forces, as discussed later in this chapter. Comparison of output variables between different reverse prosthetic biomechanical shoulder models and an investigation of the internal consistency and sensitivity of the models is a most reasonable validation for this study.

The comparison of the results of this chapter will lead to a discussion of the relative importance of reverse designs and their use compared to normal anatomy designs. In addition, in the final section of this chapter different implantation techniques and design features of reverse prostheses will be tested based on information from the literature and the shoulder prosthetic market in order to understand how different designs can affect the loading, stability and impingement of the prosthetic joint.

The aim of understanding the biomechanics of the reverse designs will be achieved by comparing modelling data between the reverse and normal anatomy shoulder model on the following aspects:

- Lengthening and moment arms of deltoid and RC muscles;
- Predicted muscle and joint contact forces during standardised activities;
- Range of arm motion with reverse shoulder and restrictions due to impingement.

5.2. *Model set-up*

In order to enhance comparability of the results between the normal anatomy model and the reverse prosthetic model, the same conditions and inputs were applied in both models.

5.1.1. Skeletal structure and shoulder girdle kinematics

No scaling factors were applied to any of the normal or prosthetic models and so the bone sizing follows the Visible Human data-set. The modifications and the virtual

implantation of the prosthetic model were described in Chapter 4. Like most of the prosthetic designs, DELTA® III provides a range of sizes in order to match the size of the skeletal structure. As described in the virtual implantation in Chapter 4, and by the surgical guidelines, the large size sphere (Rsphere=21mm) was chosen as the primary fixation. For this fixation ('standard fixation') the rim of the sphere is overlapping the inferior reamed glenoid surface. The smaller size prosthesis, where the Rsphere=18mm was also tested in order to investigate the effect of the size on the performance of the joint

It has been observed that shoulder arthropathies and joint replacements can compromise the kinematics of the scapula (Kontaxis & Johnson 2008,Mell et al. 2005) and the clavicle (Ludewig & Cook 2000). This kinematic adaptation can affect loading, stability and impingement patterns of the shoulder joint and in Chapter 6 analytical scapula kinematics data for subjects with DELTA® reverse shoulders are provided. However, for this chapter and for comparability issues with a normal shoulder both scapula and clavicle kinematics are following the normal rhythm in both the normal and reverse prosthetic models, as they were described by Barnett et al. (1999) and Marchese and Johnson (2000) and used in the original NSM (Charlton & Johnson 2006).

5.2.1. Muscle set-ups of the model

The clinical indication for the use of the reverse prosthesis is a large irreparable RC tear (Boileau et al. 2005,Grammont & Baulot 1993). In this condition the supraspinatus, infraspinatus and subscapularis muscles are not present (Full Thickness Tear – FTT). In the model, excluding the corresponding muscle lines of action simulated this RC tear.

Because information is lacking regarding the natural progression of RC tears (Ecklund et al. 2007,Jensen et al. 1999), it is possible for the infraspinatus or subscapularis muscle to be present in an irreparable RC tear, which will lead to the implantation of a reverse joint replacement. In order to investigate the effect of any remaining RC muscle, more types of tears were simulated:

- Supero-Anterior Tear (SAT – infraspinatus only present);
- Supero-Posterior Tear (SPT – subscapularis only present);
- Partial Superior Tear (PST – infraspinatus and subscapularis present).

5.2.2. Kinematic inputs (arm motion):

A set of standard activities were simulated for the dynamic and impingement predictions:

i) abduction (arm elevation in coronal plane);
ii) forward flexion (arm elevation in sagittal plane);
iii) arm elevation in scapular plane.

The activities describe arm elevation from 0 to 150 deg. The simulations were performed with both normal and reverse prosthetic anatomy at a low constant speed so that inertial effects could be considered to be negligible (quasi-static solution).

5.3. *Muscle lengthening and moment arm after reverse joint replacement*

After the DELTA® III replacement, the humerus (and, as a result, the whole arm) is positioned more medially and inferiorly compared with the normal shoulder, which can even be observed visually in real subjects (Figure 5.2,b) (Boileau et al. 2005). Measuring virtual bony landmarks on the scapula (AC) and on the humerus (under the Great tubercle) this extension, for the resting position (0 deg. of Abduction), was found to be (Figure 5.1):

Inferior displacement: $\Delta Y = \Delta Y_{DELTA} - \Delta Y_{normal} = 50.4mm - 26.3mm = 24.1mm$
Medial displacement: $\Delta X = \Delta X_{DELTA} - \Delta X_{normal} = 6.3mm - 18.8mm = 12.5mm$

Where: $\Delta Y_{DELTA,normal}$ *and* $\Delta X_{DELTA,normal}$ are the inferior and medial distances of the bony landmarks as they were measured in the thoracical frame, as shown in Figure 5.2.

These values express the length change of the upper arm (distance of from AC to elbow joint). The lengthening of the middle deltoid is 17.7% and 21.6% for size 36 and 42 ('standard fixation') respectively compared to normal anatomy (Figure 5.1). As a result of this extension the deltoid muscle, that encompasses the prosthetic joint, is significantly stretched giving a passive tension to the GH joint. In a DELTA® III biomechanical study, DeWilde *et al.* (2004) report slightly smaller but comparable deltoid extension numbers for both prosthetic sizes (36 and 42).

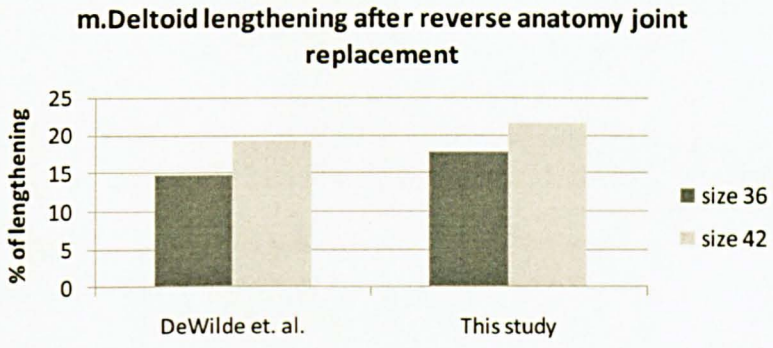

Figure 5.1:

Lengthening of the m.Deltoid after reverse anatomy joint replacement compared to DeWilde et al., (2004)

The lengthening of the deltoid muscle is rather large, especially when considering that deltoid extension of more than 20% can damage the axillary nerve (Grant et al. 1999) and paralyse the muscle. There is an additional problem resulting from the large inferior displacement of the humerus in that it creates a large space between the resected humeral head and the acromion, which increases the likelihood of infection. Clinical reviews of large series of reverse prostheses report infection as one of the most common complications after a reverse joint replacement (Wall B.T. & Walch G. 2008).

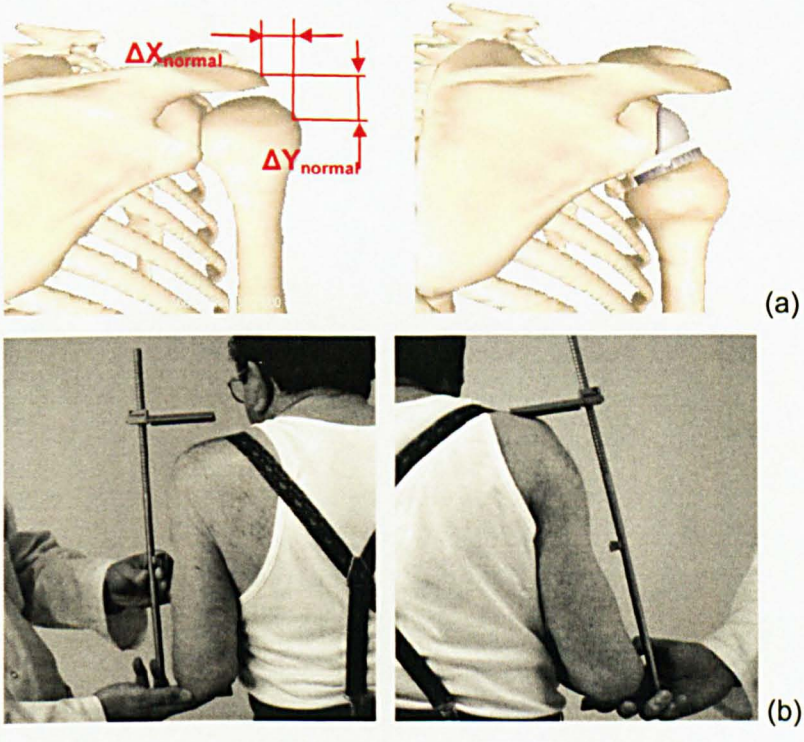

Figure 5.2: After a reverse joint replacement (DELTA III), the humerus is shifted medially and inferiorly (a) increasing the overall arm length on the operative side (b) (Adapted from Boileau et al., 2005)

The lengths of m.Teres minor, m.Infraspinatus and m.Subscapularis (if they are present after the joint replacement) are also affected by the prosthetic geometry. For the resting position the model shows that the medialisation of the arm has a shortening effect on these muscles, which means that in reality they can be subluxed. The shortening values are 16.5% and 15.5% for the m.Infraspinatus and m.Subscapularis respectively and 27.0% and 19.3% for the m.Teres minor and m.Teres major respectively. It should be noted that during high arm elevation eventually the muscles are extended to the same levels as the normal anatomy.

The lengths of the remaining two prime muscles of the shoulder (m.Latissimus dorsi and m.Pectoralis) are also affected by the prosthetic joint, yet by a lesser degree. For the resting position the m.Latissimus dorsi is 9% shorter where m.Pectoralis is shorter by an average of 6% (5% shorter for the thoracical fibres and 7% for the clavicular fibres).

5.3.1. Muscle moment arms

One of the most interesting results of the reverse prosthetic design of DELTA® III is how it affects the moment arms (and, thus, the functions) of the muscles crossing the GH joint, especially the deltoid. In the prosthetic joint the arm is rotating around the centre of the sphere, which is now attached to the scapula, in contrast with the centre of rotation of the normal shoulder where the rotational point is the centre of the humeral head. As a result moment arms of the muscles crossing the GH joint are greatly affected.

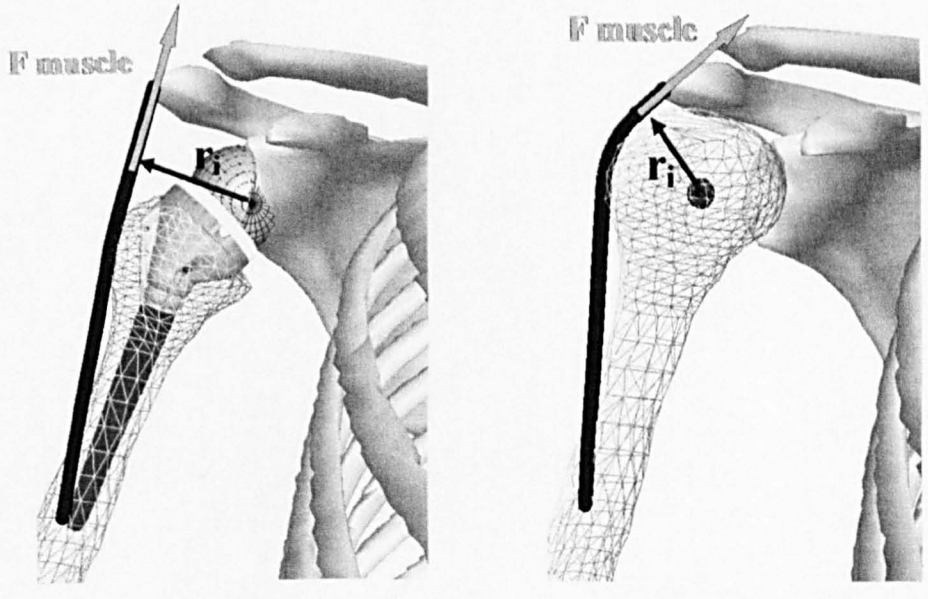

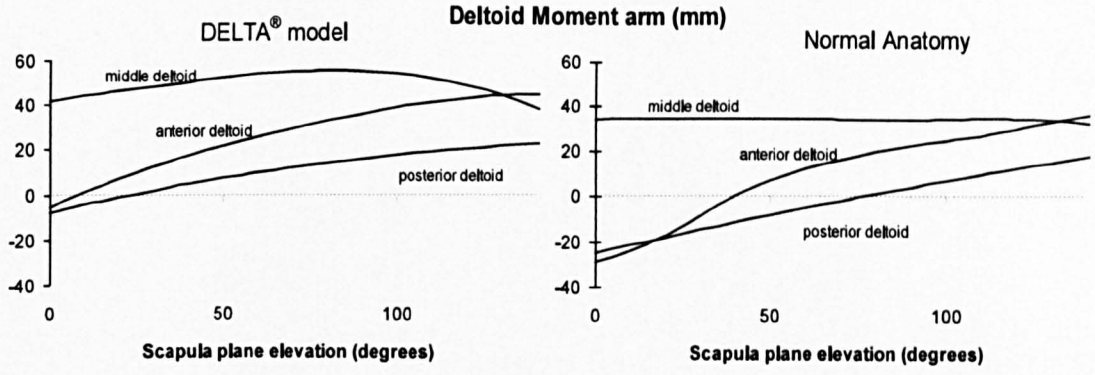

Figure 5.3: The DELTA® III geometry changes the centre of rotation of the GH joint and significantly affects the deltoid moment arm compared to the normal anatomy. In the latter the middle deltoid moment arm has almost constant value, whereas with the prosthetic geometry it has a much greater fluctuation (peak value around 90 deg. of abduction - Scapula Plane elevation).

One of the most affected muscles is the deltoid, which exhibits moment arm increases with the DELTA® III geometry that peak at an average value of 54.4mm (at 90 deg. and for the middle deltoid) for the three tasks (Table 5.1). With normal anatomy the middle deltoid moment arm is smaller and almost constant, whereas with the prosthetic geometry it has a much greater fluctuation (Figure 5.3). Interestingly, the middle deltoid moment arm in the DELTA® III model has a peak at 90 deg. of abduction, where the arm weight creates its largest adducting moment.

In order to visualise the deltoid moment arms in more of the humeral workspace, more data were calculated:

Elevation of the arm (0 to 150 deg.) for every 5 deg. of plane of elevation (azimuth, α) between abduction (where α=0 deg.) and forward flexion (where α=90 deg.). The results showed an average increase of the deltoid moment arm of 42.16% with the maximum peaks (54mm) to be at 88.5 deg. of elevation (Figure 5.4)

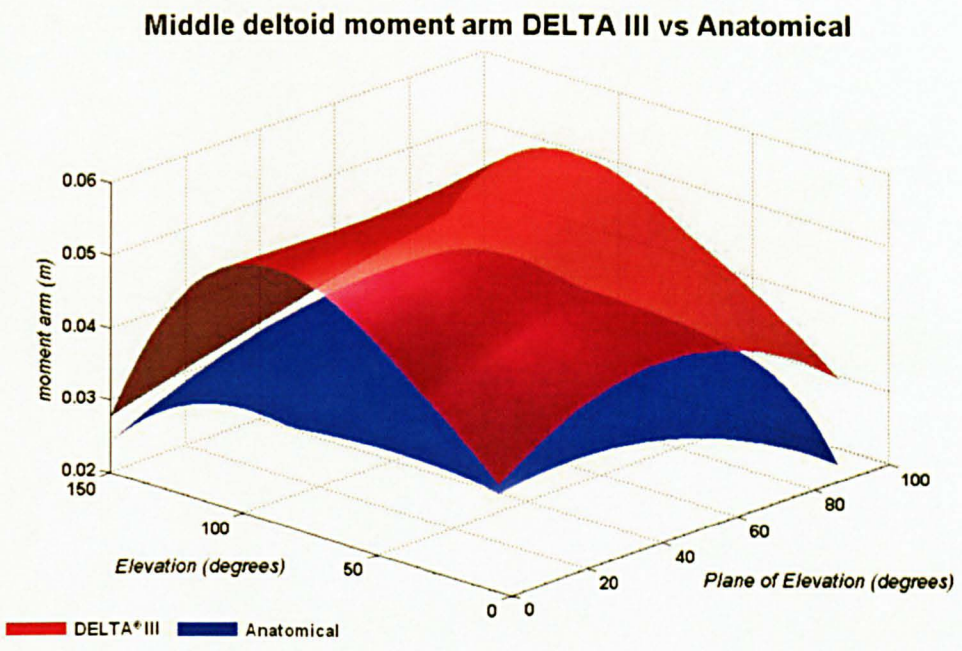

Figure 5.4: Middle deltoid moment arm in workspace for anatomical and reverse prosthetic design

The predicted results for the increased deltoid moment arms of this study agree well with the studies of De Wilde (2004) and Van der Helm (1998) the same DELTA® III geometry (Table 5.1) was used, but with different skeletal reconstruction. The slightly larger value (59.3mm) of De Wilde during scapula plane elevation can be justified by the larger skeleton used in this study, which is also reflected in the increased value of the deltoid moment arm for the normal anatomy. Terrier *et al.* (2007) using a similar type of prosthesis (Aequalis® Reversed Shoulder Prosthesis, Tornier) and, also for scapula plane elevation, reports also a similar peak moment arm of 50.0mm (Table 5.1).

As mentioned above, the increased moment arm is a result of the medialised centre of rotation, which results in an offset (*d*) from the axis of the humeral shaft (as shown in Figure 5.5). By further increasing this offset – e.g. by using either a thicker option cup or larger diameter sphere – the deltoid moment arm can be further increased in the early phase of abduction, but the peak values will be slightly reduced and appear in earlier degrees of elevation.

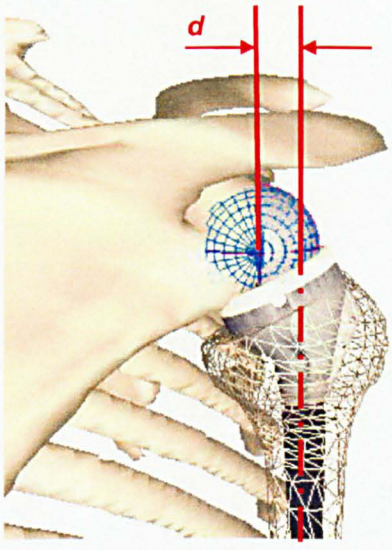

Figure 5.5

The prosthetic design medialises the centre of humeral rotation and creates an offset (d) with the axis of the humeral shaft affecting the muscle moment arms. d relates to the geometric characteristics of the reverse design.

Geometrical characteristics of the prosthesis define the medialisation of the centre of rotation as well as the offset from the humeral shaft. In theory a reverse design can medialise the centre of rotation without medialising the humerus – e.g. large diameter sphere, large offset – but such a design can dramatically increase superior impingement. The impact of the design characteristics of a reverse design on the muscle moment arms and function will be discussed analytically later in this chapter.

Study		Moment arm (mm)	
		Normal	Reverse
DeWilde *et al.* (2004) – Scapula Plane		40.0	59.3
Terrier *et al.* (2007) – Scapula Plane		28.0	50.0
Van der Helm (1998) - Abduction		35.0	52.0
This Study	Abduction	34.7	55.1
	Forward flexion	36.1	52.8
	Scapula Plane	34.6	55.3

Table 5.1: Summary of peak m.Deltoid middle moment arms and muscle lengthening in literature and in this study

The moment arms of the infraspinatus and subscapularis muscles (when present in the corresponding RC tear prosthetic models) are also affected and have an adducting moment arms throughout the motion (Figure 5.6). In contrast, in the normal anatomy the RC muscles can have abducting moment arms after 25 deg. of arm elevation (average range -3.6 to 17.9mm and -4.0 to 15.7mm respectively)

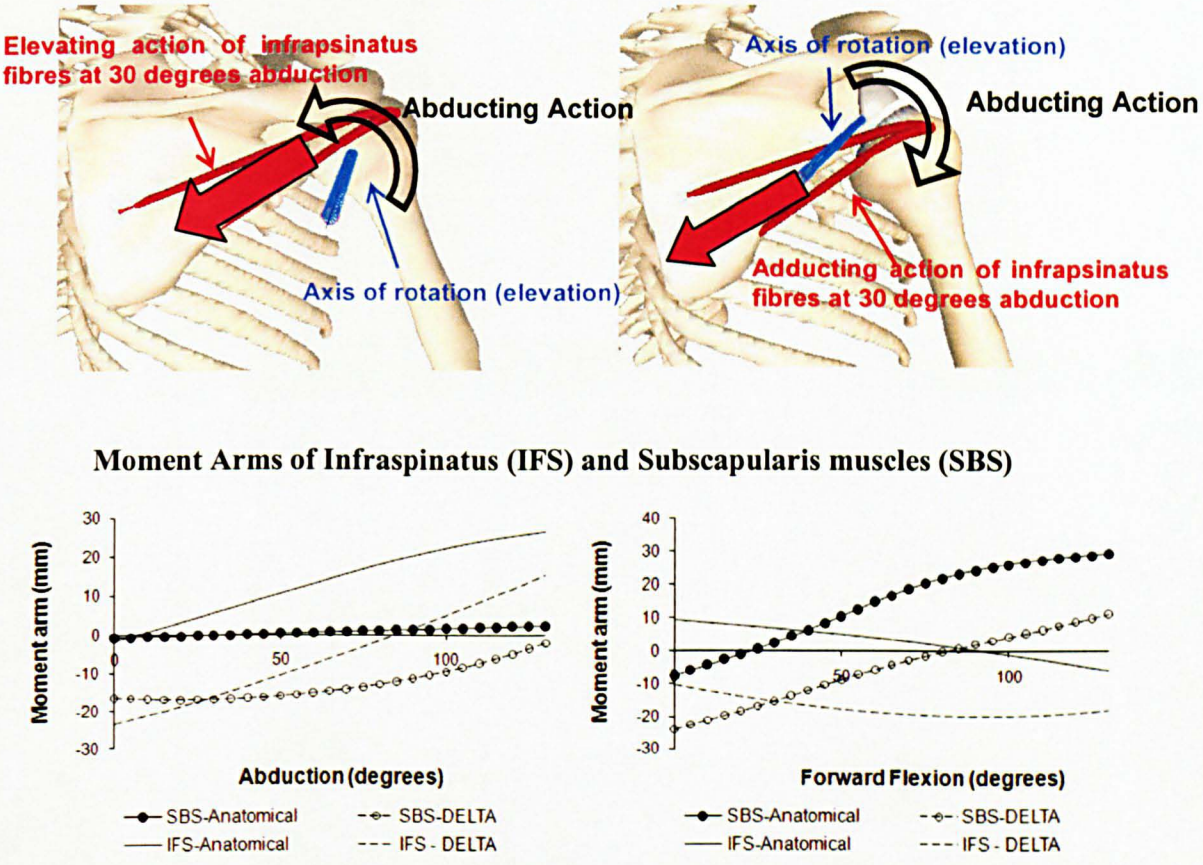

Figure 5.6: (a) An example of how the action of the RC (for infraspinatus) can change after a reverse joint replacement during arm elevation. (b) The effect of the reverse design on the moment arm of infraspinatus and subscapularis, where they have a more adducting action compared to the normal anatomy

Adduction moments at the humerus are primarily generated by the tri-articular muscles such as the m. Pectoralis major (dependent on elevation angle) and m. Latissimus Dorsi. These muscles directly transfer force to the thorax, providing simultaneous adduction moments around the GH joint and also providing joint stability acting antagonistically against the deltoid (Labriola et al. 2005,Lee & An 2002,Veeger & van der Helm 2007). Although these three muscles are prime movers of the arm, they can generate joint reaction forces that cause dislocation (Labriola et al. 2005). The m. Lattisimus Dorsi and m. Pectoralis Major are also affected by the prosthetic geometry, further increasing their adducting moment arms compared to normal anatomy (Figure 5.7).

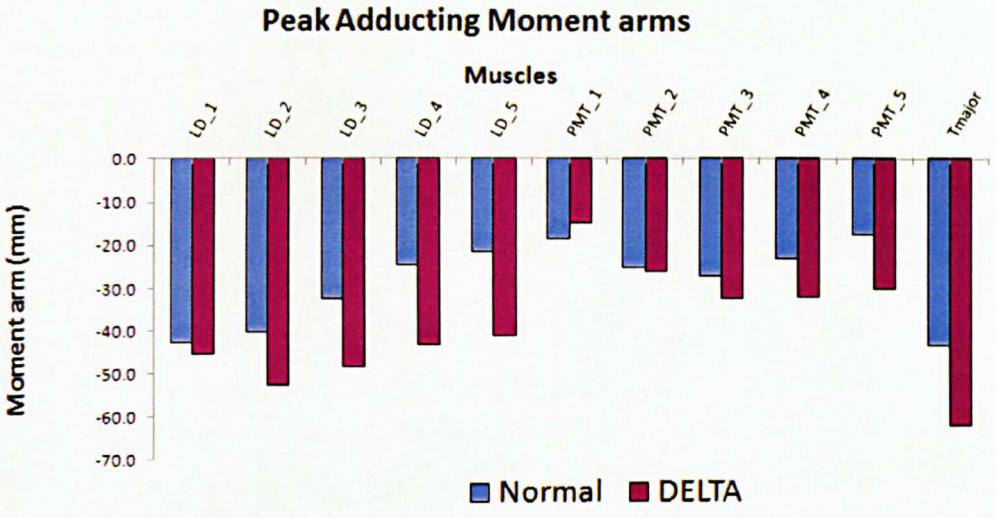

Figure 5.7: The reverse prosthesis also affects the prime movers of the arm (m.Latissimus dorsi (LD), m.Pectoralis major thoracic (PMT) and m.Teres major (Tmajor)), by increasing their already large adducting moment arms.

There is a larger difference for the clavicular part of the m.Pectoralis major, which is located very close to the fibres of the m.Deltoid anterior. In normal anatomy the action of this muscle pulls the arm medially (horizontal flexion) and only helps the m.Deltoid to lift the arm during the more extreme stages of arm elevation. With the reverse geometry the upwards pulling of the muscle starts earlier, in much lower degrees of arm elevation. The effect, however, is not as large since the moment arm peaks at only 5.53mm.

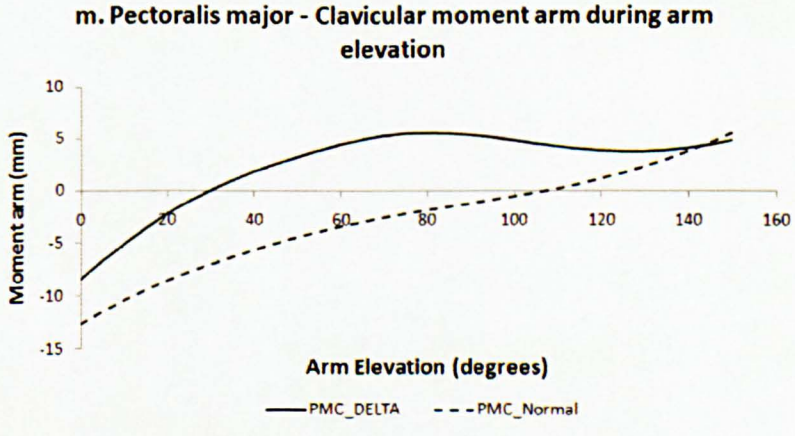

Figure 5.8: The elevating contribution of the m. Pectoralis clavicular is increased with the reverse prosthetic design

5.3.2. Moment arms during internal/external humeral rotation

It is documented that the humeral internal/external rotation range of motion in subjects with reverse prosthetic shoulder is limited (Bergmann et al. 2008,Boileau et al. 2006,Gerber et al. 2007,Grammont & Baulot 1993,Kontaxis A et al. 2007). This is expected, since the clinical indication for use of the reverse prosthesis is irreparable RC tear, which means that there is no presence of m.Infrapsinatus and m.Subscapularis to rotate the arm. Even in the rarer case where those muscles are preserved the model shows that the reverse geometry does not enhance much their rotational capability. Results of testing those muscles in external/internal rotations in adduction and abduction (90 deg. of elevation) showed a maximum increase in rotational moment arm of 20.6% (compared to normal anatomy) for the m.Infraspinatus and just 7.8% for the m.Subscapularis.

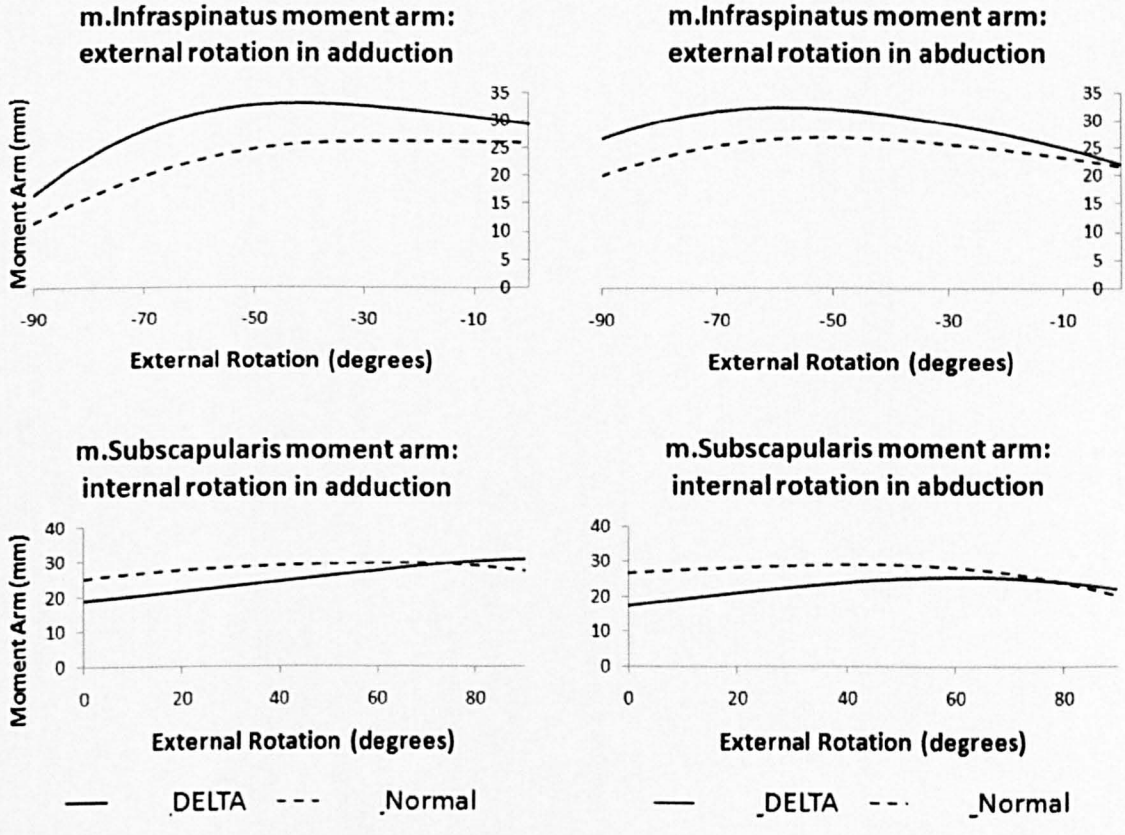

Figure 5.9: The effect of the reverse prosthetic geometry on the RC muscle in internal/external humeral rotation

In contrast with the m.Infraspinatus and m.Subscapularis, m.Teres minor is slightly more affected and its moment arm in external rotation is increased by 48.3% compared

to the normal anatomy. This muscle, with an insertion located underneath the m.Infraspinatus, is more likely to be active in a RC pathology (e.g. in RC tears m.Teres minor is the last affected muscle) and its preservation after a reverse anatomy replacement can significantly help the external rotational range of motion.

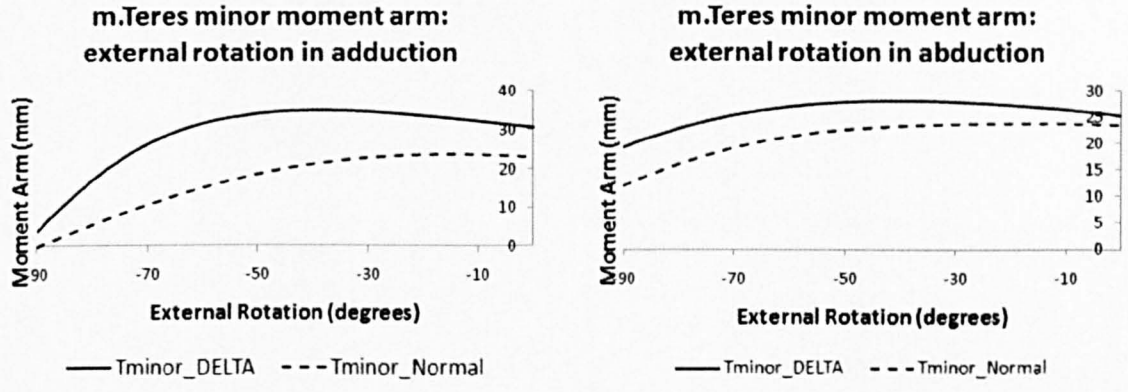

Figure 5.10: The reverse design can increase the external moment arm of m.Teres

5.4. *Muscle and joint contact forces and Glenohumeral (GH) joint stability.*

5.4.1. Normal anatomy: Simulating RC tears

In order to understand the mechanics of the reverse prosthesis, there is a need to understand what is happening to the shoulder function when there is a loss of RC muscle. As mentioned above, in a normal shoulder the RC muscles that are arranged around the superior half of the humeral head direct the joint reaction force into the glenoid and provide stability. The prime movers of the shoulder (m.Deltoid, the m.Pectoralis Major and the m.Latisimus Dorsi) can also pull the humeral head into the glenoid cavity, but the action of these muscles can also result in large antagonistic moments that could lead to dislocating forces, as discussed by Labriola et al. (2005). That study shows that even if the shoulder muscle forces can be powerful stabilisers, an active pectoralis action at the end range of abduction could create a joint reaction force that would naturally tend to dislocate the GH joint.

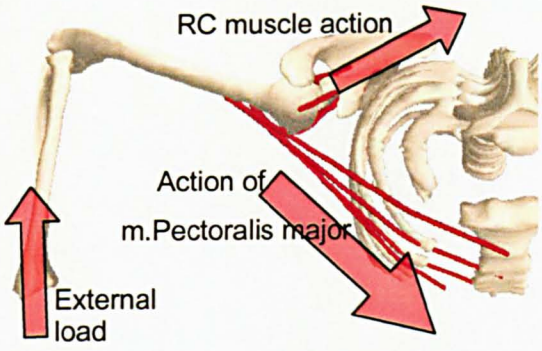

Figure 5.11

Even if the prime movers can act as shoulder stabilisers, there are positions that their natural action can create dislocation and stability of the shoulder depends upon the action of the RC muscles

Model simulations of the standard activities for the anatomical model with only a partial tear (model PST, only m.Supraspinatus missing), reached feasible solutions (i.e. the GH contact force was constrained within the stability), but the results are much different than those of the normal shoulder.

The GH joint contact force vectors are facing the superior face of the glenoid which means that the superior shear forces are increased with a shear to compressive force ratio topping 0.66 (maximum allowed 0.70 in the inferior/superior direction - the Visible Human glenoid anatomy, Figure 5.12).

The increased superior shear forces on the PST model are almost 4 times larger compared to the normal model where all the RC muscles are present (0.349 and 0.087 times BW for PST and normal model respectively). The compressive forces are dropping by 13% of BW (0.60 and 0.73 times BW for PST and normal model respectively).

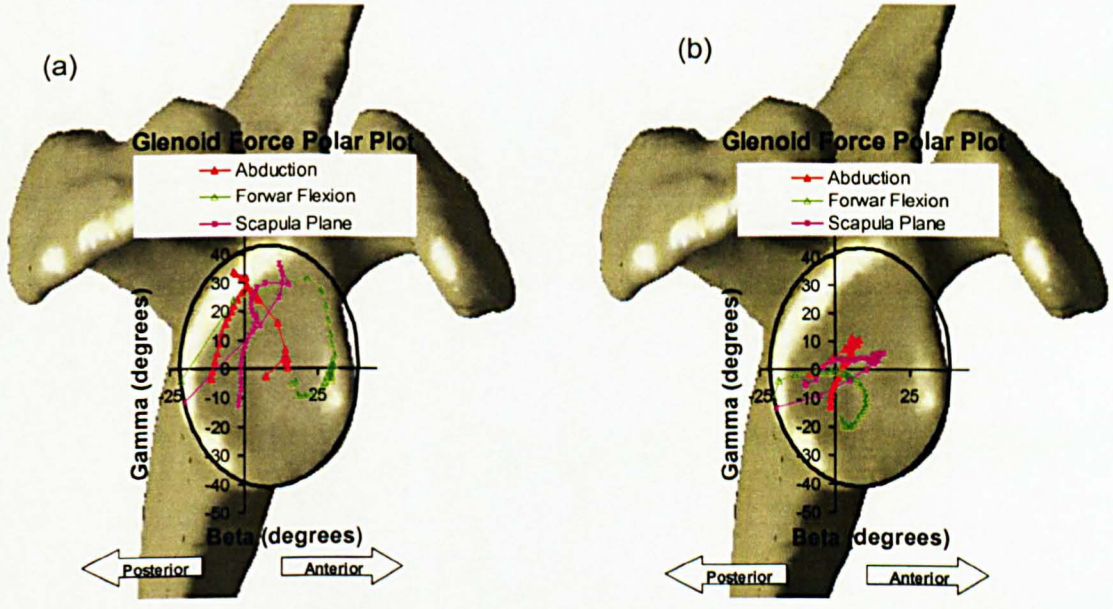

Figure 5.12: Glenoid joint contact forces in PST (a) and normal (b) model. The lack of m.Supraspinatus in the PST model shifts the contact forces to the superior face of the glenoid

In the normal model, the m.Deltoid muscle shares the elevating load of the arm with the m.Supraspinatus (max of 0.170 BW at 90 degrees for middle deltoid, and 0.171 BW at 65 degrees for m.Supraspinatus), where the latter muscle (m.Supraspinatus) also directs the contact force into the centre of the glenoid cavity. In the PST model the deltoid has to generate an excess force pulling upwards to compensate for the muscle loss and peaks at a high load of 0.267 BW (increase of 57%), increasing the overall shear joint contact forces. Even if the above simulations did not count for the large translations of the humeral head within the GH joint, as has been shown in pathological clinical cases (Ecklund et al. 2007), the results highlight the main problem of RC tear pathology, where superior migration of the humeral head and superior glenoid erosion are often reported (Sirveaux et al. 2004).

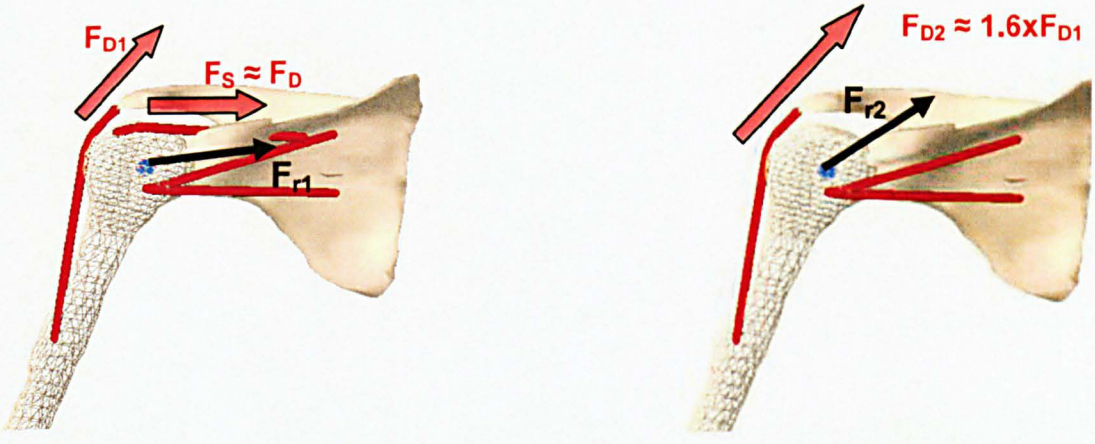

Figure 5.13: (a) In normal shoulder the m.Deltoid (F_{D1}) and m.Supraspinatus (F_S) share the load of elevation where the action of the latter muscle helps the resultant force (F_{r1}) to compress the humeral head. (b) A dis-functional m.Supraspinatus will result in a larger m.Deltoid action (FD2) to elevate the arm and, due to the resultant force (F_{r2} joint contact force), will change direction and thus increase the superior contact force acting on the glenoid

Figure 5.14

Radiographs showing superior glenoid erosion in RC arthropathies (Adopted from, Sirveaux F. et. al., 2004)

When larger RC tears were simulated, by excluding more RC muscle fibres (models SAT, SPT or full thickness tear FTT), the model could not reach feasible solutions. The results showed that the optimisation was failing to reach a global minimum value and satisfy all of the constraints of the system. When the glenoid joint contact force constraint was removed from the optimisation function, the model was able to reach a solution; this indicates that even if the deltoid has the necessary power to elevate the arm, there is no combination of muscle co-contractions that will result in the joint contact force being within the glenoid when a large portion of the RC muscles is inactive. Van der Helm has reported similar results where the Dutch interactive shoulder model did not find feasible solutions for simulation of abduction in a full thickness RC tear model (Van der Helm F.C. 1998).

At this point we need to clarify the definition of a stable joint: Veeger and Van der Helm (2007) have highlighted the difference of joint stability/instability definitions between the mechanical and clinical points of view i) in mechanical terms instability means a full dislocation of the joint (with no relocation) whereas ii) in clinical terms instability can be also synonymous with large displacement of the GH joint after force exertion on the humerus. In this study, the type of the shoulder biomechanical model that was used can investigate joint stability only by checking whether the joint contact forces are constrained within the joint stability surface (humeral cup for the reverse anatomy, and glenoid cavity for the anatomical model).

5.4.2. Joint contact forces on the reverse prosthetic joint

All simulations with the reverse prosthetic model converged to stable solutions, independently of the type of the RC tear. Analysing the full thickness tear prosthetic model, the results showed that the m.Deltoid muscle forces during all three activities were close to those of the normal anatomy model (including RC), but with the m.Deltoid

middle contributing slightly more compared to the anterior and m.Deltoid posterior (Figure 5.15). That is in contrast with the previous results: in the anatomical model when the m.supraspinatus was missing (PST model) the m.Deltoid had to exert a much higher force in order to produce the required elevating moment.

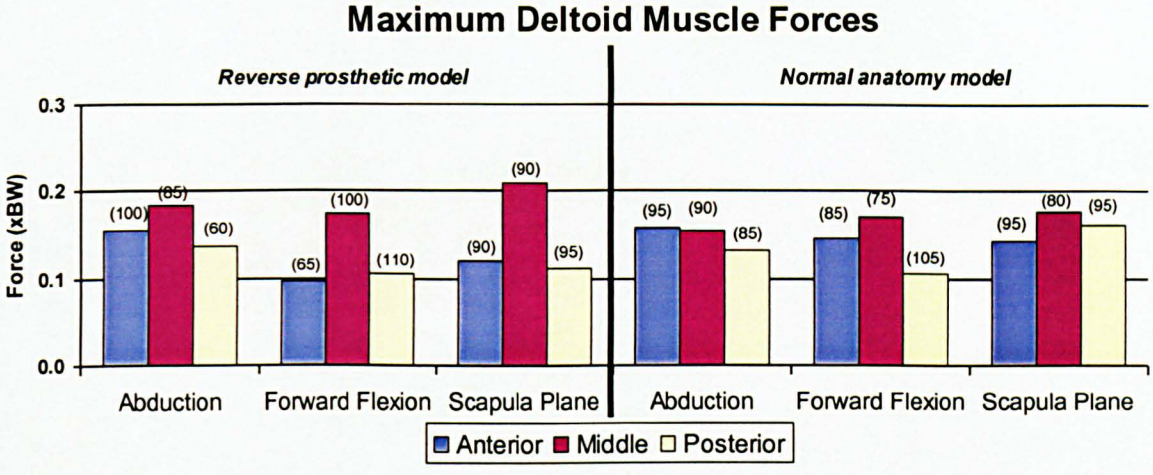

Figure 5.15: Maxima of middle m.Deltoid muscle forces during the standard elevating activities for reverse prosthetic (FFT model – no RC muscles) and normal anatomy (all muscles) shoulder. In parentheses is the humeral elevating angle (deg.) that the maxima were observed.

With the normal anatomy the m.Deltoid shares the elevating load mostly with the m.Supraspinatus. In the reverse model the elevating moment is produced mostly by the deltoid action alone. The fact that the predicted Deltoid forces are similar to the normal shoulder indicates that the reverse prosthesis provides to the m.Deltoid the necessary additional moment arm to produce sufficient elevating moment and compensate for the lack of the RC muscles. However, the resultant force during the elevating tasks in the GH joint is now largely depended by the action of the m.Deltoid and it can change direction and magnitude depending on the direction and magnitude of the muscle force.

Taking into consideration the lack of the compressive RC forces and the moderate activation of the deltoid, it is of no surprise that the predicted total contact forces for the FTT prosthetic model were reduced by an average of 41.6% compared with the normal shoulder (all the RC muscles present), ranging in values between 0.463 and 0.631 times BW.

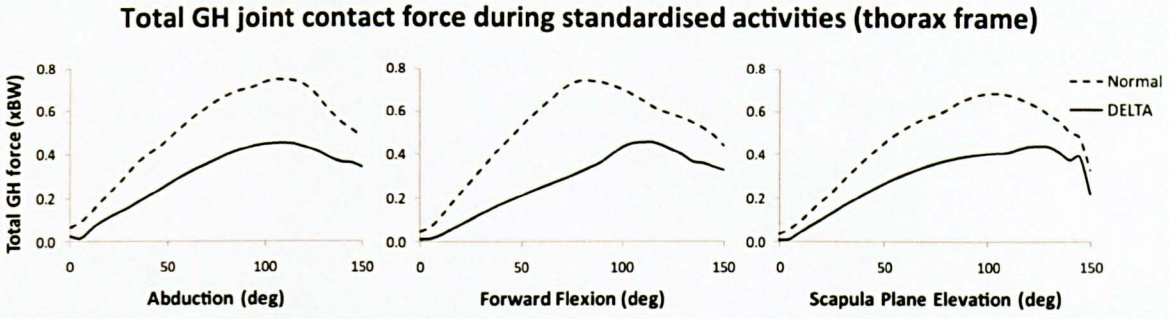

Figure 5.16: The overall joint contact force in the reverse prosthesis is reduced by an average of 41.6% compared to the normal shoulder

Transforming the total GH contact force on the glenoid site and decomposing it to its components (compressive, shear anterior/posterior and shear superior/inferior) the compressive forces were reduced by an average of 41.6% ranging from 0.435 to 0.451 times BW. As expected, shear forces were increased especially in the superior direction where there is an increase in all three activities compared with the normal model (average increase 105.4%). The values ranged from 0.285 to 0.148 times BW, compared to 0.103 to 0.076 times in the normal model (Figure 5.17).

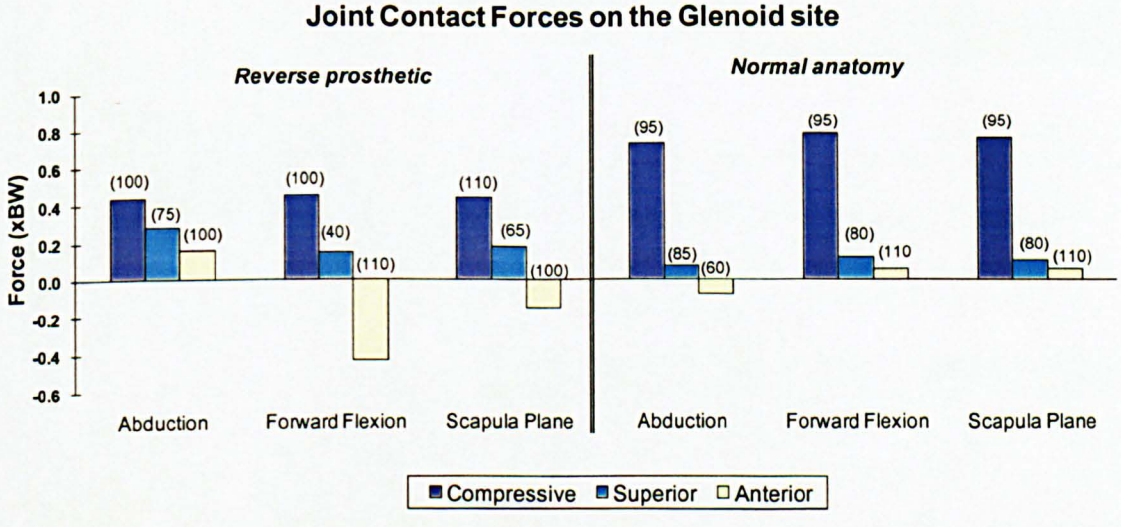

Figure 5.17: Maxima of joint contact forces on the glenoid site during the standard elevating activities for reverse prosthetic (FFT model – no RC muscles) and normal anatomy (all muscles) shoulder. In parentheses is the humeral elevating angle (deg.) that the maxima were observed.

The antero-posterior shear forces on the glenosphere site changed magnitude and direction depending on the activity. The maximum value was observed in forward flexion with the posterior shear force reaching a high 0.438 times BW where the anterior shear observed only in abduction reaching at 0.187 times BW. These results reflect how the resultant force on the GH joint (joint contact forces) depends on the action of the deltoid for elevating activities of the arm:

- During forward flexion the deltoid will push the arm upwards and backwards creating high supero-posterior shear forces on the glenosphere
- During abduction the action of the deltoid creates an upwards and slightly forward (in relation to the glenoid site) load that results in supero-anterior shear forces on the glenosphere.
-

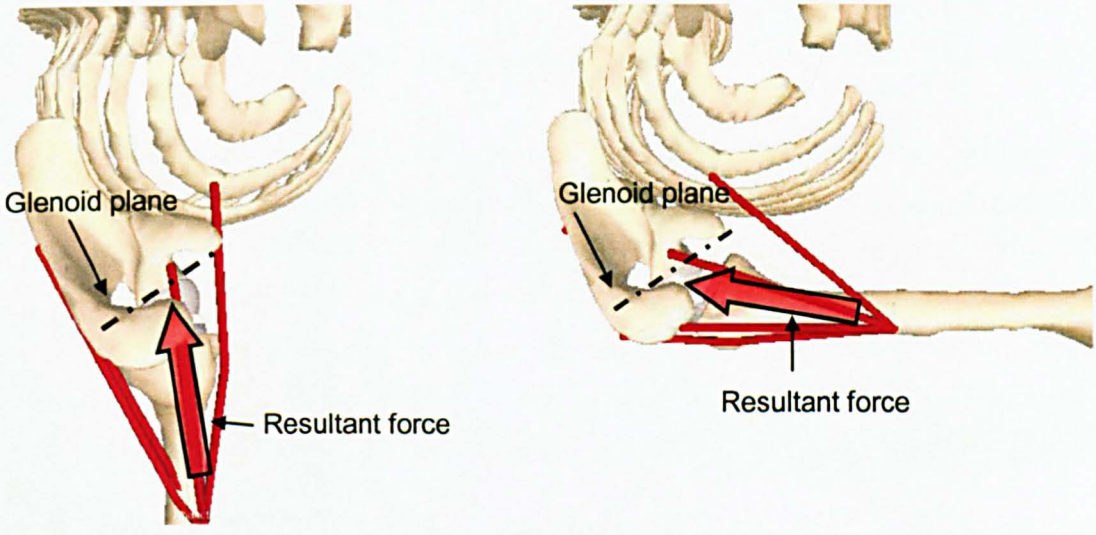

Figure 5.18: When there are no RC muscles, the resultant force on the GH joint (joint contact forces) during elevating tasks depends heavily on the action of the deltoid. As a result there are always increased superior shear forces where the antero-posterior glenoid loading depends on the plane of the elevation

Simulations with the different types of RC tears showed small differences. The remaining RC muscles exerted small forces, peaking at only 0.06 times BW. In general, subscapularis fibres reduced the anterior glenoid shear forces during abduction (0.05 times BW reduction) whereas infraspinatus reduced the posterior shear forces in forward flexion and scapula plane elevation (0.04 – 0.07 times BW respectively). The highest difference in the total joint contact force between the FTT and any of the RC tears models was only 0.07 times BW.

Terrier *et al.* (2008) predicted 50% total joint contact force reduction in a similar reverse prosthetic joint (excluding all the RC muscles) when compared to an anatomical prosthetic shoulder (all RC muscles present) and simulating only scapula plane elevation. This value is close to the current study (40.9% reduction respectively –Figure 5.16 third graph - Corresponding values: max GH 0.689xBW in normal reduced to 0.407xBW in DELTA). There are differences, however, when comparing results with the PST model (supraspinatus only missing) where Terrier *et al.* report a significant impact of the m.Infraspinatus and m.Subscapularis muscles to the total joint contact forces. A comparison between the two models is difficult since the latter includes only a limited set of muscles and there is a difference in force prediction methodology. In the current study the large adducting moments of the RC muscles forced a solution where the cost function minimised their activation. This is the reason for the small differences between the results of FTT and the rest of the RC tear models. Different and more complex kinematic inputs can show different results, where the RC muscles can have a greater effect on the GH loading.

When there is a full thickness tear, the prosthetic model shows that the m.Teres minor can contribute to the stability of the joint. This muscle, in a normal shoulder, is inactive during all three elevating tasks as its main function is to externally rotate the arm. In the prosthetic model the natural line of action of the m.Teres minor is to balance the pulling action of the deltoid, thus providing stability. The action of the muscle becomes stronger for arm elevation in the sagittal plane and towards the end range of the motion. The muscle force peaks at a maximum value of 0.18 times BW in forward flexion.

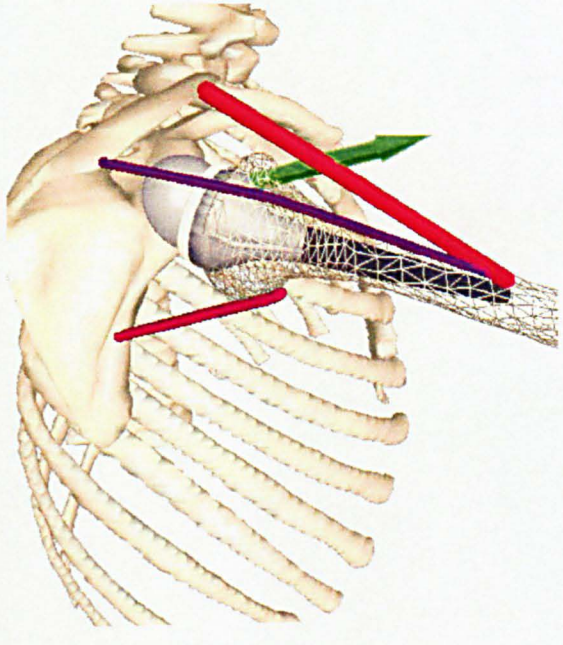

Figure 5.19

In contrast with a normal shoulder, the m.Teres minor can be active in a reverse prosthetic shoulder since its natural action provides a balance to the pulling action of the deltoid muscle.

5.4.3. Stability of a reverse prosthetic shoulder

Looking the GH joint contact forces on the humeral frame (where Xh is pointing lateral, Yh superiorly, Zh posteriorly), we can see that they are dominantly compressive.

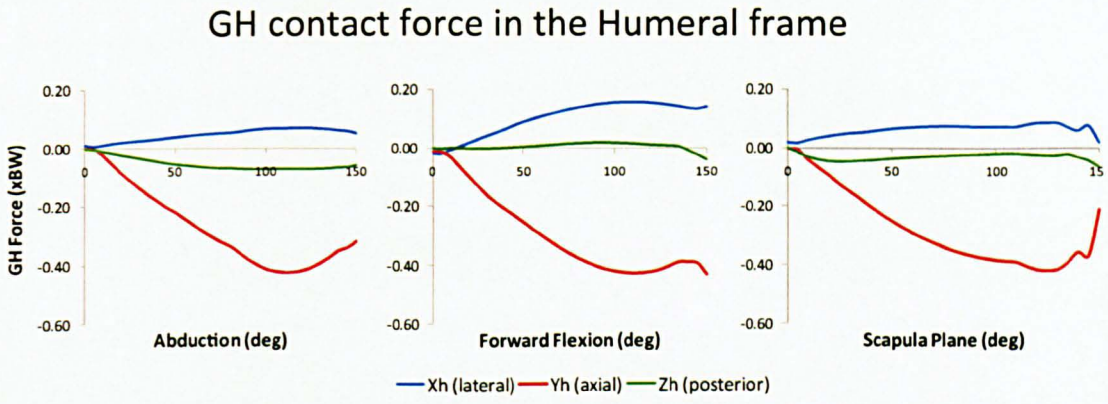

Figure 5.20: Contact loads in the humeral frame during the 3 standard activities

Transforming those joint reaction forces into the humeral cup frame, the results showed that the forces were well constrained within the stability rim, with the trace of joint contact forces located slightly inferiorly to the centre of the cup. Van der Helm (1997) and Terrier *et al.* (2008) report the same trend of stability, with the latter study to also reporting a superior trace of contact forces during the beginning of the motion. The ratio of shear/compressive peaked only at a value of 0.58 (for the FTT model) where in the DELTA® III geometry the maximum allowed ratio (for stable joint) is 1.86.

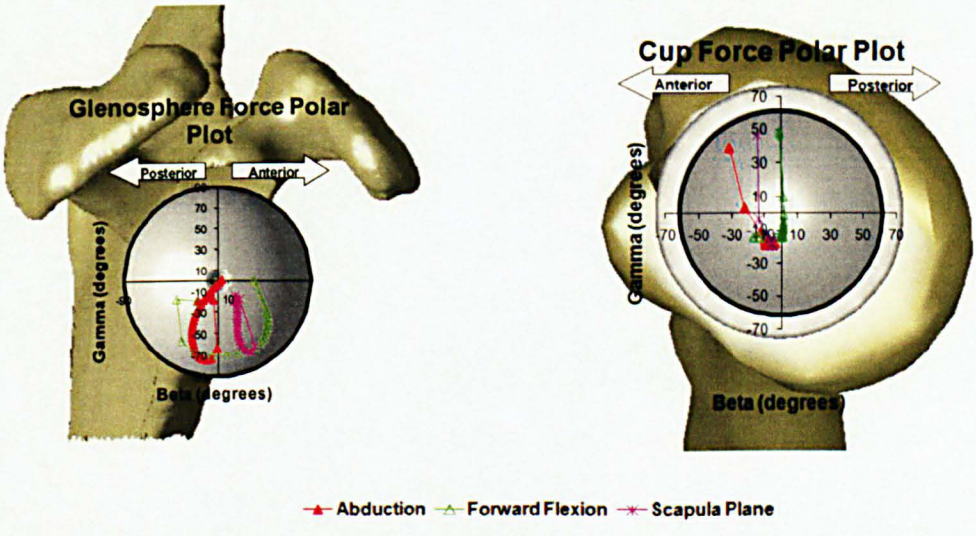

Figure 5.21: Joint contact forces in the prosthetic model with full thickness tear (FTT model). (a) In all activities there is a high superior load applied on the Glenosphere. (b) The reverse design restores joint stability, since all the joint contact forces are constrained within the stability area (the cup rim).

The joint stability results are in line with many clinical reviews (Baulot et al. 1995,Boileau et al. 2006,Sirveaux et al. 2004,Valenti P et al. 2001) that report great GH joint stability in DELTA® III geometry. The reverse prosthesis can restore the joint stability by reversing the envelope of the joint contact forces and by changing the critical articulating surface. The half-spherical glenoid fixation provides a large surface reacting to the increased shear forces. The critical stability region is now the area of the humeral cup where the depth determines the maximum dislocating shear force. The maximum allowable ratio of shear/compressive force in DELTA® is higher than an anatomical shoulder (typical value of 0.6 for the inferior/superior direction (Halder et al. 2001). In addition, the humeral cup follows the direction of the deltoid force and the high shear forces are well constrained within the cup rim.

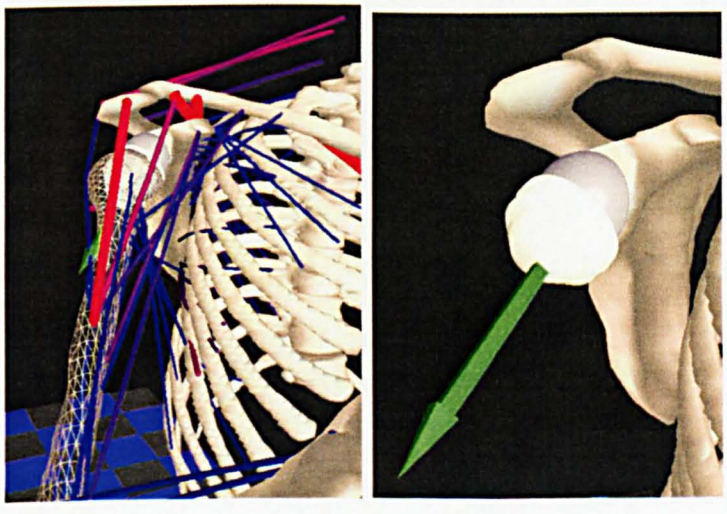

Figure 5.22

The prosthesis reverses envelope of GH forces providing stability to the joint

5.5. *Impingement: A compromise on the range of motion*

Reverse prostheses have become popular in treatment of irreparable RC tear, as the biomechanical properties of the design can restore function and stability to the joint. However, impingement and notching problems have been repeatedly reported for reverse prostheses (Boileau et al. 2006,Grammont & Baulot 1993) and have often been associated with clinical complications (Wall B.T. & Walch G. 2008) such as polyethylene wear, chronic inflammation of the joint capsule, and local osteolysis (Nyffeler et al. 2004). Furthermore, there is concern that scapular notching could be progressive and could lead to late glenoid loosening and catastrophic glenoid component failure, even if the indication so far is small (2-5%) (Valenti P et al. 2001). To date, the mechanism of the creation of the notches has been disputed, but many reports associate the problem with the contact (impingement) of the humeral cup with the scapular border.

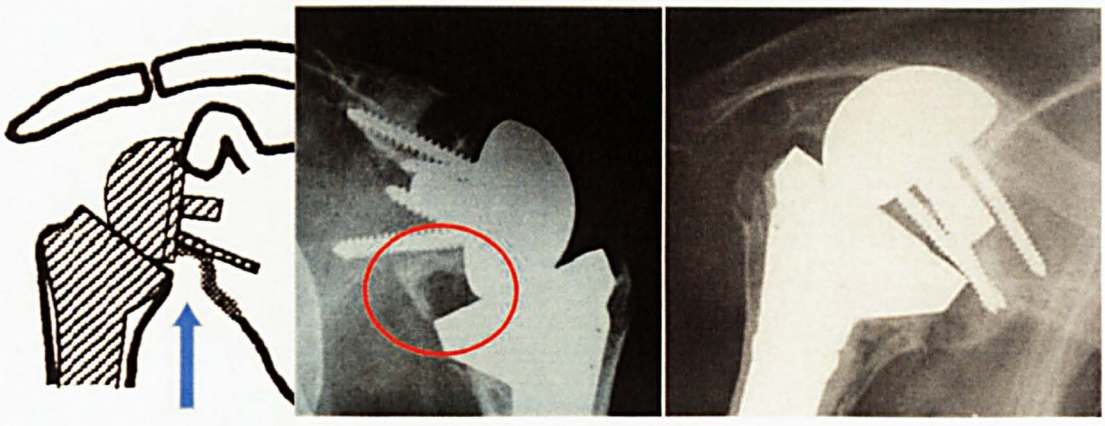

Figure 5.23: The impingement of the prosthesis with the scapular border can create notches that can even lead to glenoid loosening and catastrophic failure of the prosthesis.

Even if most of the studies in the literature refer only to the impingement of the cup, the model clearly shows that there are two kinds of impingement (Figure 5.24):

- Contact of the polyurethane cup with the scapula border (inferior impingement) at the lower degrees of arm elevation
- Bony contact of the proximal humerus (around the Greater tubercle site) with the acromion (superior impingement) or coracoid process towards the end range of motion

Several studies have reported impingement of a different form. In this study, inferior, superior and impingement free ranges of motion are measured in terms of humeral elevation angles in a humero-thoracic conversion. In case of inferior impingement, the minimum humeral angle before any contact of the cup with the bone is reported, where the maximum elevation angle before contact of the acromion with the humerus is representing superior impingement.

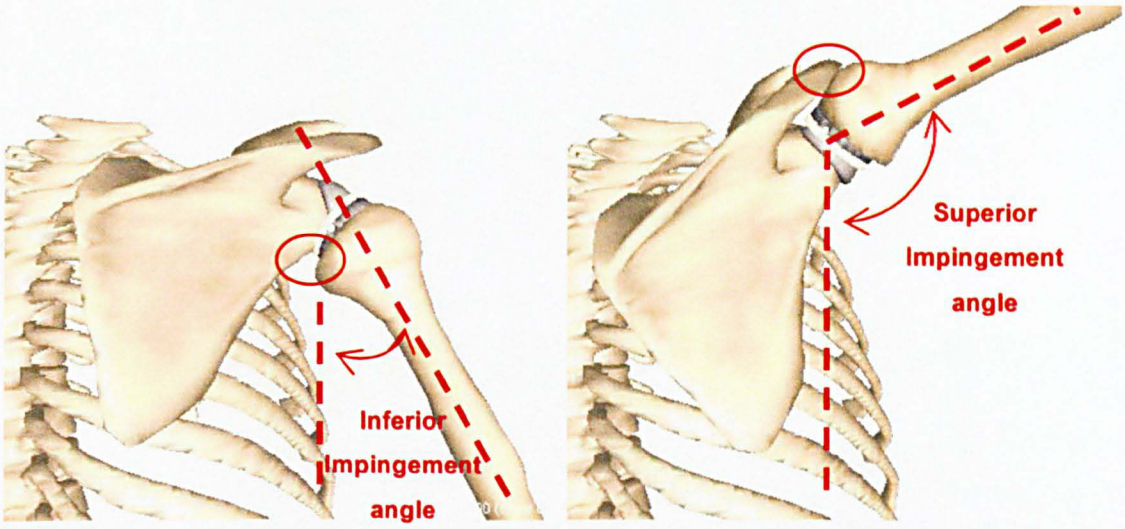

Figure 5.24: The model shows that there is a contact of the cup with the scapula border (inferior impingement) in the lower degrees of arm elevation and a contact of the humeral head to the acromion or coracoid process (superior impingement)

All three simulations of the standard activities with the prosthetic model showed inferior and superior impingement. As expected, the range of motion (with no impingent) was smaller than in the normal shoulder and was restricted to an average of 83 deg. for all 3 activities (standard fixation, Table 5.2). The graphical contact detection also showed large traces of contact of the humeral cup, and significant penetration into the scapula border when the arm is at the resting position (0 degrees of elevation).

	Standard Fixation (size 42)			
	Abduction	**Scapula Plane**	**Forward Flexion**	**Average**
Inferior (deg.)	52	32	16	*33.3*
Superior (deg.)	108	122	119	*116.3*
Range (deg.)	56	90	103	*83*

Table 5.2: Impingement in the standard reverse prosthetic joint during the three standard activities

The average predicted range of motion without impingement (83 deg.) is close to, but slightly larger than, the value of 76.3 deg. that is reported in the two dimensional study of DeWilde *et al.* (2004), with both the numbers of inferior and superior impingement being larger. The different values of this study can be explained by the different scapulo-humeral rhythm that was used in that particular study.

In a different cadaveric study Nyffeler *et al.* (2005) reported impingement averaging a range of GH motion of 40.3 deg. for three similar activities. In this study, Nyffeler measured range of motion by fixing multiple cadaveric scapulae (implanted with DELTA® III prostheses) and moving the humerus in three planes i) plane of the scapula, ii) -30 deg. posteriorly (simulating abduction), ii) 60 deg. anteriorly (simulation forward flexion). Transforming the kinematics profile and fixation set-up to match the latter study (by excluding the scapulo-humeral rhythm and fixing the scapula to the thorax), our model showed a very close agreement of an average range of motion of 41.8 deg.

The relatively large value of 33 deg. of inferior impingement indicates that the contact of the cup with the scapula border should be very frequent during everyday activities. These results, in combination with the large contact trace (of the cup to the scapula), support previous clinical studies of polyethylene wear and creation of notches. In a further chapter of this study, a set of activities of daily living (that has been recorded by reverse prosthetic subjects) is applied to the model in order to predict the site, shape and size of the notches by recording contact during the activities.

The range of external/internal humeral rotation is also affected (reduced) by the impingement problem. Unlike the normal anatomy, where a humeral rotation results in a rotation around the long humeral axis, the new kinematic constraints of the reverse prosthesis impose a different kinematic output: a simple humeral rotation means that the humeral axis rotates around a circular path with a centre that is defined by the glenosphere and radius *d* (Figure 5.25). This means that an external rotation can result in a contact of the humeral cup with the posterior part of the scapula border, where an internal rotation can result in impingement of the cup with the anterior part of the scapula border.

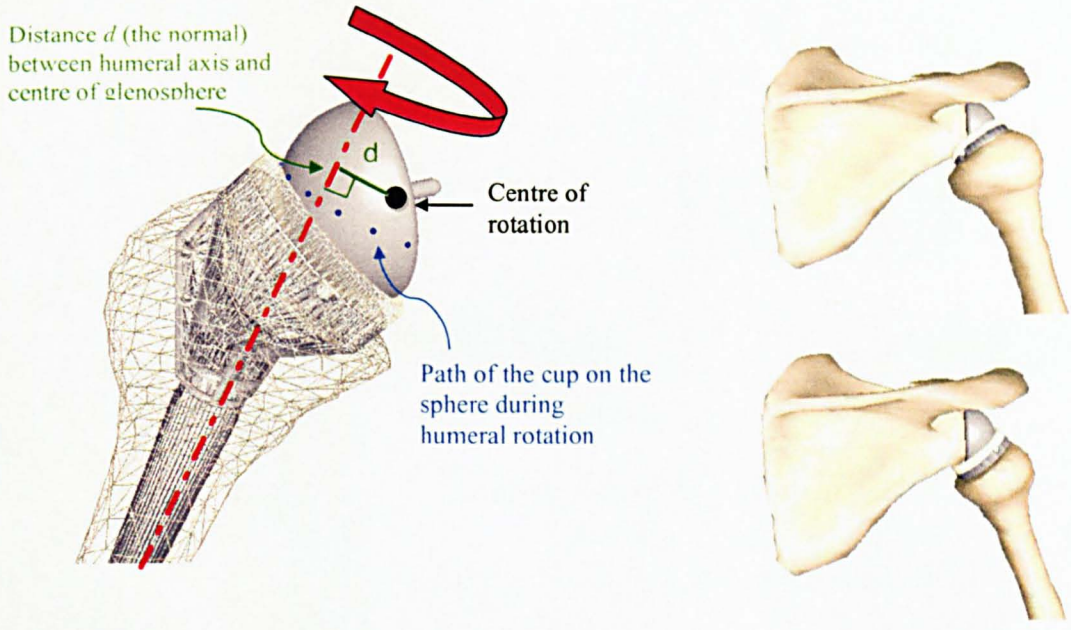

Figure 5.25: Impingement ***due to humeral rotation***

The impingement due to humeral rotation depends heavily on the humeral position and mostly on the humeral elevation. With the arm rested at 0 deg. abduction, where there is an extended penetration of the cup to the scapula border, any humeral rotation does not change the impingement. When the arm is abducted to 90 deg. there is no contact detected. When the arm is abducted 50 deg. the range of internal-external rotation is -8 (external) to 69 (internal) deg. This means that a minimisation of impingement in elevating tasks will also reduce impingement in humeral rotation.

5.6. *Fixation and Design Parameters of the Reverse Anatomy Designs*

Surgical guidelines and design alterations try to address the problem of impingement and improve survivorship. At the last stage of this chapter we present how impingement and joint stability can be affected by different surgical and design modifications as they have been found in the literature (Harman et al. 2005, Nyffeler et al. 2005, Simovitch et al. 2007). The parameters tested are shown in Figure 4 and involve:

- **Surgical modifications (Glenoid-fixations):**

i) Positioning of the Glenoid sphere (inferior D_2 and antero/posterior fixation D_1)

ii) Glenoid reaming depth D3 and angle of oblique fixation α_1

iii) Stem version fixation angle β_1

- **Design alterations:**

i) Cup depth to sphere radius ratio (h/R),

ii) Lateralisation of the centre of the sphere c from the fixation plane

iii) Neck/shaft angle of the prosthesis β_2

5.6.1. Fixation Configurations

5.6.1.1. Positioning of Glenoid sphere fixation

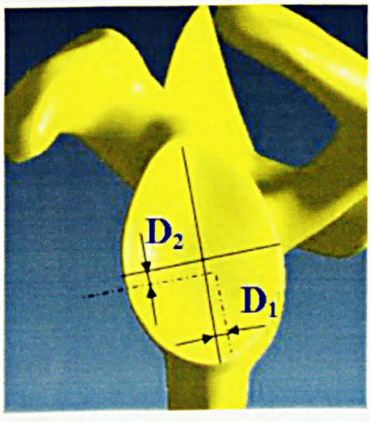

Figure 5.26

The position of the fixation of the sphere on the glenoid is important for the impingement results of the joint

i) Inferior Fixation D_1

Fixing the glenoid prosthetic component inferiorly is one of the first and most popular configurations that was tried out in clinical practice and it has been adopted as a surgical guideline from most of the current available reverse designs (Nyffeler et al. 2005,Simovitch et al. 2007). In this study, starting from the 'standard fixation', the glenoid sphere was fixed inferiorly along the supero-inferior glenoid axis, and in increments of 1mm.

The results showed that the available range of motion was greatly increased, averaging 5 deg./mm of inferior fixation. After an extreme 6mm of inferior displacement no inferior impingement could be detected, but the fixation screws were well outside the scapula border after 4mm. Deltoid elongations was also increased (1.2% lengthening increase per mm of inferior fixation) compared to an already large value of 21.6% of the standard fixation. The latter increases even further the risk of damaging the axillary nerve (Grant et al. 1999).

	Standard Fixation *D1=0, D2=0 mm*	Inferior Fixation D1 (mm) (D2=0=constant)			Antero/Posterior Fixation D2 (mm) (D1=0=constant)			
		D1=1	D1=2	D1=3	D2=-2	D2=-1	D2=1	D2=2
Inferior (deg.)	33.3	30.1	27.1	24.1	34.9	34.1	32.3	31.5
Superior (deg.)	116.3	118.6	119.6	121.6	116.7	116.1	117.2	116.9
range (deg.)	*83*	*88.5*	*92.5*	*97.5*	*81.8*	*82*	*84.9*	*85.4*

Table 5.3: Influence of Glenoid sphere positioning on the inferior and superior impingement

Predicted joint contact forces were almost unaffected, since inferior fixation had a very small impact on the muscle moment arms. For the deltoid there was a small increase of 4% on its moment arm after 3mm of inferior fixation of the sphere and it was observed gradually over 40 deg. of arm elevation (Figure 5.27)

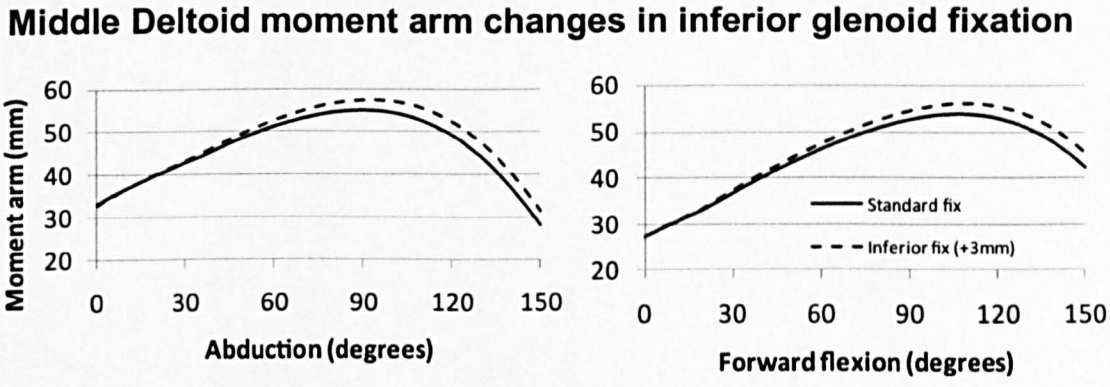

Figure 5.27: The effect of the inferior glenoid fixation on the deltoid moment arms is rather small and in high degrees of elevation

ii) Antero-Posterior fixation D_2

The fixation guidelines suggest that a fixation should be just posterior to the supero-inferior glenoid axis without specifying the exact position. Having in mind the small available fixation surface of the glenoid that limits the placement of the glenoid sphere, a ±2mm antero/posterior fixation was tested along the antero-posterior glenoid axis (positive values corresponding to a posterior direction).

The results showed small changes on the impingement with a posterior positioning of the sphere reducing only the inferior impingement by a maximum of 1.8 deg. during the three standard activities. This can be explained by the fact that the scapula border

(which is the contact site of the cup with the scapula) is slightly located posterior to the glenoid. Thus, a positioning of the sphere in a posterior direction covers more of the impingement site, but the effect is very small (Table 5.3)

Calculations of muscle moment arms and prediction of contact and muscle forces, showed small changes during an antero/posterior fixation. This happened because the ±2mm limited change of the sphere fixation did not affect the wrapping (direction) of the muscles lines around the joint.

5.6.1.2. Glenoid reaming depth and angle of oblique osteotomy

i) Reaming depth D_3

The glenoid reaming depth is defined by the instrumentation (the glenoid reamer) and for the DELTA® III design is set to 3mm.

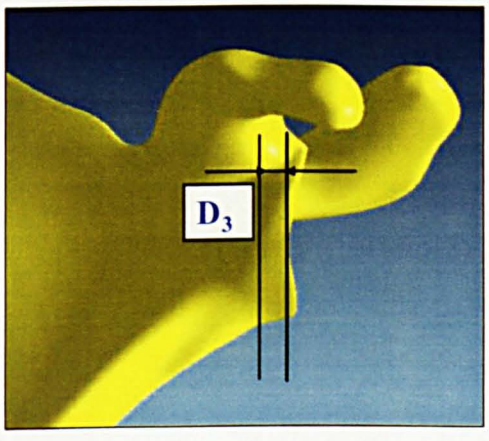

Figure 5.28

The depth of glenoid reaming had mainly negative results in impingement

As is obvious, extended reaming of the glenoid medialises the centre of rotation further, compared with the normal anatomy. However, this extra medialisation does not have the same big effect on the muscle moment arms, since the distance between the centre of rotation and the humeral shaft remains constant.

The model showed that m.Deltoid moment arm increased by only 1.4% per mm of reaming (0.7mm – average of the max difference for the three activities). The result of the latter was that the m.Deltoid exerted a slightly smaller force (4.9% smaller) and thus the total GH contact force was decreased by only 0.058 times BW. The trace of the contact force on the cup and the sphere was almost identical.

Reaming of the glenoid had a negative impact on the inferior impingement. By keeping the position of the fixation the same, the inferior impingement increased by 4.8 deg. per mm of reaming. In addition, because of the conical geometry of the glenoid, an extended reaming means an overall reduction of the available fixation surface.

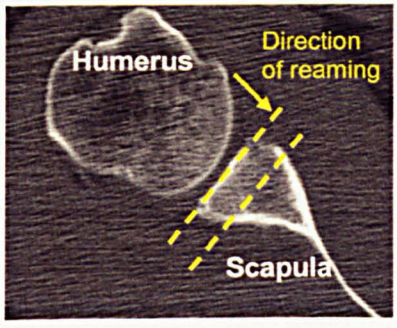

Figure 5.29

Radiographic CT image of a left shoulder. Because of the geometry of the glenoid, an extended reaming can limit the available surface of fixation

ii) Angle of glenoid osteotomy α_1

For the standard fixation the surgical guidelines and the instrumentation tools define a face glenoid reaming (where α=0 deg, Figure 5.30). There are clinical papers suggesting that an oblique glenoid osteotomy on a reverse prosthesis can minimise inferior impingement and strength of fixation (Nyffeler et al. 2005). In this study we investigated the importance of an oblique glenoid osteotomy, by maintaining the position of the standard fixation, and performing a virtual glenoid reaming at an angle of: α = 5, 10, 15 deg. (position of the fixation remaining constant). The surface of the virtual bone was remodelled accordingly each time.

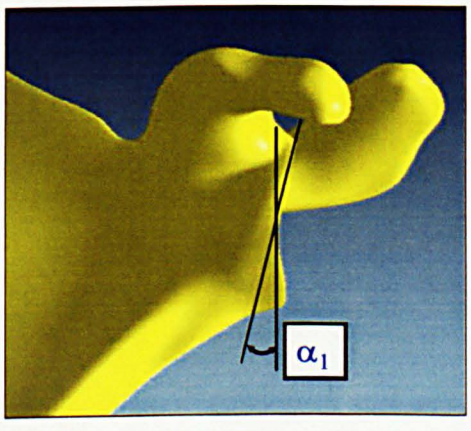

Figure 5.30

The orientation of the glenoid osteotomy can affect the loading on the glenoid site as well as the inferior impingement

Loadsharing results showed that an oblique osteotomy did not affect the total GH joint contact and muscle force predictions, since fixing the sphere in an oblique orientation had no affect on the joint geometry and to the muscle wrapping around the bones. The only difference is that the total joint contact force is decomposed in different analogies of compressive and shear force on the glenoid site (loading of the glenosphere). In general, an oblique fixation will reduce the high superior shear loads on the glenosphere, which can be important for the strength of the fixation.

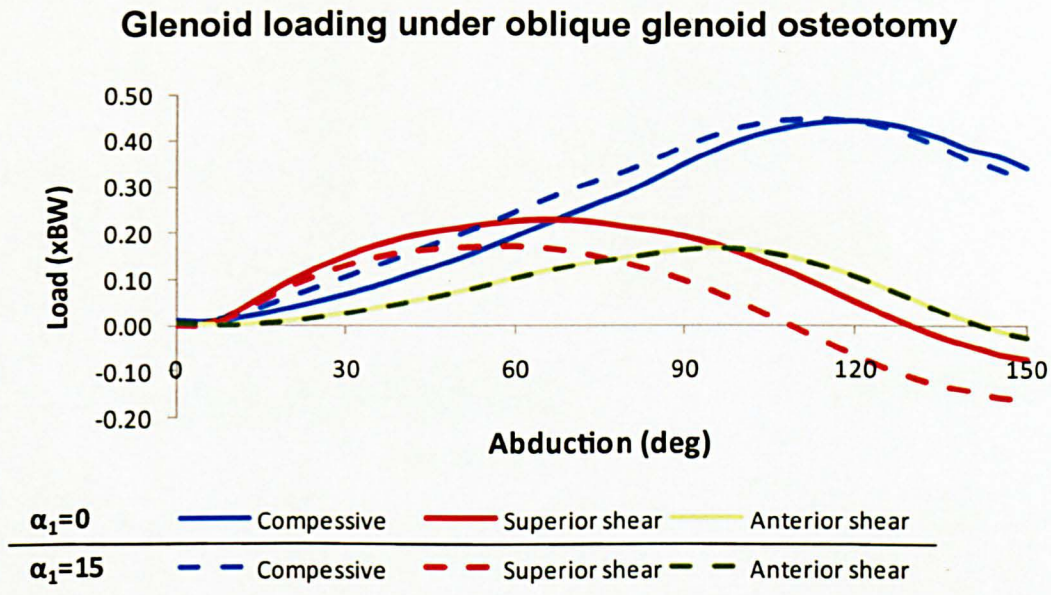

Figure 5.31: An oblique osteotomy does not change the total GH joint contact force, but it can change the ratio of compressive to shear forces that are applied on the glenoid site. Because the oblique osteotomy happens in one direction (α_1 angle in respect of the face of the glenoid - Figure 5.30) it is only the Compressive and Superior shear forces that are affected, where the projection of the Anterior shear force component remains unaffected (green dotted and continues lines coincide)

Impingement results of an oblique osteotomy (for α = 5 deg., 10 deg. and 15 deg) showed different outcomes:

a) For α =5 deg. the glenoid sphere still overlaps the inferior reamed glenoid surface and the results showed no change for the inferior fixation (Table 5.4).

b) When the sphere was fixed in a more aggressive oblique osteotomy, the inferior reamed surface was either flush or exposed under the glenoid sphere (for α=10 and 15 deg. respectively). The results for this set-up showed a small improvement, but only for the inferior impingement (Table 5.4).

Impingement	Standard Fixation	Reaming Angle α (degrees)		
	α = 0 deg	α=5	α=10	α=15
Inferior (deg.)	33.3	33.3	30.3	28.2
Superior (deg.)	116.3	116.3	116.3	116.3
range (deg.)	83	83	86	88.1

Table 5.4: ***Impingement in oblique*** *osteotomy*

The above results can be explained by the fact that oblique glenoid reaming can trim away a potential contact of the bone with the cup, but only when the sphere does not overlap the inferior glenoid surface and the inferior impingement occurs just below the sphere fixation.

5.6.1.3. Retroversion of the humeral stem fixation (β1)

Figure 5.32

The orientation of the stem fixation can affect the loading and the range of humeral internal/external rotation (due to impingement) and the loading of the cup

As described in a previous section of this thesis (Chapter 4, 'Virtual Implantation'), the surgical guidelines and the instrumentation kit are providing the surgeons with the choice of reaming the humeral head and fixing the stem in a range of different versions (from 20 deg. retroverted position (anatomical head position) to 0 ('neutral') deg. of retroversion). The stem in the standard fixation is inserted in a neutral position (β1=0 deg.).

Changing the version of the stem fixation means that the prosthesis is rotated along its long axis inside the humeral canal and, as a result, the cup changes its position on the sphere (similar effect to the internal/external rotation explained above). More specifically, and for the right arm, a neutral stem fixation (β1=0 deg.) will result in a more posterior placement of the cup on the sphere than a retroverted fixation (Figure 5.33).

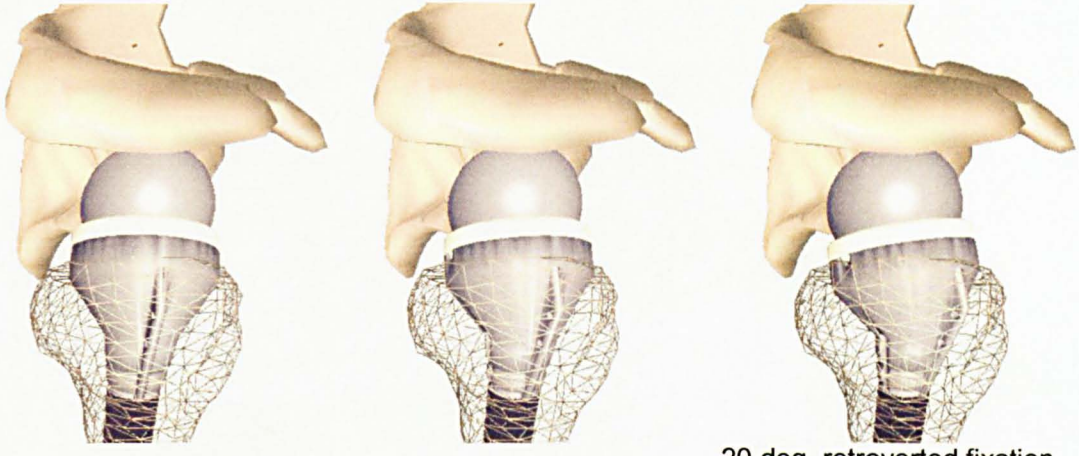

0 deg. retroverted (neutral) fixation

10 deg. retroverted fixation

20 deg. retroverted fixation (anatomical head)

Figure 5.33: The cup has different positions on the sphere for different stem fixations: a neutral fixation (0 deg. retroverted) places the cup more posteriorly, where a retroverted fixation places the cup in a more anterior position (for the same humeral orientation)

As expected, a change on the version can have an impact on the impingement, which is especially evident in the range of external/internal humeral rotation. Even if the range of the humeral rotation is not increasing or decreasing the version of the humeral fixation can shift the window of the available range of rotation such as:

- A neutral fixation will increase the internal and reduce external rotation
- A retroverted fixation will increase the external and reduce internal rotation

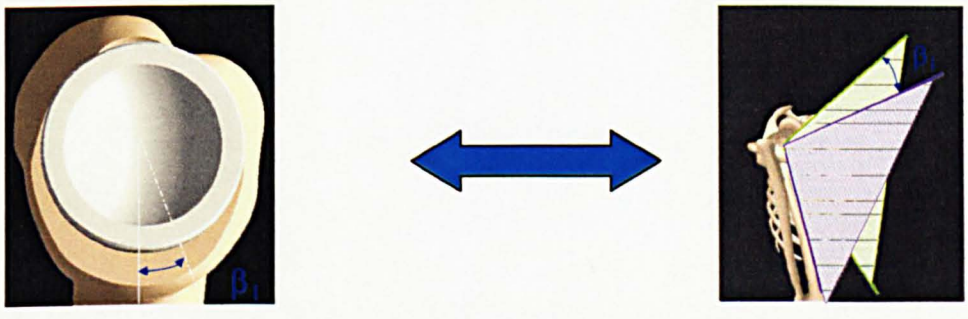

Figure 5.34: The version of the Stem fixation does not increase or decrease the range of internal/external rotation; if the shaded triangle on the right hand figure represent the range of internal/external rotation in a specific humeral position, changing the stem version by β_1 degrees does not change the range (the size of the triangles) but it shifts the window of operation of the available range of rotation by β_1 degrees

It needs to be noted that the restriction of the range of the humeral internal/external rotation due to impingement is significant only for low degrees of humeral elevation (<60 deg.).

In contrast with the impingement, the version of the fixation does not have a big impact on the muscle line of action of the prime movers and as a result does not affect their moment arms. Loadsharing results of the three standard activities for different versions of stem fixation showed a maximum increase of only 0.08 times BW in the total GH contact force, when stem was fixed in 20 deg. retroverted (compared to the standard neutral fixation). The main difference is on the loading of the cup, where a change in the version of the stem fixation changes the trace of the contact force on the cup; a retroverted fixation will increase the posterior load (cup frame). The stability of the joint was not compromised in any occasion.

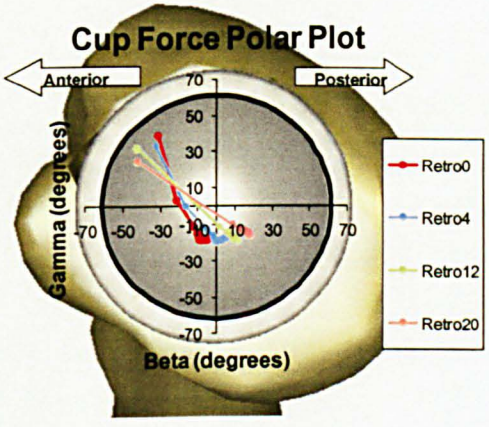

Figure 5.35

The change on the stem fixation does not change the total GH contact force, but it affects the loading of the prosthetic cup

The only muscles that are affected by the version of the stem fixation are the RC muscles (m.Subscapularis, m.Infraspinatus and m.Teres minor), where a different stem fixation can change their rotational moment arm. This is a direct result of the different position of the cup on the sphere, which changes the action of the muscle line and can increase or decrease the external/internal moment arm of the RC muscles (Figure 5.36)

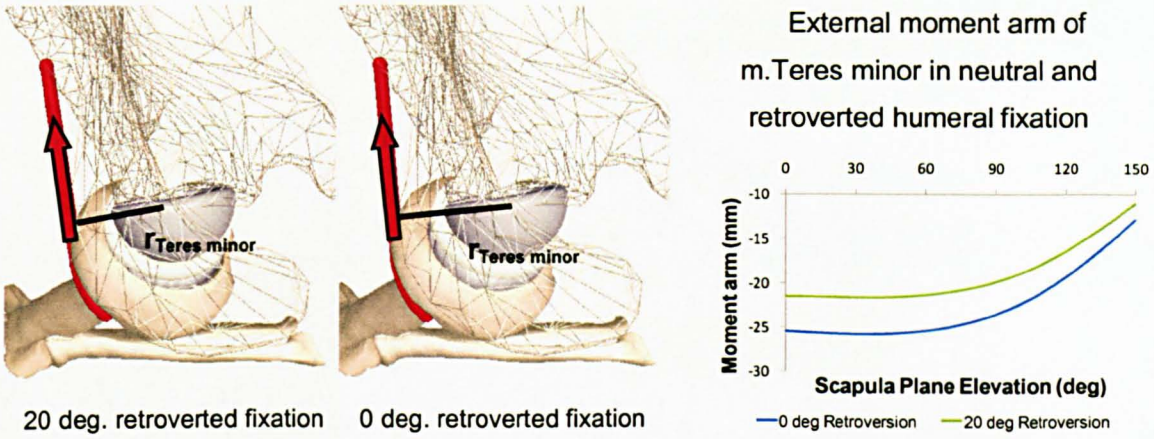

Figure 5.36: The version of the stem fixation can affect the external rotation moment arm of m.Teres minor: neutral fixation places the cup and the humerus in a more posterior position, increasing its moment arm. The difference can be up to 16%

The results show that a neutral stem fixation will help the external rotation since it increases the moment arm of m.Teres minor and m.Infraspinatus compared to a retroverted fixation (15.9% and 9.8% increase respectively). For the m.Infraspinatus the results show the opposite effect: a neutral fixation can reduce its rotational moment arm by 16.7% compared to the retroverted position.

If we compare the moment arm values with the values of a normal anatomy shoulder (Figure 5.37), it is clear that the prosthetic design, in general, reduces the ability of internal rotation and only a neutral fixation helps the m.Teres minor to externally rotate the arm.

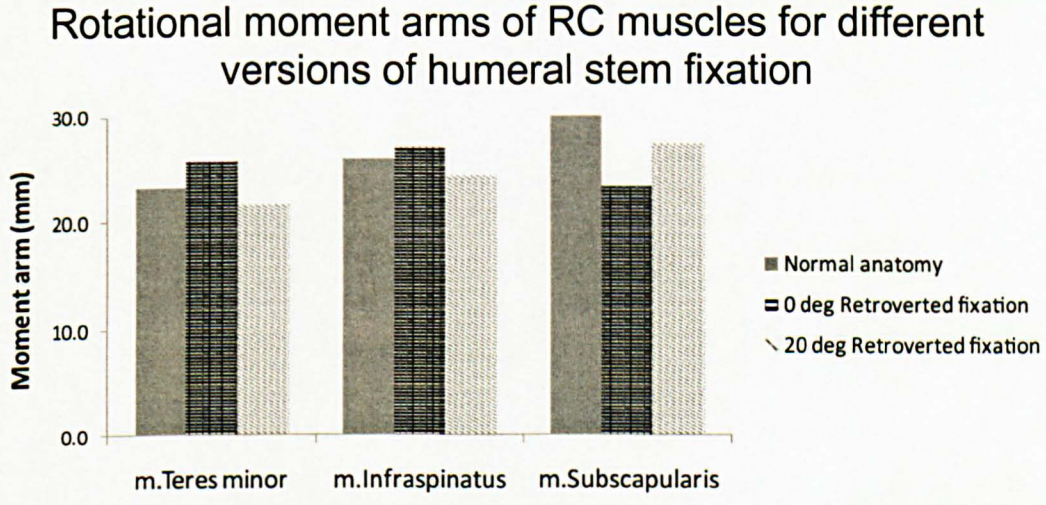

Figure 5.37: The muscle moment arm results suggest that a neutral stem fixation will help the external rotation and vice versa.

5.6.2. Design alterations

5.6.2.1. Cup depth to Sphere radius ratio (h/R)

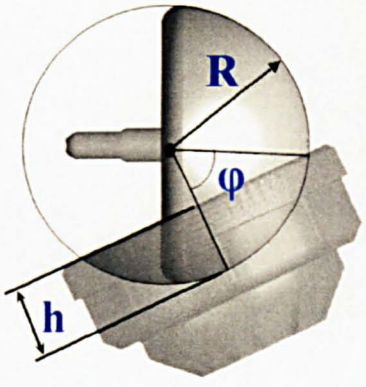

Figure 5.38

Many reverse designs introduce different sizes of the glenoid sphere or the depth of the cup, that can affect the stability and impingement of the joint

One characteristic that commonly changes in the reverse anatomical designs, is the size of the glenosphere, R, and the depth of the humeral cup h, that articulates with the sphere. Even within the same designs manufactures are giving the options of different implant sizes. For example DELTA® III design can be configured with either a sphere R=21 and cup h=11 (ratio=0.52), or sphere R=18 and cup h=8 (ratio=0.44). This ratio is related to the maximum shear to compressive force that is allowed in a stable prosthetic joint since a dislocation can happen when the resulting joint reaction force vector at the rotational centre of the joint points outside of the articulating surface.

Thus for a stable joint:

$$\left(\frac{shear}{compressive}\right)_{\max} = \frac{\sin\phi \cdot R}{R-h} = \tan\phi$$

where ϕ is the angle that defines the cup width (Figure 5.38)

A larger h/R ratio effectively means a deeper cup depth for a given sphere and, as a result, a larger shear to compressive ratio and thus a more stable joint. In case of h=R the ratio shear/compressive becomes infinite so that shear forces cannot dislocate the joint (constrained designs, (Kessel & Bayley 1979)).

Results showed that a reduction of the cup depth h (given R=constant) is an effective way to mainly reduce the inferior impingement (Table 5.5). The rim of the shallower cup is now further away from the scapula border lowering the angle of inferior impingement by almost 4 deg./mm of cup depth reduction. The superior impingement was not affected.

Loadsharing results showed no difference in muscle or joint contact forces, since the muscle moment arms and muscle lines of action remained unaffected. However, the

reduction of the cup depth means that the h/R ratio is smaller and so is the maximum allowed shear/compressive ratio (in the cup frame) for a stable joint. This ratio was reduced to 1.27 for h=8mm, which is a 32% reduction compared to the standard design h=11mm. Despite the reduced cup depth, during the simulations of the three standard activities, stability of the joint was not compromised by reducing the h only by 3mm since the contact force that was observed (maximum shear/compressive ratio 0.58) was still constrained within the stability area.

	Standard Design	**Cup Depth h (mm)**		
Impingement	h=11 mm	h=10	h=9	h=8
Inferior (deg)	33.3	29.4	25.8	22
Superior (deg)	116.3	116.3	116.3	116.3
range (deg)	83	86.9	90.5	94.3

Table 5.5: Impingement due to depth to Sphere radius ratio (h/R)

5.6.2.2. Lateralisation of the sphere centre c

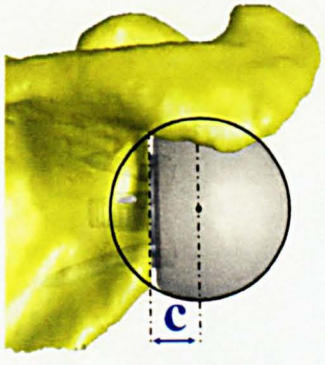

Figure 5.39

Designs that lateralise the centre of the glenoid sphere can be very effective of minimising impingement.

Some of the reverse designs currently available on the market offer a glenoid fixation that lateralises the centre of rotation away from the fixation plane. Simulation results of such a sphere (c = 1, 2, 3 mm) showed great reduction of only inferior impingement since the cup can slide more inferiorly on the sphere surface avoiding contact with the scapula border (Table 5.6). In fact, by increasing c more than 7mm no inferior impingement could be detected. Superior impingement was not affected a lot since the geometry of the acromion is extended further laterally and a contact with the humerus was unavoidable.

Impingement	Standard Design	Lateralised Sphere Centre c (mm)		
	c=0 mm	c=1	c=2	c=3
Inferior (deg.)	33.3	30.8	28.3	26.1
Superior (deg.)	116.3	116	115.8	115.8
range (deg.)	83	85.2	87.5	89.7

Table 5.6: Impingement results with a sphere that has a more lateralised centre than the original hemispherical design of DELTA® III

As with the reaming of the glenoid, the lateralisation of the centre of the sphere has a small impact on the muscle moment arms, since the distance of the humeral axis to the centre of rotation remains the same. In fact there is a small reduction in the m.Deltoid moment arm where after 3mm (c=3) the maximum value is reduced by 1.4mm (almost 3.2% reduction). This is not a significant difference especially if we consider that the original increase of m.Deltoid moment arm from the anatomical to reverse was more than 50%. Thus, joint contact and muscle force calculations were slightly affected with the overall GH contact force increasing by 0.07 times BW.

5.6.2.3. Neck/shaft angle of the prosthesis (β_2)

One of the characteristics that can change in a reverse prosthetic design is the angle of the neck, that supports the humeral cup, in relation with the stem.

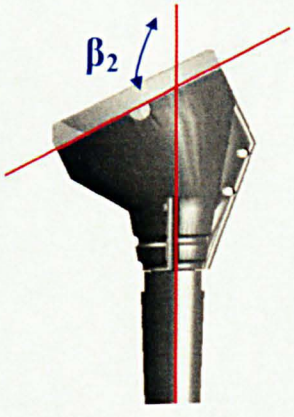

Figure 5.40

Design characteristic of a reverse design: the angle of the neck in relation with the long axis of the stem β_2

In the standard DELTA® III design this angle is equal to β_2=115 deg. This value is typical for this type of prosthesis, but there are some alternative designs that have an increased neck/shaft angle (NGR-Wright Medical).

By increasing the value of β_2 on the DELTA design, the cup will re-position itself in a more superior position on the sphere surface. That will shift the cup and the humerus

superiorly and medially, increasing the distance 'd' between the humeral shaft and the centre of the sphere.

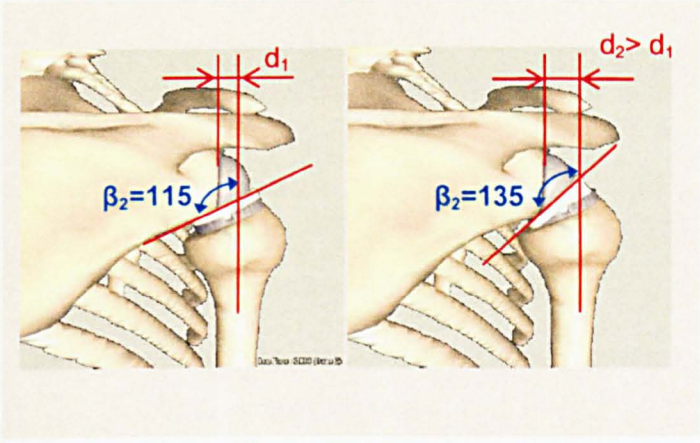

Figure 5.41

An increase of the neck/shaft angle can also increase the distance between the centre of rotation and the humeral shaft. This can affect the muscle moment arms but the change is not large

A change of the distance *'d'* also means a change in the elevating moment arm of the m.Deltoid, but overall it is rather small. The model shows that an increase of β_2 by 5, 10 and 20 deg. results in an increase the m.Deltoid moment arm by 2.5%, 4.9% and 5.4% respectively. This has a very small effect in the total GH contact load and the loadsharing results showed a maximum average (for the three standard activities) difference of 0.05 and 0.07 times BW for β_2=125 and 135 deg. respectively.

However, the trace of the contact force on the cup frame is projected inferiorly as the β_2 was increased. The stability of the joint was not compromised in any case but the maximum shear/compressive force ratio (in the cup frame) was increased. For example, in abduction the ratio of shear/compressive for β_2=115 is equal to 0.38 and is increased to 0.51 and 0.79 for β_2=125 and 135 deg. respectively with the maximum allowed ratio for the standard design cup being 1.86.

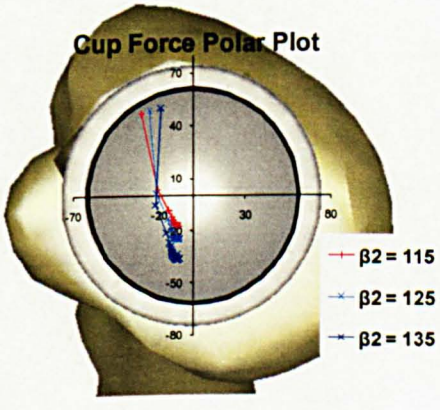

Figure 5.42

As the neck/shaft angle increases by 10 deg. the shear/compressive ratio of the contact force on the cup frame more than doubles (105.8% increase – increased risk of dislocation)

The change of neck/shaft angle of the prosthesis can also affect the impingement. As was mentioned, by increasing the value β_2 the cup moves superiorly on the sphere

surface, reducing the risk of the cup contacting the scapula border. The results show that by increasing β_2 by 5, 10 and 20 deg. there was less inferior impingement with the cup impinging the scapula in 28.2 deg., 24.2 deg. and 14.5 deg. of arm elevation (compared with the 33.3 deg. of the standard design). Unfortunately though, there is an opposite effect on the superior impingement where more bone contact was detected earlier during the high degrees of arm elevation (110.8 deg. 106.1 deg. and 94.8 deg. respectively - Figure 5.42). The overall range of motion was slightly reduced.

	Standard Fixation	**Neck/Shaft angle β2 (degrees)**		
Impingement	β2=115 deg	β2=120	β2=125	β2=135
Inferior (deg.)	33.3	30.1	27.1	24.1
Superior (deg.)	116.3	110.8	106.1	94.8
range (deg.)	83	82.6	81.9	80.3

Table 5.7: The effect of neck/shaft angle of the prosthetic stem on the impingement results

5.6.3. Summary and discussion on the fixation and design factors of a reverse prosthesis

From the results it is obvious that the position of the fixation of the glenoid sphere does not affect the contact or the muscle loading. In contrast, the impingement can be affected and the model showed, when the sphere was fixed within the reamed glenoid boundaries and without overstretching the deltoid, that inferior placement of the glenoid fixation can reduce the problem but it is difficult to eliminate it completely. The absolute lengthening of the deltoid depends also on the physical size of the skeleton, but given the large size male skeleton used in this study, deltoid over-stretching can potentially damage the axillary nerve. Subject-specific pre-operative planning could estimate deltoid lengthening and recommend optimum inferior fixation and prosthesis size.

It was also clear that reaming the glenoid was had a negative effect on the impingement where an oblique glenoid osteotomy did not show great potential compared with the inferior fixation. More significantly, such a glenoid reaming can create a more difficult and narrower fixation surface as shown by Nyffeler et al. (2005) where inferior fixation becomes more difficult.

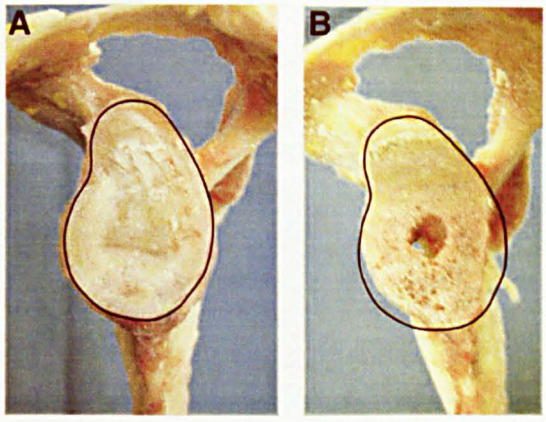

Figure 5.43: Lateral views of a shoulder specimen before (A) and after (B) an oblique resection of the glenoid was performed to increase the inclination angle. The oblique osteotomy resulted in a substantial reduction of the surface area necessary to fix the glenoid sphere (Adapted from Nyffeler et.al., 2005)

Under an oblique osteotomy or excessive reaming the scapula border can be exposed under the sphere, creating a hinge mechanism for the humeral cup. This can be a potential problem and risk for dislocation, since at lower degrees of elevation the contact of the outer rim of the cup with the flat reaming bone can create a hinge that will force the cup to dislocate from the joint.

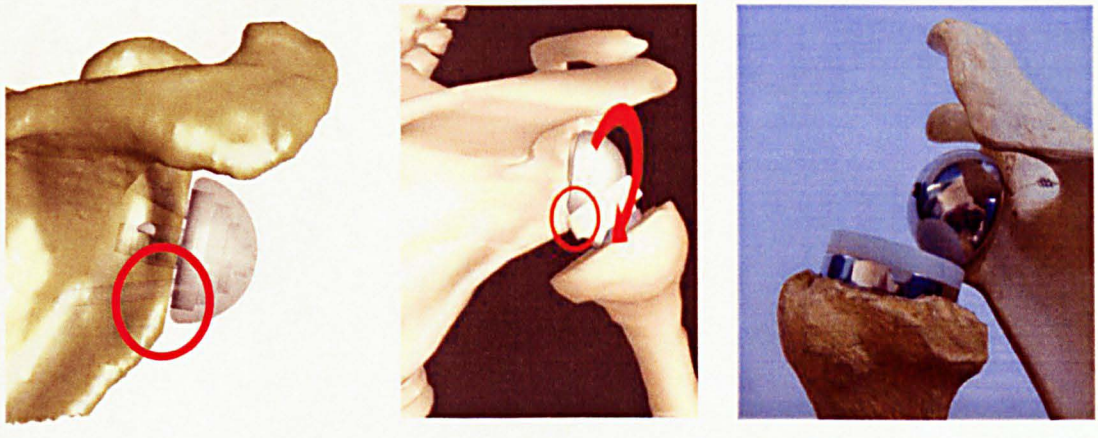

(a) (b) (c)

Figure 5.44: An extreme oblique osteotomy can expose the bone of the inferior scapula border underneath the sphere (a) creating a hinge mechanism (b) and causing possible dislocation of the joint (c).

The above clearly suggests that a face glenoid reaming will optimise the inferior fixation and thus reduce the impingement. This has also been supported by Simovitch *et*

al. (2007). They showed reduced notch volumes on scapulae with small progression border angles and face reaming.

Choosing the correct version for the stem fixation should depend on any remaining RC muscles after the joint replacement. Considering the type of the prosthesis and the clinical recommendation for use of reverse designs (massive RC tears), m.Teres minor is probably the only muscle that could be present after the joint replacement. The latter can justify why a more neutral fixation is mostly preferred in clinical practice. Nevertheless a stem fixation can change the range of internal/external humeral rotation due to impingement. A further investigation on the range of humeral rotation will be carried out in chapter 9, where impingement and scapular notch predictions are estimated during activities of daily living.

In general, changing the geometry of the prosthesis had a larger impact on joint stability and impingement compared to the surgical modification. Creating a shallow cup is an attractive solution to reduce the problem, but it can also affect the joint stability. The standard activities simulated in this study can provide a good understanding of the biomechanics of the reverse prosthesis, but they cannot represent the full range of loading during activities of daily living. An optimum cup design should have the minimum possible depth whilst also providing sufficient stability to a wider range of motion that is expected to be performed by reverse prosthetic subjects (Kontaxis A et al. 2007). Again, further investigation of GH loading will be investigated in chapter 9.

Changing the shape of the glenoid sphere by lateralising its centre (c>0) was also a highly efficient way to reduce impingement. Even if this is an attractive solution, there are considerations of excess stresses created by the bending moments of the contact forces. Harman *et al.* (2005) tested a sphere with a 6mm lateralised centre fixed on a polyurethane foam to find that the bending moment on the fixation was 69% greater than in the DELTA® III sphere (where c=0) rising fixation strength considerations over long term fatigue.

5.7. Conclusions – Stability over mobility

The preliminary results of this chapter clearly showed the advantages of a reverse prosthesis in a shoulder with RC tear pathology, where the increased deltoid moment arm helps the muscle to elevate the arm compensating for the dysfunctional RC muscles. The prosthetic design also reverses the envelope of the forces providing a large glenoidal surface and stability to the increased shear forces.

The biomechanical model also confirms the impingement as the main problem on the reverse prosthesis. The results show how the implantation can affect the impingement

and suggest an optimum fixation inferiorly placed on a non-oblique osteotomy. Anthropometric differences can affect the fixation, which is subject to limitations of bone stock and maximum deltoid lengthening, suggesting that pre-operative planning and guided implantation can help provision of the optimum fixation.

The results also show that the impingement and the stability of the joint are, in some cases, antagonistic factors cancelling each other out when changing the prosthetic design parameters. In general, results suggested that less impingement might also mean reduced joint stability or high fixation stresses. A solution to the problem is an optimisation of the design based on an objective function that can be related to the expected kinematics outcome of the joint replacement.

Chapter 6. Adaptation of Scapula Lateral Rotation after Reverse Anatomy Shoulder Replacement[3]

6.1. Introduction

The large range of available motion of the human arm is a result of the combined motion of the humerus, scapula and clavicle. In order to understand the detailed nature of this complex motion of the shoulder mechanism, there have been numerous studies of the scapula motion of normal subjects. The early two dimensional radiographic studies of scapula plane abduction (Freedman & Munro 1966;Inman et al. 1996) identified largely linear relationships between scapula and humeral abduction angles. In a second study, Poppen and Walker (1976) examined the scapula motion of a further group of normal subjects together with patients having a variety of shoulder pathologies. For the normal subjects, they found a ratio between total arm abduction and the angle of the scapula of 5:4 (Poppen & Walker 1976); the equivalent ratio of the patient group was widely variable with a tendency for a smaller glenohumeral contribution to arm abduction thus raising the question as to how scapula motion may be affected by shoulder pathology.

The complex 3-D movement of scapula is difficult to measure from two dimensional studies and de Groot (1999) showed that the range of results reported from radiographic studies could be explained by the variability in radiographic alignment. In order to meet the requirements to measure the complex scapula motion, palpation techniques were developed. First Pronk & van der Helm (1991) showed an instrumented three dimensional palpator, which was used to determine the positions of bony landmarks of the arm, trunk and scapula thus enabling calculation of the scapulothoracic and glenohumeral angles. Johnson et al. (1993) proposed the use of a palpation fixture having three palpation points connected to a rigid frame in an attempt to develop a more convenient technique for clinical use. The relative positions of the frame, arm and thorax were measured using an electromagnetic movement measurement system. In a subsequent study (Barnett et al., 1999) the technique was shown to be reliable and repeatable. A similar method has been used by Meskers et al. (1998) who further demonstrated its reliability.

[3] The material of this chapter is published in the journal of Computational Methods in Biomechanics and Biomedical Engineering, 2008, February; 11(1): 73-80, "Adaptation of scapula lateral rotation after reverse anatomy shoulder replacement".

As it was mentioned previously in this thesis, the reverse anatomy shoulder replacements have become increasingly popular, particularly for patients with rotator cuff arthropathy. In the previous chapter we analysed the biomechanics of the reverse prosthesis (for a DELTA® III design) using an interactive shoulder model (NSM) and comparing it with the function of a normal shoulder. In order to increase the comparability between the prosthetic and the normal shoulder, the arm and scapula kinematics were not modified for the two models. For a full understanding of the function of these prostheses, there is a need to measure the accompanying motion of the scapula and the aim of this chapter is to investigate and report any changes of the three dimensional scapula movements of these patients, using a validated palpation measurement technique.

6.2. *Materials and Methods*

6.2.1. Experimental set-up

Measurements were made using a published technique (Johnson et al., 1993) previously used in a study of scapula kinematics of young healthy shoulders (Barnett et al., 1995). The experimental set-up uses the ISOTRAK II™ (Polhemus Navigation, USA), a 6 degree of freedom electromagnetic movement sensor, consisting of an electromagnetic source producing low-frequency waves received by a 3-axis sensor; both source and sensor are hardwire connected to an electronics base unit which can communicate with a computer through a serial connection.

In order to measure scapula movement, a special custom-designed fixture was used together with the electromagnetic device - the Locator. The Locator has legs specially designed to enable repeatable positioning over the most palpable bony landmarks of the scapula (Johnson et al., 1993) (Figure 6.1) as follows:

i) the posterior angle of the acromion,

ii) the root of the scapula spine and

iii) the inferior angle.

The palpating legs could be adjusted along slots on the base plate in order to match and have the best possible contact with the bony landmarks. According to this arrangement, the axes of the electromagnetic source of the ISOTRAK system were aligned with the plane defined by the three contact points of the scapula landmarks.

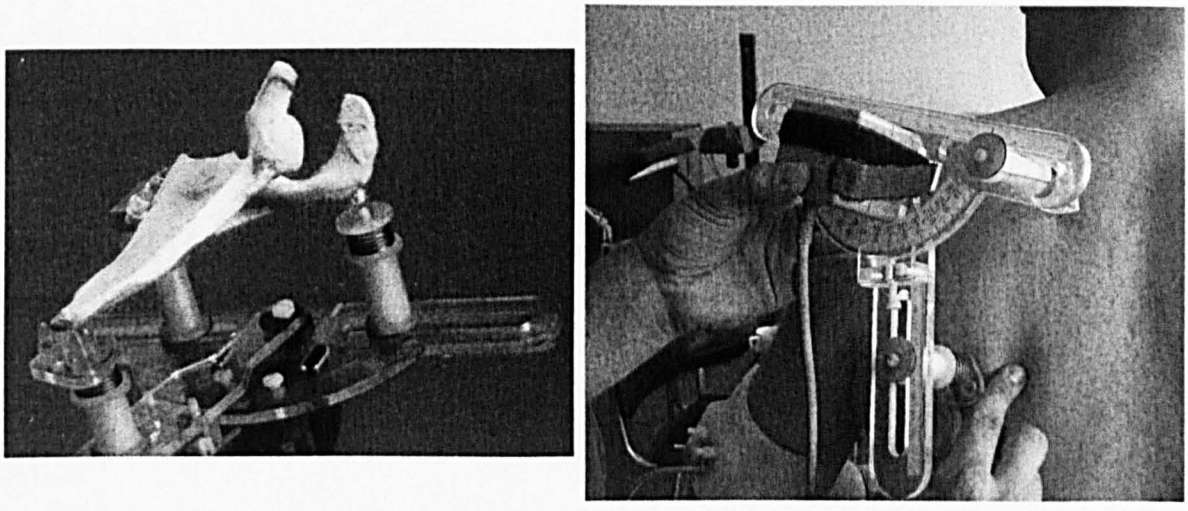

Figure 6.1:a) The scapula palpator is adjustable and specially designed in order to locate the most palpable landmarks of scapula b) The data can be recorded in static humeral positions and after palpating and locating the position of the scapula anatomical landmarks

The spatial position of the Locator was determined by the transmitter of the Isotrak II™ system. One of the receivers was mounted on an adjustable support and taped over the manubrium sterni using a mount which allowed the sternal receiver to be mounted vertically with respect to the global (laboratory) frame indicated by a bubble level. Before the receiver was taped, the subject was asked to stand in an upright position with the back against a wall. With this arrangement the alignment of the frame of the receiver matches the alignment of the thoracical frame (ISG, 1998 – Figure 6.2)

Because a direct measurement of the arm position was required, a second receiver was fixed to the arm using a moulded polythene arm splint having the elbow fixed at 90 degrees (Figure 6.2). The purpose of the flexed elbow was first introduced (Barnett et al., 1999) in order to distinguish clearly between forearm prono/supination and humeral internal external rotation.

Custom software was developed to determine the position of the arm in the frame of the receiver mounted on the sternum. This was then displayed as a real time feedback in terms of the azimuth, elevation and roll of the humerus.

Figure 6.2

Placement of the tharacical and arm receiver. An elbow splint was used in order to avoid confusion between humeral rotation and forearm pro/supination during the elevating tasks.

6.2.2. Kinematics and scapula rotation definition, measurement and task protocol

The arbitrary axes of the scapula were defined by the locator and the magnetic tracking device and converted to anatomically appropriate embedded scapula axes (Figure 6.3). In contrast with the studies of De Groot and Karduna the thoracic and humeral frames were defined with the help of the alignment of the bubble level and the elbow splint (Barnett et al., 1995), instead of digitising extra anatomical landmarks.

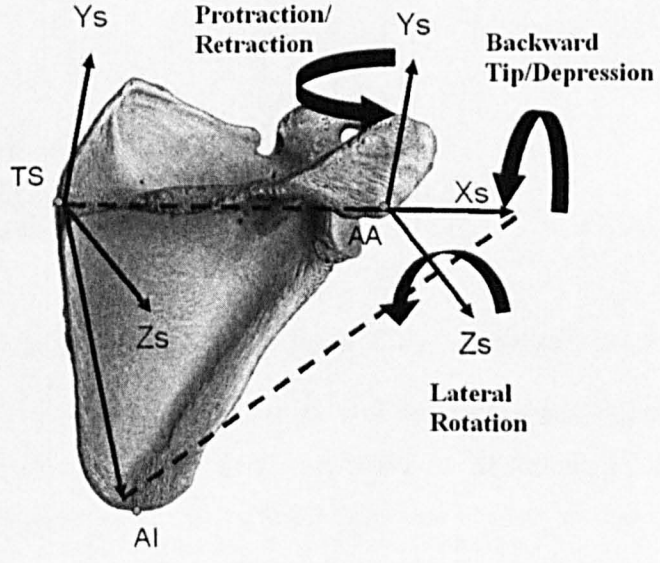

Figure 6.3

The definition of the scapula frame according to the anatomical landmarks. The scapula rotations are modelled as rotations around the anatomical axis of the embedded anatomical coordinate frame

Segment	Rotation Sequence	Rotation Terminology (in order specified)		
Scapula	$Y,Z'X''$	Scapula Protraction	Scapula Lateral Rotation	Scapula Backward Tip
Humerus	Y, Z', Y''	Humeral Azimuth	Humeral Elevation	Humeral Internal Rotation

Table 6.1: The rotation sequence of the humeral and scapula motion with respect to the thoracic frame and the corresponding clinical terminology

The directional sine and cosine of the transmitter and the receivers were recorded during the measurements and standard matrix transformation methods were used to determine the rotation matrix of the humerus and scapula with respect to the thorax (van der Helm & Pronk, 1995). Humeral and scapula rotations were calculated decomposing the Euler sequence that is used by the Newcastle Shoulder model (described in Chapter 4) and was first proposed by the International Shoulder Group (ISG - (van der Helm, 1996)). A short description/reminder of the rotation sequences and the clinical relevance is described in Table 6.1.

The scapula rotations initially were recorded with respect to the thorax, but were post processed and finally analysed in the local scapula co-ordinate system; initial resting scapula position was measured with the arm in the resting position and then the scapula motion analysed in respect of the initial scapula position. This is an effective way to minimise the effect of the anthropometric differences between the subjects (Barnett et al., 1995) and exclude the large variability of scapula resting position that has been recorded even within the normal population (Pronk 1991).

6.2.3. Data collection and task protocol

A total of 3 tasks were studied:

(1) Elevation of the arm in the frontal plane,

(2) Elevation of the arm in the scapula plane

(3) Forward flexion of the arm.

All the tasks started from 10 degrees and up to the maximum arm elevation possible. Data were collected at 20 degree increments from the starting position. Because the maximum arm elevation of each subject was variable, more points (every 10 degrees) were collected for some subjects in order to collect enough data within the functional range of the arm movement.

In contrast with the dynamic recording activities of the latest scapula kinematics studies (Karduna et al., 2001), due to the nature of the palpating technique, the recordings of the scapula position were taken in discrete static positions. The subjects elevated the arm and the exact position was evaluated each time by the visible feedback of the humeral position on the computer screen. Prior to collecting data for each motion, a couple of practice trials were performed. The investigator could monitor real-time humeral motion, which was displayed on a computer screen, and provided the subject with feedback. The subject was instructed to maintain a forward gaze and not to look either at their arm or the computer screen during the experiment. As with the practice trials, the investigator was able to monitor the humeral motion pattern during the data collection and give feedback for correct humeral position.

Data were collected for 10 subjects: 10 shoulders in total. All the subjects had a reverse total shoulder replacement (DELTA® III) for more than 1 year and the average age was 67.7 (sd 13.5). There were 5 male and 5 female subjects and 4 out of 10 shoulders suffered from osteoarthritis, 2 from rheumatoid arthritis and 4 subjects from tumour in the humeral head. All the subjects were right handed but 4 of them had a non-dominant (left) shoulder joint replacement. The protocol for the left shoulders was the same, but all the measured data were mirrored before any analysis, since the definitions of the rotations and the euler sequences are only valid for the right arm.

The measurements took place in a clinical environment (Ravenscourt Park Hospital, Ravenscourt Park, London) with the presence of an orthopaedic surgeon and a chaperone (when necessary). All the subjects were previously informed of the measurement procedures and agreed to participate on the study by a formal letter sent prior to them, as it was described in the documentation of the ethical application, which was approved by the local ethical committee.

6.2.4. Validation of the device in prosthetic subjects

The palpating measurement technique is based on an electromagnetic tracking device ISOTRAC II™ (Polhemus Navigation, USA) and is validated for scapulohumeral kinematic measurements in healthy subjects. In order to investigate whether there is an influence of the metallic prosthesis in the measurements, a simple plastic linkage where only 1 DOF was adjustable was constructed. By adjusting the linkage it was able to simulate humeral abduction or forward flexion.

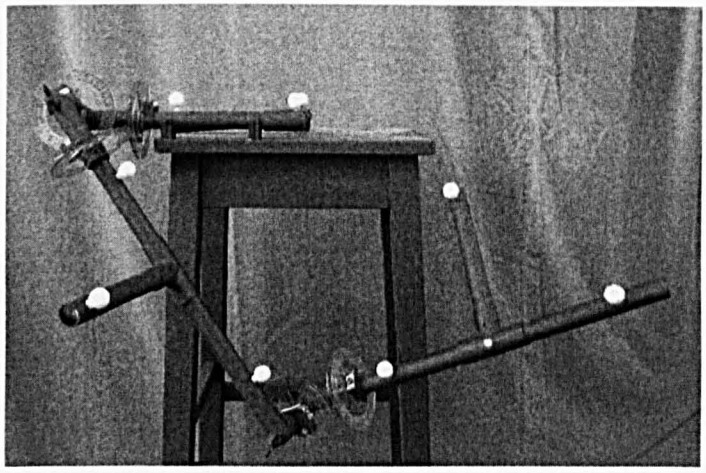

Figure 6.4: The simple plastic linkage mechanism could simulate abduction and forward flexion in order to investigate the effect of the metallic prosthesis on the measurements

The receivers and transmitter were placed in similar position to a subject set-up (defining thoracical, humeral and scapula plane), and simple tasks of abduction and forward flexion were simulated, starting from 10° to 120° with a 10° interval. The scapula palpator was kept fixed during the experiment. Humeral and scapula readings could be measured through the computer visual feed-back and with simple goniometers.

The two tests of abduction and forward flexion were repeated at 5 different fixed positions of the palpator and with and without the presence of a real DELTA® III reverse prosthesis attached to the plastic linkage.

6.3. Results

6.3.1. Sensitivity test

The sensitivity tests for the influence of the metallic prosthesis in the experimental set-up, showed that the DELTA® III does not affect the recorded output of the electromagnetic device. The differences in the recorded outputs of humeral and scapula angles, with or without the prosthesis, in all 10 recorded activities (5 abductions and 5 forward flexion with different fixed palpator position) showed that there was not a significant difference ($p>0.05$ with $a=0.95$, original hypothesis H0: average of differences between models with and without the prosthesis=0).

6.3.2. Subject studies

All the subjects were able to complete all 3 activities, but the maximum arm elevation within the activities and within the subjects were very variable. The lowest average value was for abduction with 95.81° (sd 8.01°) and the highest for forward flexion with 119.07° (sd 15.2°); the average elevation for scapula plane was 103° (sd 7.14°) – Table 6.2. All the maximum values of the lateral scapula rotation for each subject and for every activity were greater than the expected healthy scapula rhythm (Barnett 1996) (Figure 6.5). The average maximum lateral rotation was 49.57° (sd 4.92°), 50.57° (sd 2.58°), 52.98° (sd 4.96°) for abduction, scapula plane and forward flexion respectively. The corresponding values for the other two scapula rotations (Backward Tip and Retraction/Protraction) were much smaller and even if the averages were different from the normal scapulothoracic rhythm, were within the 95% Predictive Intervals (PI) of the generic model for healthy shoulders. Because of the uncertainty of the results in the above two rotations, the analysis of the results focuses only on lateral rotation of the scapula.

	Maximum Arm Elevation		
Subject	Abduction	Scapula Plane Elevation	Forward Flexion
1	77.8	100.0	99.1
2	95.8	92.7	90.9
3	95.8	92.7	100.9
4	90.0	94.5	108.3
5	82.1	90.5	118.6
6	84.2	89.4	94.8
7	87.7	91.3	118.3
8	91.2	103.4	119.1
9	91.4	92.2	102.1
10	70.9	76.2	69.9

Table 6.2:. Maximum arm elevation of all the subjects during the scapula measurements

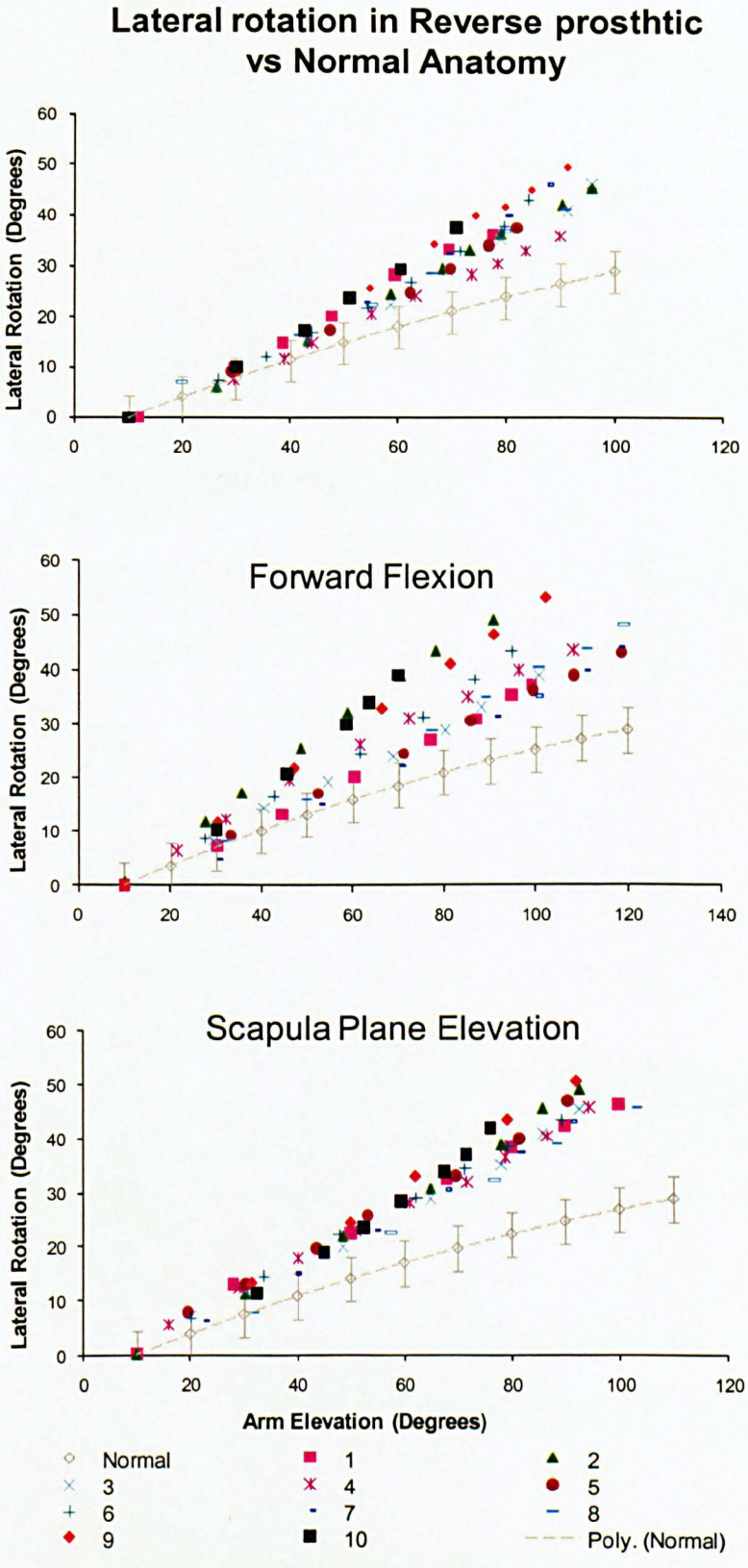

Figure 6.5: Recorded data of lateral scapula rotation compared with the predicted lateral of a healthy scapula rhythm (Barnett 1996) a) Abduction, b) Forward Flexion, c) Scapula Plane Elevation

6.3.3. Regression analysis

All the data were analysed in the local scapula frame of the resting position. In this way was possible to minimise the effect of anthropometric differences and investigate the scapula rotation from its resting position and for a certain arm elevation. Because of the variability of the maximum arm elevation within the subjects and within the three different activities, a comparison of average and maximum scapula rotation values could lead to wrong conclusions. For this reason the differences of the scapula lateral rotation have been calculated between the collected data and the corresponding predicted value for normal scapulothoracic rhythm (eq 6.1,):

$$\begin{aligned} Alpha = &- 0.0275 \circledcirc a + 9.74e\text{-}5 \circledcirc a^2 \\ &+ 0.3866 \circledcirc e - 6.48e\text{-}4 \circledcirc e^2 \\ &+ 0.0171 \circledcirc r - 1.06e\text{-}4 \circledcirc r^2 - 3.8184 \end{aligned} \qquad \text{eq. 6.1}$$

Where:

Alpha	Scapula Lateral Rotation
a	Arm Azimuth
e	Arm Elevation
r	Arm Rotation

In order to investigate the differences and define the changes in the scapulohumeral kinematics a regression analysis was performed in the calculated data. A linear and a quadratic model have both been analysed:

$$Alpha' = \beta \cdot e + c \qquad \text{eq.6.2}$$

$$Alpha' = \beta_1' \cdot e - \beta_2' \cdot e^2 + c' \qquad \text{eq.6.3}$$

Where:

$Alpha'$	Difference in Lateral Rotation
β, β_i'	Linear and quadratic coefficients
c, c'	constants

The regression analysis showed good correlation for both linear and quadratic models. The average R squared values for all the subjects and all the activities were 0.989 (sd 0.009) and 0.972 (sd 0.026) for the quadratic and linear models respectively. Because the correlation factor does not necessarily indicate the accuracy of the model, an analysis of the 95% of the Confidence Intervals (CI) of the errors (residuals) was also performed. For each activity and each model, the difference of the lateral rotation between normal and prosthetic shoulder was calculated from the recorded arm position. Then the error was calculated between: i) the predicted values (from the linear and quadratic models) and ii) the recorded differences. The 95% CI were calculated from the formula:

$$CI = c_a \cdot stdev_i \cdot \sqrt{\frac{1}{n_i}}\Bigg|_{a=0.95} \qquad \text{eq. 6.4}$$

where:

$stdev_i$	= Standard Deviation of the i^{th} sample
n_i	= number of the data of the i^{th} sample
c_a	= constant for level confidence a ($c=1.96$ *for* $a=0.95$)

All the 95% CI for each subject and for each activity are presented in Table 6.3 and Table 6.4. The results show that an increase in the order of the model does not affect the 95% CI for most of the subjects. Only the models of the subjects 3 and 9 showed inconsistencies within the 3 activities with the 95%CI being significantly smaller in the quadratic models.

Subject	1	2	3	4	5	6	7	8	9	10
Abduction	0.705	0.200	0.620	0.575	0.481	0.642	0.670	0.818	0.219	0.582
Scapula Plane	0.671	1.232	0.532	0.654	0.405	0.364	0.381	0.329	0.426	0.349
Forward Flexion	0.321	0.294	1.383	0.282	0.543	0.603	0.400	0.539	0.710	0.711

Table 6.3: 95% Confidence Intervals of the residuals for the Quadratic Model

Subject	1	2	3	4	5	6	7	8	9	10
Abduction	0.851	0.446	1.008	0.429	0.523	0.890	0.894	0.727	0.254	0.573
Scapula Plane	0.810	1.507	0.988	0.681	0.455	0.367	0.540	0.637	1.263	0.685
Forward Flexion	0.483	0.336	1.200	0.554	0.480	0.847	0.701	0.412	1.189	0.322

Table 6.4: 95% Confidence Intervals of the residuals for the Linear Model

The linear coefficients of the linear models in Table 6.5 represent the increase of the scapula lateral rotation in a reverse prosthetic shoulder in comparison to the healthy population. The average values of coefficient for Abduction, Scapula Plane and Forward Flexion were 0.261(0.055), 0.257(0.058), 0.215(0.111) respectively. The maximum and minimum values were observed within the subjects performing forward flexion, an activity that shows the biggest variability within the linear coefficients (min 0.105, max 0.440). The overall average of all the coefficients was 0.244 but the standard deviation was high (0.079). Four of the subjects showed a similar increase in lateral rotation (sd 0.245) during the 3 activities, three subjects showed a small difference in one of the activities (sd 0.453) and three more subjects indicated a much larger scapula adaptation within the 3 activities (sd 0.801). The last group includes the subjects that the linear model shows large 95%CI.

	Abduction		Scapula Plane		Forward Flexion	
Subjects	*c*	*β*	*c*	*β*	*c*	*β*
1	-4.525	0.251	-0.372	0.206	-2.124	0.165
2	-3.392	0.250	-5.054	0.241	-3.317	0.327
3	-3.580	0.244	-3.290	0.227	-1.879	0.105
4	-0.013	0.189	-0.736	0.209	0.001	0.160
5	-2.348	0.243	-2.326	0.273	-2.504	0.124
6	-3.425	0.273	-1.556	0.233	-2.560	0.209
7	-3.347	0.295	-3.336	0.233	-1.649	0.120
8	-1.197	0.183	-3.298	0.221	-2.601	0.177
9	-3.711	0.330	-1.470	0.368	-0.576	0.322
10	-3.024	0.355	-4.799	0.355	-4.155	0.440

Table 6.5: The constant and the linear coefficient of each subject in every activity of the linear models that describe the increase of lateral rotation in a prosthetic shoulder

6.4. Discussion

With the development of sophisticated three-dimensional shoulder models (Charlton & Johnson 2006;van der Helm 1994), accurate description of scapula motion on the thoracic cage is of great importance. Since the scapulothoracic rhythm can affect the stability and loading of the shoulder, customisation of models with patient specific scapula kinematics is necessary when investigating shoulder pathologies.

Evidence exists that adaptation to scapula motion is related to shoulder pathology (Johnson et al. 2001). There are studies based mainly on medical imaging or electromagnetic palpating tracking devices, correlating the change in scapulohumeral kinematics with specific shoulder pathology like impingement or rotator cuff tears (Hallstrom & Karrholm, 2006, Lukasiewicz et al., 1999, Mell et al. 2005). The results always report a statistical significance in the change of the scapula motion when compared to normal scapula rhythm, but the results also indicate large variability within the pathological shoulders.

In this study a static palpation method that has been shown to produce reliable measurements was used to record possible changes on the scapula rhythm after reverse total shoulder arthroplasty. A disadvantage of the palpation approach is the near

impossibility of making dynamic measurements of the scapula moving beneath the skin. To overcome this limitation, Karduna et al (2001) have made measurements using an electromagnetic sensor attached to the skin overlying the acromion. Since then several studies replicated this method to investigate scapula kinematics in healthy or pathological shoulders (McClure et al., 2006, Mell et al., 2005). A recent study by Meskers et al., (2007) also suggests that there is a good agreement between dynamic and static palpating techniques, but there is a deviation on the recorded scapula rotations in the higher degrees of arm elevation (more than 120 degrees). However both of the studies were performed in young healthy subjects and in addition they report that a single sensor attached on the acromion site can be affected by the anthropometric differences and especially the soft tissue and fat concentration around the sensor attachment point. In pathological shoulders (where often correlates with older age and loose skin) glenohumeral motion is likely to be compromised (De Wilde et al., 2005, Kontaxis & Johnson, 2008) and the technique of dynamic scapula tracking is still uncertain. Therefore upper arm motion analysis recommendations have proposed static measurements for the investigation of scapula kinematics in pathological shoulders (Kontaxis et al., 2009).

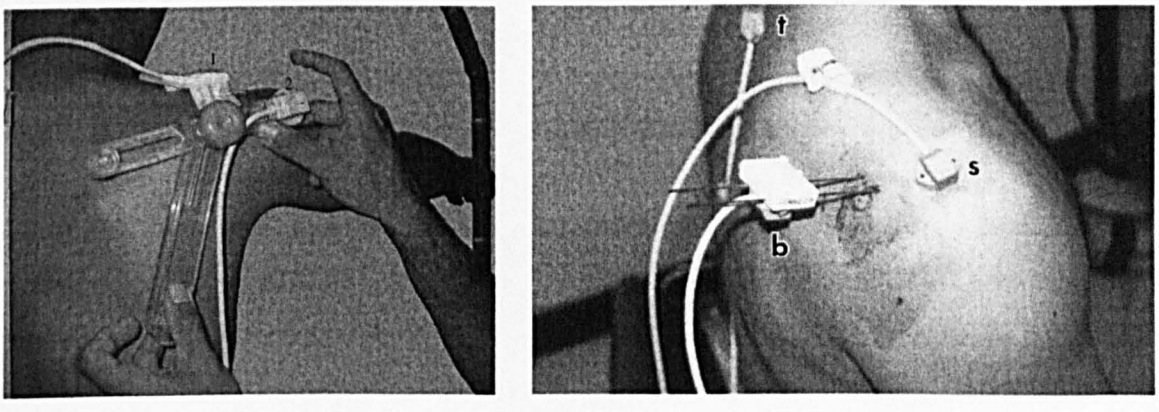

(a) (b)

Figure 6.6: The dynamic scapula measurements can be performed with a single sensor placed on the scapula and close to the acromion. The method has been validated only for young healthy subjects and show good accuracy for measurements up to 120 degrees of arm elevation (a) Validation of dynamic scapula measurements with a palpator - adopted from (Meskers et al., 2007) (b) Validation of dynamic scapula measurements with bone fixed pins - adopted from (Karduna et al., 2001)

Using the dynamic measurement technique, Mell et al. (2005) have recently published a study comparing scapula kinematics of a group of healthy shoulders with a

series of 14 shoulders suffering from rotator cuff tears. In this study the subjects had a smaller average humeral elevation (85.6°) but the average lateral scapula rotation was increased by a similar amount (linear coefficient of increased scapula rotation: 0.21 – 0.16 for phase 1 and 2 respectively). In the same study the authors also reported that the change in the other two scapula rotations had no statistical significance from the healthy group.

There are limited published data for scapula kinematics in patients after total shoulder replacement. A study from de Wilde et. al. (2005), used the palpation method to evaluate the functional recovery of prosthetic patients using reverse shoulder prosthesis. The study is using scapulohumeral data to describe only the lateral rotation of the scapula during scapula plane elevation and calculate muscle moment arms. A group of 4 patients was reported to show an average increased scapula lateral rotation of 118% compared to healthy shoulders. This value is lower than the average value for scapula plane elevation found in this study (125.7%), but the small number of the sample limits further statistical analysis.

The results of the regression analysis show that the differences calculated from the increased scapula rotation and the normal scapula rhythm can be described with a linear relationship. This is in contrast with the study of Mell et. al.(2005), who reported a 3-phase scapula rhythm change in patients with rotator cuff tears. The fact can be justified by the difference of the shoulder pathology, but they may also reflect differences between the measurement techniques followed in the studies (static-palpating and the dynamic). Even if results from Mell show a good correlation with this study in phase-1 (early degrees of arm elevation), they also indicate a smaller increase of scapula rotation during phase-2 and a match to the normal scapula rhythm in the last phase-3 (the higher part of humeral elevation). In contrast the results of this study indicate a linear increase of scapula rotation throughout the range of humeral elevation.

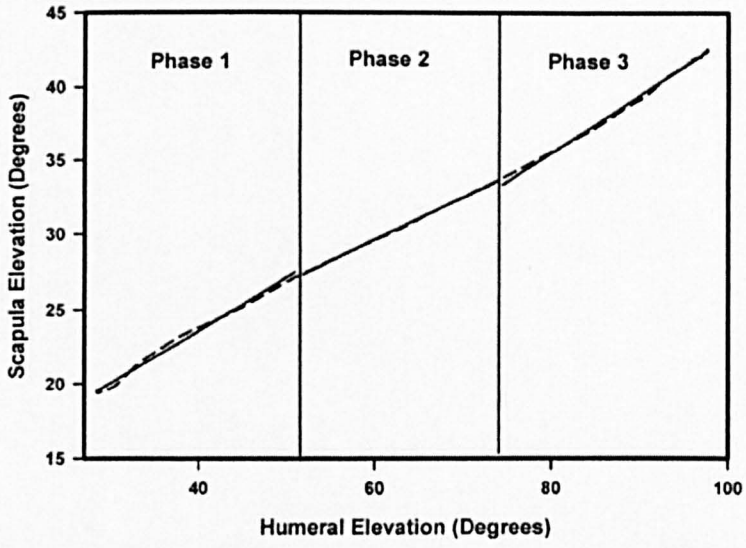

Figure 6.7: The three different phases reported in the scapula lateral rotation (referred as scapula elevation) by (Mell et al. 2005) can be an effect of the dynamic measurements that was applied in this study – adopted (Mell et al. 2005)

The results from the residual analysis indicate that a linear fit of the calculated differences provides a good correlation. For most of the subjects, an increase of the order to a quadratic model does not decrease significantly the 95% CI of the residuals. For some subjects, however, (subjects 3 and 9) the R squared values and the 95% CI indicate that the rotation of the scapula does not have a linear increase compared to the normal rhythm. Analysing further the specific data, it becomes clear that lateral rotation has two phases in which the rate of lateral rotation is seen to increase above an abduction of 40 deg. The mechanism for this different change is not clear but it maybe a result of impingement or human error during the palpating measurements.

It is difficult to compare directly the recorded data of the increased scapula lateral rotation within the subjects of the group. The maximum rotation (52.98°±2.51°) was observed at 102.98°±2.12° of forward flexion which was not the maximum arm elevation (119.07°±2.12°) for that subject. Since the maximum arm elevation for each subject and each activity is different, the linear coefficient of the differences between the recorded values and the expected normal scapula rhythm is a better indication of the adaptation (increase) of the scapula rotation. This coefficient actually shows a decrease in the GH joint rotation indicating joint stiffness after the joint replacement. However, it should be remembered that the values of all the coefficients of this study are highly variable. A second regression analysis with the modelled values was performed in an attempt to create a generic model that describes the increased scapula rotation. The mean

coefficient was 0.220 with a poor correlation (R squared 0.633), but an error analysis showed that the 95% of the Predictive Intervals for the estimated error are very large (9.490°).

Since there are studies indicating that adaptation to scapula motion is related to shoulder pathologies (Hallstrom & Karrholm, 2006, Johnson et al., 2001, Lukasiewicz et al. 1999, Mell et al., 2005) a further analysis of the data was performed to show if there is any correlation of the increased lateral rotation with the sex, age or shoulder pathology of the group. A factorial analysis of the variance of the sample did not reveal any significant trend since the size of the sample is rather small (n=10). A similar study with more subjects could be more conclusive.

Even though there was a large variability within the results, there was a correlation between maximum arm elevation and the recorded scapula rotation. From the linear correlation (that shows the increase of the scapula lateral rotation compared to the normal scapula rhythm) it seems that the lower the maximum achieved elevation the larger the scapula rotation increase (larger coefficient). The graph in Figure 6.8(a) shows the correlation of the mean "linear coefficient" of each subject (for all 3 activities) with the corresponding mean "maximum achieved humeral elevation" during the recorded activities. The original correlation factor for all the subjects is not strong (R squared: 0.573). Investigating the correlation further, the residuals of each point (to the linear regression) in Figure 6.8 were calculated. A Kolmogorov-Smirnov normality test showed that the residual data are normal (P=0.150>0.05, H0:Sample is normal), but one of the residuals of the sample is significantly larger than the mean (subject no. 9). The probability of this residual to be in the normal distribution (mean x=-0.0016, sd=0.0441) is very small (Φ(-2.37)=0.0089) and, therefore, by applying the Chauvenet's Criterion it can be excluded from the sample. This is not a surprise if we consider that the linear model of subject 9 had the largest 95%CI of the residual errors of the recorded scapula rotations. The re-calculated correlation of figure 4, excluding subject 9, is increased dramatically to 0.829.

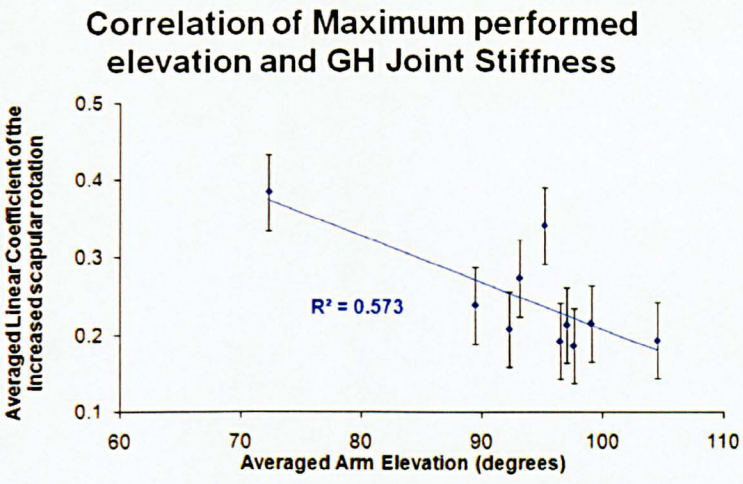

(a)

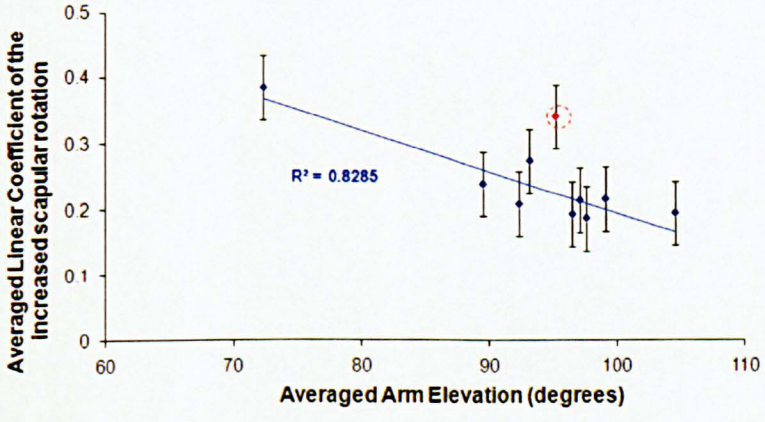

(b)

Figure 6.8:

There is a correlation between the averaged maximum performed elevation and the averaged linear coefficient of the increased scapula rotation that represents GH joint stiffness. The correlation is not strong (a) but one of the points has larger residuals from the rest of the points. By applying the Chauvenet's Criterion, we can exclude this point increasing the correlation up to 0.8285 (error bars=2 standard deviations)

6.5. *Effect of the adapted scapula kinematics in moment arms and GH loading*

The adaptation in the scapula kinematics can affect the biomechanical properties of the prosthesis. In order to investigate the effect of the scapula rhythm adaptation, the larger coefficients of the regressions (subject no.10) were applied to the reverse prosthetic model that was described in chapter 5. Three standard activities were again simulated: abduction, forward flexion and scapula .plane elevation.

The results of the model suggest that the moment arms of the muscles crossing the GH joint are not significantly changed (Figure 6.9). For example the peak moment arm of the middle m.Deltoid is almost unaffected (average increase 0.7 mm) with the largest

differences observed at the end range of the motion (higher than 90 degrees of arm elevation)

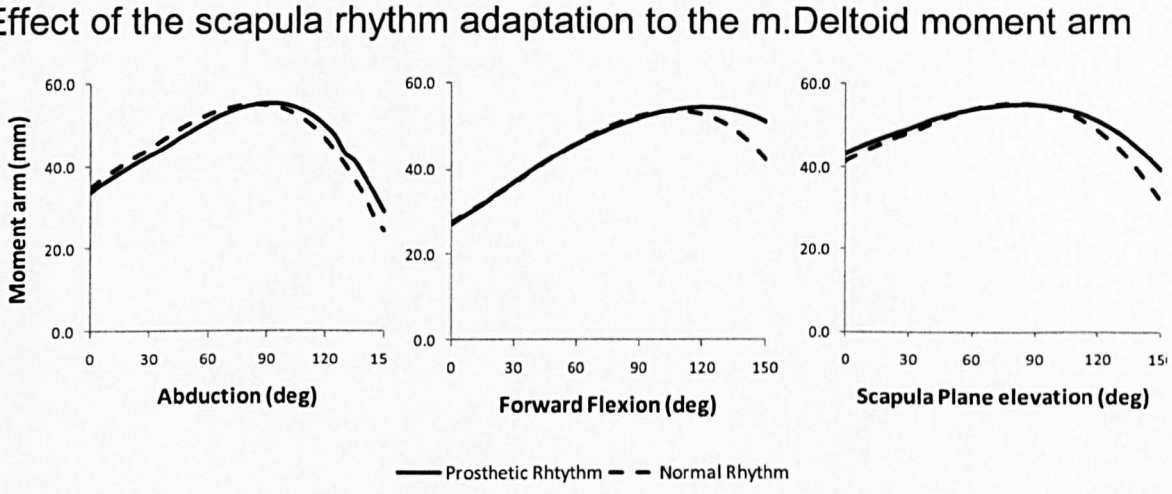

Figure 6.9: The increase of the scapula lateral rotation does not change the m.Deltoid moment arm significantly

The small difference in the moment arm also means small differences in the total GH loading. The total GH load was only 0.3 times BW smaller in average when the prosthetic scapula rhythm was simulated.

There was a bigger difference on the loading of the Glenosphere. Because of the more rotated position of the scapula, the GH loading is pushing the glenoid sphere in a more superior direction, increasing the superior shear forces (average increase of 19% in the 3 standard activities). The compressive forces are reduced by 12% where the impact on the antero/posterior shear forces was smaller (increase of 4% on the anterior shear forces during abduction, increase of 7% on the posterior shear forces during forward flexion).

The different scapula kinematics is also affecting the impingement problem. As it is expected the increased lateral rotation is also increasing the inferior impingement, since there is a contact of the cup with the scapula border in higher arm elevation. The results showed that inferior impingement occurred at 37.5 deg of elevation (average for the 3 activities), which is 4.2 deg more than the results with the normal scapula rhythm. In contrast the superior impingement was improved since the contact between the humerus and the acromion occurred also in higher degrees of elevation (average 121.1 deg instead of 116.3 deg of the normal rhythm). The impingement results reflect the linear increase of scapula lateral rotation and the small differences between inferior and superior impingement can be explained by the bone morphology.

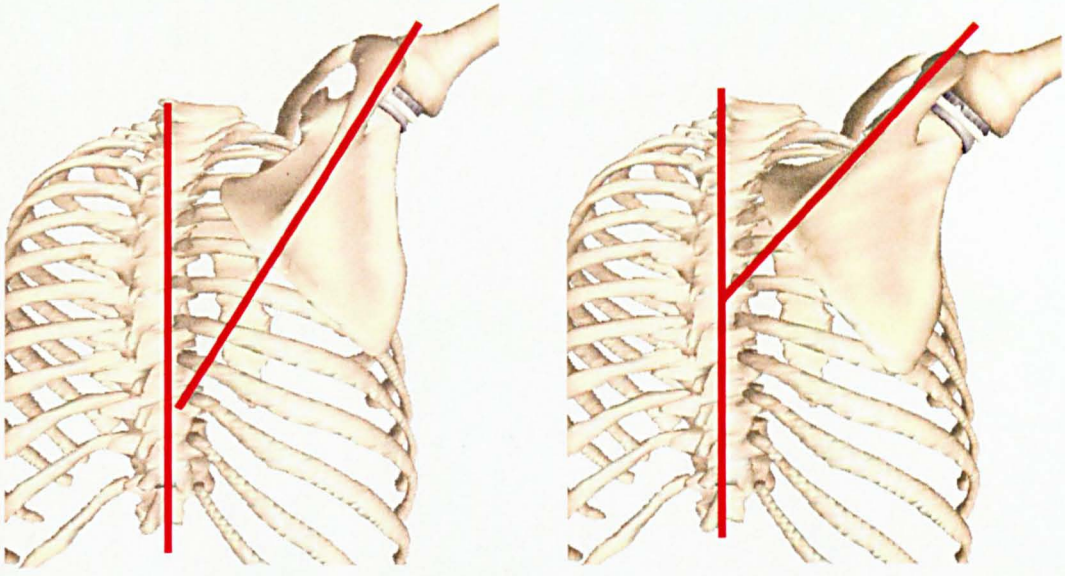

Figure 6.10: The increased lateral rotation can affect the loading of the on the glenoid sphere (increased superior shear forces) and the impingement (increased inferior and reduced superior impingement)

6.6. Conclusions

The results of this study clearly indicate that there is increased lateral scapula rotation in patients with reverse shoulder arthroplasty compared to healthy shoulders. However, the increase is highly variable within the subjects making it difficult to create a generic model. For this reason detailed customisation of biomechanical shoulder models with patient specific scapula rhythm should be considered in the case of biomechanical analysis of reverse prosthesis, since the kinematics adaptation can increase the shear contact forces on the glenoid site by 19%. All the regression data will be used in further chapters (7 and 8) in order to customise the model and compute muscle and joint contact forces for activities of daily living (ADLs) that have been recorded from the same prosthetic subjects

It is difficult to explain the reason behind the adaptation, since there is no clear indication which can correlate the increase of the scapula rotation (e.g. pathology, sex or age) with the recorded data. However, there is a strong trend showing that patients with good recovery and large range of humeral elevation after the surgery have small change in their scapula rhythm whereas those with muscle weakness and small range of movement minimise the glenohumeral rotation and have large scapula rotation. A pre

and post operative study of scapula kinematics with a large number of subjects would be required to give a clear indication whether the adaptation is influenced by the joint replacement and rehabilitation process or is connected only with shoulder pathology (Mell et al., 2005)

Chapter 7. Upper Arm kinematics analysis in reverse prosthetic subjects

7.1. Introduction

The use of motion analysis in clinical gait is established in the treatment of clinical conditions affecting the lower extremities (Gage 1994). Likewise, analysis of upper extremity function by means of 3-D kinematics can also be an important tool in clinical decision making and outcome measure in patients with upper extremity disorders. Quantifying upper extremity dysfunction, as seen in orthopaedic and neurological disorders, is technically complex because of the multi-joint structure and the variability of the possible movements.

Compared to gait analysis, motion analysis of the upper extremity carries several disadvantages, with the most important being that there is no single most relevant functional activity. However, while lower limb studies concentrate almost exclusively on gait, the tasks performed by the upper limb are much more varied and therefore, the necessary design data can only be collected using a variety of tasks which may be regarded as representative of normal daily activity. Several activities of daily living (ADL) have been suggested in the literature (Anglin & Wyss 2000a, Buckley et al. 1996, Murray & Johnson 2004, van Andel et al. 2008). Recently, it was attempted to implement functional tasks in clinical studies, but the variety of possible functional tasks complicates standardization procedures (Fitoussi et al. 2006,Petuskey et al. 2007).

This chapter presents a kinematics analysis of a group of subjects with reverse prosthesis shoulders, who perform a set of activities of daily living. Results will be compared with a set of normal subjects (with asymptomatic shoulders - control group) that performed the same set of activities in the same environment as suggested by Kontaxis et al. (2009). Also, the aim of the dataset is to be used as an input to the biomechanical shoulder model in order to investigate, in depth, more realistic GH loadings as well as the impingement problem that was presented in chapter 5.

7.2. Materials and methods of the kinematic recordings

7.2.1. Motion analysis system and experimental set-up

The measurements took place in a clinical environment (Ravenscourt Park Hospital, Ravenscourt Park, London) with the presence of an orthopaedic surgeon and a chaperone (when necessary).

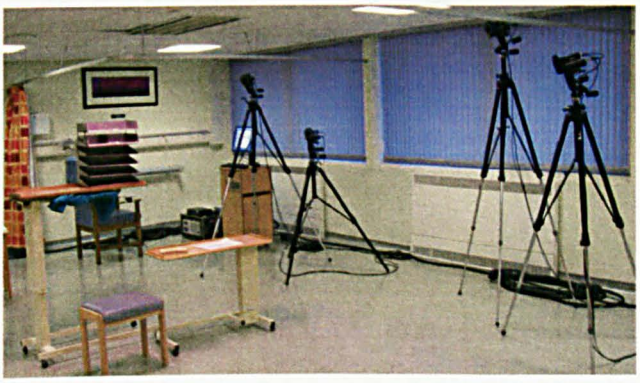

Figure 7.1

The kinematic recordings were captured in one of the wards of the Ravenscourt Park Hospital.

A VICON® optical motion analysis system (VICON® type 512) was used to record the kinematics data. This optical system uses cameras and image-processing technology to track reflective markers (Figure 7.2). For the specific set-up, 7 cameras sampling at 50Hz were used around the position of the subject. The cameras use infrared lighting to get high-contrast images of the high reflective markers. VICON then correlates the data from each camera to generate a three dimensional map of all of the markers. This results in a 3-D reconstruction of the captured movement. Those data are then extracted as trajectories (X, Y, Z trajectories) in large text files where they could be loaded and processed in Matlab and by the Newcastle Shoulder model's custom code.

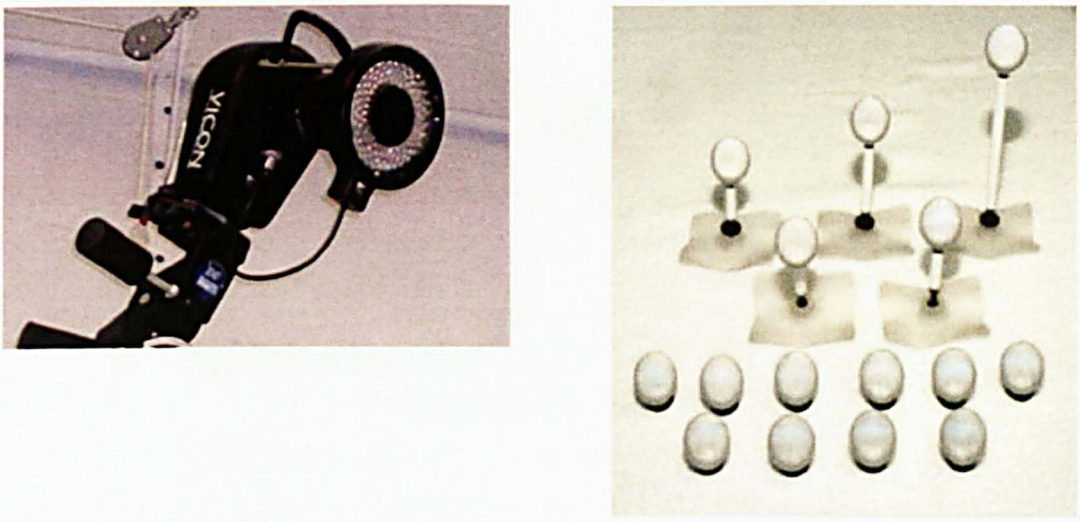

(a) (b)

Figure 7.2: The VICON system uses recordings from multiple cameras (a) which use infrared light to record high contrast digital images between the background and the reflective markers (b) and then correlate the data to generate a 3D map of all the markers

The main drawback of this optical technology is that each of the markers needs to be seen by at least 2 cameras at any time for its position to be interpolated correctly. Also, since VICON uses passive markers (they can only reflect and not emit light), they can not be differentiated. This makes the placement of the markers and the cameras very important in order to avoid marker obstructions.

The activities recorded in this study do not require a large workspace to be covered by the cameras, since they were all performed with the subject sitting on a stool. This allowed the cameras to be placed very close to, and around, the subject reducing the residuals on the 3-D reconstruction of the markers. Because of the high mobility of the upper extremity and the nature of the recorded activities, placement of the cameras was still challenging in order to avoid marker obstructions during the recordings. The optimal configuration was found to be a circular arrangement (around the subject), where four cameras are placed in front of the subject, one camera on the side of the performing hand and two additional cameras on the back. The cameras were placed in multiple levels in order to cover specific activities where marker visibility was difficult (hidden markers).

7.2.2. Marker set-up

In chapter 4 there is an analytical description of all the anatomical embedded frames of each segment. In order to track the frames with the VICON system they must be linked to a set of markers of the measurement system. This requires:

- to define marker locations over the subject's body, and
- to establish the relationship between the segment coordinate systems and the markers, which define the 'technical frames'.

On any limb segment, at least three markers must be visible at any moment to define its position and orientation in three dimensions and they should be as widely spaced as possible (Soderkvist & Wedin 1993).

Anglin and Wyss (2000b) have presented an extended review on marker set-ups and landmark location. However, no methodological study is yet available to recommend the optimum set-up for a specific type of pathology or group of subjects, where movement constraints, loose skin and fat issues can create inaccuracies (Kontaxis et al. 2009).

The positioning of markers on the upper limb presents particular challenges because of the large and complex excursions of the segments of the upper limb. It should be noted that marker placement over anatomical landmarks can create large skin artefacts (Cappozzo et al. 1996). Kontaxis et al. (2009) proposed – specifically for the upper limb marker placement – to:

- Not attach markers on anatomical landmarks, (e.g lateral and medial epicondiles),
- Use a set of markers on each segment ('technical markers') that is easy to track and allow the definition of intermediate co-ordinate frames ('technical frames') between the global (laboratory) and anatomical frames as described by Cappozzo et al. (1995)
- Use anatomical calibrations to define anatomical landmarks and thus anatomical axes and frames (Cappello et al. 1997,Cappozzo et al. 2005)

Considering all the above points, the current study follows the methodology of Murray (2000) and Murray & Johnson (2004), where they used four video cameras and APAS (Ariel Dynamics Inc, San Diego, CA, USA) software for 3D reconstruction of the markers to study the kinematics and dynamics of the upper limb of 10 healthy subjects performing 10 ADL. Reflective markers were attached at 10 locations on the upper limb and trunk to define all the technical frames, and static trials were performed in order to calibrate the anatomical landmarks of the 7^{th} cervical vertebrae, and the lateral and medial epicondyles (Figure 7.3). In his study, Murray also demonstrated that the data of the kinematic measurements can be inherently repeatable, i.e. there is good

repeatability between repetitions of the whole experiment (including the positioning of markers) on different occasions.

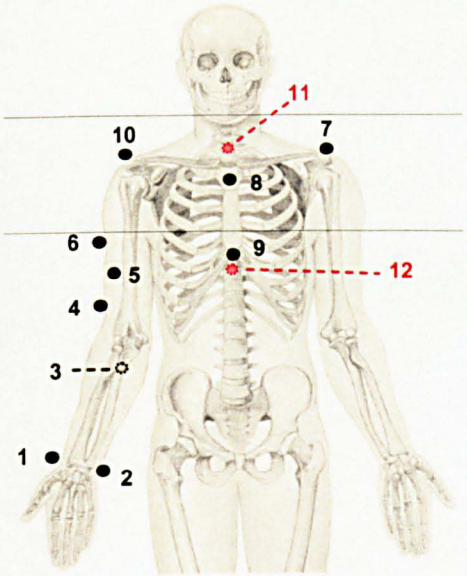

Figure 7.3:

The marker set-up that defines the technical frames of the upper arm. The placement of the markers 1-10 (black) follows the Murray and Johnson (2000) configuration. Two additional markers (markers 11 and 12 – red) were used to set-up an extra thoracic technical frame in order to minimise skin artefacts and obstruction of markers 8 and 9

Marker	Symbol	Attachment point	Marker	Symbol	Attachment
1	US	Ulnar Styloid	6	DI	Deltoid insertion
2	RS	Radial Styloid	7	LA	Left Acromion
3	PU	Proximal Ulna	8	MA	Manubrium
4	BI	Brachioradialis ins.	9	XI	Xiphoid Process
5	BB	Biceps belly	10	RA	Right Acromion
11	*C7*	*7th cervical vertebrae*	*12*	*T8*	*8th thoracic vertebra*

Table 7.1: The marker set-up

Technical Frames

Forearm	Humerus	Thorax1	Thorax2
$\overline{X_{Ft}} = \frac{(\overline{US} - \overline{RS})}{\lvert(\overline{US} - \overline{RS})\rvert}$	$\overline{Y_{Ht}} = \frac{(\overline{DI} - \overline{BI})}{\lvert(\overline{DI} - \overline{BI})\rvert}$	$\overline{Y_{Ht}} = \frac{(\overline{DI} - \overline{BI})}{\lvert(\overline{DI} - \overline{BI})\rvert}$	$\overline{Y_{Ht}} = \frac{(\overline{DI} - \overline{BI})}{\lvert(\overline{DI} - \overline{BI})\rvert}$
$\overline{Z_{Ft}} = \frac{(\overline{PU} - \overline{US}) \times \overline{X_{Ft}}}{\lvert(\overline{PU} - \overline{US}) \times \overline{X_{Ft}}\rvert}$	$\overline{X_{Ht}} = \frac{(\overline{BB} - \overline{DI}) \times \overline{Y_{Ht}}}{\lvert(\overline{BB} - \overline{DI}) \times \overline{Y_{Ht}}\rvert}$	$\overline{Z_{Tt1}} = \frac{(\overline{LA} - \overline{MA}) \times \overline{Y_{Tt1}}}{\lvert(\overline{LA} - \overline{MA}) \times \overline{Y_{Tt1}}\rvert}$	$\overline{Z_{Tt2}} = \frac{(\overline{LA} - \overline{T8}) \times \overline{Y_{Tt2}}}{\lvert(\overline{LA} - \overline{T8}) \times \overline{Y_{Tt2}}\rvert}$
$\overline{Y_{Ft}} = \overline{X_{Ft}} \times \overline{Z_{Ft}}$	$\overline{Z_{Ht}} = \overline{X_{Ht}} \times \overline{Y_{Ht}}$	$\overline{X_{Tt1}} = \overline{Y_{Tt1}} \times \overline{Z_{Tt1}}$	$\overline{X_{Tt2}} = \overline{Y_{Tt2}} \times \overline{Z_{Tt2}}$
Origin = US	*Origin = BI*	*Origin = MA*	*Origin = C7*

Table 7.2: Technical frames defined by the 12 markers attached on the skin. The Forearm, Humerus and Thorax1 are defined according to Murray & Johnson (2000)

Some changes had to be made to the anatomical calibration and marker placement in order to fit the definition of the new prosthetic model:

i) Murray uses a different definition of the anatomical trunk frame which is based only on the anatomical landmark of 7th cervical vertebrae (C7) and the markers of Xiphoid Process (marker 8) and Manubrium (marker 9) to define the thoracic superior axis – Figure 7.4. Extra landmarks had to be recorded since the anatomical trunk frame of the current model (as described in chapter 4) follows the ISG recommendations (van der Helm 1996) using the anatomical landmarks of the 8th thoracic vertebrae (T8), Jugular notch (JI), tip of Xiphoid Process (PX) as well as the C7.

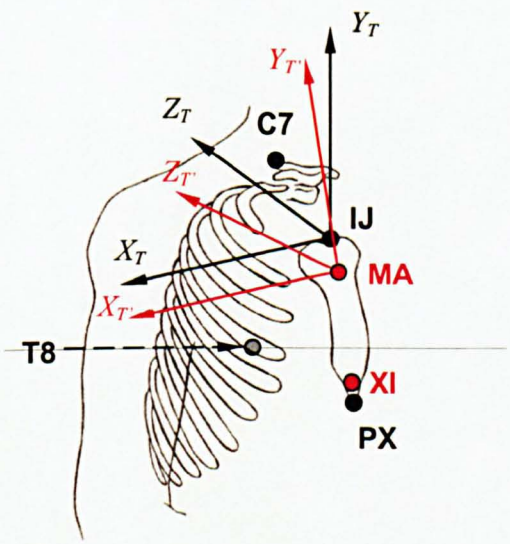

Murray & Johnson (2000)

$$\overline{Y}_{T'} = \frac{\left(\overline{MA} - \overline{XI}\right)}{\left|\left(\overline{MA} - \overline{XI}\right)\right|}$$

$$\overline{X}_{T'} = \frac{\overline{Y}_{T'} \times \left(\overline{C7} - \overline{XI}\right)}{\left|\overline{Y}_{T'} \times \left(\overline{C7} - \overline{XI}\right)\right|}$$

$$\overline{Z}_{T'} = \overline{X}_{T'} \times \overline{Y}_{T'}$$

Origin = MA

ii)

This study

$$\overline{Y}_T = \frac{\left(\overline{IJ} + \overline{C7}\right)/2 - \left(\overline{PX} + \overline{T8}\right)/2}{\left|\left(\overline{IJ} + \overline{C7}\right)/2 - \left(\overline{PX} + \overline{T8}\right)/2\right|}$$

$$\overline{X}_T = \frac{\overline{Y}_T \times \left(\overline{PX} - \overline{T8}\right)}{\left|\overline{Y}_T \times \left(\overline{PX} - \overline{T8}\right)\right|}$$

$$\overline{Z}_T = \overline{X}_T \times \overline{Y}_T$$

Origin = IJ

Figure 7.4: Differences in thorax anatomical frames used in Murray&Johnson (2000) and the current study, in which the anatomical frame follows the recommendations of International Shoulder Group

ii) In addition to the existing markers, two extra markers were placed close to the 7th cervical and 8th thoracic vertebrae and along the spine. Murray uses only 3 markers (markers 7, 8 and 9) to define a technical thoracic frame. The extra cameras of the

VICON system make it easy to follow the extra two markers on the spine and define an extra technical thoracic frame (Table 7.1). This extra frame helps to minimise skin artefacts from the thoracic markers by minimising any relative rotation between the two frames but, most importantly, it allows the reconstruction of the Manubrium and Xiphoid markers that can be obstructed during the movement of the upper arm during the recordings of the activities.

iii) In addition to the original static anatomical calibration, further anatomical landmarks were recorded (Table 7.3) in order to provide data for the clavicle and scapula lengths and resting positions as described by Charlton (2003). Those data are used by the Newcastle Shoulder model to define scaling factors to customise the skeletal structure to the individual subjects recorded with VICON.

The anatomical landmark calibrations were performed with a pointer constructed from a rigid rod with two attached markers at 300 and 600mm from the tip (the same pointer as used by Murray & Johnson).

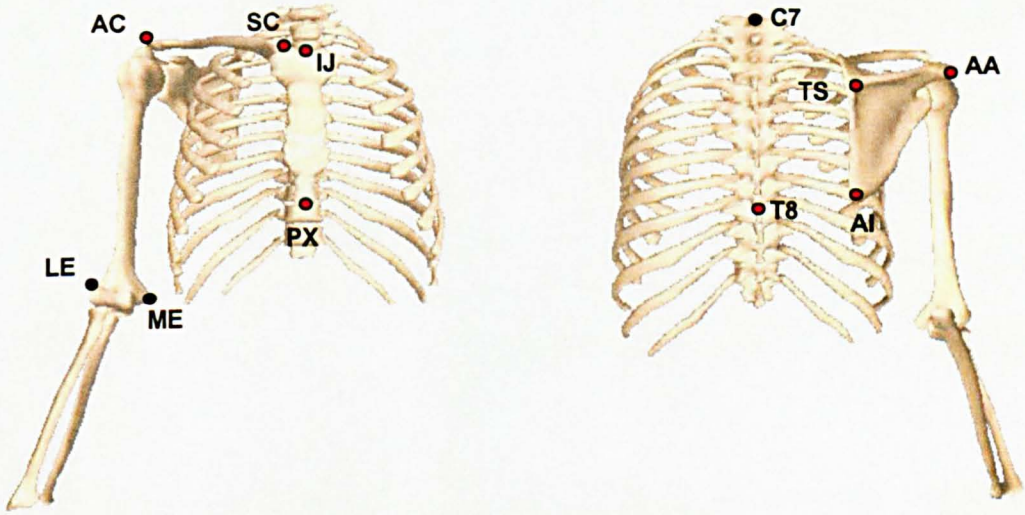

Figure 7.5: Anatomical landmarks calibration: i) Black dots are the landmarks as they used by Murray&Johnson (2000), ii) Red dots landmarks as they used from Charlton (2003) and the current study

Bony Landmarks for Anatomical Calibration			
LE	Lateral Epicondyle	AC	Acromioclavicular Joint
ME	Medial Epicondyle	SC	Sternoclavicular Joint
C7	7th cervical vertebrae	IJ	Incisura Jugularis (jugular notch)
T8	8th Thoracic vertebrae	AA	Angulus Acromialis (acromion tip)
AI	Angulus Inferior (inferior angle)	TS	Trigonum Scapulae (root of spine)
PX	Tip of Xiphoid Process		

Table 7.3: All the bony landmarks that were calibrated during the static trials (Figure 7.5)

7.2.3. The groups of subjects

A group of 12 subjects that had DELTA III joint replacement was selected to perform the set of activities that are described below (section 7.2.4). The same group also had scapula kinematics measurements (with the methods that were described in chapter 6), just after the VICON recordings. Unfortunately 2 subjects (in total 3 pathological shoulders) had to be excluded from the latter measurements due to technical problems of the scapula measurement system.

The DELTA group had an average age of 70 years (range 50 to 85) with an average weight and height of 67.0 kg and 166.8 cm respectively. The group was equally divided into 6 female and 6 male subjects. All of them had a right dominant hand side, but 6 out of the 12 subjects had a joint replacement on the non-dominant side. Interestingly only two subjects (subjects 2 and 9) were fitted with the larger size of the prosthesis (DELTA 42), which has a glenoid sphere diameter of is 42 mm. Unfortunately, excepting the size of the prosthesis there was no detailed information about muscle structure (e.g. size of the original RC tear pre-operatively) or whether there were any remaining RC muscles after the joint replacement.

Joint Replacement (DELTA) group

Subject	Age (years)	Weight (kg)	Height (cm)	Operated Arm	Dominant arm	Sex	DELTA® III size
1	67	73.0	169.00	R	R	f	36
2	80	79.0	185.42	R	R	m	36
3	65	59.0	172.00	L	R	m	36
4	63	94.0	170.18	R	R	f	36
5	85	44.0	144.78	R	R	f	36
6	67	81.0	160.00	L	R	m	42
7	70	56.2	157.50	R	R	f	36
8	65	66.0	162.50	R	R	m	36
9	50	89.0	177.80	L	R	m	42
10*	84	51.0	160.02	L & R	R	f	36
11	66	52.0	180.34	L	R	m	36
12*	83	60.0	162.00	L	R	f	36
Average	*70*	*67.0*	*166.8*				

**subjects 10 and 12 were the only subjects that were not included in the scapula kinematics study*

Table 7.4: Details of the DELTA III group. The same group also had scapula kinematics measurements (chapter 6) except for subjects 10 and 12

In order to be able analyse, in depth, the kinematics of the DELTA group, it is necessary to compare the kinematics with the normal population. There are studies that have shown that for normal (non-symptomatic) shoulders, even if there is inevitably a variation in executing the same tasks (by different subjects), the kinematic patterns show acceptable confidence intervals (Anglin & Wyss 2000a,Murray & Johnson 2004,van Andel et al. 2008).

Thus, a group of normal subjects (with non-symptomatic shoulder) were recorded to perform the same activities in order to act as a control group. The recordings were captured in the same environment using the same objects, since environmental changes can affect the kinematic output (Kontaxis et al. 2009). The control group consisted of 10 subjects but with a younger average age (ranging from 23 to 57 years old). Six out of ten subjects were male. 2 had a left dominant hand. All of the subjects performed the activities with their dominant hand.

Normal (control) group

Subject	Age (years)	Weight (kg)	Height (cm)	Dominant arm	Sex
1	37	70.0	170.2	L	f
2	23	70.0	183.0	R	m
3	50	69.0	162.5	R	f
4	24	61.0	168.0	R	f
5	45	80.5	177.8	R	m
6	57	78.0	175.3	R	m
7	25	50.0	160.0	R	f
8	27	73.0	182.0	R	m
9	26	73.0	180.0	R	m
10	32	80.0	183.0	L	m
Average	*35*	*70.5*	*174.2*		

Table 7.5: Details of the Normal (control) group. All the subjects performed the activities with their dominant hand

All the subjects were previously informed of the measurement procedures and agreed to participate on the study by a formal letter sent to them, as described in the documentation of the ethical application, which was approved by the local ethical committee.

7.2.4. Testing protocol

7.2.4.1. Calibration activities

Except for the anatomical landmark calibration, there is additional information needed in order to define all of the anatomical and functional frames of the upper limb. One of the points that cannot be calibrated, but is essential for the definition of the humeral anatomical frame, is the centre of rotation (CoR) of the GH joint. For the normal shoulder, Murray (1999) has developed a technique where the GH CoR can be found using certain regression equations that take into account the skeletal size and the position of the acromion.

This method is not valid for the prosthetic group, since the reverse joint replacement changes GH CoR in comparison to the normal shoulder (described in chapters 4 and 5). In order to define the new CoR, small circumductions of the arm were recorded with the VICON system. Since the arm is moving around the glenoid sphere, all the humeral markers (markers 4, 5 and 6), should move on a surface of a sphere with constant radius. Thus using a simple sphere regression algorithm and minimising the error of all

three markers, it was possible to define and express the new CoR in relation to the humeral technical frame.

In order to decrease the errors of the procedure and produce consistent results, the circumductions were assisted by the orthopaedic surgeon. The subjects had to relax their arm while the surgeon was a) guiding their arm in small circumductions and b) suppressing the scapula (by pressing the top of the acromion) in order to minimise any scapula motion. The procedure was repeated 3 times for 3 different humeral positions.

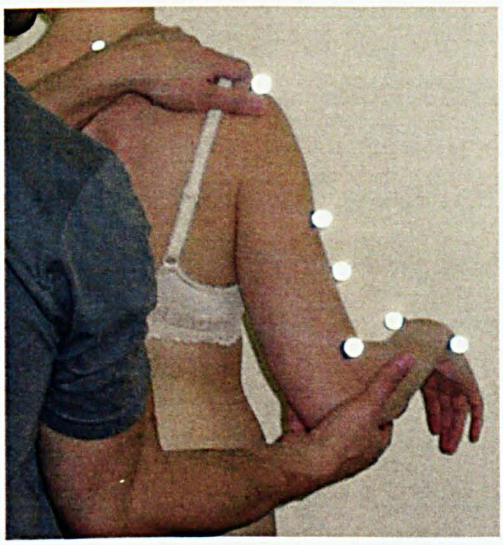

Figure 7.6:

Calibration recordings: Finding the glenohumeral CoR by recording small humeral circumductions

Two extra calibration activities of full elbow flexion/extension and forearm prono/supination (with the elbow flexed at 90 deg.) were recorded in order to define the flexion/extension axis (V_{flex}) and the prono/supination axis (V_{pron}). Both axes were defined by calculating the mean instantaneous helical axis, as described by Biryukova et al. 2000. The V_{flex} was expressed in the technical and anatomical humeral frames, where the V_{pron} was expressed in the technical and anatomical forearm frames.

7.2.4.2. The set of the recorded activities

Defining the number and set of activities to be measured is challenging. Most of the clinical studies that investigate pathological shoulders (e.g. joint replacement) often report only range of motion (ROM) in abduction, flexion and internal external rotation (Bergmann et al. 2008,Ludewig & Cook 2000,McClure et al. 2004).

From another point of view, several studies have investigated kinematics of functional activities on normal shoulders to demonstrate that there are repeatable kinematic patterns (Murray 1999,van Andel et al. 2008). A number of user function studies have recommended different sets of activities in order to challenge several aspects of the shoulder joint (Anglin & Wyss 2000a,Murray 1999,Peterson & Palmerud 1996,Veeger et

al. 2006). Bukley et al. (1996) and more recently Anglin & Wyss (2000) have an extended review of ADLs used in upper extremity studies.

For this study it was decided to record both, i) standardised activities (ROM of the prosthetic subjects) and ii) a set of ADL. The data will provide information to investigate whether:

a) there are differences or any constraints in kinematic patterns of the joint replacement compared to the normal shoulders

b) provide a kinematics dataset which, when analysed with the biomechanical shoulder model, will provide a wide range of glenohumeral loading that will be useful for mechanical testing or finite element analysis.

The set of the standard activities included in the testing protocol are commonly tested in clinical examinations and clinical scores and include 3 elevating tasks (in coronal plane – abduction, in sagittal plane –forward flexion and in scapula plane) as well as internal external rotation in adduction and in 90 deg. of abduction (Table 7.6).

The testing protocol also includes recommendations of Murray & Johnson (2000) who had selected activities recommended also by Buckley et al. (1996). The protocol includes hygiene and feeding activities, and those using everyday objects. Murray showed that even if there is a variation between the normal subjects on how they execute each task, there is also a certain consistency, and the kinematic patterns show acceptable confidence intervals that can be used to identify irregular patterns of pathological shoulders. The same kinematic dataset was later used by Charlton (2003) to investigate joint and muscle loading of normal shoulders using the Newcastle Shoulder Model. Charlton discussed that the Murray & Johnson dataset produced a wide variety of loadings to the glenohumeral joint providing useful information for using to investigate strength and wear of joint replacement.

In order to make the testing protocol more complete, two extra activities were also included:

i) The original 10 ADLs as described by Murray and Johnson do not include any activity that requires a large amount of internal activity, as concluded by the same authors. 'Reach and clean the lower back' was added to the protocol specifically to test the available humeral internal rotation of the joint replacement subjects.

ii) Sit to stand is also a very popular functional task in kinematics studies (Anglin & Wyss 2000a,Packer et al. 1994,Wheeler et al. 1985) and has been also used to predict GH loading (Anglin et al. 2000). This specific activity was included in order to provide useful GH loading rather than kinematic information as shown by Anglin and Wyss (2000).

Testing protocol – Kinematic activities recorded			
Range of Motion (Standardise activities)			
Abduction Forward flexion Scapula plane elevation		Internal/external rotation in adduction Internal/external rotation in abduction (90deg.)	
Activities of Daily Living (ADL)			
Activity	**Area of Use**	**Activity**	**Area of Use**
1. Reach to opposite axilla	Hygiene	**6.** Eat with spoon	Feeding
2. Reach to opposite side of neck	Hygiene	**7.** Answer telephone	Everyday object
3. Reach to back of head	Hygiene	**8.** Combing hair (contra-lateral side)	Hygiene
4. Eat with hand to mouth	Feeding	**9.** Lift block to shoulder height	Everyday object
5. Drink From Mug	Feeding	**10.** Lift block to head height	Everyday object
11. *Reach lower back*	*Hygiene*	***12.*** *Sit to stand and stand to sit*	*Everyday activity*

Table 7.6: Complete set of tasks of the testing protocol. The ADL follow the Murray and Johnson (2000) protocol except tasks 11 and 12 that were added specifically for this study

7.2.4.3. Preparation of the recordings

All the ADL were recorded with the subjects sitting on a stool in order to increase marker visibility. Only in task 12 (sit to stand) a different but standard chair with back and armrest was used. Two additional adjustable tables were also used for most of the activities, in order to place some of the objects that were used during the activities.

All the subjects had to adapt an arm resting position before the start of any of the activities with the arm on the side slightly lifted, the elbow flexed at 90 deg. and the palm rested on the table. The lifted humeral position was around 20 deg. and it was measured manually with a simple goniometer. This position was adopted in order to avoid Gimbal lock, which is observed with the humeral position at 0 deg. of elevation (van der Helm 1996,Wu et al. 2005). The table (where the arm was resting – initial position), was always adjusted for each subject so the same resting position could be achieved, regardless the height of the subject.

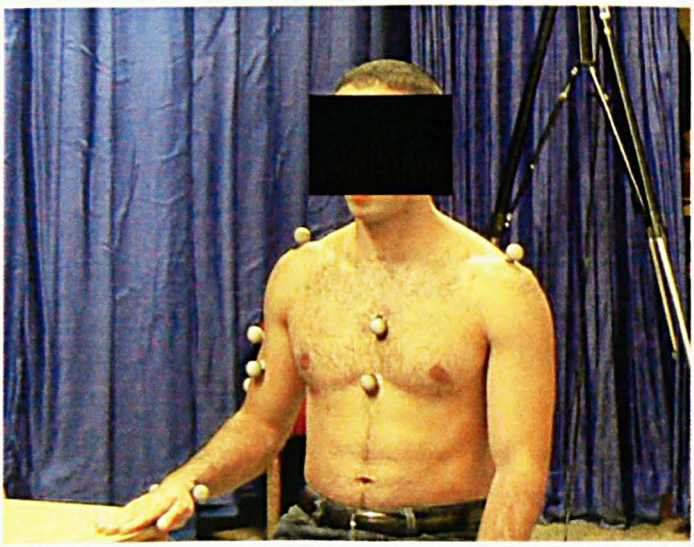

Figure 7.7:

Resting position of the hand on the table

All the subjects were instructed to start and finish every task from the resting position. Before every task there was a verbal description of the activity. The subjects were asked to perform all the tasks in their own time and in a natural way and any descriptive details or visual examples of how to perform the activity were avoided in order to prevent guidance, as suggested by Kontaxis et al. (2009).

In order to investigate inter-subject repeatability, all the healthy subjects were asked to repeat each activity 5 times. For the prosthetic group though, considering their shoulder weakness and disability, the subjects were ask to perform the activity a maximum of 3 times, if that was not too tiring for them.

Some extra objects were used during the activities in order to promote a more natural performance of the tasks. Objects and their weight are listed on Table 7.7

Object	Used in task:	Weight of the object (kg)
Biscuit	4	Negligible
Plastic spoon	5	Negligible
Half full mug (water)	6	0.400
Table telephone	7	0.112
Hair brush	8	0.120
Block	9 & 10	0.500

Table 7.7: Objects that were used during the ADL

For the 'sit to stand' activity a standard chair with a back and armrests was used. The chair was not height adjustable, in order to represent a more realistic day-to-day action. As shown by Anglin and Wyss (2000), this type of activity can generate large GH joint forces because of the reaction forces when a subject uses the armrests to stand up or to

sit down. Thus, it was important to record the reaction forces (on the hand) that are developed when the subjects were pushing the armrest. A 6-DOF load cell was mounted rigidly onto one of the arms of the chair, on the operated shoulder side (a block with similar dimensions and profile as the load cell was fitted on the contralateral side (Figure 7.1)). The load cell was marked with VICON markers and the loads were recorded simultaneously on the VICON PC. A time stamp on the data provided a synchronisation point of the recorded loads and the kinematic recordings.

In contrast with the other ADL, a specific instruction was given to all the subjects to specifically use the armrests to stand up and sit down, since most of them in the normal group and few on the prosthetic group declared that they were capable (or used to be capable) of naturally performing the activity without using their hands.

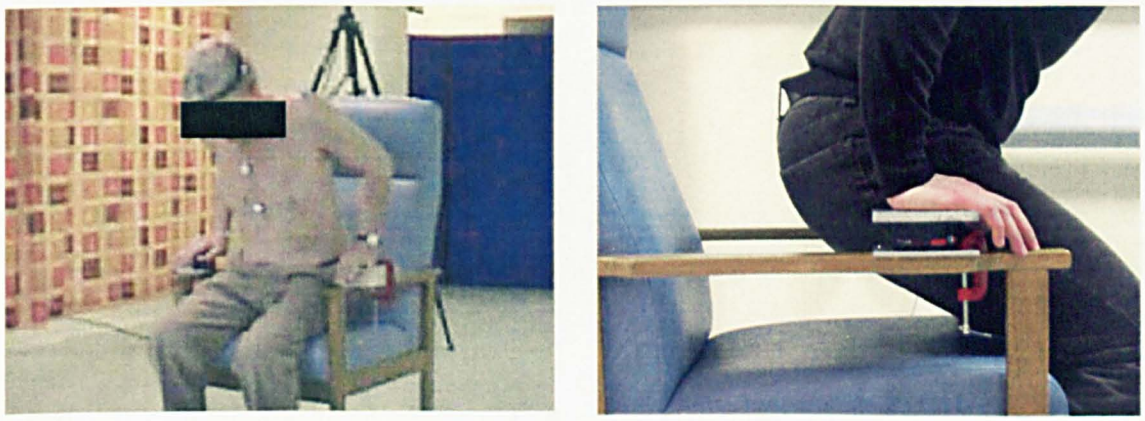

Figure 7.8: Sit to stand activity. The reaction forces on the hand were measured with a AMTI 6-DoF load cell

7.2.5. Clinical scores

Clinical scales have been used extensively in clinical studies in order to report performance and rehabilitation after a joint replacement (e.g. hip, elbow, shoulder, knee). In an effort to investigate whether there is any correlation between the results of the kinematics of the ADLs and the clinical scales, both groups (normal and prosthetic) completed (after the VICON session) 2 sets of questionnaires that represent the Oxford shoulder scale (Dawson et al. 1996) and the Standard score SF36 (Ware, Jr. & Sherbourne 1992). Both scales have been extensively used in shoulder studies (shoulder replacement, fractures, RC repairs etc) and even if the Oxford shoulder has gained large popularity within recent years, the SF36 includes many questions that are relevant to the ADL that were included in this study.

Both of the questionnaires as well as the methodology of the scoring system are shown in the appendix.

7.3. Results and Discussion

7.3.1. Range of Motion (ROM) - Standard activities

The results of the standard activities within the control (normal) group showed great consistency especially for the three elevating tasks (average standard deviation 3.9). The maximum elevation was 148.8, 179.4 and 167.7 deg for abduction, forward flexion and scapula plane elevation respectively (Figure 7.9). It needs to be noted that when the normal subjects were asked to freely abduct their arm they could reach a full elevation of 180 deg. in all three planes, but for abduction and scapula plane elevation they could only achieve that with a humeral internal rotation at the end range of the motion. This is not a surprise since at high degree of abduction and with no humeral rotation there is an impingement between of the humeral head and the acromion (Kapandji, 1982). In order to prevent any humeral rotation the subjects were asked to slightly bend their elbow (in order to control the humeral rotation and not confused with forearm pronation) and try not to rotate their arm during the activity.

The ROM of internal/external rotation was more variable than the elevation ROM, since two of the female subjects achieved larger external rotations than the rest of the group. The average range of humeral rotation in abduction was 184.7 deg. (96.4 deg external, 88.3 deg internal), with the maximum external rotation in adduction averaging 82.8 deg. (Figure 7.9)

As expected, the values of ROM for the DELTA group – for both elevation and humeral rotation – were smaller than the control group. The results also showed a large variability within the subjects.

Even if the maximum elevation values were relatively high (average: 103.7 deg abduction, 125.8 deg forward flexion, 118.3 deg scapula plane elevation – Figure 7.9) the range of the values were large. Some of the subjects achieved only a maximum elevation of 66.0 (abduction), 69.0 (forward flexion) and 76.0 (scapula plane) deg while the maximum values were 128.0 170.0 146.0 deg respectively. The average overall elevation (of all three elevation activities) was 115.9 deg and this seems to agree well with other DELTA clinical studies (e.g Boileau et al. 2006) that report 121 deg of elevation for a large group of DELTA III subjects). The large variability within the results is reported in studies that investigate not only DELTA but also different type of reverse prosthesis (Bergmann et al. 2008).

The elevation results that are reported here are slightly different from the results shown in chapter 6 (scapula measurements). If we exclude subjects 10 and 12, who did not take part in the scapula kinematics, the maximum achieved elevation was, on average, 17 deg. less compared to the results obtained with the VICON system. The small difference is believed to be a result of the electromagnetic equipment and specifically of the elbow splint that was used for the scapula measurements: it seems that, for some reason, the splint was constraining – to some degree – the movement of the subjects' shoulder girdles, as well as their elbows.

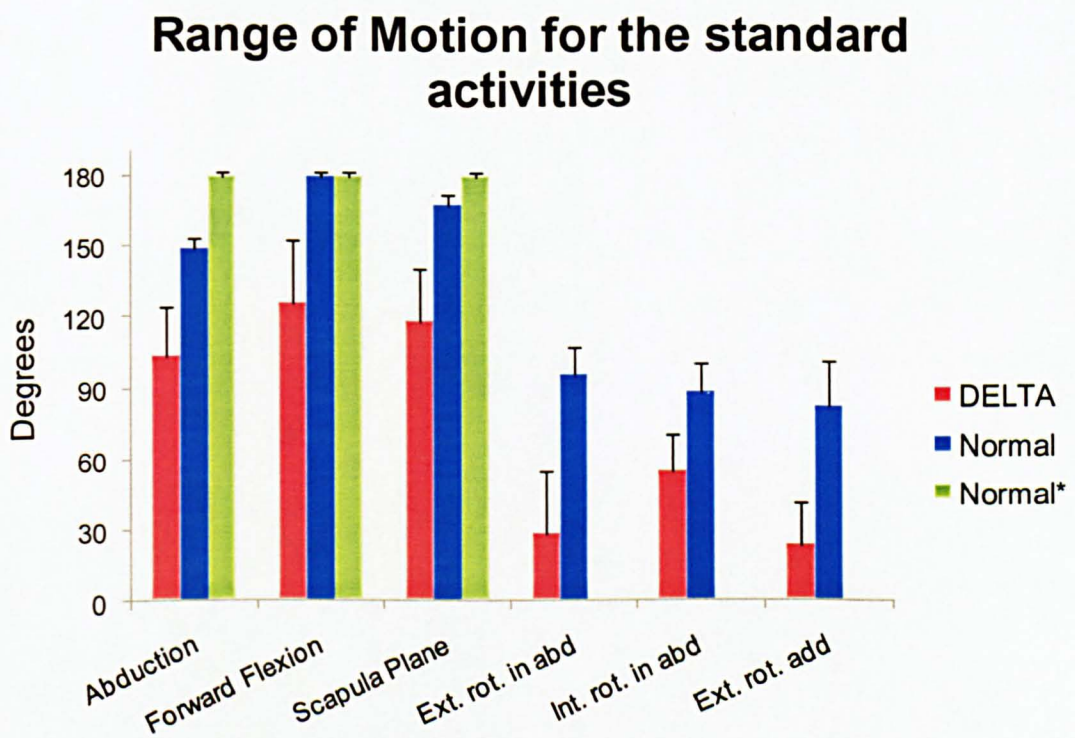

Figure 7.9: ROM during the standard activities. Error bars indicate the standard deviation within the groups. The 'Normal' is the same group of subjects as the 'Normal' but elevating the arm without the constriction of humeral rotation*

The humeral rotation ROM values were even smaller compared to the control group. The external rotation in both abduction (90 deg) and in adduction (10 deg) were especially low, averaging only 28.9 and 23.6 deg respectively. This is much smaller than the 96.4 and 82.8 deg of the control group (Figure 7.9). Again there was large variability within the DELTA group, with one subject being able to externally rotate up to 86 deg., but also with four subjects (3 male and 1 female) unable to perform any external rotation when the arm was at 90 deg. of abduction. The latter subjects were asked to perform the

same activity in a position of their own comfort, but their ability to perform external rotation was very low (range 5 to 11 deg.).

The results of the poor humeral rotation range were expected since a primary indication of a DELTA III joint replacement is large and irreparable RC tears. The lack of RC muscles results not only in loss of joint stability (as it was explained in chapter 5) but also in loss of humeral rotation. The large variability of humeral rotation amongst the DELTA subjects indicates that there may be remaining functional fibres of the RC muscles after the joint replacement and, as shown in chapter 5, the reverse design allows m.Teres minor to externally rotate the arm.

It was also noticeable that some DELTA subjects (subjects 5, 6, and 10) were performing a combined motion of external rotation while lifting and extending the arm. Their maximum rotation was 19, 35 and 33 deg respectively (for each subject). This motion can indicate a different muscle recruitment strategy for external rotation; the biomechanical model shows that the posterior fibres of m.Deltoid posterior have the moment arm to externally rotate the arm and an activation of those muscle fibres can result in humeral rotation. However, with no co-contraction of the RC muscles, a posterior deltoid activation will result not only in rotation but also in elevation and extension of the humerus.

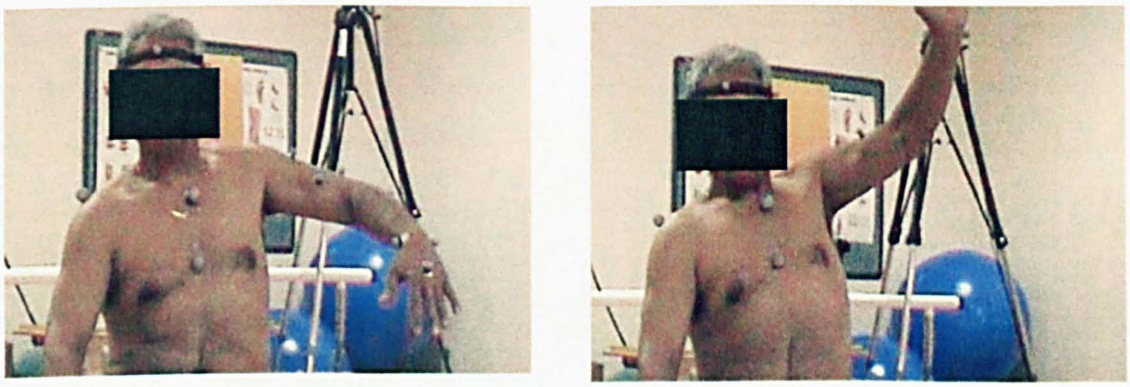

Figure 7.10. External rotation in abduction is achieved with a combined motion of humeral elevation and shoulder extension which may suggests m.Deltoid posterior activation

7.3.2. Activities of Daily Living (ADL)

7.3.2.1. Repeatability

In order to analyse kinematic patterns and compare the Normal with the DELTA group there is first a need to establish whether there is consistency of a subject performing a specific activity (intra-subject repeatability).

For the normal group, all the subjects performed the activity at least 5 times and the results showed that every individual subject was performing each activity with the same approach for every repetition (Figure 7.11). If we consider that every activity begins from a resting position, goes to the target point and completes the activity by returning to the resting position, the values of azimuth, elevation and humeral rotation for the target position were almost identical for each repetition. The only parameter that was slightly changing was the time of completion of the activity, which was decreasing slightly (increase of speed) while the subjects were repeating the task.

To consider the comfort of the subjects of the DELTA group, only 4 subjects agreed to repeat all the ADL and only up to three times. However, the results were similarly repeatable.

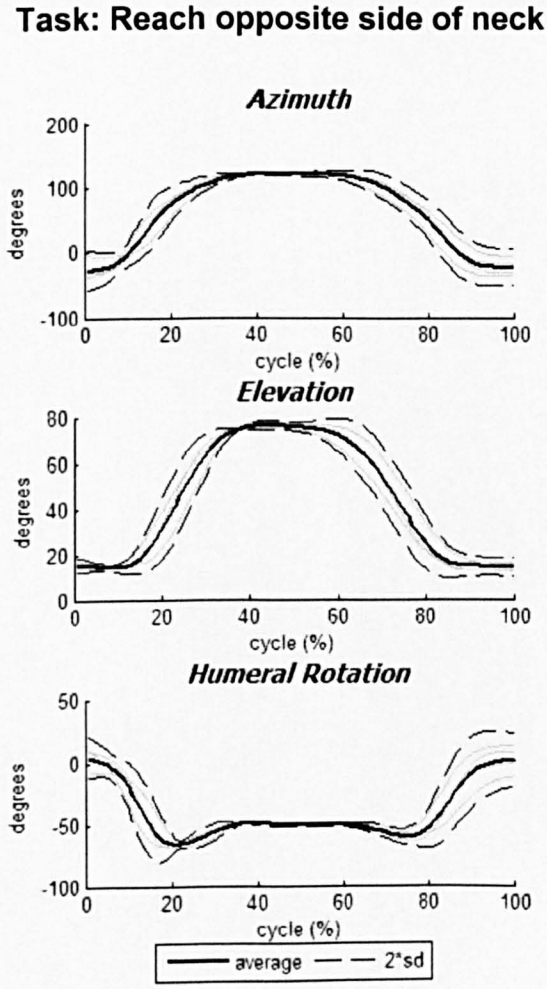

Figure 7.11:

Example of normalised results of Azimuth (plane of elevation), Elevation and Humeral rotation for one of the ADL. There was an inter-subject repeatability for all the normal subjects and all the ADL. The dotted lines represent 2 times Standard Deviation (sd). The small widening of the sd during the approach of the arm to the target is due to the increase of the speed in which the subjects were performing the activity during the repetitions.

7.3.2.2. Kinematic range and variation between the groups

It was easy for all of the subjects of the control group to complete all 12 ADL of the protocol. The DELTA group also managed to perform most of the activities of the protocol. It was only a few subjects who failed to complete the task of 'Reach back of the head' (failed n=3) and 'Block to head height' (failed n=2). In contrast, all the subjects of the DELTA group failed to complete task 11 ('Hand to lower back'). This specific activity is analysed later in this chapter (section 7.3.2.9).

As in other studies, the control group showed consisted kinematic patterns within the activities (Figure 7.12). The standard deviations for all of the 3 DOF (azimuth elevation and humeral rotation) were consistent, and are comparable with Murray (2000) for the 10 ADL (average 2*SD - 17.1 this study, 16.6 Murray).

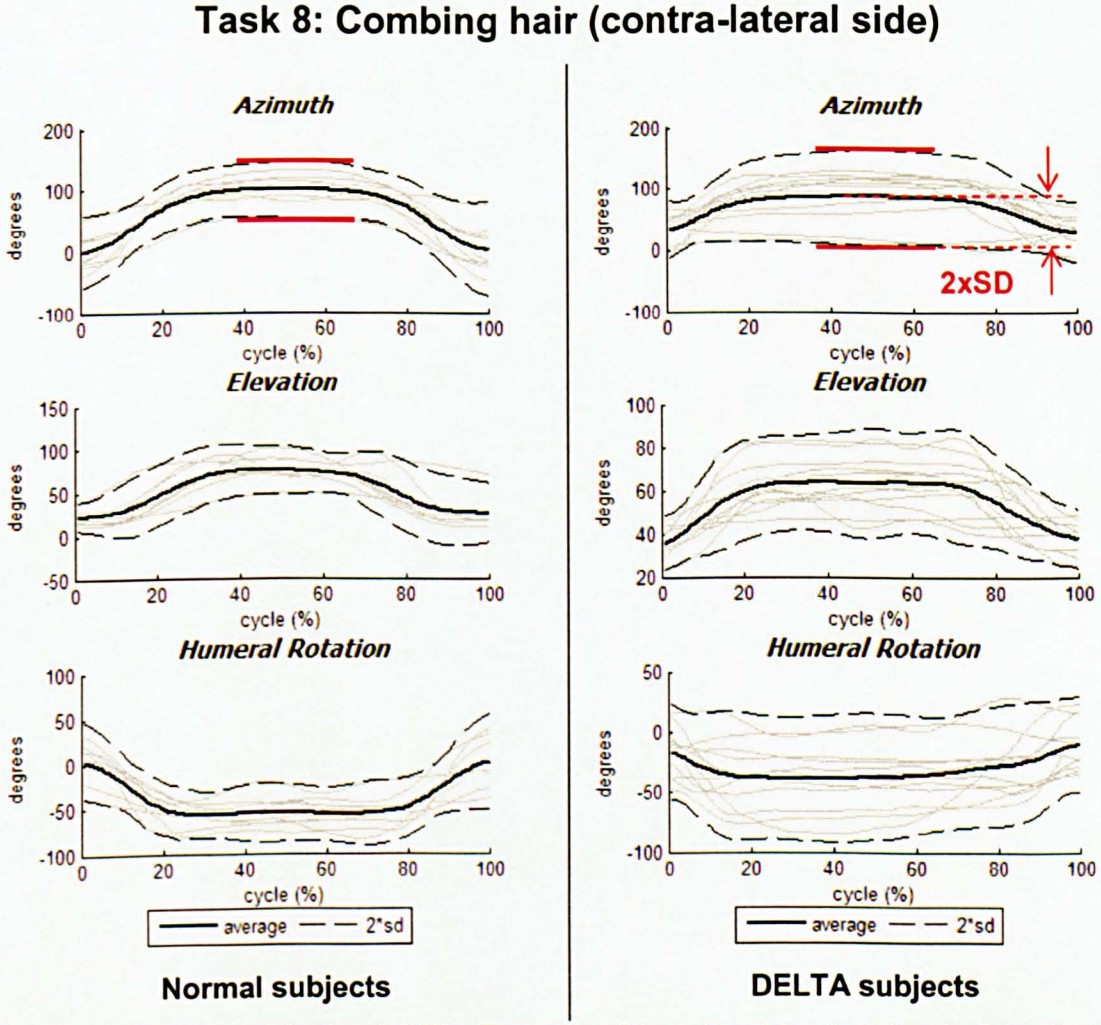

Figure 7.12: Intra-subject variability: Example of task 'combing hair (contralateral side)'. The Normal (control) group shows a consistent kinematic pattern, while there is a large variability within the DELTA group.

There are only 2 tasks showing inconsistent kinematic patterns within the normal group:

- The feeding task 'Spoon to mouth' shows a much higher standard deviation of 36.2 (Figure 7.13). This is due to the lack of standardisation for this activity, where the subjects used only a plastic spoon to pretend feeding. Because there was no detailed verbal instruction and no real food, it was observed that most of the subjects approached the task with a different degree of attention.
- The 'Sit to Stand' task also showed a large variability (2*SD=30.2 – Figure 7.13). This was expected since the chair that was used for the activity had no adjustable arms, thus dictating the resting positions of the subjects' arms. Thus, the variability of the size (height) of the subjects is reflected in the arm kinematics. Anglin and Wyss (2000) also reported large kinematic variability for the same activity.

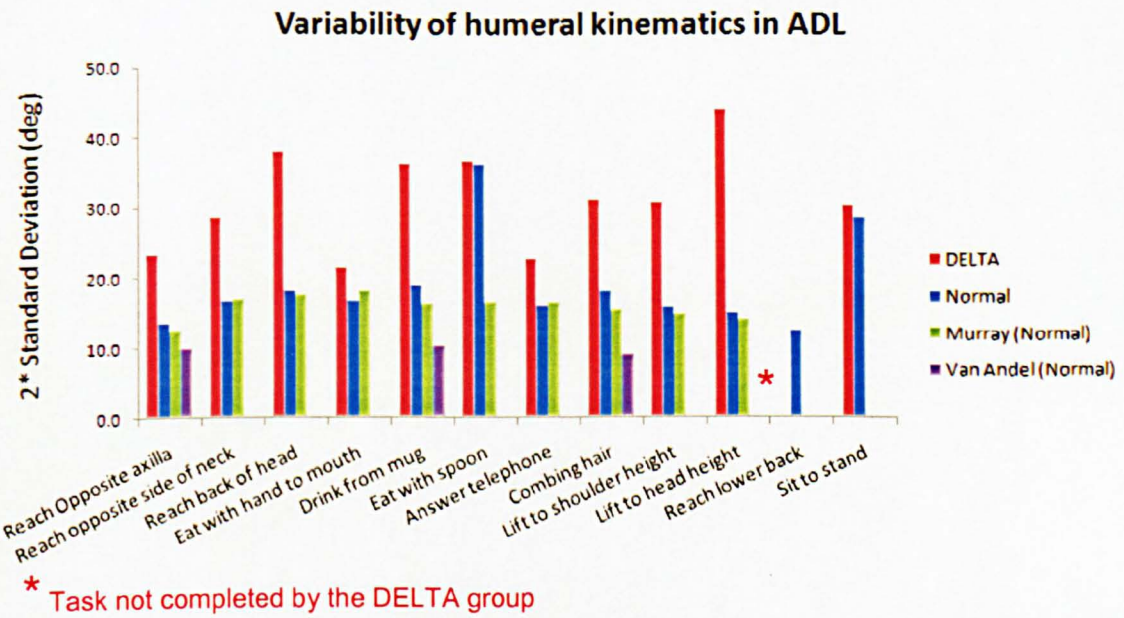

*Figure 7.13: Variability (2*SD) of the kinematic results between the control (Normal) and DELTA (group) for all 3 deg. of freedom (average). The control group shows consistency and reasonable deviation comparable to the literature (Murray (2000), van Andel et. al (2008), where the values of DELTA group is significantly larger for most of the activities*

As with the standard activities, the kinematic pattern of the DELTA group was much more variable for most of the ADL (Figure 7.13). The average standard variation for all three deg. of freedom was almost double that of the normal group. It was only the feeding task of 'Eat with hand to mouth' and the task of 'Answer telephone' that there

was consistency within the group (compared to normal group), yet the overall movement of the arm during those activities was rather small.

The data of the range of motion for each ADL showed that, in general, the elevation values of the DELTA group were particularly high and matched the Normal group for most of the activities, with an average difference being 11 deg (max values: 109.5 deg Normal, 98.7 deg DELTA - Figure 7.14). In a way, those results support the findings of the biomechanical model; that the geometry of the DELTA prosthesis enhances the performance of the m.Deltoid, which compensates for the non-functioning RC muscles (especially the m.Supraspinatus) that normally contribute to arm elevation.

The range of the azimuth values (plane of elevation) was also comparable between the two groups, covering values up to 139 deg and 134 deg for Normal and DELTA respectively. Even if the DELTA group showed a wide range of azimuth values, in some activities the target position was achieved in a different plane of elevation, as is shown later in this chapter.

There was a difference between the groups in the range of the humeral internal/external rotation, which for the DELTA group was smaller for some of the activities with the average difference in the range being 18.1 deg. If we exclude task 11 ('reach lower back' – not completed by DELTA group) and task 12 ('Sit to stand' – large variability by both normal and DELTA group), the other 10 ADL were shown to require mostly external, and almost no humeral internal rotation.

Finally, the range of elbow flexion/extension was also slightly different between the two groups, with the DELTA group showing slightly larger extension values in some activities. However, this is expected, since the elbow compensates for lack of movement of the upper arm in order the forearm to reach the target position of the activity.

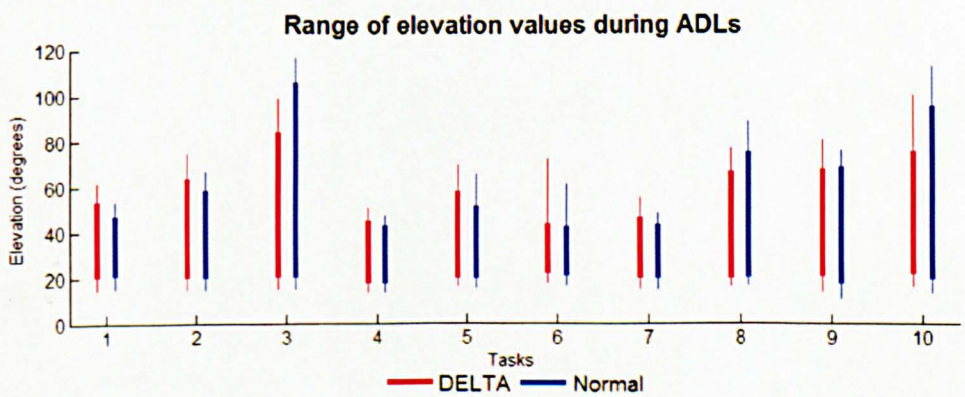

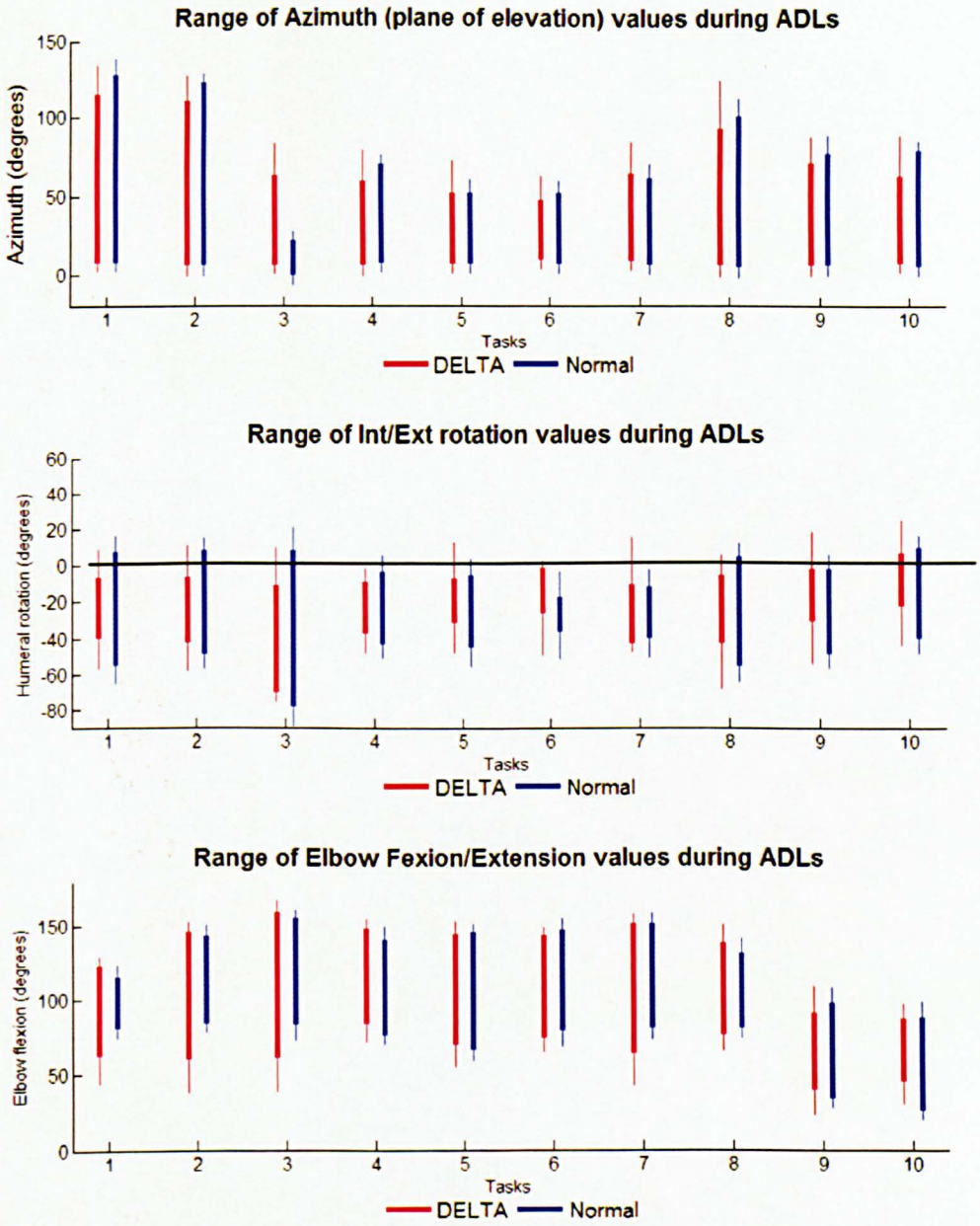

Figure 7.14: Range of elbow and humeral motion (all 3 degrees of freedom)

7.3.2.3. Activities of the contra-lateral side

Within the protocol of the ADL there is a set of 3 hygiene activities for which the target position is on the contra-lateral side (Task 1 - 'Reach opposite axilla', Task 2 - 'Reach opposite side of neck', Task 8 - 'Combing hair'). All of those activities require a horizontal flexion of the humerus (increase of azimuth values) but the target is effectively in a higher position.

Even if all the subjects were able to complete all 3 activities, it was clear that some of them found Tasks 2 and 8 – where the target was higher – to be more difficult (Figure

7.15). Plotting the azimuth and elevation values of the target position, the data showed that for Task 2 all the subjects reached the elevation values of the normal group, but for some this happened in an earlier plane of elevation and they had to compensate with more elbow flexion.

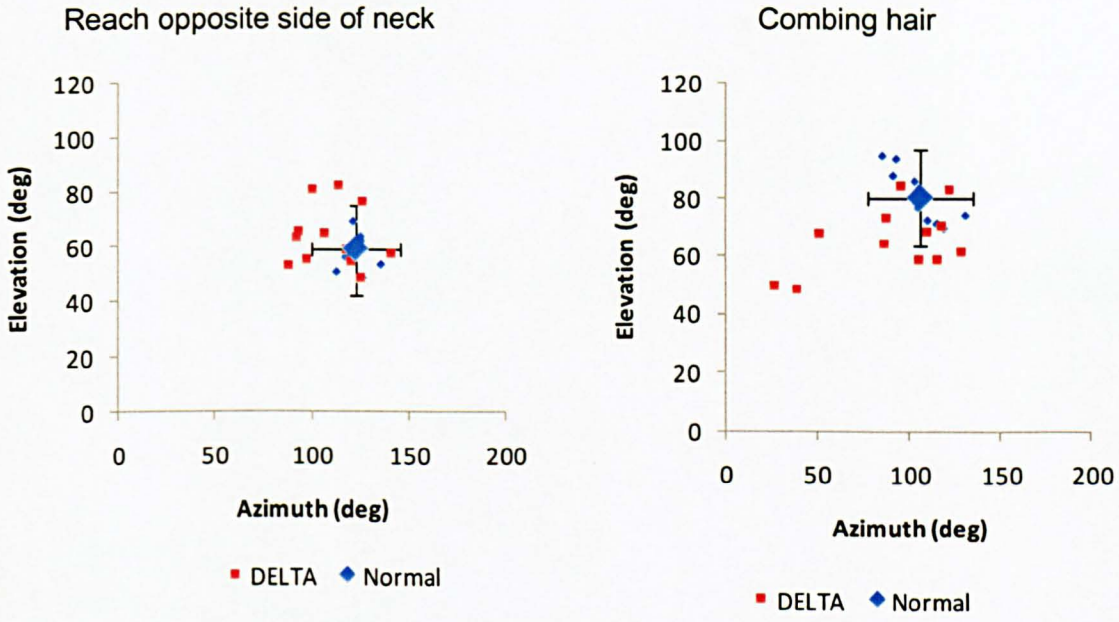

* Error bars indicate 2*SD of the normal group

Figure 7.15: Azimuth vs Elevation values for the target position in Task 2 and 8. The data show that some of the DELTA subjects adopted different strategies to reach the target position, with lower elevation. Those subjects compensate with more external rotation and elbow flexion extension.

Task 8 showed even larger differences, with some of the subjects also achieving less elevation. Those subjects had a different approach to the activity; with the elbow closer to the body (lower elevation) they used more external rotation to reach the target. Even if the instruction of the activity was to keep looking forward, within the DELTA group there larger movement of the head was noticeable during the activity (combing their hair).

The activity of combing hair in healthy subjects has been studied for kinematic analysis previously (van Andel et al. 2008), but Veeger et al. used this activity to study the kinematics of joint replacement subjects. Despite studying a group with a different type of joint replacement, they also reported that the subjects that managed to perform the activity had a different approach, using more external axial rotation.

7.3.2.4. Feeding activities

As explained above, out of the three feeding activities, the task 'Spoon to mouth' showed large variation between both groups and it was excluded from further kinematics analysis.

The 'Hand to mouth' showed very small range of humeral motion for both groups and also small and similar variability. The humerus elevated only up to an average of 43.1 deg (sd 6.5) in an azimuth of 60 deg (sd 6.1) and external rotation of 62.9 deg (sd 8.2). All the subjects used large elbow flexion (151.2 deg, sd 6.9) to approach the target.

The 'Hand to mouth' and 'Drink from mug' are very similar activities for the subjects of the Normal group and showed similar approaches and similar humeral ROM, in agreement with Murray (2000) and van Andel et al. (2008). Surprisingly though – and in contrast with the previous activity – some subjects of the DELTA group do not follow the same approach to complete the 'Drink to mouth'; rather than a small elevation in a frontal plane, they prefer to elevate the arm in a more coronal plane.

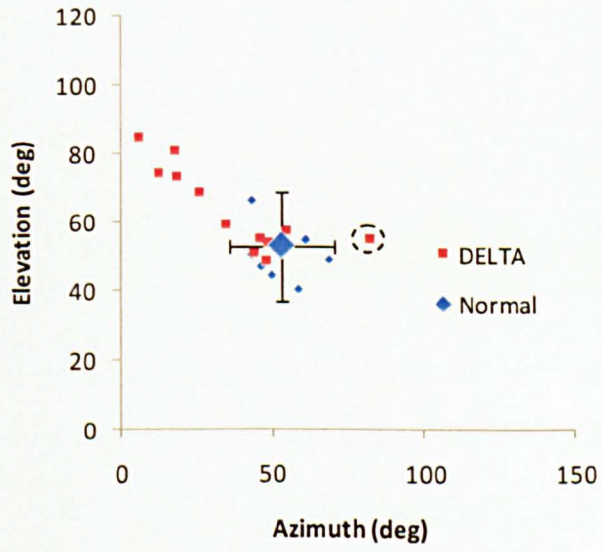

* Finger arthritis on one of the Delta subjects (outlined) forced a different mug grip and an un-natural approach of the activity

Figure 7.16: Some Delta subjects had a very different approach of the activity 'Drink from Mug', compared to the Normal group

It is not clear whether the different approach of the activity is correlated with the specific joint replacement, or it is just related to personal style (that can be related to the age difference).

7.3.2.5. Answer telephone

This activity requires only small movement of the upper arm in order the subjects to reach the target position. The activity requires extensive elbow flexion (127.8 deg sd 5.1) and both groups showed consistent activity with small values of humeral elevation (33 deg. sd 3.5, Normal group, 31.3 deg. sd 4.8, DELTA group). Even if the activity requires external rotation of the arm (77,6 deg. sd 8.9 for the Normal group), the DELTA group was able to perform the activity with the same approach to the Normal group, since the external rotation is happening in the sagittal plane.

7.3.2.6. Hand behind the head

The 'Hand behind the head' activity was one of the most challenging activities for the DELTA subjects; 3 of them did not manage to complete it (did not reach the target position).

The subjects within the Normal group were very consistent in elevating the arm high (average elevation 101.3 deg) in a more coronal plane (average azimuth 7.6 deg) and reaching the target with external rotation (average 89.0 deg) and large elbow flexion (average 148.0 deg). As shown in the standard activities the DELTA subjects had a very small range of external humeral rotation in abduction and as such they had to approach the target position from a different plane of elevation (average azimuth 64.4 deg, sd 19.3). The humeral elevation was slightly smaller (92.4 deg sd 11.2) and so was the humeral external rotation (79.8 deg sd 14.5).

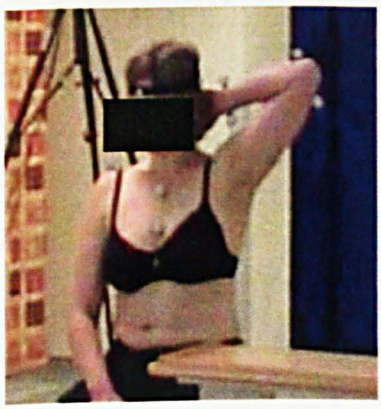

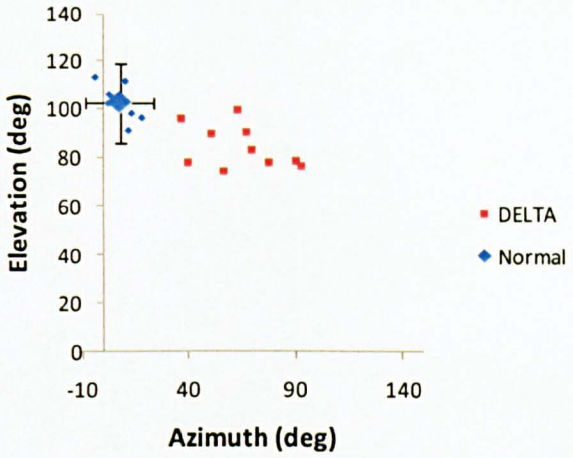

Figure 7.17: All the DELTA subjects were elevating the arm in a different plane in order to reach the 'Back of the head'

It must be noted that some of the DELTA subjects (4 out 9) were elevating the whole shoulder girdle (shoulder shrug) in order to reach the target. Shoulder elevation values are shown in section 7.3.3.

7.3.2.7. Lifting activities

Out of the two lifting activities, the 'lift block to head height' was more challenging for the DELTA group with 2 subjects failing to place an object on a shelf (at head height). This is in contrast with the suggestions of Murray (2000) and Charlton (2003) who found that lifting and placing an object at shoulder height (effectively 90 deg. of elevation) creates larger adducting moment on the shoulder than lifting to head height and thus more demanding for the m.Deltoid.

For this study the kinematics data showed that for the 'Lift to shoulder height' the DELTA subjects averaged the elevation values of the Normal group (87.1 deg sd 11.6 for DELTA, 91.3 sd 5.9 for Normal). For the 'Lift to head height' the normal subjects elevated the arm higher than the previous activity (107 deg sd 6.3), approaching the target from the side (azimuth 63.1deg sd 6.4), while some of the DELTA subjects (n=4)

preferred to approach the target by elevating the arm in a sagittal plane (as forward flexion with a bent elbow) using the length of their forearm more in order to reach the height of the target (Figure 7.18).

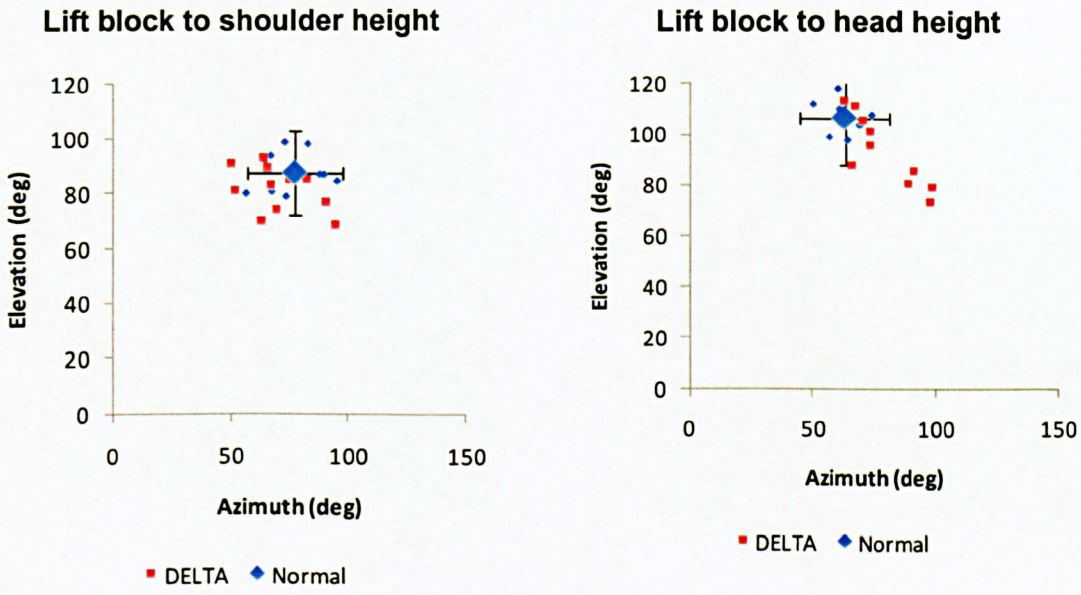

Figure 7.18: The 'Lift block to head height' was challenging for the DELTA subjects

In both activities (and especially in 'Lift to head height') most of the DELTA subjects showed significant movement of the body (thorax) in order to compensate for the restricted humeral elevation. While the Normal group showed almost no thorax flexion (average 3.4deg sd 0.8) the DELTA group averaged a range of thorax flexion extension of 19.8 deg (sd 5.3).

7.3.2.8. Reach lower back

As mentioned above, task 'Reach hand to lower back' was the only task that was not completed by any of the DELTA subjects. In contrast, the Normal group was approaching the target with a humeral extension (negative azimuth, average -22.0 deg sd 6.9) in a slightly elevated position (31.3 deg, sd 7.1) and then internally rotating the arm (92.8 deg, sd 9.1) and flexing the elbow to complete the activity (Figure 7.19). Even if the DELTA group had the same approach (humeral extension and then internal rotation) they failed to internally rotate the arm enough in order to approach the target. Their average maximum internal rotation was much lower than the normal with an average of 41.2 deg (range 22.0-52.0 deg). This average value is even lower than what the DELTA subjects achieved during the standard activities (internal rotation in

abduction), which was 55.5 deg (sd 15.1). The reason for the reduced range of rotation is not clear, but when the subjects were performing internal rotation at 90 deg. of abduction, they had their elbow 90 deg flexed. In this position the weight of the forearm naturally creates a rotational moment that may help the subjects to increase their internal humeral rotation range in abduction.

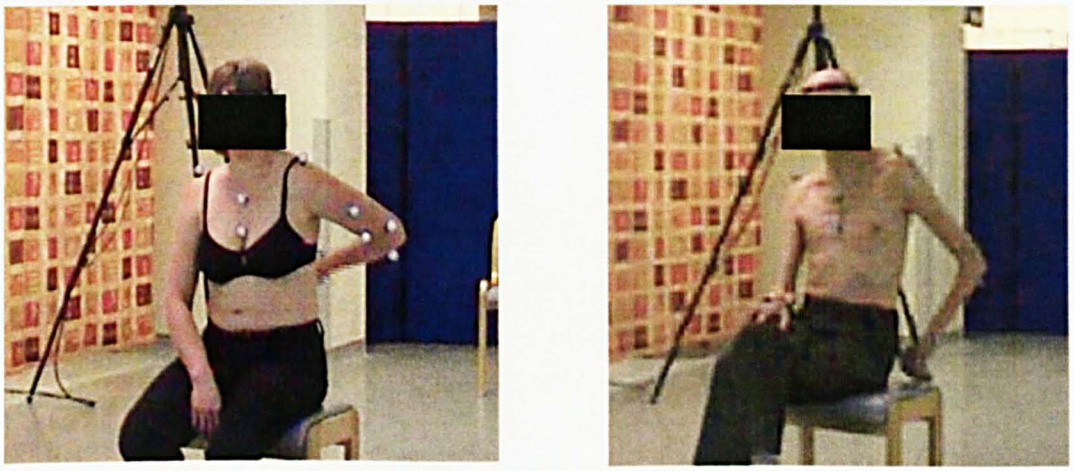

Figure 7.19: All the subjects of the DELTA group failed to complete the 'Reach lower back' activity.

The lack of RC muscles probably prevented the subjects from completing the task. Analysing the activity with the biomechanical model, it is clear that there is no muscle to create a positive (internal) rotational moment, other than the m.Subscapularis, when the arm is extended backwards in adduction (Figure 7.20).

The model also indicates that this specific activity creates a larger inferior impingement, with a large portion of the plastic cup penetrating the scapula border. This may well mean that even if the DELTA subjects have the ability to internally rotate the arm in this position (with remaining m.sabscapularis fibres), the heavy collision of the prosthesis with the scapula may prevent the motion of the arm.

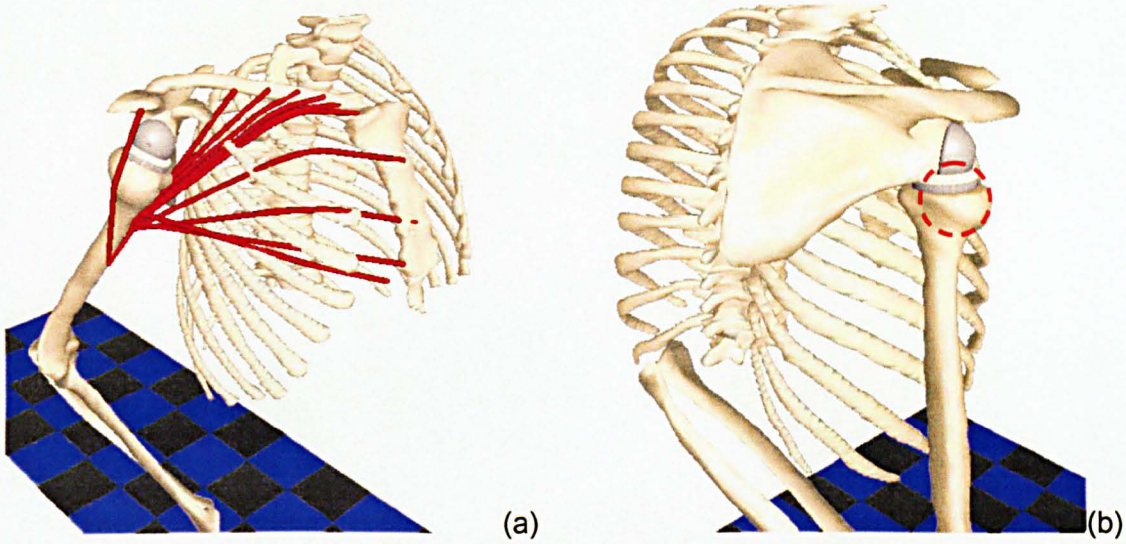

Figure 7.20: (a) When the arm is extended backwards in adduction the model shows that, other than the m.Subscapularis, there is no muscle to create a positive (internal) rotation moment. (b) The model shows that with the hand reaching the lower back there is a large impingement of the prosthesis and the scapula

7.3.2.9. Sit to stand (external load)

The activity of 'Stand to sit' showed large variation even if the ROM of the humerus was rather small. The biggest kinematic difference between the two groups was on the trunk movement. The DELTA group showed a wider range of thorax bend (rotation around the anatomical x axis) with an average maximum of 32.0 deg (sd 9.2), while the subjects of the Normal group adopted a more up-right position (20.1 sd 5.8).

This activity is different to the other ADL of the protocol, since it creates a rather large external reaction force to the hand while the subjects are pressing the arm of the chair. The activity can be divided into two separate phases a) Standing up from sitting position and b) Sitting down from standing position.

The maximum hand load that was recorded by the load cell for the Normal group was 0.224*BW (sd 0.096) and was recorded during the first phase of the activity, where the maximum load for the Sitting down phase was slightly smaller (0.204*BW, sd 0.093 Figure 7.21). Those values are larger but close to the loads reported by Anglin and Wyss (2000), who also presented slightly smaller loads for the sitting down phase (0.19*BW sd 0.06 for standing up, 0.16 sd 0.06 for sitting down)

Interestingly, the maximum load recorded in the DELTA group was noticeably lower, topping only 0.127*BW (sd 0.072 - standing up phase). The load was almost the same for the two different phases of the activity (sitting down phase: 0.126*BW sd 8.1). This

may indicate that the DELTA subjects were exerting higher loadings with the non-operated force, but there was no lateral thorax bending to support such a hypothesis.

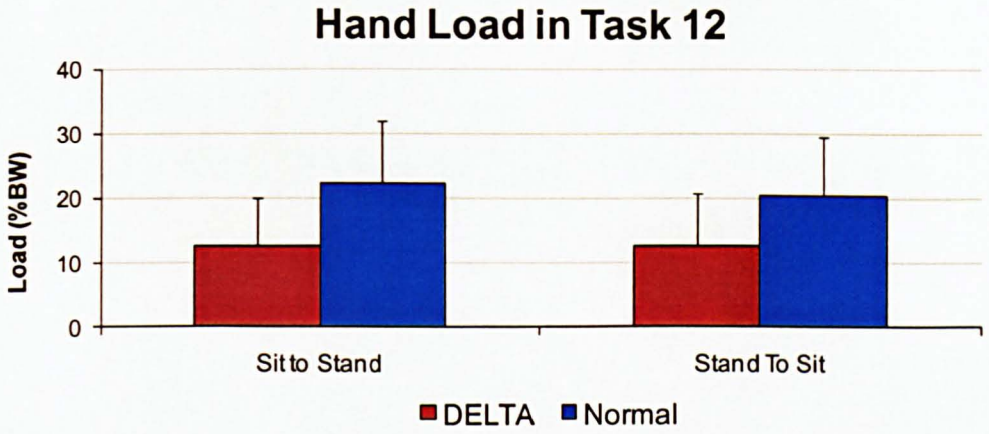

Figure 7.21: The maximum hand load that was recorded from the load cell was significantly smaller for the DELTA group

Breaking down the load cell readings into inferior loads (pushing down), posterior (pulling backwards to the chair) and lateral (pushing to the side and out of the chair), it is clear that the main force component is in the inferior direction (Table 7.1). The difference between the two groups is that the DELTA subjects are exerting slightly higher posterior loads only during the standing up phase; a fact that may be correlated with their more bent thorax position.

	Sit to Stand forces (xBW)					
	Posterior		Lateral		Inferior	
DELTA	0.008	(0.006)	0.007	(0.015)	0.125	(0.074)
Normal	0.003	(0.005)	0.011	(0.019)	0.205	(0.130)

	Stand to Sit forces (xBW)					
	Posterior		Lateral		Inferior	
DELTA	0.003	(0.008)	0.004	(0.015)	0.125	(0.082)
Normal	0.002	(0.009)	0.010	(0.018)	0.184	(0.121)

Table 7.8: The maximum posterior, lateral and inferior (compressive) load that was recorded during the 'sit to stand activity' and 'stand to sit activity'

7.3.2.10. Task difficulty and performance index

As is clear from the kinematics data, some subjects performed better than others. If we consider the target position of each task as the standard of achievement for each subject of the Delta group, then we can score each subject with:

- 0 for not completing the task;
- 1 for completing the task but with different approach from Normal subjects (different values of azimuth, elevation and rotation);
- 2 for completing the task similar to Normal subjects (humeral position values within the 2*SD of the Normal subjects)

By constructing a table with all the scores for all subjects for all activities, the normalised summaries of each task and of each subject can relate to how difficult an activity was (*Difficulty index*) or how well the subjects performed in ADL (*Performance index*). All values and indexes are shown in Table 7.9

From the scoring results it is clear that reaching the back of head and lifting block to head height were the most challenging activities, where 3 subjects (3 shoulders) were performing almost as well as the normal group.

Even if the indices on the Table 7.9 only give a rough indication of difficulty (of an activity) or performance (of a subject), the scoring of 0, 1 and 2 cannot represent the large variability of the movement of the DELTA group.

	Task No												***Performance index***
	1	***2***	***3***	***4***	***5***	***6***	***7***	***8***	***9***	***10***	***11***	***12***	
1	1	1	1	2	2	2	1	1	2	1	0	2	0.67
2	1	2	1	2	1	2	2	2	1	2	0	2	0.75
3	2	1	0	2	1	2	2	1	2	1	0	2	0.67
4	2	2	1	2	2	2	2	2	2	1	0	2	0.83
5	2	2	1	2	2	2	2	1	2	2	0	2	0.83
6	2	2	1	2	1	2	2	1	2	2	0	2	0.79
7	1	1	1	2	2	2	2	1	1	1	0	2	0.67
8	2	2	1	2	2	2	2	2	2	2	0	2	0.88
9	2	2	1	2	2	2	2	2	2	2	0	2	0.88
10 R	2	2	1	2	2	2	2	2	2	2	0	2	0.88
10 L	2	1	1	2	2	2	2	1	2	1	0	2	0.75
11	1	1	0	1	1	2	2	1	2	0	0	2	0.54
12	2	1	0	2	2	2	1	1	1	0	0	2	0.58
Difficulty Index	*0.88*	*0.77*	*0.38*	*0.96*	*0.85*	*1.00*	*0.92*	*0.69*	*0.88*	*0.65*	*0.00*	*1.00*	

Subject No

*Table 7.9: Scores of each subject on each activity. The normalised summaries are related to how difficult an activity was (*Difficulty index*) or how well the subjects performed an ADL (*Performance index*).*

7.3.3. Shoulder girdle elevation (shoulder shrug)

The shoulder girdle elevation is related to the movement of the clavicle and scapula. Recently, a study of Garofalo et al. (2009) tested a group of healthy shoulders and found that there is a consistent relationship between humeral elevation and shoulder elevation/depression or shoulder retraction/protraction.

Calculating the shoulder elevation for the maximum observed humeral elevation in each task of the ADL, the data of the Normal group showed a linear relationship with a rather high R squared value.

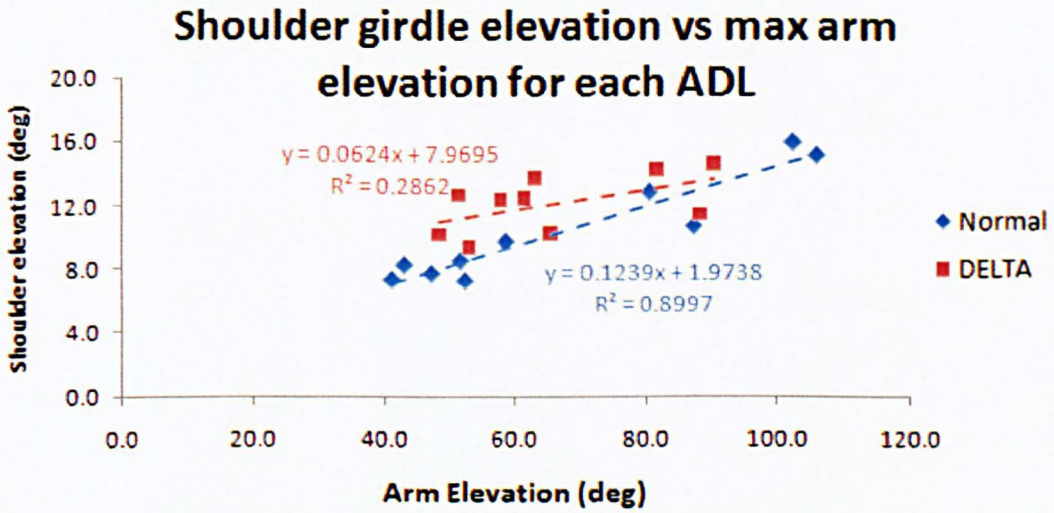

Figure 7.22: In contrast with the DELTA group, the normal subjects show a consistent linear relationship between shoulder elevation and humeral elevation

In contrast, for the DELTA subjects there is not such a clear relationship; they seem to elevate their shoulder girdle more in lower humeral elevation (Figure 7.22).

An interesting observation in the DELTA group was that some of the subjects (n=2 shoulders) were elevating and holding the shoulder girdle from the beginning of the activity (shoulder shrug - Figure 7.23). Even if this mechanism naturally lifts the whole arm upward (shifting) it is not clear whether this is the main purpose of the shoulder shrug, or there is an internal muscle optimisation that helps the subjects to elevate the arm. Unfortunately, it was not possible to record the precise scapula position during the shoulder shrug, since the subjects were not replicating the same motion during the static recordings of scapula kinematics.

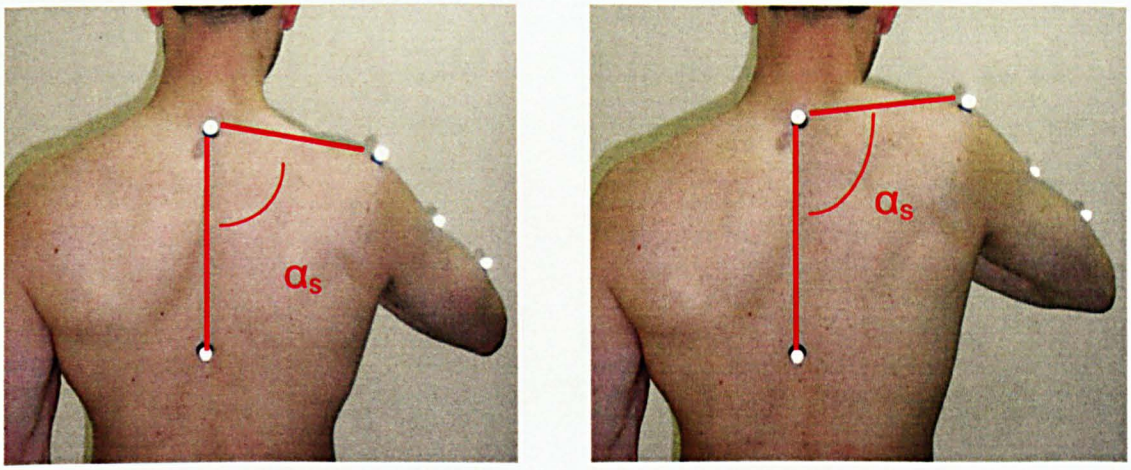

Figure 7.23: The 'shoulder shrug' mechanism where the subject elevates the shoulder girdle even in low deg. of humeral elevation

7.3.4. Task completion time

Except the differences in the kinematics patterns between the Normal and the DELTA group, the data showed that the latter group also required more time to complete an activity. The average time to complete an activity for the Normal subjects was 2.65 sec (sd 0.39) with a range of 2.16 sec to 3.34 sec. For the DELTA group this was 4.52 sec (sd 1.16) but with a larger range (3.13sec to 6.52 sec) (Figure 7.24)

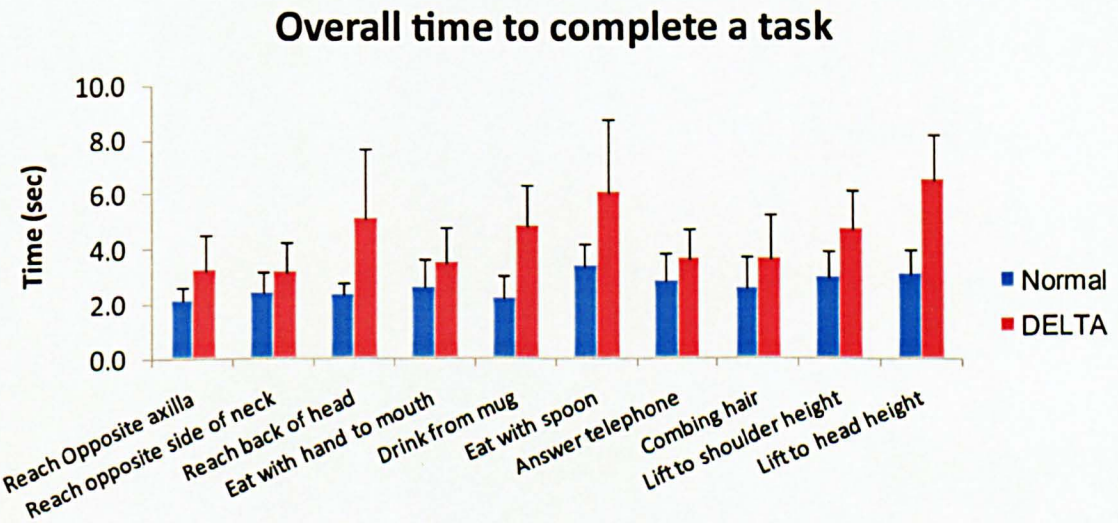

Figure 7.24: The overall time to complete an activity was much larger for the DELTA subjects

Even if the DELTA subjects required more time for all the ADL, the difference for 5 of the activities was larger that the rest. The greater times (and differences with the Normal subjects) were observed for the high elevating tasks ('Reach back of head', 'Lift block to head height', 'Lift block to shoulder height'), but also for the feeding tasks.

The overall increased time in all the ADL of the DELTA subjects may suggest an overall weakness (muscles) of the operated shoulder. The larger time difference in some of the activities that require more precision may also suggest a lack of muscle control. In a normal shoulder the co-contraction of the RC muscles can balance out large moments of the prime movers of the shoulder (m.Deltoid, m.Pectoralis, m.Lattisimuss Dorsi) to provide control and precision to the humeral movements (Veeger et al. 2006). As the data suggest (Figure 7.25), the DELTA subjects lack this specific control and thus they approach a target with a much slower speed, requiring more time to reach it (compared to the Normal subjects).

Target Approach time for 'Lift block to Head height' activity

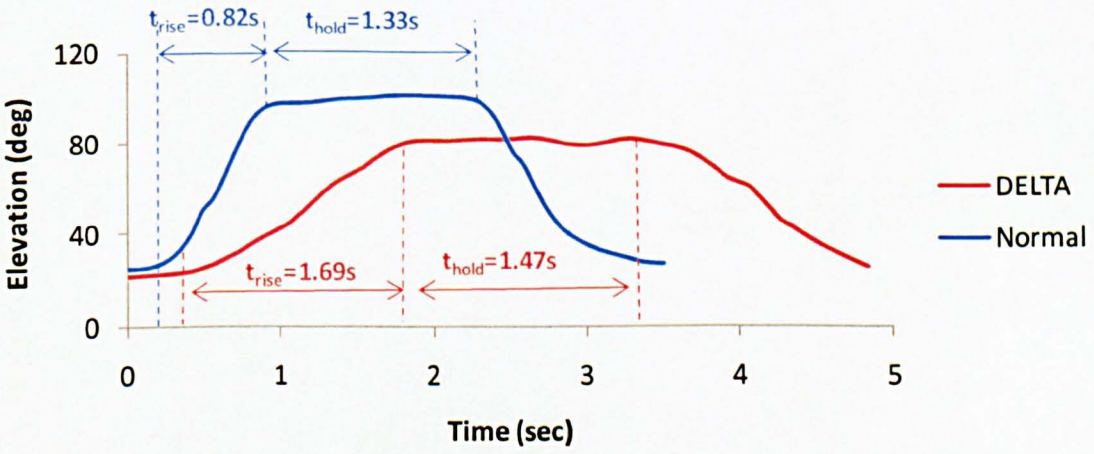

Figure 7.25: Specific example of two subjects on 'Lifting block to head height'. The time of the DELTA subject to reach the target 't_{rise}' is much larger and disproportional to the holding time 't_{hold}' compared to the normal subject

7.3.5. Clinical scores and correlations

All subjects completed the 2 different clinical scale questionnaires after the completion of the recordings of scapula and ADL. The Standard Score SF_36 is a clinical scale that includes 36 questions and has a scoring scale of 0 to 100 points. The Oxford clinical scale is a shorter test (12 questions) that has a reverse scale scoring system with 48 points being the worse result and 0 being the best.

Shoulder No.	Oxford	SF_36
1	42	78
2	34	95
3	31	65
4	29	71
5	26	74
6	43	42
7	40	71
8	15	80
9*	24	87
10*	20	89
11	39	61
12	26	81
13	40	61
Average:	***31***	***73***

* Right and left shoulder of same subject

Table 7.10: both clinical scores of all the DELTA subjects. The scoring was performed by an orthopaedic surgeon

Both of the scores were tested for normality with an Anderson-Darling normality test and found to follow a normal distribution (Oxford $p=0.462>0.05$, SF_36 $p=0.843>0.05$). For better presentation and comparison purposes the Oxford scale was reversed (0 being the minimum and 48 being the maximum) and then both scales were normalised (by dividing with their maximum value) so that both cover a range from 0 to 1 (min to max) – Figure 7.26.

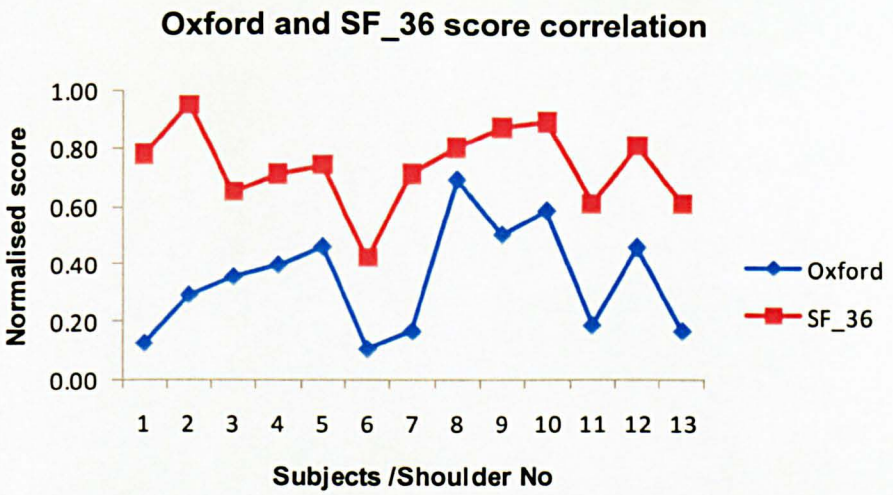

Figure 7.26: The normalised scores of Oxford and SF_36 scales for all the DELTA group shoulders show a rather small correlation.

In order to investigate the correlation between the two different clinical scores, the Pearson correlation coefficient was calculated using the eq. 7-1

Pearson correlation coefficient:

$$r = \frac{\sum(x_i - \overline{x}) * (y_i - \overline{y})}{(N-1) * s_x * s_y} \qquad \textit{eq. 7-1}$$

Where

x_i, y_i is the value of the variable (e.g Oxford – x and SF36 – y) of a specific observation (e.g. specific subject)

$\overline{x}, \overline{y}$ is the mean of the population of the x and y variables

s_x, s_y is the standard deviation of the x and y population

The correlation coefficient is a standardised form of the covariance between two samples and shows if there is a dependency between any changes in the 2 variables of the groups. The range of the coefficient lies between -1 and +1. A coefficient of +1 indicates that the two variables are perfectly correlated and thus a change in one of the variables means a proportionate amount of change to the other variable. Negative values indicate a reverse proportionate relationship where 0 indicates that there is no correlation.

Surprisingly, the coefficient between the two clinical scores of the DELTA group was rather small (***r* = 0.590**), indicating a poor correlation between Oxford and SF_36.

Correlation between the clinical scores and the performance indices on Table 7.9 were also calculated, but the values of ***r =0.524*** and ***r =0.209*** (for Oxford and SF_36 respectively) show no significant correlation either.

7.3.5.1. Correlation between ROM in ADL and clinical scores

In order to investigate whether there was any correlation between the clinical scores and the kinematics data of the ADL, the values of elevation, azimuth and humeral rotation, of each DELTA subject was normalised against the mean of the corresponding values of the Normal group for each task.

So if the average value of each DoF (elevation, azimuth and humeral rotation) between the Normal group for each task is:

$$\overline{Ndof_i} = \sum_{s=1}^{10} \frac{Ndof_{s,i}}{Ns} \qquad \text{eq. 7-2}$$

Where:

$Ndof_{s,i}$ is the value of each DoF (elevation $Nel_{s,i}$, azimuth $Naz_{s,i}$, humeral rotation $Nr_{s,i}$), for the Normal subject No s in the i^{th} task

Thus the normalised average value (for all the task) of each of each DoF of each DELTA subject is:

$$\overline{Ddof_s} = \sum_{i=1}^{10} \frac{Ddof_{s,i} / \overline{Ndof_i}}{Ni} \qquad \text{eq. 7-3}$$

Where:

$Ddof_{s,i}$ is the value of the DoF (elevation $Del_{s,i}$, azimuth $Daz_{s,i}$, humeral rotation $Dr_{s,i}$), for the DELTA subject No s in the i^{th} task

Ni is the number of tasks

The correlation coefficient was calculated for each subject and each DoF (correlation between Oxford or Standard score with $\overline{Del_s}$, $\overline{Daz_s}$, $\overline{Dr_s}$,), as well as with the combined contribution of all of the DoF

$$Cs = \sqrt{\overline{Del_s}^2 + \overline{Daz_s}^2 + \overline{Dr_s}^2}, \qquad \text{eq. 7-4}$$

(Combined normalised contribution of all the DoF for each subject s)

The correlation coefficients are presented in Table 7.11

Correlation between ADL and clinical scores

	Azimuth	Elevation	Hum. Rot	Combined
Oxford	0.19	0.07	0.45	0.59
SF_36	0.12	0.29	0.44	0.21

Table 7.11: All the Correlation coefficients between the normalised range of motion during the ADL and the clinical scores were low

From the results it is clear that there is not a significant correlation between the range of motion during the ADL and the clinical scores. Surprisingly, the highest value was observed between the Oxford score and the combined value (0.59), even if the SF_36 questionnaire includes specific questions of ADL that are similar to the ADL protocol of this study.

The highest correlation value was observed between the ADL (combined value) with the subject performance indexes on Table 7.9 (***r = 0.612***). Even if this value is the highest correlation value, it is still small and does not reflect straight forward correlation between the two. The performance indexes are clearly reflecting on the ability of a subject to perform the ADL, but the discrete scoring of 0, 1 and 2 cannot represent the large variability of the movement within the DELTA group fact that reducing the correlation factor.

7.3.5.2. Correlation between RoM in Standard activities and the clinical scores

Many clinical studies often report RoM of standard tasks (abduction and internal/external rotations) as a measure of performance of the joint replacement.

Thus, the last set of correlation coefficients were calculated for range of humeral motion in the standard activities (Figure 7.9). The range of the elevation values of the abduction, forward flexion and scapula plane were averaged and – together with the range of the internal/external rotational values (in 90 deg abduction) – compared with the clinical scores.

Correlation between Standard activities and clinical scores

	vs Elevation	vs Rotation	vs Combined
Oxford	0.12	0.40	0.31
SF_36	0.31	0.55	0.48

Table 7.12: The correlation coefficients show that there is no significant correlation between the range of motion that is measured in standard activities and the clinical scores.

Again all of the correlation coefficients were low (suggesting poor correlation). The highest value of 0.55 was observed between the SF_36 and the range of humeral rotation.

7.3.5.3. Short conclusions on the correlations

From the results it is clear that there is not a straightforward correlation between the clinical scores and any of the kinematics data (standard activities or ADL). The clinical scales have been validated in many clinical studies and they have been optimised in order to reflect patient satisfaction after the joint replacement. Even if both scores include questions of functional activities, there are also many subjective questions related to pain and overall personal satisfaction. Thus, the outcome of the clinical scores is reflecting not only the kinematic performance/rehabilitation after the joint replacement but also the overall personal health of the patient. However, the kinematics results of this study are focused only on the performance of the shoulder by comparing its function with the normal activity, which can explain the low correlation between the kinematics data and the clinical scores.

7.4. *Short Summary – Conclusions on arm kinematics*

The kinematics analysis of the ADL have shown that the DELTA group, in general, was able to perform well, completing most of the activities in the protocol where in general achieved high humeral elevation (comparebale to Normal subjects). It was also clear that the DELTA subjects had a limited range of humeral internal/external rotation, which was reflected in the failing of the activity 'Reach hand to lower back'. The lack of the RC muscles have forced some of the subjects to adopt different approaches to some

tasks in order to reach the target position of the activity. Thus, the variability on the kinematics data was large, while the Normal group was very consistent in most of the activities

In this study there was no tracking of the hand (wrist movement). Van Andel (2006) argued that tracking the movement and orientation of the hand is a major determinant in the accomplishment of functional tasks, since the arm may be considered as a positioning instrument for the hand. For example, if shoulder ROM is increased following a joint replacement, functional gain will be absent when the hand is not able to use this extended ROM. To some degree, this was obvious to one of the subjects of this study (subject 11) where finger arthritis forced the subject to hold the objects used in tasks 5, 9 and 10 with a different grip and as a result changed the movement of the whole upper arm in order to approach the target.

It was a surprise not to find any significant correlation between the results of the two clinical scores (Oxford and SF_36) and any set of the kinematics data of this study. This reflects the difference of the objective of the two: where the clinical scales' target is to show overall satisfaction, the kinematics analysis shows only general performance. Even if the kinematics analysis of the upper extremity is not very popular yet, future studies should consider the development of a more unified protocol whereby a correlation (to some degree) can be achieved between clinical scores and kinematic analysis: this would provide a unified database to benefit clinical diagnosis and monitoring of different rehabilitation techniques.

Chapter 8. Glenohumeral range of loading in a reverse prosthesis during Activities of Daily Living

8.1. Introduction

Forces at the shoulder have typically been dismissed as being small compared to other joints like the knee and hip. Typical values of 0.9 times body weight (BW) for unloaded arm abduction such as those suggested by Poppen and Walker (1978) have been extensively referenced and used in various biomechanical studies. Since, more recent and sophisticated models (Charlton 2003,Karlsson & Peterson 1992,Runciman & Nicol 1994,van der Helm 1994) have studied GH loading in range of activities (e.g ADL) to estimate a wider range of GH loads, which can be up to 2.4 BW for tasks with external loads (Anglin et al. 2000).

However, most of the above GH contact forces are cited with reference to the normal shoulder and, unfortunately, there is not much information regarding reverse joint replacement. Very recently, Westerhoff et al. (2009b) used an instrumented prosthesis (Westerhoff et al. 2009a) and published the first in vivo set of GH loading results, of four subjects performing ADL, reporting a range of GH loading values that is as large as 1.38xBW. However, those loading values that recorded during ADL with small to moderate hand load (1.5 – 2.0 kg) are measured from an anatomical instrumented prosthesis. Loading of a reverse prosthesis is expected to be different.

The objective of this chapter is to use the kinematic dataset that was presented in chapter 7 and to use the biomechanical model to create a database of GH loadings that act on a reverse prosthesis during ADL. The predicted loads that - as shown in chapter 5 - are expected to be different from those in a normal shoulder (and in general any anatomical joint replacement) will provide useful information for those performing mechanical testing and/or finite element analysis of reverse shoulder prostheses.

In addition, some wear approximation will also be presented in this chapter as well as a summary of the activity of the GH muscles in order to understand the effect of the reverse joint replacement on the shoulder function.

8.1.1. Model set-ups and results format

The biomechanical model was scaled accordingly to simulate each individual subject of the Normal and DELTA group (table 7.4 and 7.5). The scaling technique follows the Newcastle Shoulder model (Charlton 2003) where thorax, clavicle, scapula, humerus

and forearm (ulna/radius) are scaled individually (non-homogenous scaling) from the bony landmarks that were palpated in the kinematic recordings (chapter 7, Figure 7.5 and Table 7.3).

Following the medical record of the DELTA group, the small size prosthesis (DELTA 36) was fitted to 10 of the subjects (11 shoulders) where the remaining 2 subjects were fitted with the larger size DELTA 42. The models were further customised to fit the individual subjects by including the scapula kinematics data shown in chapter 6 (for 10 out of the 12 subjects).

As mentioned earlier, there was no detailed information regarding the size of the RC tear or on whether any remaining RC fibres were still attached after the surgery. Thus, (as in chapter 5) all the individual models were set up with the m.Teres minor as the only remaining RC muscle (FTT - Full Thickness Tear). Models of Supero-Anterior Tear (SAT – infraspinatus only present), Supero-Posterior Tear (SPT – subscapularis only present) and Extended Tear (ET) were also simulated for the DELTA subjects.

Of key importance in examining the muscular activity and loadsharing in many subjects is the normalisation of muscle force. Muscular activation is defined as muscle force divided by maximum force and will hence be used in all places where muscle forces are examined directly. As in most of the literature, joint contact forces are presented in subject bodyweight (BW) for comparison purposes and the GH forces will be displayed on the joint replacement in order to better comprehend the force direction and the stability of the joint.

As a reference, the ADL are shown on Table 8.1. Results of Task 12 are usually presented in individual graphs, since the specific activity creates larger scale values than the other tasks in the protocol.

Activities of Daily Living

1	Reach to opposite axilla	**7**	Answer telephone
2	Reach to opposite side of neck	**8**	Combing hair (contra-lateral side)
3	Reach to back of head	**9**	Lift block to shoulder height
4	Eat with hand to mouth	**10**	Lift block to head height
5	Drink from mug	**11**	*Reach lower back*
6	Eat with spoon	**12**	*Sit to stand and Stand to sit*

Table 8.1: ADL that were analysed in this study

8.2. *Summary of GH moments*

The kinematics data in the previous chapter showed that the most difficult activities (where difficulty was calculated using the 'Difficulty index' (section 7.3.2.9)) were the 'Reach back of head' (Test 3), 'Lift block to head height'(Test 10) and 'Lift block to shoulder height'(Test 9) (excluding the 'Reach lower back' activity, which all the subjects failed to complete).

The total net moments generated at the GH joint from the ADL for the DELTA group are summarised in Figure 8.1. The moment results show slightly different activities as the most demanding (highest moments) with the Test 9 and 10 generating the highest moments followed by Test 5 and 8.

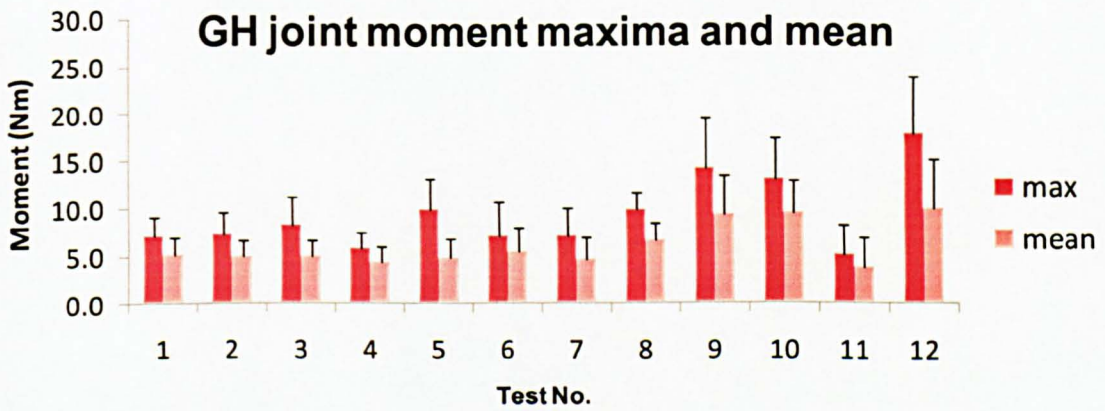

Figure 8.1: Maxima and mean of GH moment during ADL

Naturally, the highest moment was observed during the 'Sit to Stand' and 'Stand to Sit activity' because of the high reaction force on the hand. The maximum moment values of this task have ranges of 18.10 Nm (sd 5.89) for the standing phase and 18.02 (sd 5.58) for the Sitting down phase. Considering the high external load compared to the other tests, this value is rather close to the maximum moment of Test 9, but this can be explained by the direction and place of application of the external force. In the sitting and standing activity, the maximum load on the hand occurs while the hand is close to the body and, as a result, the external force points close to the centre of rotation of the arm. In contrast, during the lifting activities of Test 9 and 10, the subjects had to extend the arm in order to reach the target of the activity and thus the combined weight of the arm and the object are much further from the GH joint and so generate high moments. However, the high external force on Test 12, even if it generates moderate GH moments, is expected to increase the joint contact forces.

8.3. *Joint contact forces in the Glenohumeral Joint*

The results of the total joint contact force in the GH joint showed values peaking at 0.77xBW (sd 0.11) for the DELTA group in Test 10, while the values in the high loaded Test 12 were as high as 1.47xBW (sd 0.48) for the standing phase and 1.38 (sd 0.47) for the sitting phase (Figure 8.2).

Comparing the same values for the Normal group, it is clear that the values are larger, with an average difference of 0.16xBW (sd 0.06) and a range of 0.09 to 0.31xBW, for the first 11 activities. This difference goes up to 0.73xBW for Test 12. The values for this specific activity are larger from what Anglin et al. calculated using the Swedish Shoulder model (Karlsson & Peterson 1992), but so was the external hand load that was recorded during the activity (chapter 7)

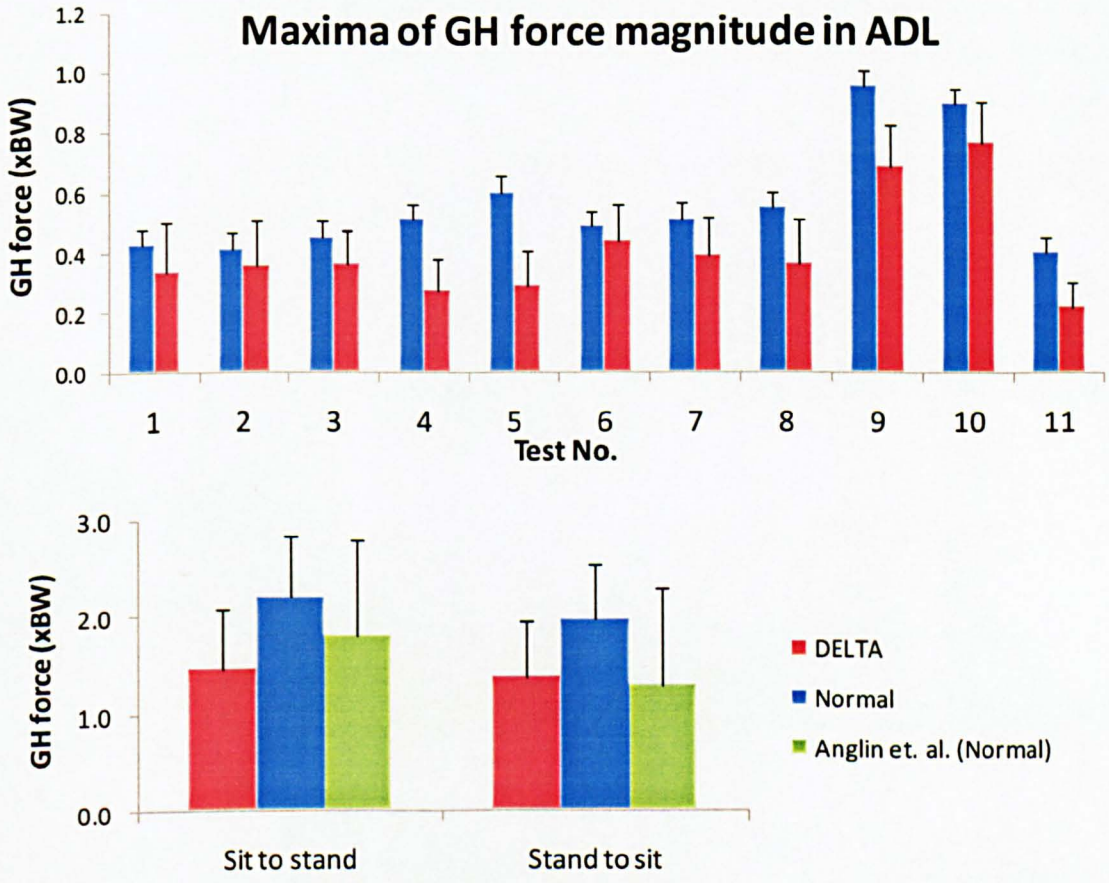

Figure 8.2: The results show that the maxima of GH contact force in the Normal group are larger for all the activities

The values of GH contact forces shown above are rather large, considering the upper limb accounts for only 5% of the total BW. The large forces are due to the large external

moments and to the fact that many of the muscles that act as prime movers or stabilisers do so to a joint that has a rather small articulating surface. For the small prosthetic joint (DELTA 36) the articulating surface of the cup is just 9.05 cm^2 and, considering the highest predicted load is 968 N (in Test 12), the maximum stress is 1.07 MPa. This value is much smaller than the yield stress of the UHMWPE material of the cup, which is 23MPa (Avallone E.A. et al. 2006).

In order to further understand the action of the joint contact forces, they are analysed and presented below on both the glenoidal and the humeral sites.

8.3.1. Glenoid loading

The results of the glenoid loading for the DELTA and the Normal group, and for the first 11 tests, are presented in Figure 8.3. The values of the graphs in the Figure 8.3 represent the maxima of each component of the GH force (compressive, superior and antero/posterior shear forces) and they usually appear in a different phase during the motion (eg. Figure 5.31). Thus the composition of the three components does not correlate with the respective maximum value of the magnitude of the total GH force that is presented in the graph of Figure 8.2.

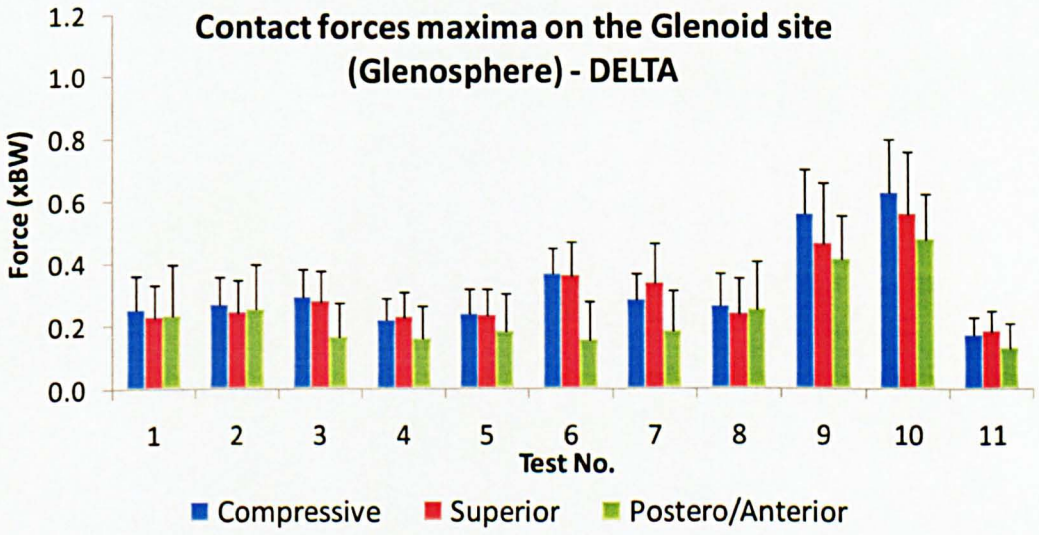

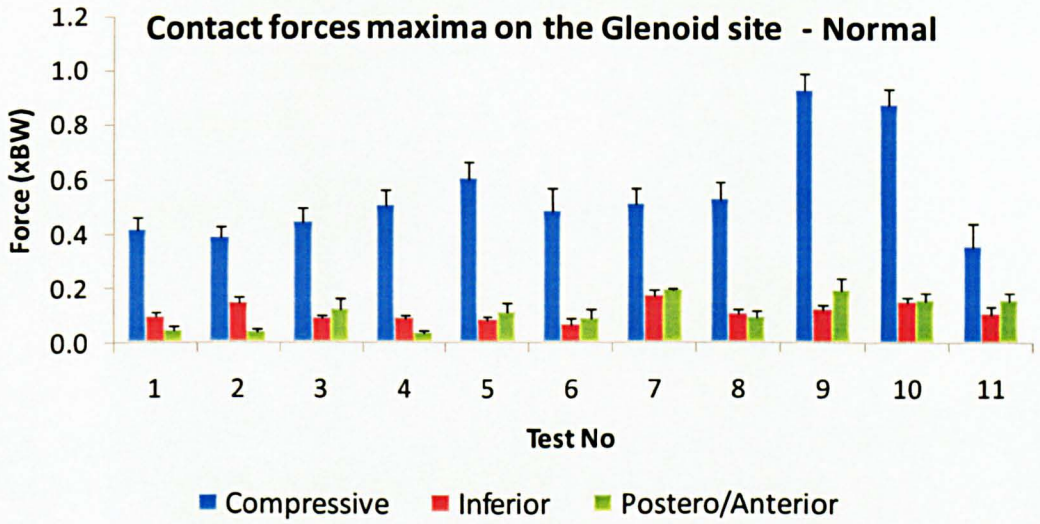

Figure 8.3: The contact force maxima on the Glenoid (Glenosphere) for the DELTA group showed large shear forces (especially the superior), whereas in the Normal group it is the compressive force that is dominant

From the results, the difference between the two different loading patterns is clear: in the Normal group the dominant component is the compressive force that accounts for almost the 78% (in average) of the total GH force and is 4.3 times larger than the shear forces (combined inferior and antero/posterior together). This relationship seems to agree with the findings of Charlton (2000), even if the absolute values of compressive and shear forces were lower for the Tests 3, 9 and 10.

In contrast with the above results, the glenoid loading (on the glenoid sphere) of the DELTA group shows large shear forces. The magnitude of the superior loading is almost as large as the compressive loading with a ratio of 1.05 (compressive/superior). The compressive load was less than the Normal group, with an average of 0.323xBW (sd 0.138) and a range of 0.631 to 0.176xBW, and with the maximum value observed in Test 10 instead of Test 9, which is (Test 10) the activity with the maximum compressive load in the Normal group.

The increase of the superior loading that now ranges from 0.181 to 0.557xBW is a direct result of the upward pulling of the m.Deltoid and the lack of RC muscles to provide any compressive stability. Even at high levels of arm elevation the increased scapula lateral rotation in the DELTA subjects (described in detail in chapter 6) more exposes the inferior part of the glenoid sphere to the resultant GH contact force (and as such increases the superior loading - Figure 8.4).

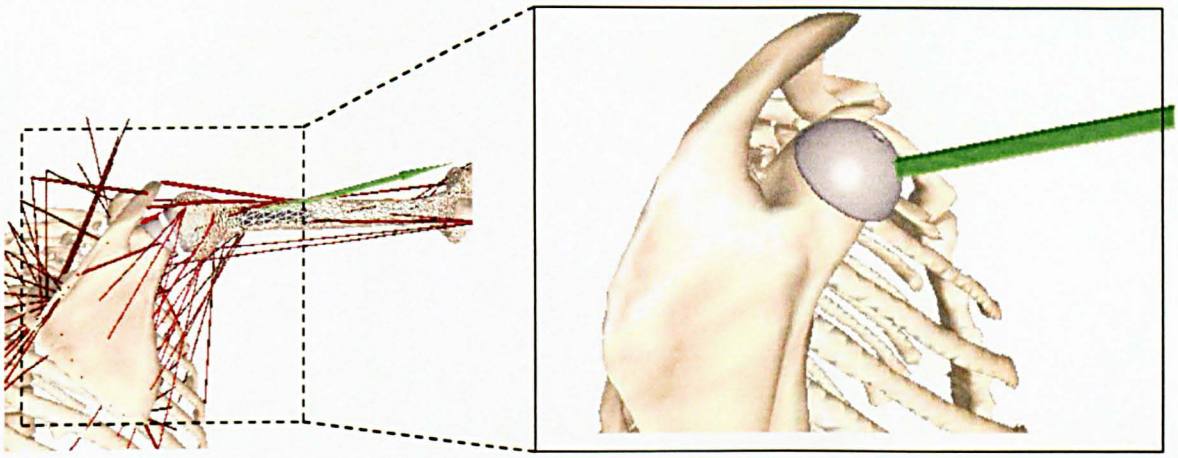

Figure 8.4: When the arm is elevated the resultant force (green vector) is generated by the m.Deltoid and, in combination with the increased scapula lateral rotation, this force is loading the inferior part of the glenoid sphere (Superior shear glenoid force)

The antero/posterior forces are not as large as the compressive or the superior forces, but they are also increased significantly compared to the Normal anatomy with an average maximum value of 0.237xBW (sd 0.113). The direction of the loading (anterior or posterior) is mainly defined by the plane of elevation of the arm. Most of the ADL required the arm motion to be in front of the subject and, as a result, the posterior contact forces were generally larger than the anterior forces (ranges: 0.127 to 0.483xBW posterior, 0.062 to 0.355 anterior (Figure 8.3)).

The direction of the loading is very significant for the fixation of the rather large sphere on the small glenoid surface. So far, most reports of the clinical and biomechanical studies of reverse prostheses have focused on the high superior loading and so most currently available designs primarily address the fixation by using screws on the supero/inferior axis. The findings of this study, however, also highlight rather large loads in the antero/posterior direction, indicating that a secure fixation in this direction is very important.

(a) (b)

Figure 8.5: Different approach on glenoid fixation: (a) only 2 fixation screws on the supero/inferior direction (b) multiple direction of fixation screws to withhold forces in postero/anterior and supero/inferior directions

The point of application of the GH contact force on the glenoid sphere for tests 1-11 and for all the subjects, are shown below in Figure 8.6. From the results it is clear that the GH forces cover only the inferior half of the sphere.

GH contact force on Glenosphere

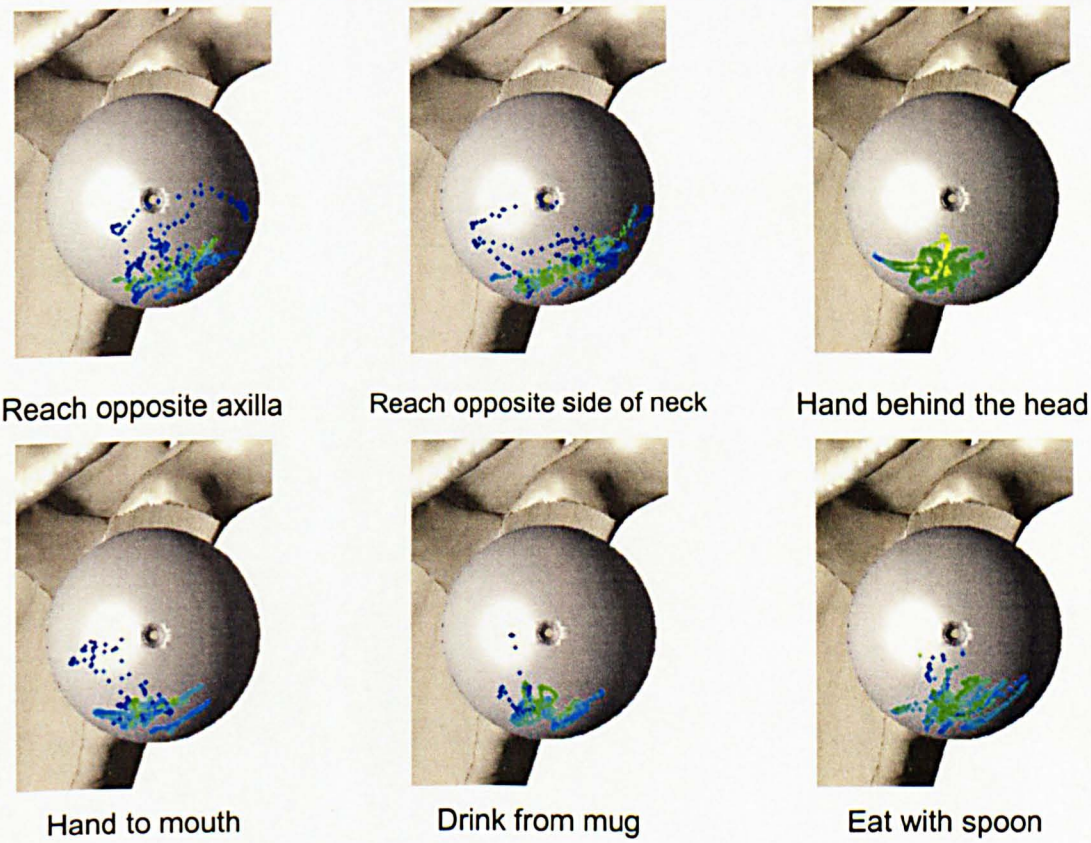

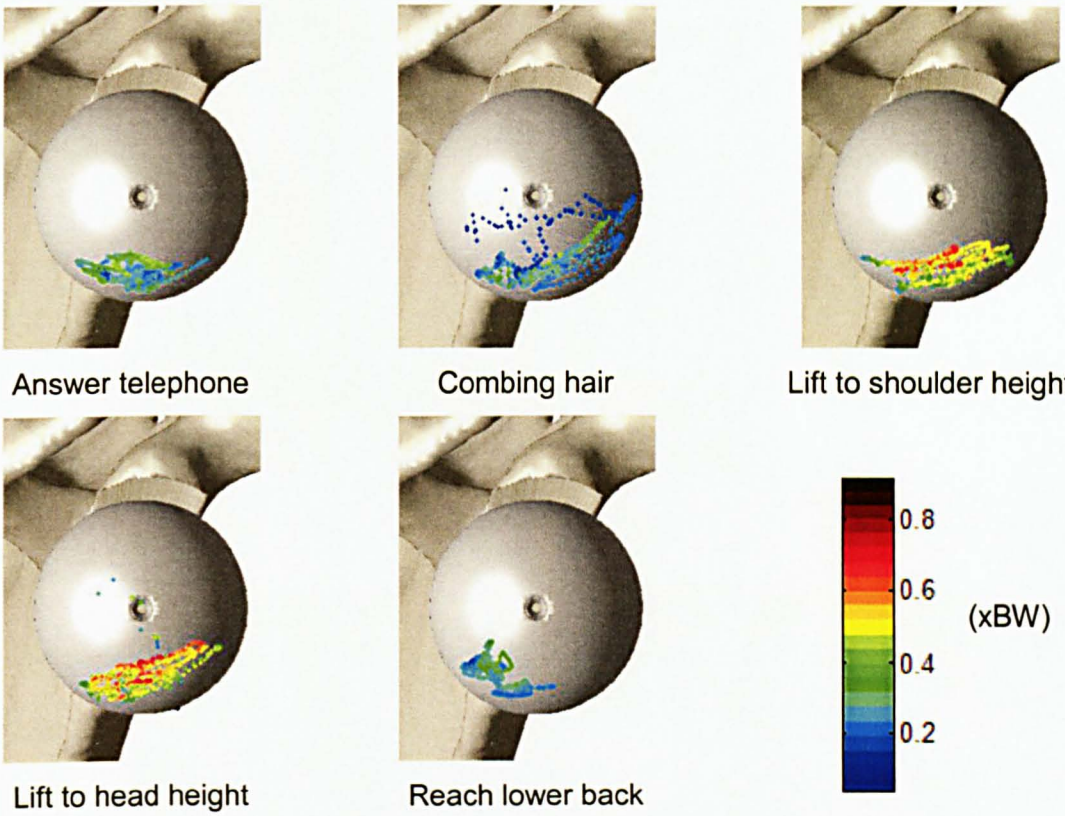

Figure 8.6: Contact force point of application on the glenoid sphere for the ADL

As shown above, Test 12 created the largest GH contact force, which was almost the same for the 2 phases (1.474xBW standing up and 1.385xBW sitting down). As expected, in both phases the superior loading is dominant (Figure 8.7) and it reflects the effect of the external reaction force on the hand, but the other two GH force components were also large. This is due to the contraction of the triceps, which balances the elbow flexion moment and the contraction of m.Latissimus Dorsi and m.Pectoralis major thoracic; muscles that balance the abducting moment that the external force is creating.

In addition, the loading of the glenoid sphere shows slightly different patterns for the two phases: in the standing phase, the compressive and posterior forces are larger than those in the sitting down phase. Even if the arm kinematics are not very different between the two phases, there is a difference in the application of the external force (reaction force between the hand and the arm of the chair) as described on chapter 7 (section 7.3.2.8). During the standing up phase the subjects push the arm in the beginning of the activity - when the elbow is still flexed - and relax the arms while they are getting into an up-right position. During the sitting down phase, the subjects apply the force again in the beginning of the activity where the elbow is less flexed and relax the arm while they are sitting down.

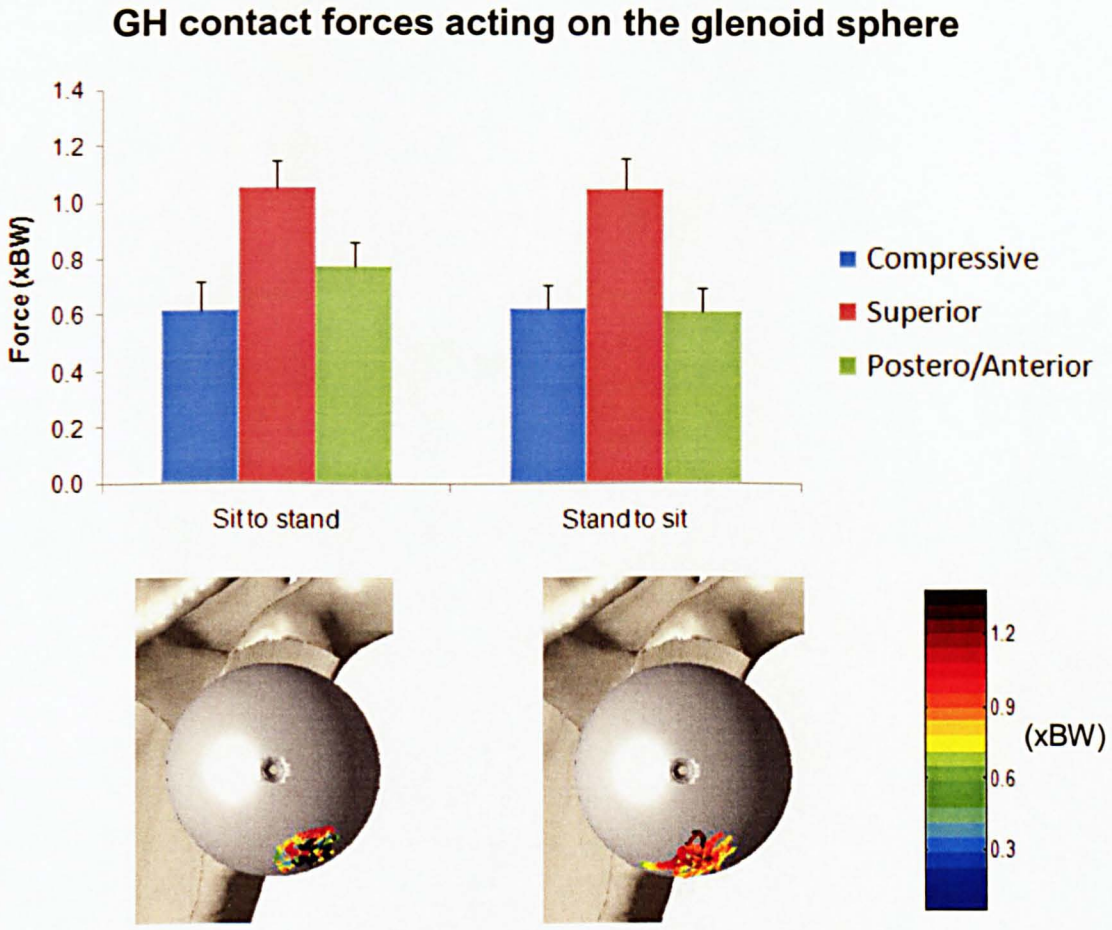

Figure 8.7: The superior forces are dominant in both phases of Test 12, but there is a difference in the ratio of the superior and Postero/anterior forces due to the difference in the external application of the force on the hand

8.3.2. Humeral loading

Analysing the GH contact force on the humeral frame, the results again show the difference on the loading between the Normal and the DELTA group.

The compression/stability forces (on the glenoid) that the RC muscles are generating in the normal shoulder are translating as lateral loads on the humerus in the DELTA group. The lateral loading is dominant during Tests 1, 2, and 4-8 where the humerus has a moderate elevation (<40 deg). As the humerus is lifted higher (Tests 3, 9 and 10) the superior part of the humeral head is pressed against the glenoid and, as a result, the humeral axial loading is increased (Figure 8.8).

The GH force in the DELTA subjects is loading the humerus (and thus the implant) with a different pattern. The high superior loading on the glenoid sphere that was reported above is now translating into a compressive force of the humerus and the

implant. This is the dominant loading (average maximum 0.401xBW sd 0.08) and is increasing as the humerus is elevated higher (range 0.223 to 0.6149xBW) (Figure 8.8).

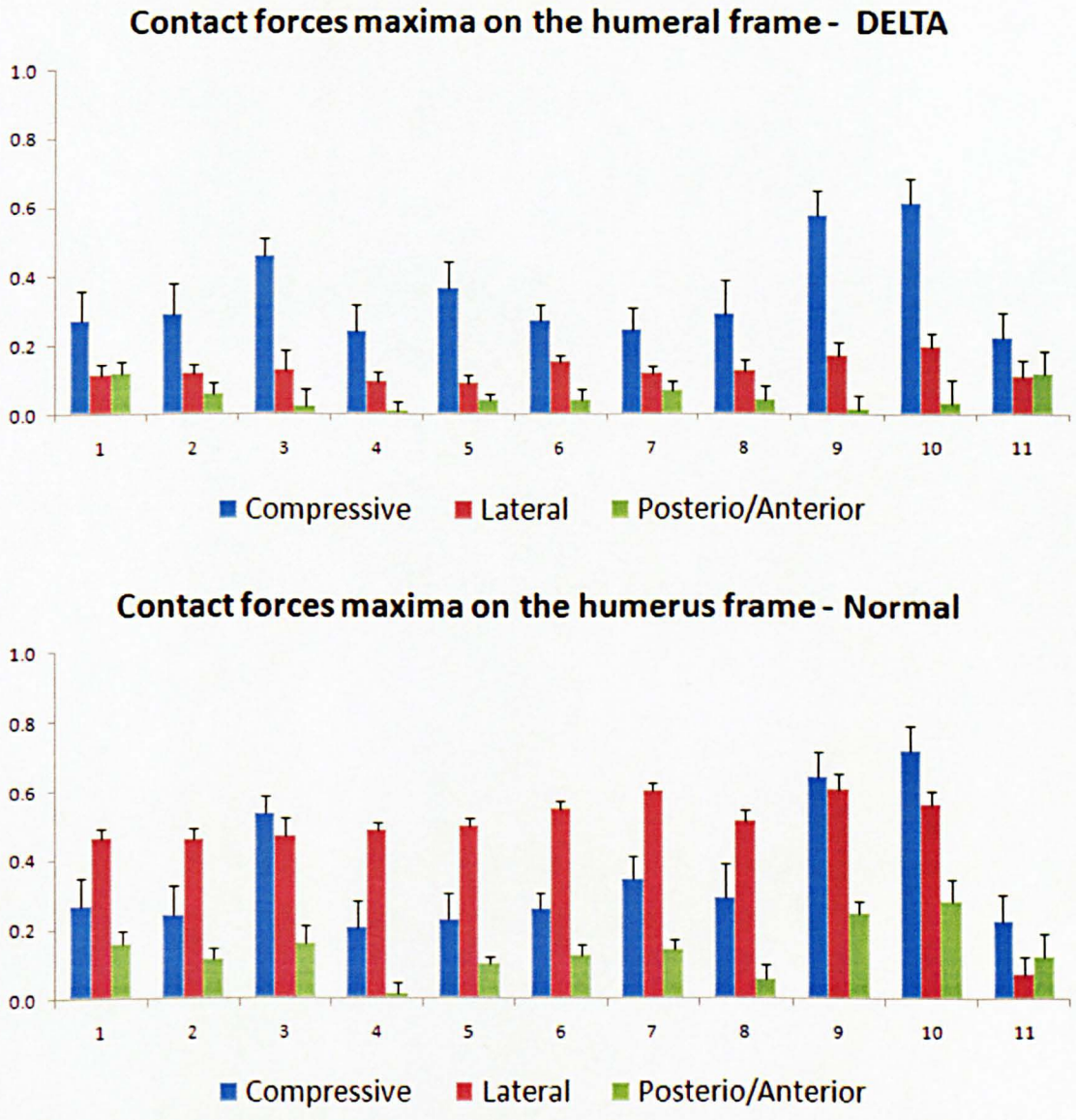

Figure 8.8: The contact forces maxima on the humeral frame for the DELTA group showed large compressive forces, while in the Normal shoulders lateral forces can be as large as the compressive forces, depending on the humeral position.

Like in the values in Figure 8.3, the data above represent the maxima of each component of the GH force which usually appear in a different phase during the motion and thus their composition does not correlate with the respective maximum value of the magnitude of the total GH force (Figure 8.2).

The point of application of the contact force on the humeral cup for each activity and for all the subjects is shown in Figure 8.9. It is clear that the cup is compressed mainly at the inferior part, which translates to high humeral compressive forces.

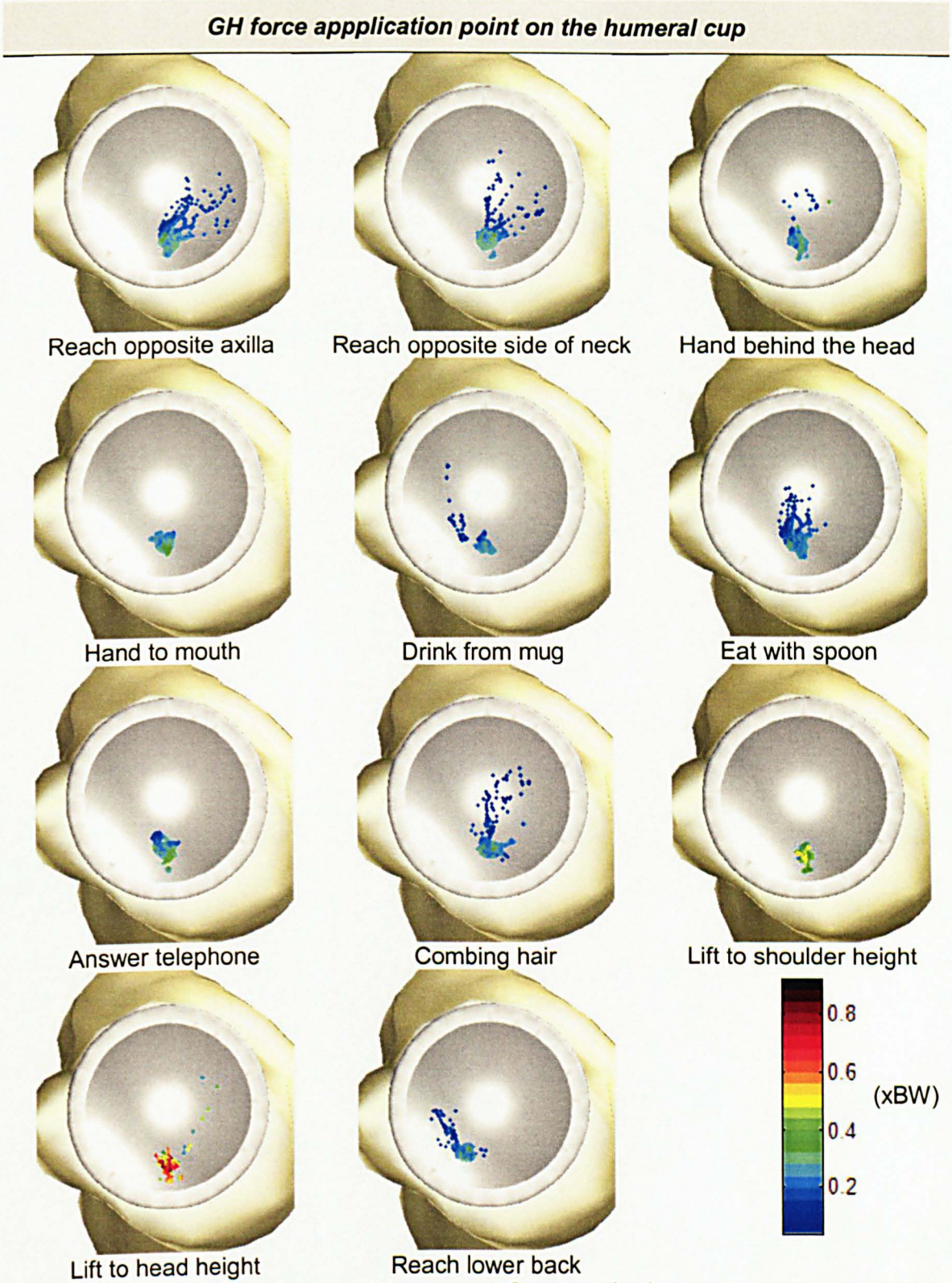

Figure 8.9: Point of application of the contact force on the humeral cup for each of the ADL

As expected, the compressive forces on the humerus were dominant during the 'Sit to stand' and 'Stand to sit' activities, reaching values of just over 1xBW(1.097xBW in 'Sit to stand' and 1.185xBw in 'Stand to sit). As with the glenoid, the anterior loading of the humeral cup during the standing up phase was larger compared with the anterior loading in the sitting down phase. This is for the same reason that was explained above (Figure 8.10).

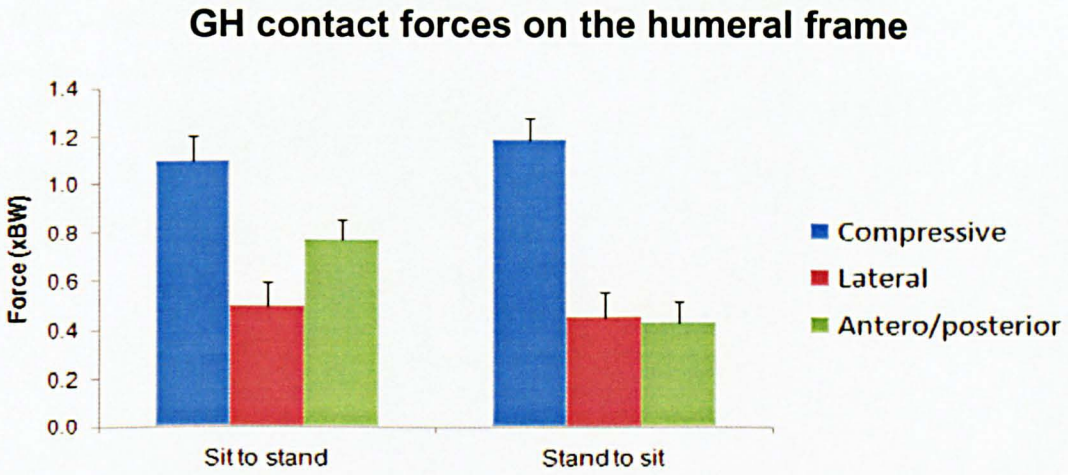

Figure 8.10. The compressive forces were also dominant in the humeral frame during the Sit to stand and Stand to sit activities

8.3.3. Stability of the joint replacement

Stability of the GH joint is an area of great interest; the bony structure of the joint is intrinsically unstable and is prevented from dislocation or subluxation through forces in the surrounding muscles and ligaments. The physiological mechanisms by which stability is maintained from a motor control perspective are still under discussion and are most likely complex and varied (van der Helm et al. 2000).

The criteria for stability in this study are straightforward, merely that the vector of the GH contact force should not pass outside the stability area which, for the DELTA anatomy, is the area of the concave humeral cup and for the normal anatomy is the glenoid cavity.

The GH joint contact results presented above (paragraph 8.3.2) showed that when there are no RC muscles the resultant force that is generated primarily by the prime movers of the shoulder (m.Deltoid, m.Latissimus Dorsi, m.Pectoralis) follows the direction of the humeral shaft (thus the large compression values on the humeral frame). The great advantage of the reverse prosthesis is that it restores the joint stability by

reversing the critical articulating area (the stability area) to match the direction of the contact force by placing the cup on the humerus. In contrast with the glenoid in the normal shoulder, the Glenosphere provides a very large articulating surface and does not compromise the joint stability in any occasion.

The results in Figure 8.9 show the joint stability of the reverse shoulder with all the joint contact forces to be constrained within the rim of the humeral cup. Despite this, a numerical measure of the stability of the GH joint during the examined activities would be useful.

In chapter 5 (section 5.6.2.1) it was shown how the ratio of the depth of the cup *h* to the radius of the sphere (h/R) can affect the stability of the joint, since it defines the maximum allowed ratio of the shear to compressive force:

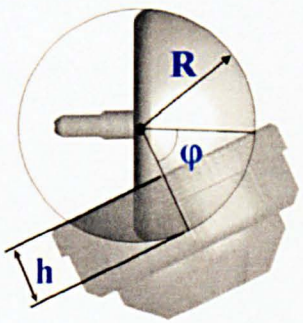

$$\left(\frac{shear}{compressive}\right)_{\max} = \frac{\sin\phi \cdot R}{R-h} = \tan\phi$$

If we define as "safety dislocation factor S_d" the ratio of:

$$Safety\ dislocation\ factor\ (S_d) = \frac{Max\left(\frac{shear}{compressive}\right)_{cup}}{\left(\frac{shear}{compressive}\right)_{loading}} \qquad eq.\ 8\text{-}1$$

Where:

$shear = \sqrt{Fx^2 + Fz^2}$ is the combined supero/inferior (Fx) and anterior/posterior (Fz) shear forces on the cup frame

$\left(\frac{shear}{compressive}\right)_{loading}$ is the ratio of shear to compressive joint contact force on the cup frame during a task

$Max\left(\frac{shear}{comp\ ressive}\right)_{cup}$ is the maximum ratio of shear to compressive joint contact force that can be constrained within the stability area of the cup. The values for the 2 different cup sizes of DELTA® 36 and 42 are 1.85 and 1.50 respectively.

then the mean value of the safety factor ($\overline{S_d}$) for each loading of every subject during a specific task can show the "stability or instability" of each task. A value of $\overline{S_d}$ smaller than 1 suggests that the stability of the joint is compromised, where a large value translates to a stable activity.

The results of the mean Safety dislocation factor show that even if all the activities converged to stable solution, Test 12 was the closest to 'instability', with Tests 4 and 6 being the most stable.

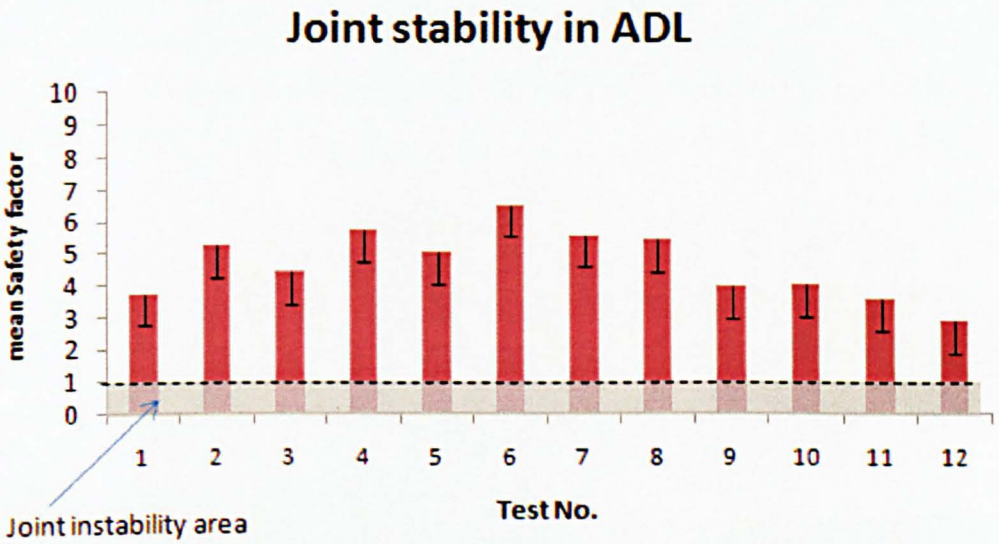

Figure 8.11: Even if all the activities converged to stable solutions the safety factor suggests that test 12 is the most possible to cause joint instability.

The average value of $\overline{S_d}$ for all the tasks was 4.7 (sd 1.1) suggesting that the locus of GH loading on the cup is not close to the rim of the cup. In theory the cup depth can be reduced by: $\overline{S_d} - 2 * sd - 1 = 4.7 - 2 * 1.1 - 1 = 1.5$ times and still provide GH stability to the current ADL, but in some of the activities the trace of the GH contact force will be very close to the rim of the cup (instability). It is arguable that a very large force near the rim of the humeral cup would lead to greater instability than a lesser force, but any force outside the glenoid could equally theoretically dislocate the joint. The Safety dislocation factor, $\overline{S_d}$, does not account for the magnitude of the GH load.

However, the results suggest that a cup with a smaller depth *h* and for the same glenoid radius *R* can provide GH stability and, as shown in chapter 5 and discussed

further in the next chapter, a shallower cup can significantly reduce the impingement problem.

8.3.4. Rotational and bending moments

The results of the contact forces have shown large compressive forces on the humeral frame. These forces are usually acting on the inferior half of the humeral cup and in an offset direction from the stem of the prosthesis. This naturally creates a moment around the stem which is the primary fixation element of the humeral component. The contact forces can create a multi-axial moment with the lateral and the compressive forces to create bending, and with the postero/anterior forces to create torsion. Making an assumption of a rigid fixation only along the shaft of the prosthesis the three moments (Mx-antero/posterior bending, My-torsional moment, Mz-Lateral bending – Figure 8.12) were calculated:

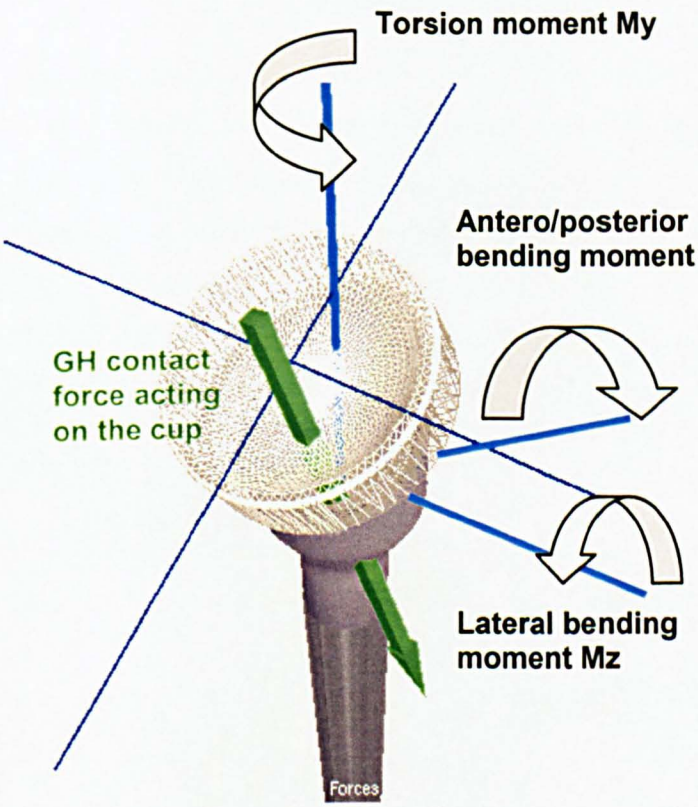

Figure 8.12: The application of the GH contact force on the humeral cup can create moments around the 3 axes.

The results show that the contact force can create a large lateral bending moment on the fixation averaging 3.9 Nm (sd 163). Torsion moment was surprisingly high, averaging 1.8 Nm (sd 1.3), while the moment around the x axis (antero/posterior bending) averaged only 0.9 Nm (sd 0.4)

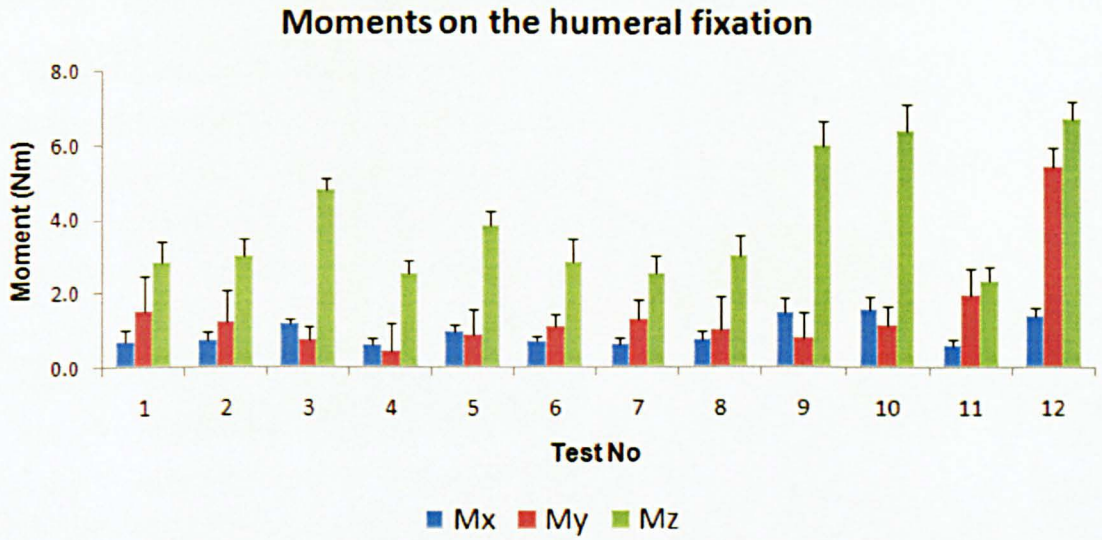

Figure 8.13: The GH contact force create large lateral bending on the fixation

The above values are rather large for the strength of the fixation, but the assumption of a rigid fixation only in the stem is also an underestimation. Most of the prostheses (e.g. DELTA) also use the neck to provide extra fixation by either applying a coating of Hydroxyapatite (HA) for osteo-integration or fixing it with bone cement.

The fixation of the long axis along the humeral canal offers a good resistance to the lateral and antero/posterior bending. In contrast, it can provide less resistance to the large values of torsion, which is probably why modern stem designs are adopting a more rectangular design in the profile of the stem or the neck of the prosthesis.

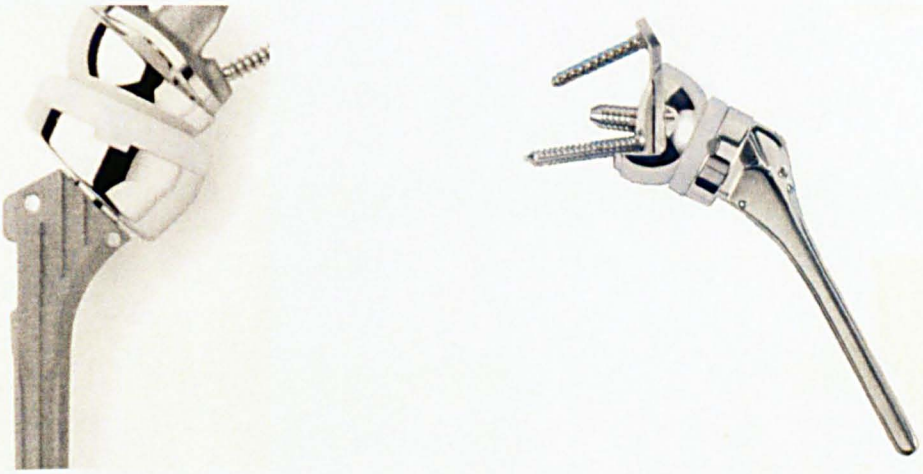

The Zimmer reverse/anatomical design Doucentric reverse (Aston Orthopaedics)

Figure 8.14: Some of the reverse design are adopting a more rectangular stem in order to resist the high torional loads

8.4. Basic estimation of joint wear

Wear of joint replacements is always a concern especially in high loaded joints like the hip and the knee. So far, the results of this chapter showed that the loadings of the GH joint are smaller than the knee or the hip, but are still considerably high. Certain ADL load the glenoid more and thus are considered as more 'demanding'. However, estimation of a GH wear rate would be a much more physiological basis for distinguishing activities as being "demanding" of the GH joint and can have a direct implication in implant design.

Charlton (2000) estimated the wear rates of a normal anatomy GH joint, given a known pressure distribution and the joint angle history.

Starting from Archard's wear model (Archard J.F. 1953) that gives a wear depth, h, for a finite surface element, i, per cycle:

$$h_i = \sum_{t=0}^{T} K \cdot P_t \cdot d_t \qquad \text{eq. 8-2}$$

Where:

d_t, is the slipped distance over an individual time step,

K is the wear coefficient and

P_t is the pressure on the articular surface over time step t.

Charlton estimated the volume V_t of the wear material generated over a finite time step t.

$$V_t = K \cdot F_t \cdot \sum_{t=0}^{N} \frac{(d_i)_t}{\bar{v}_i} \qquad \text{eq. 8-3}$$

Where:

Ft is the force acting on the finite element surface

A full analysis of the above equation is difficult, as the terms $(d_i)_t$ – the slipped distance over the i^{th} element over time step t – and $\bar{v}_i$ – the surface normal – require a finite element representation of each joint surface for calculation. However, Charlton obtained some comparative estimates of the wear depth (or volume) of the normal glenoid by making some broad assumptions:

- If an element experiences an equal slip of dt of the angular velocity, times the humeral head radius, the error in the slipped distance should be approximately equal for each test.

- Large changes in the pressure distribution on the glenoid surface from the GH contact force application are neglected.

Thus, the summation of $\sum_{i=0}^{N} \frac{(d_i)_t}{\bar{v}_i}$ becomes trivial, and it reduces to:

$$V = K \cdot R \cdot \Delta t \sum_{t=0}^{T} F_t \cdot \omega_t \qquad \textit{eq. 8-4}$$

Where

R is the humeral head radius and Δt the uniform time step.

Following the same methodology an "average" wear depth of the humeral cup was obtained for the kinematics and load dataset of this study. The only difference is that Charlton also assumed a constant contact surface A for the glenoid, where in this study the articulating surface of the cup with the glenoid sphere (A_t) is changing and depends on the relative humeral position in respect to the scapula over time step t.

Thus the estimated wear depth per cycle is given by:

$$\hat{h} = K \cdot R \cdot \Delta t \sum_{t=0}^{T} \frac{F_t \cdot \omega_t}{A_t} \qquad \textit{eq. 8-5}$$

For the calculations the wear coefficient of UHWMPE was used where K=10.656x10^{-7} mm^3/Nm (Maxian et al. 1996).

The results of the wear rate that is measured in nm/Cycle (of each activity) are presented in Figure 8.15 :

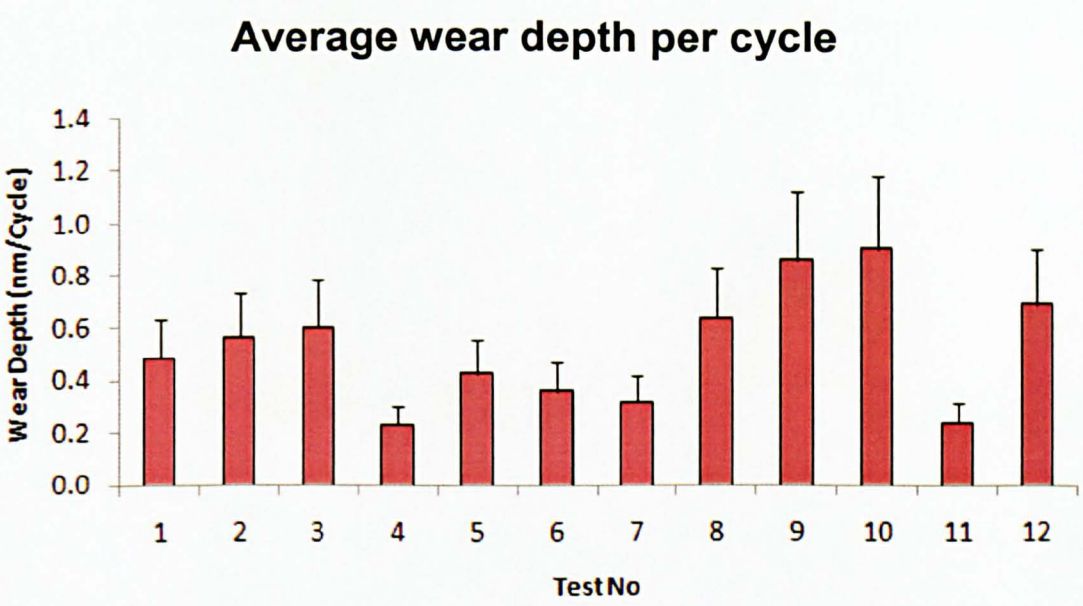

Figure 8.15: Average wear depth per Cycle for each test of ADL

From the results it is clear that Test 9 and 10 produce the most wear on the GH joint in a rate of 0.86 and 0.91 nm/cycle due to the combination of the rather large angular displacements of the cup to the sphere and the high loads.

Following this, Tests 12, 8 and 3 show the greatest potential for wear. Tests 3 and 8 are showing high values due mainly to the increased angular displacements, and Test 12 due to the highest GH load. The lowest wear depths per cycle within the ADL were produced by Tests 11, 4, 7 and 6 averaging only a wear depth rate of 0.29nm/cycle.

Overall, the range of wear depths across the tests averaged on 0.53 nm/cycle (sd 0.23) compared to the 0.77 nm/cycle (sd 0.35) found in Charlton for the normal anatomy. This is due to the slightly smaller GH loads found in the reverse joint and the larger average articulating surface of the cup that distributes the pressure in eq. 8-5

These wear figures should be a fair approximation of the true wear depths (or at least total wear volumes) produced in a reverse joint replacement shoulder. Charlton also recommend a rough estimate of 2000 cycles per day (counting of all of the various types of activity), since there are no standardised numbers for wear testing in shoulders. With this frequency the estimated wear volume of the reverse prosthesis (of the humeral cup) is 38.1 mm^3/year (sd 7.1 mm^3/year).

This number is close to the 44.6mm^3/year wear prediction of Terrier *et al.* (2009) who used a similar type of reverse prosthesis (Aequalis reverse, Tornier) in a finite element model. The average maximum GH contact force was 648N, which was calculated from a customised reverse prosthesis biomechanical model (Terrier et al. 2008). The larger

wear prediction value was mainly because of the increased number of cycles that they used (3500 cycles/day) that was recommended by Hopkins *et al.* (2007).

If we compare this number to the wear volumes of 57 mm^3/year that are predicted for the hip prosthesis (with similar articulation of UHMWPE to metal) (Pietrabissa et al. 1998,Raimondi et al. 2000), the value for the reverse shoulder wear appears reasonable considering the assumptions made. The contact force in the hip ranges from approximately 1 kN to 2 kN (more than 20 times the GH force range) and the number of cycles used is frequently 250,000 per year (more than 2 times as many as used by Charlton).

Of course, the model used for these prediction is extremely simplistic and should by no means be used for calculations other than the preliminary comparisons. However, knowing the probable over-prediction of these calculations, it seems safe to say that wear in reverse prostheses would not greatly exceed the predicted wear of 38 mm^3/year. Given the depth and level of detail of the database of GH contact forces and ROM gathered here, much more conclusive studies of wear in GH endoprosthesis could be performed using FEM techniques.

8.5. *Effect of RC tears on GH loading*

The effect of the reverse design on muscle function has already been discussed in chapter 5. The loadsharing results of the standard activities (in chapter 5) showed that if there are any RC muscle fibres left after the joint replacement (of m.Infraspinatus, mSubscapularis or m.Teres minor) they do not contribute to the elevation of the arm; they have an increased adducting moment arm.

The ADL introduce a more complex kinematic profile with a wide range of humeral rotations and, as such, loadsharing simulation of the ADL can exploit whether a different type of RC tear (as they described in section 8.1.1) can affect the GH loading.

The FTT model (where only the m.Teres minor is present) was used for all the GH loading results that were presented above. By averaging the values of maximum and mean activation of each subject for each activity, the muscle activation results clearly showed that m.Teres minor was active in all the ADL (Figure 8.16).

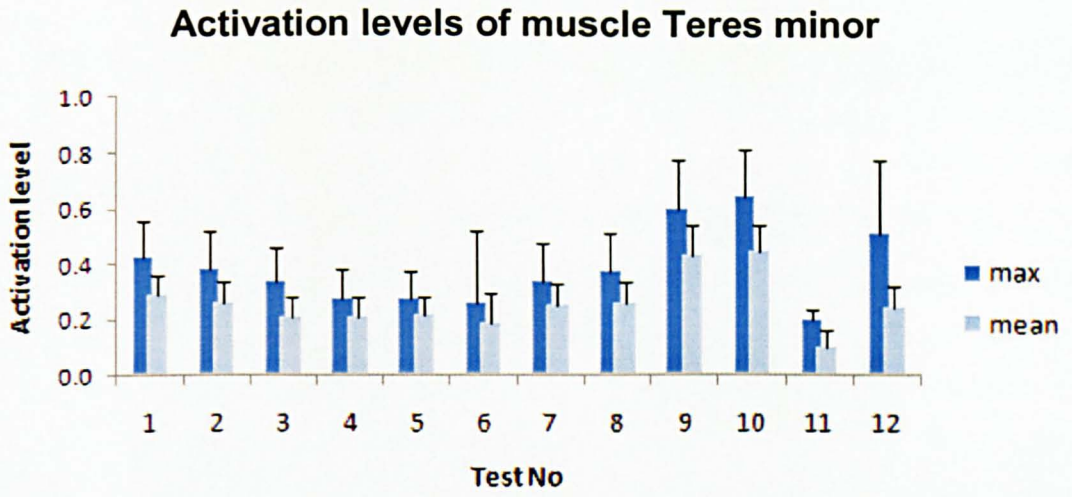

Figure 8.16: From the results it is clear that m.Teres minor is active in all the ADL

The average maximum and mean activation was 0.39 (sd 0.14) and 0.26 (sd 0.10) respectively and shows that action of m.Teres minor is required during the ADL in order to counter-balance the rotational moments that are generated in the shoulder joint during the activities.

As the above results suggest, different types of RC tears should result in different muscle activation; this is reflected in the results of the contact forces for the different types of RC tear models that are presented in Figure 8.17.

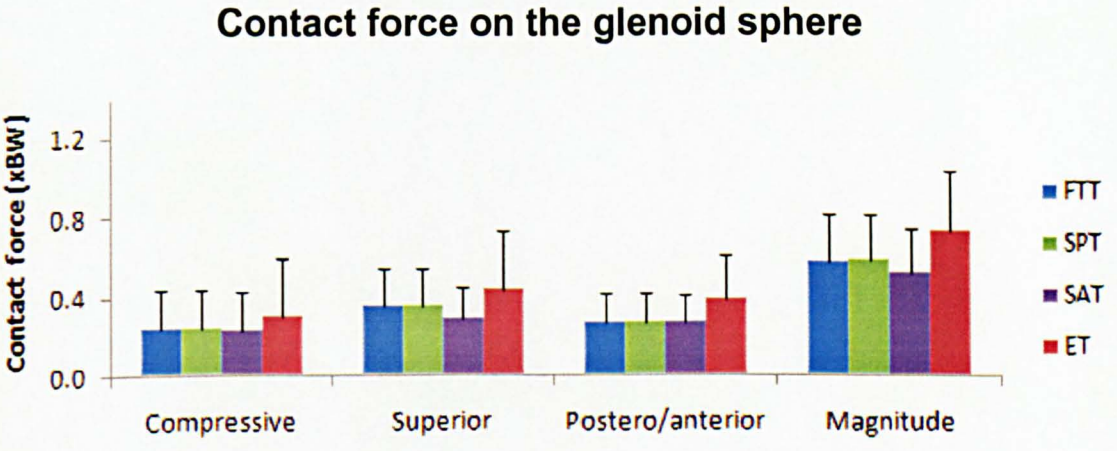

Figure 8.17: There is only a increase of the GH contact forces when there is an extended RC tear.

From the above results it is clear that when there is an extended tear (where none of the RC muscles are present – model ET) the GH contact force is increased by 0.15xBW

(26.5% increase) with respect to the FTT model. The largest increase is seen on the postero/anterior shear forces (30.8%) where the compressive and the superior forces were increased by only 0.07 and 0.08xBW respectively. The slightly uneven increase of the shear forces (with respect to the compressive forces) also affected the 'potential instability' of the joint by reducing the safety dislocation factor, but only by a small amount (average $\overline{S_d}$ for all ADL = 3.96, which is only 0.73 smaller than the FTT model).

In contrast, the differences between the FTT and the SAT model are much smaller, with the forces being slightly reduced by 0.03xBW. Surprisingly, the SPT model has the same compressive, shear and force magnitude values as the FTT model, suggesting that even if the subscapualris muscle is present it remains inactive during the ADL (Figure 8.18).

The values of the mean muscle activation (for all ADL Figure 8.18) also show that in the ET model there is an increased activation of the middle and especially the posterior part of the Deltoid. In this model there are no fibres of Teres minor or Infraspinatus muscle which means that the internal rotation moments had to be balanced by the action of the posterior Deltoid. This increased Deltoid activation is reflected also on the increased values of the GH contact forces that were presented on Figure 8.17

The results of the SAT model also show that even a moderate activation of the Infraspinatus muscle can balance the rotational moments and thus the action of Teres minor is even more reduced. This is reflected in the small reduction of the GH contact forces, even if the difference is small.

The function of m.Lattisimus dorsi and m.Pectoralis major thoracic was not affected by the different type of tears, and in general except Test 12 they stay relatively inactive (average maximum activation level 0.12 and 0.14 for m.Lattisimus dorsi and m.Pectoralis major respectively) like in the normal shoulders.

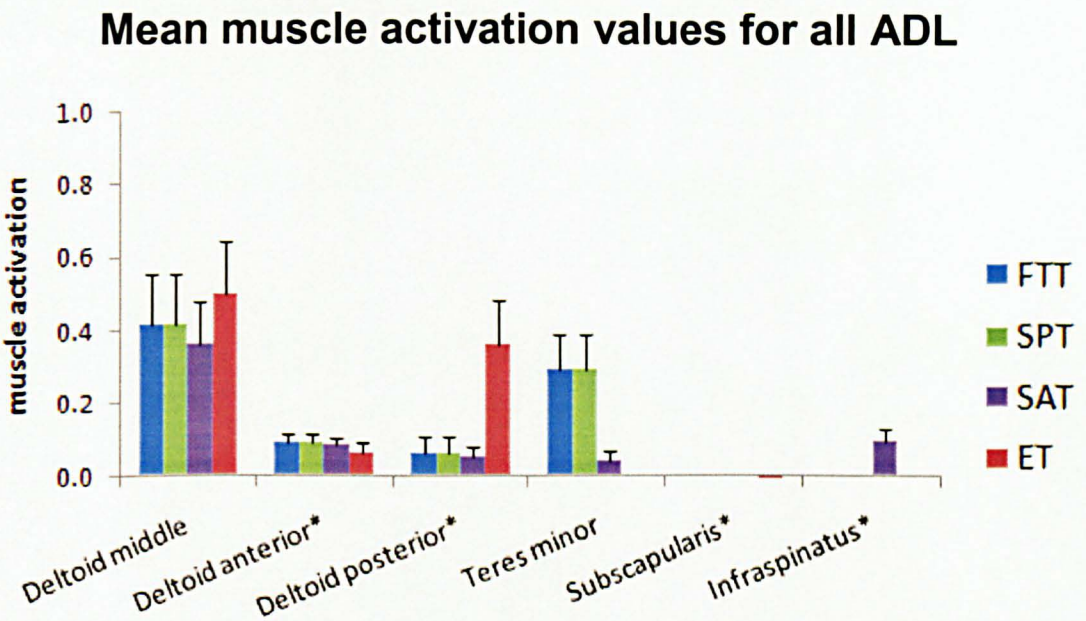

*Muscles that are represented with more than one line of action were averaged

Figure 8.18: There is a noticeable increase in the activation of the posterior part of the Deltoid in the ET model, in order to balance the rotational moments in the shoulder. Surprisingly the m.Subscapularis stays inactive in the SPT model (even if it is present)

8.6. Modelling inaccuracies – Scaling and muscle wrapping problems

8.6.1. Scaling of the model

As mentioned above, in this study a certain model customisation was achieved by scaling the shoulder model to describe the skeletal structure of the subjects that were recorded performing the ADL. This is a common practice for most of the biomechanical models of upper extremity in the literature (Karlsson & Peterson 1992,Runciman & Nicol 1994,van der Helm 1994). This technique is proven for normal and healthy subjects, but it may lead to inaccuracies when the model is scaled to match pathological shoulders.

One of the main problems begins with the use of the same PCSA values that are used to describe the muscles in the normal and DELTA group. The shoulder joint replacement subjects were older and, naturally, the pathology that led to the joint replacement is likely to have also caused some muscle wasting in the shoulder. This was not accounted in this study since there were no detailed imaging data for individual

subject skeletal and muscular reconstruction. As a result this could have caused some overestimation of the muscle activation in the shoulder and thus the GH loading. However, Charlton (1993) showed that 10% decrease of the Deltoid PCSA (on VH anatomy) resulted on a very small change of the GH loading (<2%) in standard activities. This study presents a wide range of GH values which is a result of the multiple kinematics input (ADLs) and so the percentage of the overall error in the range can be considered small.

8.6.2. Muscle wrapping problems

The shoulder biomechanical model that was used in this study represents the action of the muscles as elastic strings that wrap around simple geometrical shapes (e.g. sphere, cylinder, ellipse) that fit the bone geometry (Charlton & Johnson 2001,Marsden & Swailes 2008). Muscles with large attachment sites are usually modelled as a set of strings in order to replicate their action (e.g Deltoid, Pectoralis, Trapezious etc).

Most of the current biomechanical models of the upper limb are using the same string approach to represent the muscles (Charlton 2003,Karlsson & Peterson 1992,Runciman & Nicol 1994,Terrier et al. 2008,van der Helm 1994), but there are certain limitations. Marsden et al, (2008a, 2008b) described the 'muscle flipping problem' and how the wrapping of the muscle string can jump around a wrapping object when they adopt the shortest path. In addition, the independent movement of the muscle strings of a large muscle can cause unrealistic muscle wrapping positions where the fibres of the same muscle split to follow different paths (Figure 8.19).

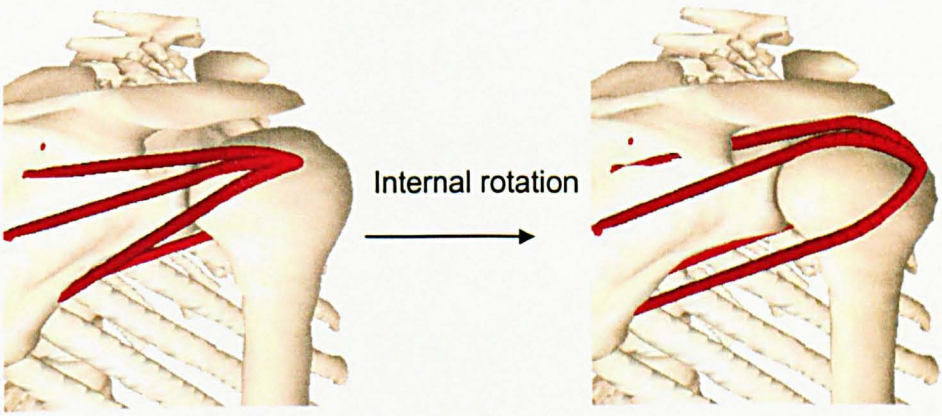

Figure 8.19: Large internal rotation of the humerus in adduction can cause the fibres of infraspinatus to separate (Normal anatomy – Newcastle model)

Some muscle wrapping problems were also observed in this study mostly on the Deltoid muscle. Posterior Deltoid is primarily a retro-flexor of the humerus (i.e. suited to

elevation in planes "behind" coronal) and the activity in this muscle in some tests highlights some possible limitations of the muscle wrapping. The posterior part of the Deltoid (which includes two fibres/lines of action) is not supposed to be active in activities where the arm is elevated in a sagittal plane (e.g. forward flexion). However the independent movement of each muscle string is adapting a muscle path which is very close to the fibres of the middle Deltoid like in Tests 9 and 10 where the arm is elevated in a frontal plane. This causes the unnatural activation of the posterior deltoid fibres which act together with the middle Deltoid to balance the flexion moment.

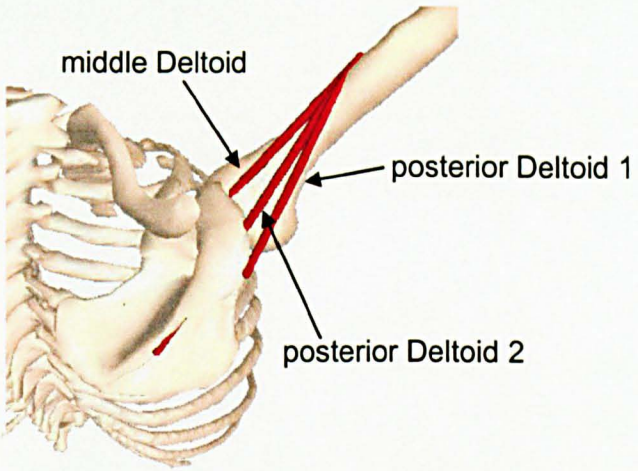

Figure 8.20: The muscle wrapping algorithm forces the posterior fibres of the Deltoid to adapt an unnatural position close to the middle Deltoid, which this results in their activation in tasks with arm elevation in the frontal plane (e.g Tests 9 and 10)

In addition, there were some sporadic wrapping problems in some activities in a few of the subjects: the scaling of the model caused some failings to the wrapping algorithm forcing the line of action to wrap in a completely unrealistic manner, or not wrap at all around the wrapping objects. These failings were not consistent for specific subjects or tests (they usually occurred only in a few frames of a task), but the problem was observed only for the Deltoid and the RC muscles. These specific muscle wrapping failings were usually reflected in the GH loading results (unusual high or low values) or even in the representation of the contact points of the GH force on the glenosphere or cup (Figure 8.6 and Figure 8.9) where they were offset from the rest of the locus.

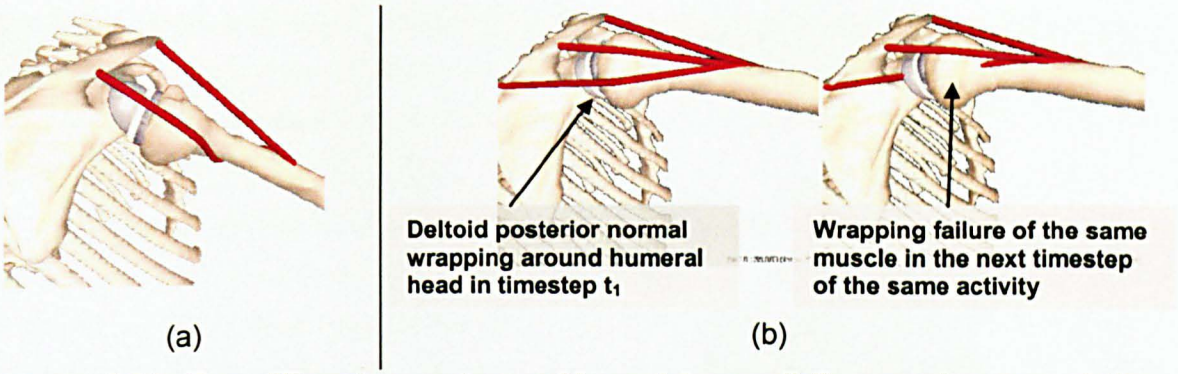

Figure 8.21: Two different wrapping problems (a) unrealistic wrapping around the humeral column was very rare, but it resulted in some jumps on the calculations of GH force (b) failing of wrapping around the humeral head of the posterior Deltoid in two consecutive frames of the same test.

8.7. *Short summary – Conclusions*

The loadsharing results show that the GH contact forces in the reverse joint replacement can rise up to 0.8xBW during ADL with low or no external hand loading where an activity such as 'Sit to stand' can double the GH loading.

Compared to the normal shoulders these values are slightly smaller and this is mainly due to the characteristics of the prosthesis, which enables the m.Deltoid to perform better (by increasing its moment arm) and compensate for the lack of the RC muscles. This was also clear by the muscle activation results where the m.Deltoid was never saturated (activation levels<1).

As a result of the constant upward pulling of the m.Deltoid and the lack of any compressive muscles (e.g RC muscles), the GH loading results show that there is a constant compressive loading on the humerus (thus the implant stem), which also translates to high superior and antero/posterior loading on the Glenosphere. This is in contrast with the GH loading of a normal shoulder, where there is a constant compressive force on the glenoid site, which is mainly generated by the action of the RC muscles.

Analysing more the GH loadings, it is clear that one of the biggest advantages of the reverse prosthesis is that it reverses the envelop of forces and the critical stability (articulating) area and provides joint stability, with a large surface of the sphere resisting to the upward pulling of the m.Deltoid and the humeral cup providing enough articulating surface in a direction such as to constrain all the humeral compressive forces.

The stability analysis of the current DELTA cup design showed that it offers a very large safety factor, but as it has already been suggested in chapter 5, stability and impingement are antagonistic factors and a cup with large safety factor may also cause extended impingement problems.

The muscle activation results suggest that the preservation of the m.Teres minor can be very beneficial to the GH joint loading (or function) as it can balance out the internal rotation moments on the shoulder joint. Surprisingly the inclusion of the m.Subscapularis in the simulations of the ADL did not affect the GH loading results and stayed inactive. However, the set of ADL did not include any activities (except reach lower back) that can create high external moments and thus the activation of the m.Subscapularis was unnecessary. In addition the large adductive moments that this muscle can create in a reverse shoulder anatomy (as it was explained in chapter 5) forced the model to minimise its action.

Chapter 9. Prediction of impingement and notches during activities of daily living

9.1. Introduction

As it has been mentioned before in this thesis, reverse anatomy prostheses (and especially the DELTA® III design) has been extensively used in Europe and are very popular for treatment of massive RC arthropathies. There are many clinical data demonstrating good performance of the reverse prosthetic designs (Sirveaux et al. 2004,Woodruff et al. 2003), and the biomechanical analysis in chapter 5 support the advantages of the reverse prosthesis in RC arthropathies. The results of the biomechanical analysis also confirm the impingement problems that have been reported to create bone notches on the inferior border of the scapula and possibly glenoid loosening after long term use (Nyffeler et al. 2004,Valenti P et al. 2001) .

In chapter 5, impingement was analysed in terms of available range of motion (which is free of impingement) during three standardised activities (abduction, forward flexion and elevation in scapula plane). The results showed great agreement between other cadaveric, radiographic and modelling studies (De Wilde et al. 2004,Nyffeler et al. 2004,Nyffeler et al. 2005). However the range of motion can only provide a basic understanding of the impingement and the notching problem since the multi-axial and high mobility of the shoulder joint during every day activities can only enlarge the problem.

In this chapter we try to analyse the impingement and the notching problem of the DELTA® (and in general the reverse) designs in more depth using the contact detection of the interactive shoulder model and a larger set of kinematics data that will include not only elevating tasks but also extensive internal/external humeral rotation. Based again on the hypothesis that the mechanical contact between the polyethylene cup and the bone at the inferior scapular neck is closely related to the scapula notching, this chapter has tried to predict shape and volume of the notches in more detail.

In chapter 5 the influence of many different implant fixation and design alterations were discussed in order to determine how they can affect not only the impingement but also the mechanics of the prosthetic joint. Having established the relationship between impingement/mechanics, this chapter will investigate again the same fixation and design alterations but only from the impingement point of view.

9.2. Methods

9.2.1. The kinematic input

The set of the kinematic recordings of the 12 Activities of Daily Living (ADL) that was described in chapter 7 was the input to the model. Since the kinematic profile of the ADLs showed great variability within the prosthetic subjects (chapter 7), instead of averaging a kinematic profile for each task, the impingement was calculated separately for each of the 12 prosthetic subjects.

9.2.2. Model configurations

Impingement simulations run first for the standard fixation which represents the configuration that was found following the surgical guidelines of the manufacturer. A detailed configuration of the 'standard fixation' (Glenosphere size 42 fixed slightly postero/inferiorly to the centre of the glenoid and a stem inserted in neutral humeral version) is shown in detail in chapter 4. Like the methods followed during the biomechanical analysis of the DELTA III (chapter 5) in order to investigate impingement in depth, simulations were performed not only for the original design geometry and the standard fixation but also for a number of parameters. Like before, those parameters were separated into two categories:

i) Surgical modifications, which relates fixation of the glenoid sphere and stem

ii) Design alterations as they have been introduced by different manufactures

A quick summary of those factors is shown below

9.2.2.1. Surgical modifications - Fixation configurations (Figure 9.1)

a. Antero/posterior (D1) and inferior fixation (D2) of the glenoid sphere: For standard fixation D1=D2=0mm

b. Reaming depth (D3) and angle (α) of the prosthesis: For the standard fixation D3=3mm and α=0 deg

c. Retroversion of the humeral stem fixation (β1): For the standard fixation β1=0 deg

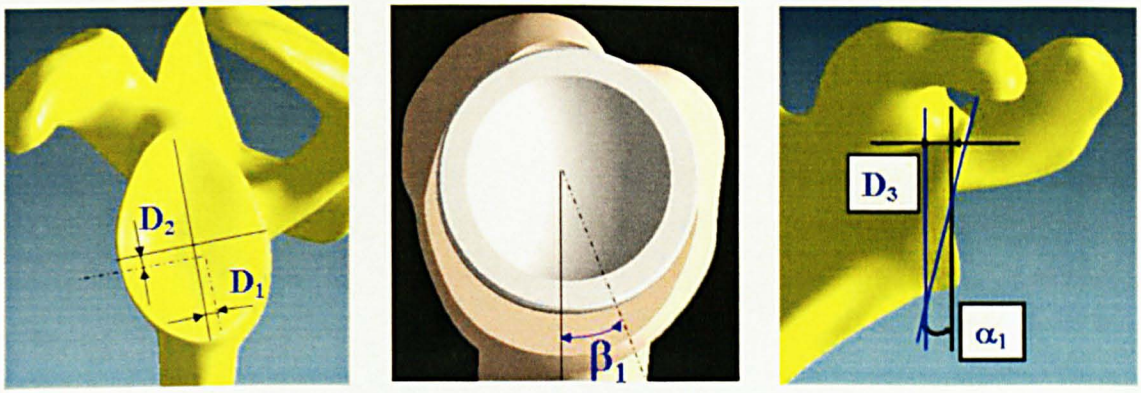

(a) (b) (c)

Figure 9.1: Surgical modifications: ***a)****Position of the fixation (inferior D2, antero-posterior D1),* ***b)****Retroversion of the stem fixation (β1,)* ***c)****Glenoid Reaming (Depth D3, angle α),*

9.2.2.2. Design alterations (Figure 9.2)

d. ***Size of the sphere (R) and relative cup depth (h):*** For DELTA III size 42 R=21mm and the h=11 mm.

e. ***Sphere centre lateralisation (c) from the fixation plane:*** For standard DELTA III c=0 mm.

f. ***Neck/shaft angle of the prosthesis (β2):*** For standard DELTA III, β2=115 deg

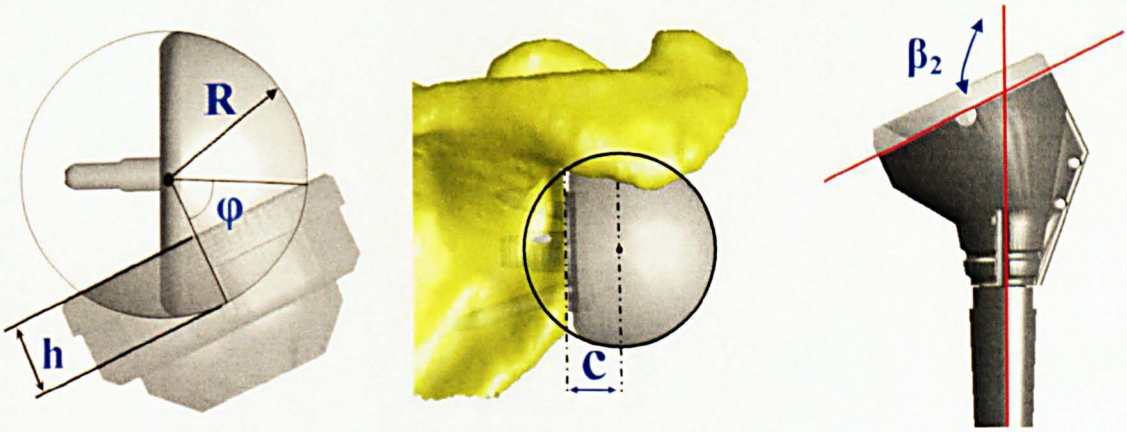

(d) (e) (f)

Figure 9.2: ***d)*** *Cup depth h to sphere size R ratio (h/R),* ***e)****Lateralisation of the sphere centre,* ***f)*** *Neck/Shaft angle of the stem (β2)*

9.2.3. Presentation of the results

In each simulation the contact detection algorithm was used to detect all instances of inferior or superior impingement during the kinematic inputs. Only one of the above

parameters was changed in each simulation in order to identify its impact to the impingement. The results are presented as an average percentage of the detected contact per all the cycles of all the ADLs that performed by all the subjects (AICD = % of Average Inferior Contact Detection, ASCD = % of Average Superior Contact Detection, ATCD = % of Average Total Contact Detection).

9.3. Results

9.3.1. Standard fixation

Like during the simulations of standard activities, the results clearly identified

i) contact between the humeral cup with the inferior scapular border (inferior impingement) and

ii) contact of the resected humerus (around the area of the greater tubercle) with the acromion or the coracoid process (superior impingement).

The results for the standard fixation showed a heavy impingement averaging a total contact of ATCD = 42.1% (SD 13.2). From the latter results AICD was 38.6% (SD 15.9) and ASDC was only 3.5% (SD 6.1). The recorded volume between the contact of the polyethylene cup with the inferior scapula border created a large size scapula notch in the inferior border, which extends behind the metallic fixation plate (8.1 mm wide) and up to the inferior fixation screw (10.37 mm). The contact trace of the scapula to the humeral cup also revealed a wide notch on its latero-inferior side occupying in length the 28.7% of the cup perimeter and extending 5.5mm in depth down to the rim of the humeral metallic support (the Epiphysis – Figure 9.3 (c)).

Standard Fixation

D_1	D_2	D_3	α	β_1
2.1mm	*2.3mm*	*3mm*	*0 deg*	*0 deg*

Original prosthetic geometry

h	c	β_2	R_{sphere}	
8 mm	*0 mm*	*115 deg*	*21 mm*	

Average impingement during all ADL cycles		
Inferior *(AICD)*	38.6%	15.8 (sd)
Superior *(ASCD)*	3.5%	6.1 (sd)

Table 9.1: Average superior and inferior impingement as calculated for all the subjects and all the ADLs

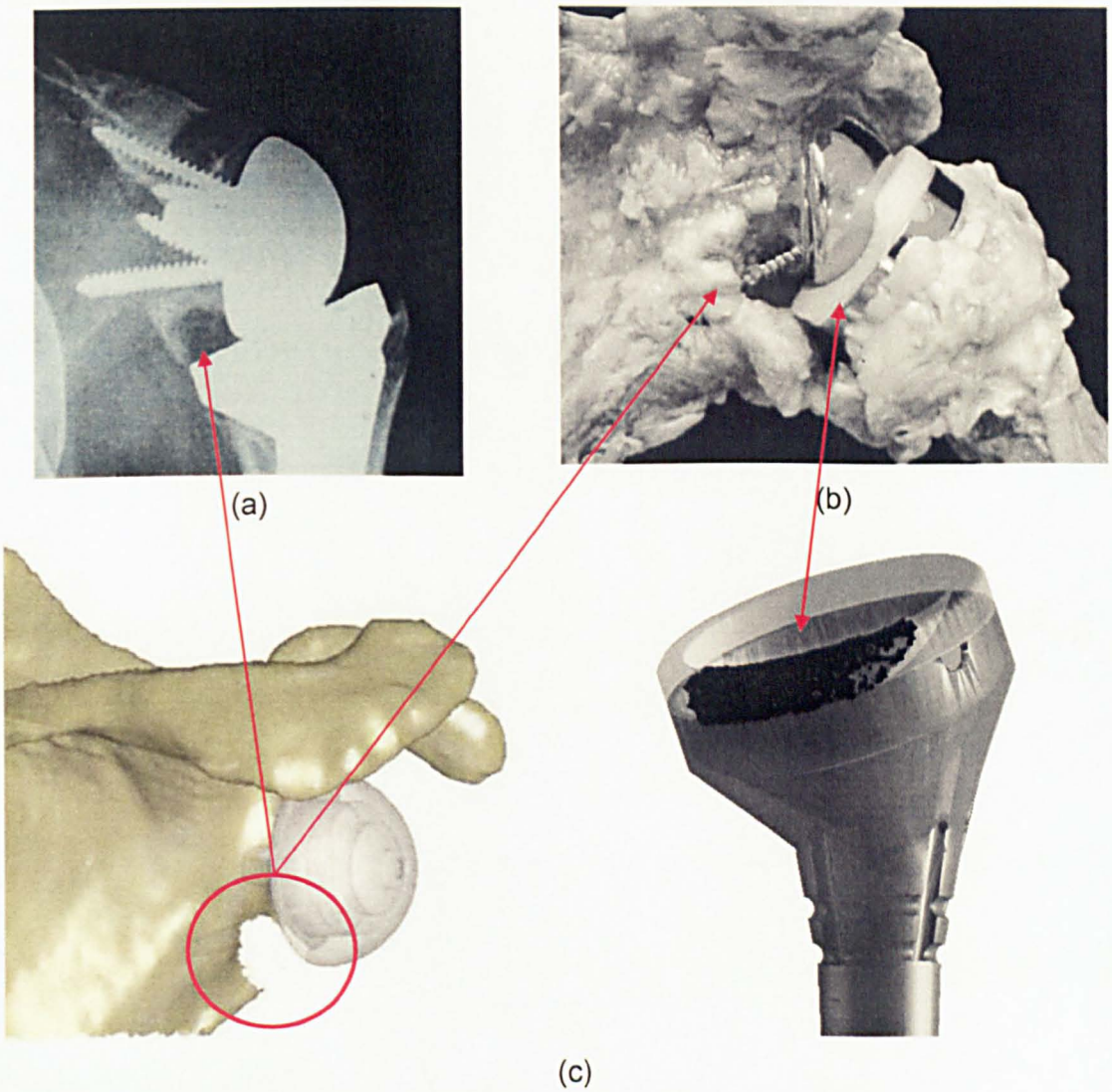

Figure 9.3: (a) Radiographic image of scapular notches in DELTA III design (adopted from Simovitch et.al (2007) (b) Retrieved DELTA III (adopted Nyffeler et. al., (2004), c) Scapular and Cup notching prediction from the contact detection algorithm.There is an apparent similarity between the predicted and the real notches in both the scapula and in the polyethylene cup

9.3.2. Surgical modification - Fixation configurations

9.3.2.1. Position of the Glenoid Fixation (D1, D2):

Changing the glenoid fixation on the antero/posterior axis had a small but negative impact in the impingement. Results showed that posterior fixation reduced the AICD and vice versa. The maximum increase was by 3.2% (Figure 9.5) and it was observed just 1.8mm posteriorly to the standard fixation. An even more posterior fixation created

impingement site on the anterior part of the glenoid border when simulating tasks of the arm reaching the contra-lateral side (e.g tasks 1 and 2).

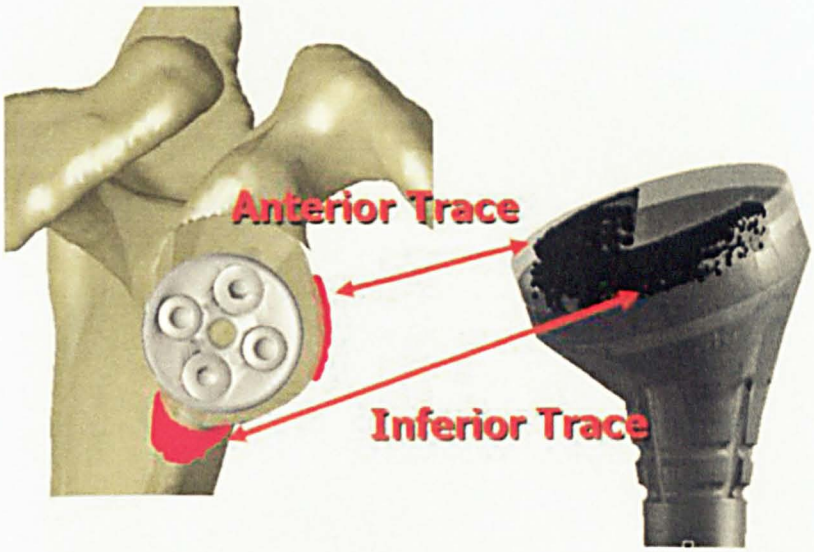

Figure 9.4: An extreme posterior fixation (D1=-2mm, Figure 9.5) reduced even further the impingement on the scapula border, but it created an impingement trace on the anterior wall of the glenoid

An inferior positioning of the sphere (D2) had very effective result in reducing both superior and inferior impingement (Figure 9.5) averaging 4.8% per mm decrease in the ATCD. Even if the improvement was constant, it should be noted that after 3mm of extra inferior fixation from the standard fixation, the fixation plate and screws was graphically outside the scapula bone.

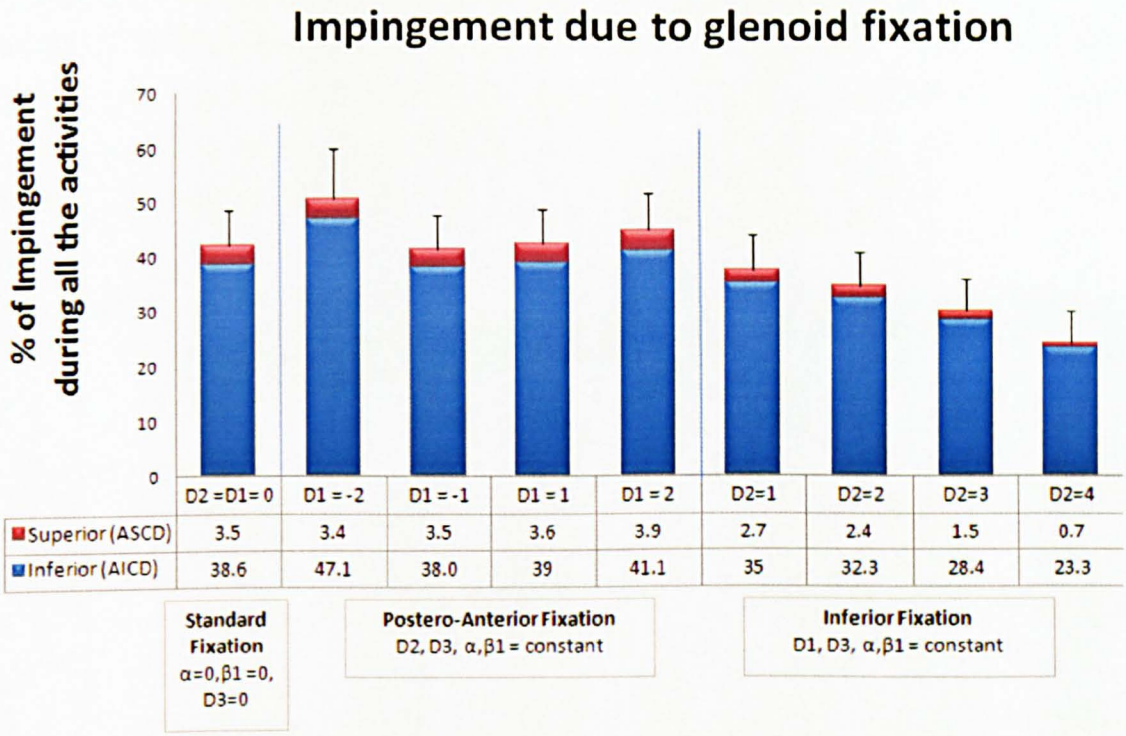

Figure 9.5: Inferior placement of the glenoid sphere is very effective in reducing impingement, where antero-posterior fixation did not have a desired effect

9.3.2.2. Reaming of the glenoid (α, D3):

Reaming depth D3: The results show that an increased reaming depth (given that the position of the fixation is constant) increased the AICD by 3.5% per mm (Figure 9.7). As it was also discussed in chapter 5, the excess reaming (from 3 to 6 mm) also reduced the overall fixation surface by 27.8%.

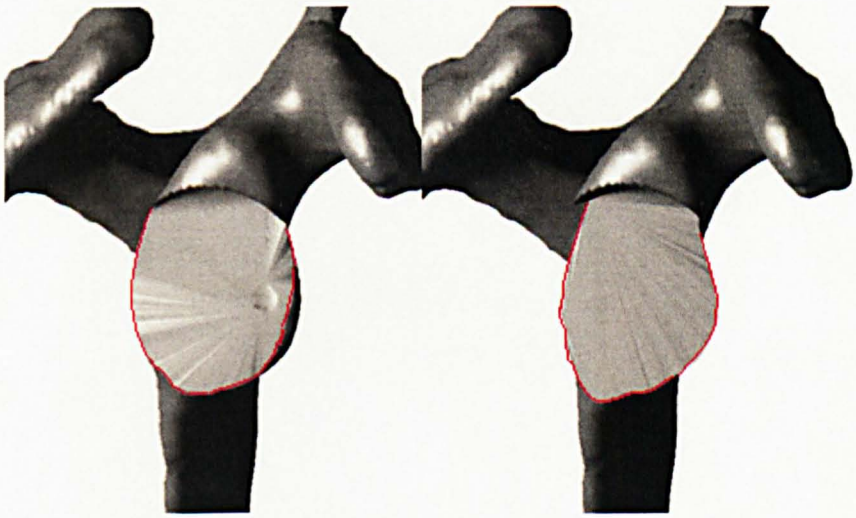

Figure 9.6: Excess reaming of the glenoid can reduce the fixation site

Oblique osteotomy α: An oblique osteotomy improved only the inferior impingement, showing a 7.1% decrease of the AICD for the maximum reaming angle (α=15 deg – Figure 9.7). It needs to be noted that the oblique reaming of the glenoid resulted also in a reduction of the surface area of the inferior part, exposing the posterior fixation screw out of the scapula bone.

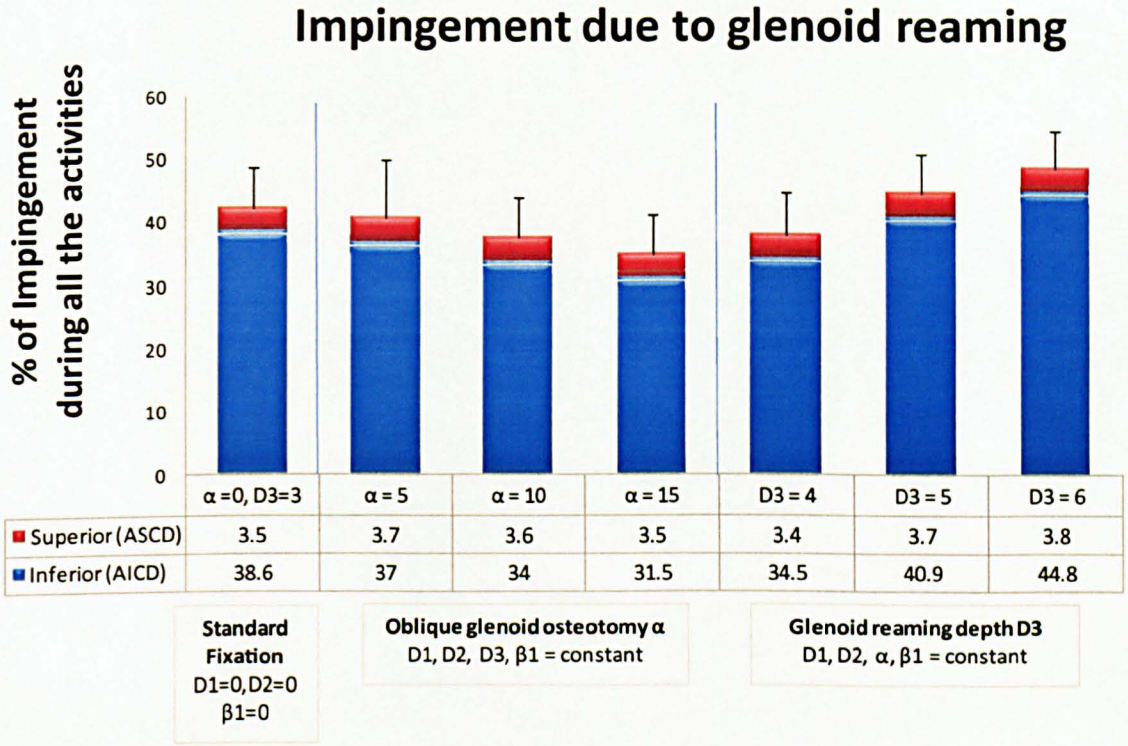

Figure 9.7: Oblique osteotomy can improve the impingement problem, but excessive reaming should be avoided

9.3.2.3. Humeral stem fixation (β1):

The results show that there was a decrease in inferior and a small increase on the superior impingement when the stem was fixed in a more retroverted position. The maximum change was observed in β1=20 deg where the ATCD dropped by 6.1% compared to the standard fixation (Figure 9.8).

This was also visible on the cup notch, where it was located in a different place and had a smaller trace.

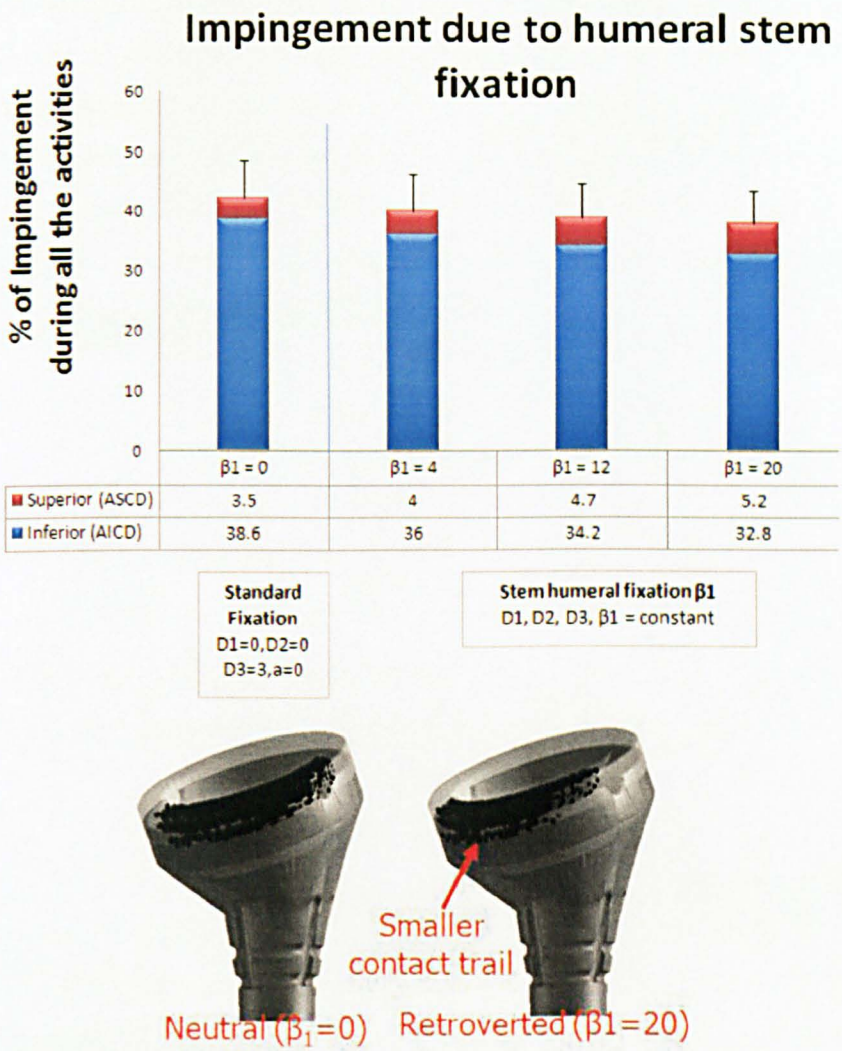

Figure 9.8: A retroverted fixation showed a small improvement on the impingement results

9.3.3. Design alterations

9.3.3.1. Cup depth (h) to sphere size (R) ratio

Reduction of the ratio h/R was very effective on reducing inferior impingement. Testing shallow polyethylene cup (depth h=11, 10, 9, 8) for the same sphere size (R=21) the result showed a linear decrease of inferior impingement with the superior impingement unaffected. For the standard fixation, reduction of h by only 3mm (which means ratio h/R dropping from 0.52 to 0.38 – 27.2% reduction) dropped the AICD by 41.7% (Figure 9.10). Superior impingement remained unaffected.

Except the large size prosthesis (DELTA size 42) that was tested up to now DELTA design is also available in a smaller size (DELTA 36) where Rsphere=18mm. Fixing the small size prosthesis in the same place and alignment as the large size the overall contact was slightly increased (Table 9.2). Those results seem to contradict the above

data since the h/R ratio of DELTA 36 is reduced in relation to DELTA 42 (0.44 and 0.52 respectively) and in theory should reduce impingement. This is not a surprise though, since the smaller size sphere does not overlap the scapula border as much as the larger diameter sphere of the DELTA 42 when both are fixed in the same place. If DELTA 36 is fixed in a more inferior position in order to cover the same overlap of the scapula border as the DELTA 42, then the impingement results are in favour of the smaller size prosthesis.

	DELTA 42 R=21, h=11 (h/R=0.52)	DELTA 36 R=18, h=8, (h/R=0.44)
Inferior (AICD)	38.6%	39.7%
Superior (ASCD)	3.5%	3.6%

Table 9.2: Impingement for the 2 available sizes of the DELTA prosthesis: large(42) and small(36). Both prostheses had the same fixation position and alignment

9.3.3.2. Sphere centre lateralisation (c)

Results showed that lateralisation of the sphere centre can reduce significantly the inferior impingement, showing an average decrease of AICD by 3.9% per mm. For the maximum c = 5mm tested in this study the AICD reduced down to 19.0% (50.8% less than the original DELTA design).The superior impingement was not affected significantly and any difference are due to the dip of the acromion bone (Figure 9.10).

9.3.3.3. Neck/Shaft angle of the stem (β2)

Increasing the angle of the neck/shaft of the stem, inferior impingement was reduced, but, as expected, the superior impingement was also increased (Figure 9.10). Excessive increase of the neck/shaft angle (tested for β2=130 deg) resulted in contact of the polyethylene cup with the superior part of the glenoid surface before any superior impingement of the humeral head with the acromion (Figure 9.9).

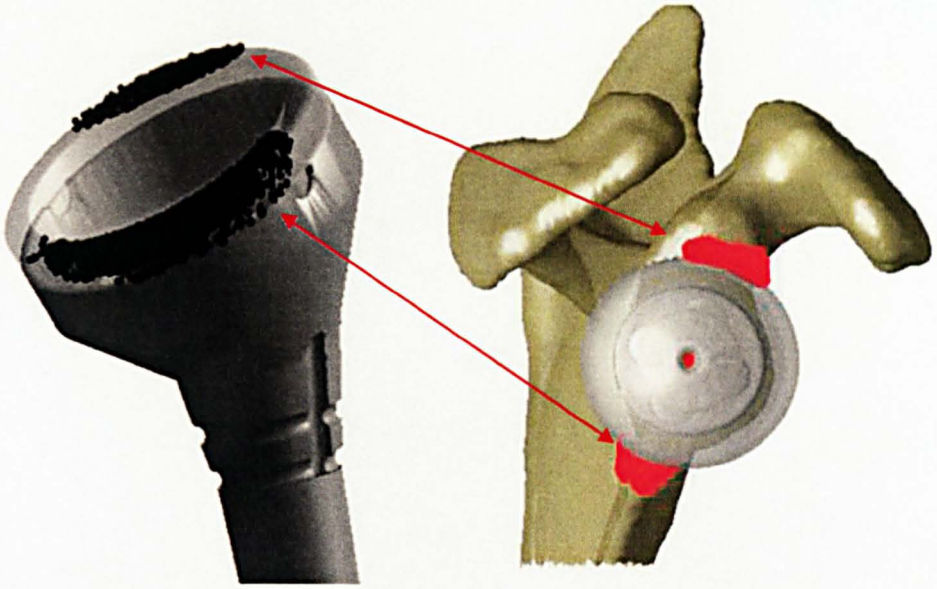

Figure 9.9: When a neck/shaft angle of β2=130 deg was tested an impingement of the superior part of the polyethylene cup with the superior face of the glenoid was detected

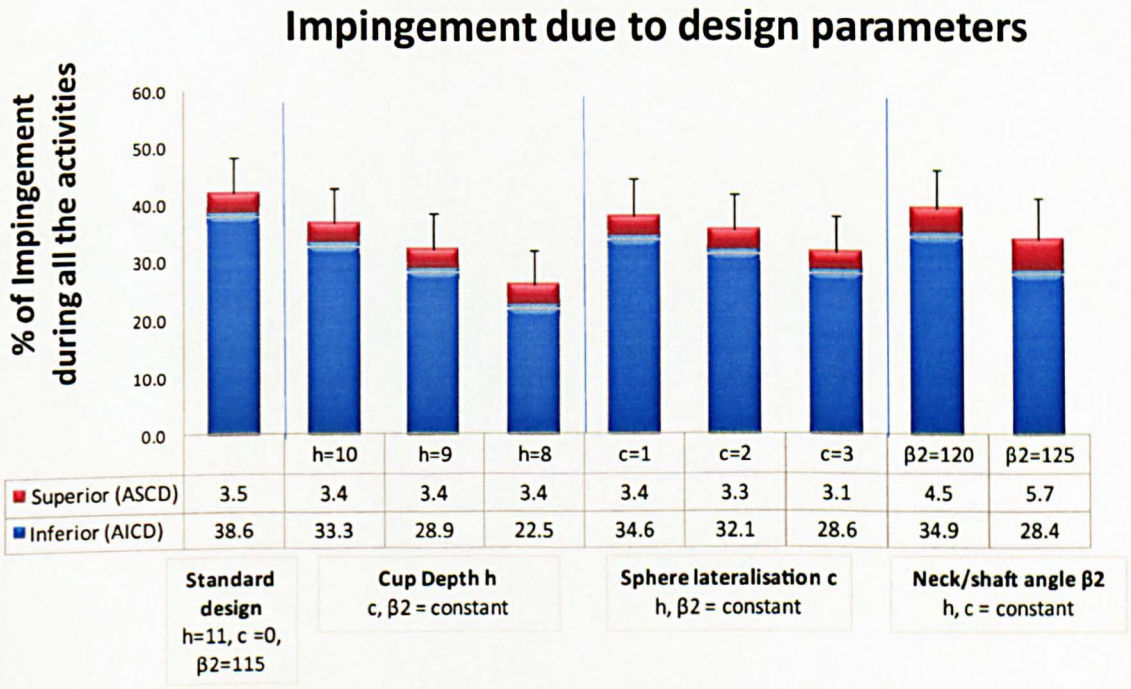

Figure 9.10: Changing the design parameters can affect (reduce) the impingement problem

9.4. *Discussion*

As it is already mentioned the impingement problem and the creation of bone notches is of major concern for the reverse prosthesis that has caused controversy over its

appropriate use (Rockwood, Jr. 2007). Even if there are a few studies that investigate the problem (De Wilde et al. 2004,Nyffeler et al. 2005), most of them investigate simple elevating tasks and report only range of motion. This study investigates impingement and the notching problem by applying a set of kinematic data that are recorded from prosthetic subjects in order to increase the understanding of notching.

The data of this chapter support the concerns of impingement and predicts scapula notches that are very similar in volume and shape with notches that have been observed in cadaveric and radiographic studies(Boileau et al. 2006,Nyffeler et al. 2004,Simovitch et al. 2007,Sirveaux et al. 2004) (Figure 9.3). In some way the agreement of the modelling results with the real samples also give a bigger validity to the kinematic reconstruction of the model which is used further to investigate the effect of surgical techniques or prosthetic design alterations on the impingement.

Glenoid preparation and optimum fixation of the sphere are defined by the surgical procedure and the instrumentation tools and can reduce inferior contact appreciably decreasing the volume of notches and minimising the risk of loosening. The results showed that the most frequent contact was between the inferior border and the polyethylene cup. It was clear that for the DELTA geometry, the impingement was decreased when the glenoid sphere was overlapping the reamed glenoid surface, especially over the inferior scapula border. It also becomes clear that inferior placement of the sphere was the most effective factor to minimise impingement without altering the original prosthetic geometry. It reduced not only the inferior but also the superior impingement. Results indicate that the more inferior fixation the better, but the physical size of the glenoid poses specific limitations that vary depending on the morphology of the individual scapula. The importance of inferior fixation to the impingement has been demonstrated also by other clinical and biomechanical studies(Nyffeler et al. 2005,Simovitch et al. 2007). Despite that, caution should be taken during inferior fixation since as it has shown in chapter 5 it can stretch the deltoid muscle more than 20% of its anatomical length, with a risk of damaging the auxiliary nerve(Colohan AR et al. 1996).

Figure 9.11: The amount of overlap (l) of the glenoid sphere over the inferior scapula border is critical for the results of the inferior impingement. Inferior implantation of the sphere is one of the most effective ways to increase the overlap and reduce impingement

When inferior fixation of the sphere is limited (small glenoid) fixing a larger size sphere is a highly effective solution for increasing the overlap of the reamed glenoid surface (similar effect to the inferior fixation), but it naturally can create a greater superior impingement in reaching activities that require high arm elevation. The results of the small size prosthesis (Rsphere = 18mm) did not show any marked improvement of impingement, even if the h/R ratio is reduced, demonstrating the significance of inferior fixation. Despite the attractive solution of a larger size sphere, joint size limitations in small subjects can pose fixation difficulties during surgery.

In contrast with the data of chapter 5, oblique glenoid osteotomy was the second most effective factor reducing only the inferior impingement (without altering the prosthetic design). Additionally, as shown by (Nyffeler et al. 2005) an oblique osteotomy can result in a much reduced and narrower (oval shaped) glenoid reamed surface affecting the fixation of the sphere. Inferior fixation was limited after an extreme oblique reaming of 15 deg and because inferior fixation leads to a greater reduction of impingement compared with an oblique reaming the optimum sphere fixation was identified as the most inferior placement that could be achieved (considering that plate and screws are interacting with the bone material) on a small α=0 to 5 deg cut.

A minimum reaming depth of the glenoid minimised the risk of the inferior impingement. This can be explained from the presence of the small flat glenoid neck that is beneficial for the impingement when the sphere overlaps the glenoid reamed surface. Excessive reaming will shave off the scapula neck exposing more the inferior border to the impingement site creating also bigger volume of notches. The importance of the scapula neck to the impingement and the big variability of its shape is also highlighted in

the radiographic study of Simovitch et al. (2007) where he investigates and correlates the developed notches of seventy seven shoulders with DELTA III joint replacement with the inferior fixation and the scapula neck morphology.

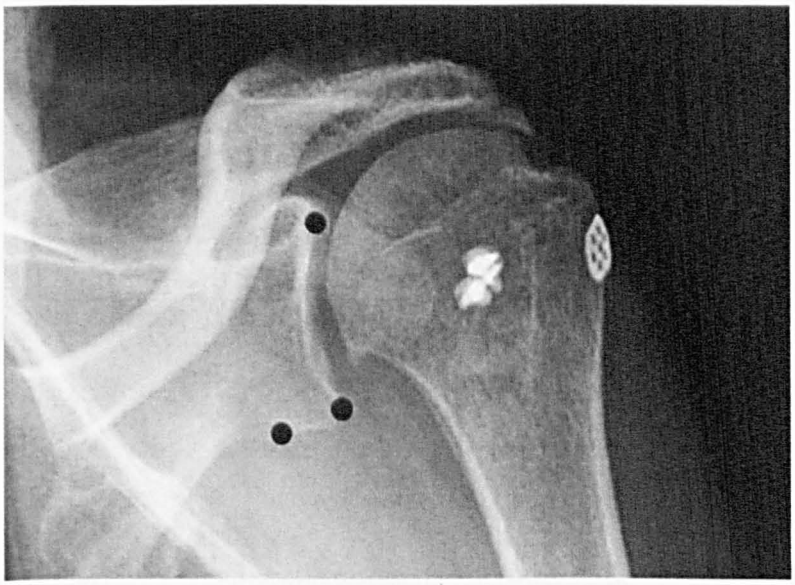

Figure 9.12: A small glenoid reaming before the sphere implantation is very beneficial in some scapulae that have a very flat neck before the inferior border (Adopted by Simovitch et al. 2007)

The version of the fixation of the humeral stem had also an impact in the inferior impingement, but rather small. The mechanics and the kinematic alterations following a change on the version of the humeral stem fixation has been analysed in chapter 5 (section 5.6.1.3). In general a neutral stem fixation can improve internal rotation, whereas a retroverted stem fixation will increase the range of external rotation. For the kinematic profile of the ADL tested in this study the results showed that the most retroverted stem fixation (α=20 deg) decreased the contact trace, but only by a small amount. As it has also shown in chapter 5, a retroverted fixation can reduce the moment arm of teres minor thus reducing the external rotation of the arm. This creates a dilemma for the choice of the version of the stem fixation. In common practice surgeons prefer a neutral stem fixation (personal communication), but if m.Teres minor is not functioning a retroverted fixation should be preferred.

Like in the preliminary results (chapter 5), changing the design of the prosthesis (parameters c, h, β2) had in general a bigger impact on the reduction of impingement and the volume of notches. By changing dramatically the shape of the sphere (increasing c) or making a very shallow cup (h/R ratio small), it was actually possible to eliminate the inferior impingement and avoid notching, something that was impossible by

only changing the fixation. In contrast though with the placement of the fixation and the glenoid preparation, where there is an optimum configuration (given the prosthetic geometry and the morphology of the scapula), a change on the design parameters of the prosthesis can have an impact on the joint stability or the strength of the fixation (analysed in chapter 5)

Reducing cup depth (reduction of h/R ratio) was the most effective way to minimise the impingement, but taking into consideration the high shear loads calculated during the ADLs, the choice of the cup depth should be such to always provide stability to the joint. The stability results of the ADL tested on this study showed that DELTA design provide a very safe cup depth, but a 20% reduction on the cup depth can improve the impingement without also compromising the joint stability.

By increasing the neck/shaft angle, the cup articulating surface is adapting a more lateral and superior position on the sphere and results of impingement showed that can reduce inferior impingement but it will also increase the superior contact of the Greater tubercle to the acromion during high elevating tasks. An even more extreme neck/shaft angle can result in impingement of the cup with the superior part of the glenoid which can restrict the maximum arm elevation. Considering the rather small impingement benefits and the dislocation risks of a big neck/shaft angle (as they analysed in chapter 5 – section 5.6.2.3) a value between 115 to 120 degrees is recommended.

Changing the shape of the glenoid sphere by lateralising its centre (c>0) was one of the most efficient ways to reduce the volume of scapular notches. Even if this is an attractive solution the excess stresses applied on the fixation by the bending moments that the contact reaction forces can create must be taken into account.

9.5. *Conclusions on the impingement*

In summary, this study has shown impingement to be a major problem on the reverse prosthetic designs and predicts notches on the scapular bone and the humeral cup similar to those observed in the literature. The results highlighted the importance of a good glenoid preparation with an inferior fixation of the sphere, but anthropometric differences can affect the fixation, which is subjected to limitations of bone stock and maximum deltoid lengthening. The latter suggests that pre-operating subject specific planning and guided implantation can help defining the optimum fixation reducing the impingement. In this study it proved difficult to completely avoid scapula notching without changing the design of the original DELTA III prosthesis. Unfortunately the results confirm that impingement and stability of the joint are antagonistic factors cancelling each other out during design alterations. Less impingement can also mean reduced joint stability or high fixation stresses. A design optimisation can balance the problem out

maximising the range of motion (minimum impingement) but also providing sufficient joint stability over a set of kinematic activities that the prosthetic shoulder is expected to perform.

The optimum solution for minimum impingement is a combination of the several parameters that were tested above. In this study, numerous design changes have been combined (for the optimum solution) but the findings of this optimisation are the subject of a patent application and cannot be presented in this thesis. It is up to the reader to interpret the results that are presented above in order to reach an optimum solution.

Chapter 10. Conclusions and recommendations for further work

The work carried out and presented here has enabled better understanding of the function of a reverse shoulder joint replacement by using an established interactive upper limb biomechanics model.

The Newcastle Shoulder model has been successfully adapted to describe the reverse joint replacement. Partial validation of the model was undertaken through comparison of various data from the literature mostly in the form of muscle moment arms and range of motion (impingement). The model was able to clearly show the benefits and the disadvantages of the reverse prosthesis and predict a range of GH loading during selected activities of daily living.

The summary and conclusions of the various findings of the study are presented below.

10.1. Summary of the results/Conclusions

10.1.1. Model Adaptation

The established Newcastle Shoulder Model was used in this study as the core of the investigation of the reverse joint replacement. The model proved to be highly adaptable, but several techniques of graphical manipulations and definition of new frame and kinematic constraints had to be developed to fully describe accurately and realistically the new prosthetic geometry.

A virtual implantation of a joint replacement in a computerised model is far easier than in the operating theatre, since it is mostly about aligning embedded coordinate frames according to technical drawings. Nevertheless, for this study a standard procedure of the real surgical implantation was followed using representative models of the real instruments. This resulted in a realistic alignment of the implant on the bones and revealed implantation parameters that can change during a surgical procedure (e.g reaming depth and precision of glenoid alignment) which can affect the function of the prosthesis.

In order to investigate the joint replacement, the biomechanical model had to be improved in some areas such as bone visualisation and the ability to detect contact of the prosthesis with the scapula.

10.1.2. Reverse prosthesis biomechanics and validation

Model validation in this stage is difficult since preliminary *in vivo* data of GH joint loading have only recently been published. However, a certain validation of the model was achieved by comparing results of moment arms and range of motion (impingement) against published data from either cadaveric or modelling studies. Most of the data showed great agreement with the literature.

That gives us the confidence to interpret the results of the model which shows the advantages of the reverse prosthesis when it is used in subjects who suffer from irreparable RC tears. The modelling data show how the geometry of the reverse designs can increase the moment arm of the Deltoid muscle (as much as 50%) and enhance its performance compensating for the loss of the RC muscles.

The model also showed the potential function of any (possible) remaining RC muscle after a reverse joint replacement, where their action is slightly changed compared to the normal shoulder. Even if the reverse geometry maintains the internal/external rotation moment arm of the m.Subscaularis and m.Infraspinatus, their line of action also implies more adducting moments and thus should be less active during arm elevation.

10.1.3. Kinematics analysis

There were two sets of kinematics measurements in subjects with reverse joint replacement in this study, including scapula rhythm and arm kinematics during representative ADL. Both kinematic measurements were used to customise the model and obtain more realistic predictions from the model.

All the data clearly indicated that there is a kinematics adaptation in reverse joint replacement subjects compared to normal. The scapula-rhythm results indicate that there is increased lateral scapula rotation in reverse shoulders compared to normal. However, the increase is highly variable within the subjects with a range of 1.2 – 1.9 times the normal scapula rhythm. It is difficult to explain the reason behind the adaptation since there is no clear indicator which correlates the increased scapula rotation with any physiological parameter (e.g. sex, age). However, there is a trend showing that patients with good recovery and large range of humeral elevation after the surgery have small change in their scapula rhythm whereas those with muscle weakness and small range of movement minimise the glenohumeral rotation and have large scapula rotation.

The large variability in the kinematic patterns is also clear in the results of the arm kinematics during ADL, where the results showed that subjects with reverse shoulder

replacements completed ADL in a different approach compared to normal subjects. However, the kinematics results also showed that the reverse replacement subjects in general were able to perform well completing most of the activities on the protocol and demonstrating very high humeral elevating capabilities. The limited range of humeral internal/external rotation is a reflection of the lack of the RC muscles.

The lack of tracking in the hand and wrist orientation was clearly a limitation of the study, since the hand is a major determinant in the accomplishment of functional tasks and future kinematics study should include methods of its accurate wrist kinematic recordings.

The lack of correlation of the kinematics results with the clinical scores reflects the different objectives of the two approaches, since clinical scales reveal overall satisfaction where kinematic analysis shows more performance of the recovering shoulder.

10.1.4. GH results

Even if historically the forces at the shoulder have typically been dismissed as being small compared to other joints like knee and hip, the loadsharing results of this study show that the GH contact forces in the reverse joint can rise up to 0.8xBW during ADL with low or no external hand loading where an activity such as 'Sit to stand' can increase the contact forces up to 1.6xBW.

The GH loading results also offer a greater understanding of the loading of a reverse prosthesis, since the data showed how the constant upward pulling of the m.Deltoid and the lack of any compressive forces increase the compressive loading on the humerus (thus the stem of the implant) which also translates to high superior and antero/posterior loading on the Glenosphere.

The analysis of the GH loadings also greatly supports one of the biggest advantages of the reverse prosthesis, which is joint stability. The prosthesis reverses the critical stability (articulating) area and provides stability by placing the large surface of the sphere to resist to the upward pulling of the m.Deltoid and the humeral cup in a direction to face and constrain all the humeral compressive forces.

The results though also revealed some modelling limitations that concern the representation of the muscles as elastic strings and their wrapping around simple geometrical shapes that fit the bone geometry. This simplistic assumption over the string muscle representation creates inaccuracies on the line of action and thus the performance of a muscle. Future musculoskeletal studies should take into consideration the volumetric quantity of each muscle and the interaction/interconnection of the fascicles.

10.1.5. Impingement results and recommendations for implantation and prosthesis design

In summary, this study confirmed that impingement is a major problem on the reverse prosthetic designs and predicts notches on the scapular bone and the humeral cup similar to those observed in the literature. These results also validate to some extent the kinematic reconstruction of the model and enhance the investigation for implantation and design optimisation.

The results highlighted how the positioning of the implant can affect the impingement and suggested that an optimum fixation of the glenoid sphere is when it is fixed inferiorly (on the glenoid) on a non oblique osteotomy. The version of the stem fixation can shift the window of internal/external rotation and a neutral fixation can provide increased internal range while providing more muscle efficiency (moment arm) to m.Teres minor.

Anthropometric differences can affect the fixation, which is subjected to limitations of bone stock and maximum deltoid lengthening suggesting that pre-operating planning and guided implantation can help identify the optimum placement of the implant.

The results also show that the impingement and the stability of the joint are in some cases antagonistic, cancelling each other out when changing some aspect of the prosthetic design (e.g cup depth). In general, results suggests that less impingement can also mean reduced joint stability or high fixation stresses.

From the impingement data it was clear that reducing the cup depth or increasing the sphere lateralisation centre is the most effective way to reduce the impingement. Considering the large safety dislocation factor that was calculated for the DELTA® III design in chapter 8, a reduction of the cup depth should show benefit on the impingement without compromising the joint stability. The percentage of the reduction though is arguable since a highly reduced cup will eventually result in a more unstable joint. The optimum depth should reflect the amount of joint stability that is aimed for by the prosthesis, since if it is targeted for highly active subjects that often perform activities with higher loads than the ADL the cup depth should be large and vice versa. However, reverse prostheses are usually used in more elderly subjects where muscle wasting and the extended RC tears usually constrain their activities and this should be considered in a reverse prosthetic design.

10.2. Recommendations for further work

During the discussion of the findings of this study, it was clear that there were some important limitations especially on the Newcastle Shoulder Model. These limitations are in the form of current assumptions made by the model, unknown effects in the model's behaviour and other software constraints.

Various improvements that could be made in future studies are suggested below.

10.2.1. Measurement of Upper Limb Kinematics

This study has demonstrated that kinematic analysis of the upper limb can provide useful information about the joint function, but the data capturing process poses several difficulties. Even if in this study there are some improvements for the correction of the kinematic cross talk on the elbow (by introducing the second functional frame on the humerus – chapter 4), there is a need for further improvements.

In shoulder motion analysis, soft tissue artefacts can also corrupt the calculation of some joint angles. In particular there are reports that all axial rotations tend to be substantially underestimated (Cappozzo et al. 2005) and they should be analysed with caution. In particular, while intra-subject comparisons may still be possible, intersubject comparison may not be valid. Compensation techniques have been developed and/or tested recently on upper-limb kinematics such as the correction of the humeral axial rotation (Cutti et al. 2005a, Cutti et al. 2005b). However, these techniques are not yet fully or extensively validated for all of the segments of upper extremity.

As the kinematics results suggested the humeral rotation is important for the completion of ADL and in this study the marker set-up and kinematic analysis has probably underestimated the internal/external rotation in the subjects of the Normal and the DELTA group. In a future study the NSM should integrate techniques for accurate humeral estimation, based on frame coupling of the humerus with the forearm that was first proposed by Cutti *et. al.* (2005a). Even if this technique is promising it does not provide an analytical solution to the problem and is based on a discrete correction factor. A further development of the technique, where a second functional forearm frame is defined and projected to the humeral functional frame can provide continues solution to correct the humeral rotation (Kontaxis and Johnson, 2009).

10.2.2. New ADL and task protocol

In the expansion of the application of the Newcastle Shoulder Model, one area of utmost importance is the addition of more ADLs to the established database of kinematics, dynamics and loadsharing results. The particular areas which the database lacks are more tasks with GH internal rotation like dressing and interaction with other everyday objects (opening a door, driving etc.). Examining the biomechanics of dressing using optical motion capture techniques is quite a challenge and different methods should be exploited (e.g. inertial sensors) as proposed by other authors (Cutti et al. 2008). Interaction with everyday objects where larger forces are exerted at the hand (e.g in gripping) requires measurements of reaction forces from gripping and holding (load cell implementation).

In addition to the everyday activities, occupational tasks are also of interest, with particular reference to injury mechanisms and safety. In these cases more instrumentation will undoubtedly be required, together with the wrist and hand expansion to the model.

10.2.3. Dynamic scapula tracking

As the variability of the scapula kinematic results showed, measurement of subject specific scapula and clavicle kinematics is key for improving the individuality of the models. This study followed the methodology of subject specific regression equations that relate scapula angles to humeral rotations (Veeger et. al., 1993, Barnett 1996). This is a direct limitation of the static acquisition of the kinematic data as proposed by Johnson *et, al.* 1993. As discussed in chapter 7, the shoulder 'shrug' that was obvious on some of subjects during the recording of the ADL was not replicated during the static data collection of the scapula measurements and thus poorly simulated in the model.

The solution to the problem would be a more dynamic tracking of the motion of the scapula as proposed by Karduna *et. al.* (2001) and Meskers *et.al.* (2007). As mentioned in chapter 6, the above techniques are not validated for pathological shoulders. A future kinematics study of pathological shoulder girdle should include valid dynamic measurements of the scapula, in order to increase the reliability of the kinematic reconstruction in the biomechanical model and enable the investigation of different muscle strategies that are often observed in subjects with joint replacements. The result of such study can also include pre and post operative follow up providing significant information of any rehabilitation progress.

10.2.4. Muscle modelling and wrapping

Many of the techniques used to represent the behaviour of the muscle elements on the Newcastle Model are basic and not truly physiologically accurate.

The modelling of the muscles as elastic strings together with the simplifications made to describe their paths when interrupted by bony structures has been the cause of many of the deficiencies of the model as discussed in chapter 8.

Simply the ability to wrap muscle around any number of arbitrary polygonal surfaces – e.g bone face triangles – would offer an immediate improvement over the rather simplistic constraints currently provided (simple geometric wrapping objects). Techniques for prescribing such paths for simple strings have been developed and are already finding their way into biomechanical modelling software (e.g. the AnyBody software, Rasmussen et al., 2002).

But the real challenge is the development of muscles with volume and mass properties where they could wrap not only around bone geometries, but also around other muscles, as happens in reality. Some researchers in that respect are beginning to use finite element models in order to better understand the force distribution within muscles. These techniques are becoming more efficient and rather than using full finite element models of muscle, more simple volumetric models based on the more homogenous properties could also be used for producing physiologically representative muscle paths (finite volume methods (Teran J. et al. 2009)).

10.2.5. The Newcastle Shoulder Model as an orthopaedic tool for pre-operative planning tool

Even if the NSM has been used as a research tool to investigate total shoulder joint replacement, the adaptation of the model in its current form is rather difficult and very time consuming. As mentioned in chapter 4, the model is based mainly on modular code that is developed in a mathematical programming language (MatLab) where most of the visualisation of the bone and muscle structure is performed in specialised musculoskeletal software (SIMM®) which also requires specialised code development.

Based on the findings of the impingement and loading results there is clear evidence that pre-operative subject specific planning will provide the optimum results during a joint replacement operation. Based on this assumption, there is a necessity for development of a user-friendly orthopaedic clinical tool, where surgeons would be able to quickly perform a virtual implantation and get immediate feedback for an optimum fixation of a shoulder prosthesis.

This clinical tool can be based on the Newcastle Shoulder Model and the techniques that were developed in this study, but with integration of a quick, user-friendly clinical interface. Enhancements of model customisation with automatic skeletal and muscular reconstruction from CT and MRI imaging are techniques that have been recently developed and could be integrated to the model as well.

10.2.6. Forward dynamics modelling

Finally, the trend in musculoskeletal modelling seems to have recently moved on, from the inverse dynamic, loadsharing approach, towards forward dynamic simulation. This type of simulation involves "driving" the model with either muscle force or neural input and optimising the input to achieve a desired output, frequently measured joint trajectories. Achieving viable solutions to these problems requires a great deal more computing power and time, but this limitation is constantly being eroded by the progress in computing speeds. In addition a deeper understanding of the dynamic response of the central nervous system and the effect of muscle contraction parameters should be well understood in order to develop forward dynamics models. Such models will be able to investigate ballistic movements, joint instability, impingement and dislocation mechanisms and include more accurate ligament constraints where in inverse dynamics models are mainly modelled as rigid links.

References

An, K.N., Browne, A.O., Korinek, S., Tanaka, S. and Morrey, B.F., 1991, "Three-dimensional kinematics of the glenohumeral elevation". *Journal of Orthopaedic Research*, vol 9, pp. 143-149

Anglin, C. & Wyss, U. P. 2000, "Review of arm motion analyses", *Proc.Inst.Mech.Eng H.*, vol. 214, no. 5, pp. 541-555.

Anglin, C. & Wyss, U. P. 2000, "Arm motion and load analysis of sit-to-stand, stand-to-sit, cane walking and lifting", *Clin.Biomech.(Bristol., Avon.)*, vol. 15, no. 6, pp. 441-448.

Anglin, C., Wyss, U. P., & Pichora, D. R. 2000, "Glenohumeral contact forces", *Proc.Inst.Mech.Eng H.*, vol. 214, no. 6, pp. 637-644.

Antuna, S. A., Sperling, J. W., & Cofield, R. H. 2008, "Shoulder hemiarthroplasty for acute fractures of the proximal humerus: a minimum five-year follow-up", *J Shoulder Elbow Surg*, vol. 17, no. 2, pp. 202-209.

Archard J.F. 1953, "Contact and Rubbing of Flat Surfaces", *Journal of Applied Physics*, vol. 24, no. 8, pp. 988-998.

Avallone E.A., Baumeister T., Sadegh A., & Marks L.S. 2006, *Mark's Standard Handbook for Mechanical Engineers*, 11th, Illustrated edn, McGraw-Hill Professional.

Barnett, N. D., Mander, M., Peacock, J. C., Bushby, K., Gardner-Medwin, D., & Johnson, G. R. 1995, "Winging of the scapula: the underlying biomechanics and an orthotic solution", *Proc.Inst.Mech.Eng H.*, vol. 209, no. 4, pp. 215-223.

Barnett, N. D. 1996, *Measurement and modelling of three dimensional scapulohumeral kinematics,* Ph.D., University of Newcastle upon Tyne.

Barnett, N. D., Duncan, R. D. D., & Johnson, G. R. 1999, "The measurement of three dimensional scapulohumeral kinematics - a study of reliability", *Clinical Biomechanics*, vol. 14, pp. 287-290.

Baulot, E., Chabernaud, D., & Grammont, P. M. 1995, "[Results of Grammont's inverted prosthesis in omarthritis associated with major cuff destruction. Apropos of 16 cases]", *Acta Orthop.Belg.*, vol. 61 Suppl 1, pp. 112-119.

Baulot, E., Garron, E., & Grammont, P. M. 1999, "[Grammont prosthesis in humeral head osteonecrosis. Indications--results]", *Acta Orthop.Belg.*, vol. 65 Suppl 1, pp. 109-115.

Bergmann, G., Graichen, H., & Rohlmann, A. 1993, "Hip joint loading during walking and running, measured in tow patients", *Journal of Biomechanics*, vol. 26, no. 8, pp. 969-990.

Bergmann, G., Graichen, H., Rohlmann, A., & Linke, H. 1997, "Hip joint forces during load carrying", *Clinical Orthopaedics & Related Research* no. 335, pp. 190-201.

Bergmann, G., Deuretzbacher, G., Heller, M. O., Graichen, H., Rohlmann, A., Strauss, J., & Duda, G. N. 2001, "Hip contact forces and gait patterns from routine activities", *Journal of Biomechanics*, vol. 34, pp. 859-871.

Bergmann, J. H., de, L. M., Janssen, T. W., Veeger, D. H., & Willems, W. J. 2008, "Contribution of the reverse endoprosthesis to glenohumeral kinematics", *Clin.Orthop.Relat Res.*, vol. 466, no. 3, pp. 594-598.

Biryukova, E. V., Roby-Brami, A., Frolov, A. A., & Mokhtari, M. 2000, "Kinematics of human arm reconstructed from spatial tracking system recordings", *J Biomech.*, vol. 33, no. 8, pp. 985-995.

Blasier, R. B., Soslowsky, L. J., Malicky, D. M., & Palmer, M. L. 1997, "Posterior glenohumeral subluxation: active and passive stabilization in a biomechanical model", *J Bone Joint Surg Am.*, vol. 79, no. 3, pp. 433-440.

Boileau, P., Trojani, C., Walch, G., Krishnan, S. G., Romeo, A., & Sinnerton, R. 2001, "Shoulder arthroplasty for the treatment of the sequelae of fractures of the proximal humerus", *J Shoulder Elbow Surg*, vol. 10, no. 4, pp. 299-308.

Boileau, P., Watkinson, D. J., Hatzidakis, A. M., & Balg, F. 2005, "Grammont reverse prosthesis: design, rationale, and biomechanics", *J Shoulder Elbow Surg*, vol. 14, no. 1 Suppl S, pp. 147S-161S.

Boileau, P., Watkinson, D., Hatzidakis, A. M., & Hovorka, I. 2006, "Neer Award 2005: The Grammont reverse shoulder prosthesis: results in cuff tear arthritis, fracture sequelae, and revision arthroplasty", *J Shoulder Elbow Surg*, vol. 15, no. 5, pp. 527-540.

Boileau, P., Chuinard, C., Le Huec, J. C., Walch, G., & Trojani, C. 2006, "Proximal humerus fracture sequelae: impact of a new radiographic classification on arthroplasty", *Clin.Orthop.Relat Res.*, vol. 442, pp. 121-130.

Boyd, A. D., Jr., Thomas, W. H., Scott, R. D., Sledge, C. B., & Thornhill, T. S. 1990, "Total shoulder arthroplasty versus hemiarthroplasty. Indications for glenoid resurfacing", *J Arthroplasty*, vol. 5, no. 4, pp. 329-336.

Brostrom, L. A., Wallensten, R., Olsson, E., & Anderson, D. 1992, "The Kessel prosthesis in total shoulder arthroplasty. A five-year experience", *Clin.Orthop.Relat Res.* no. 277, pp. 155-160.

Buckley, M. A., Yardley, A., Johnson, G. R., & Carus, D. A. 1996, "Dynamics of the upper limb during performance of the tasks of everyday living--a review of the current knowledge base", *Proc.Inst.Mech.Eng H.*, vol. 210, no. 4, pp. 241-247.

Cappello, A., Cappozzo, A., La Palombara, P. F., Lucchetti, L., & Leardini, A. 1997, "Multiple anatomical landmark calibration for optimal bone pose estimation", *Human Movement Science*, vol. 16, pp. 259-274.

Cappozzo, A., Catani, F., Croce, U. D., & Leardini, A. 1995, "Position and orientation in space of bones during movement: anatomical frame definition and determination", *Clin.Biomech.(Bristol., Avon.)*, vol. 10, no. 4, pp. 171-178.

Cappozzo, A., Catani, F., Leardini, A., Benedetti, M. G., & Croce, U. D. 1996, "Position and orientation in space of bones during movement: experimental artefacts", *Clin.Biomech.(Bristol., Avon.)*, vol. 11, no. 2, pp. 90-100.

Cappozzo, A., Della, C. U., Leardini, A., & Chiari, L. 2005, "Human movement analysis using stereophotogrammetry. Part 1: theoretical background", *Gait.Posture.*, vol. 21, no. 2, pp. 186-196.

Carey, J., Small, C. F., & Pichora, D. R. 2000, "In situ compressive properties of the glenoid labrum", *J Biomed.Mater.Res.*, vol. 51, no. 4, pp. 711-716.

Cazeneuve, J. F. & Cristofari, D. J. 2006, "[Grammont reversed prosthesis for acute complex fracture of the proximal humerus in an elderly population with 5 to 12 years follow-up]", *Rev.Chir Orthop.Reparatrice Appar.Mot.*, vol. 92, no. 6, pp. 543-548.

Charlton, I. W., Murray, I. A., Pandyan, A. D., & Johnson, G. R. "A new technique for the derivation of elbow flexion and forearm pronation angles from landmark co-ordinate data", Cape Town, S. Africa.

Charlton, I. W. & Johnson, G. R. 2001, "Application of spherical and cylindrical wrapping algorithms in a musculoskeletal model of the upper limb", *J Biomech.*, vol. 34, no. 9, pp. 1209-1216.

Charlton, I. W. 2003, *Model for the Prediction of the Forces at the Glenohumeral Joint,* PhD, Newcastle university.

Charlton, I. W. & Johnson, G. R. 2006, "A model for the prediction of the forces at the glenohumeral joint", *Proc.Inst.Mech.Eng [H.]*, vol. 220, no. 8, pp. 801-812.

Cruess RL. 1985, "Corticosteroid-induced osteonecrosis of the humeral head". Orthop Clin North Am. vol, 16, no 4, pp. 789-96.

Colohan AR, Pitts LH, & Rosegay H. 1996, *Injury to the peripheral nerves.*

Cutti, A. G., Paolini, G., Troncossi, M., Cappello, A., & Davalli, A. 2005, "Soft tissue artefact assessment in humeral axial rotation", *Gait.Posture.*, vol. 21, no. 3, pp. 341-349.

Cutti, A. G., Cappello, A., & Davalli, A. 2005, "A new technique for compensating the soft tissue artefact at the upper-arm: in vitro validation", *Journal of Mechanics in Medicine and Biology*, vol. 5, pp. 1-15.

Cutti, A. G., Raggi, M., Davalli, A., & Cappello, A. 2006, "Definition of two reference elbow models from cadaver data", *Gait.Posture.*, vol. 24, no. S2, p. S224-S225.

Cutti, A. G., Giovanardi, A., Rocchi, L., Davalli, A., & Sacchetti, R. 2008, "Ambulatory measurement of shoulder and elbow kinematics through inertial and magnetic sensors", *Med.Biol.Eng Comput.*, vol. 46, no. 2, pp. 169-178.

Dawson, J., Fitzpatrick, R., & Carr, A. 1996, "Questionnaire on the perceptions of patients about shoulder surgery", *J Bone Joint Surg Br.*, vol. 78, no. 4, pp. 593-600.

de Groot, J. H. 1998, *The shoulder: a kinematic and dynamic analysis of motion and loading,* Ph.D., Delft University of Technology, Netherlands.

de Groot, J. H. 1999, "The scapulo-humeral rhythm: effects of 2-D roentgen projection", *Clin.Biomech.(Bristol., Avon.)*, vol. 14, no. 1, pp. 63-68.

de Leva, P. 1996, "Adjustments to Zatsiorsky-Seluyanov's segment inertia parameters", *Journal of Biomechanics*, vol. 29, no. 9, pp. 1223-1230.

De Wilde L. 2008, "Replacing shoulder joints," in *Joint Replacement Technology: New Developments*, 1st edn, Woodhead Publishing Ltd.

De Wilde, L. F., Audenaert, E. A., & Berghs, B. M. 2004, "Shoulder prostheses treating cuff tear arthropathy: a comparative biomechanical study", *J Orthop.Res.*, vol. 22, no. 6, pp. 1222-1230.

De Wilde, L. F., Plasschaert, F. S., Audenaert, E. A., & Verdonk, R. C. 2005, "Functional recovery after a reverse prosthesis for reconstruction of the proximal humerus in tumor surgery", *Clin.Orthop.Relat Res.* no. 430, pp. 156-162.

DePuy. DELTA CTA Reverse Shoulder Prosthesis. [9072-78-032]. 2005. Ref Type: Catalog

Ecklund, K. J., Lee, T. Q., Tibone, J., & Gupta, R. 2007, "Rotator cuff tear arthropathy", *J Am.Acad.Orthop.Surg*, vol. 15, no. 6, pp. 340-349.

Ellman MH & Curran JJ 1988, "Causes and management of shoulder arthritis", *Comprehensive Therapy*, vol. 14, no. 2, pp. 29-35.

Favre, P., Moor, B., Snedeker, J. G., & Gerber, C. 2008, "Influence of component positioning on impingement in conventional total shoulder arthroplasty", *Clin.Biomech.(Bristol., Avon.)*, vol. 23, no. 2, pp. 175-183.

Fenlin JM Jr. 1975, "Total glenohumeral joint replacement.", Orthop Clin North Am. vol 6, no 2, pp. 565-83.

Fick, A. E. & Weber, E. 1877, "Anatomisch-mechanische studie ueber die schultermuskeln II.", *Verhandl.Wurz.Phys.Med.Ges.*, vol. 11, p. 157.

Fitoussi, F., Diop, A., Maurel, N., Laassel, e. M., & Pennecot, G. F. 2006, "Kinematic analysis of the upper limb: a useful tool in children with cerebral palsy", *J Pediatr.Orthop.B*, vol. 15, no. 4, pp. 247-256.

Freedman, L. & Munro, R. R. 1966, "Abduction of the arm in the scapular plane: scapular and glenohumeral movements. A roentgenographic study", *J Bone Joint Surg Am.*, vol. 48, no. 8, pp. 1503-1510.

Gage, J. R. 1994, "The role of gait analysis in the treatment of cerebral palsy", *J Pediatr.Orthop.*, vol. 14, no. 6, pp. 701-702.

Garofalo, P., Cutti, A. G., Filippi, M. V., Cavazza, S., Ferrari, A., Cappello, A., & Davalli, A. 2009, "Inter-operator reliability and prediction bands of a novel protocol to measure the coordinated movements of shoulder-girdle and humerus in clinical settings", *Med.Biol.Eng Comput.*, vol. 47, no. 5, pp. 475-486.

Gerber, C., Pennington, S. D., Lingenfelter, E. J., & Sukthankar, A. 2007, "Reverse Delta-III total shoulder replacement combined with latissimus dorsi transfer. A preliminary report", *J Bone Joint Surg Am.*, vol. 89, pp. 940-947.

Graichen, H. & Bergmann, G. 1991, "Four-channel telemetry system for *in-vivo* measurement of hip joint forces", *Journal of Biomedical Engineering*, vol. 13, pp. 370-374.

Graichen, H., Bergmann, G., & Rohlmann, A. 1999, "Hip endoprosthesis for *in-vivo* measurement of joint force and temperature", *Journal of Biomechanics*, vol. 32, pp. 1113-1117.

Graichen, H., Pennington, S. D., Lingenfelter, E. J., & Sukthankar, A. 2007, "Reverse Delta-III total shoulder replacement combined with latissimus dorsi transfer. A preliminary report", *J Bone Joint Surg Am.*, vol. 89, pp. 940-947.

Grammont PM, Trouilloud P, Laffay JP, & Deries X 1987, "Etude et réalisation d'une nouvelle prosthèse d' épaule", *Rhumatologie*, vol. 39, pp. 407-418.

Grammont, P. M. & Baulot, E. 1993, "Delta shoulder prosthesis for rotator cuff rupture", *Orthopedics*, vol. 16, no. 1, pp. 65-68.

Grant, G. A., Goodkin, R., & Kliot, M. 1999, "Evaluation and surgical management of peripheral nerve problems", *Neurosurgery*, vol. 44, no. 4, pp. 825-839.

Gristina, A. G., Romano R.L., Kammire G.C., & Webb L.X. 1987, "Total shoulder replacement", *Orthop.Clin.North Am.*, vol. 18, no. 3, pp. 445-453.

Guihard, M. & Gorce, P., 2000, "An artificial arm with muscles", 12th Conference of European Society of Biomechanics, Dublin, Rep. Ireland.

Halder, A. M., Kuhl, S. G., Zobitz, M. E., Larson, D., & An, K. N. 2001, "Effects of the glenoid labrum and glenohumeral abduction on stability of the shoulder joint through concavity-compression : an in vitro study", *J Bone Joint Surg Am.*, vol. 83-A, no. 7, pp. 1062-1069.

Hallstrom, E. & Karrholm, J. 2006, "Shoulder kinematics in 25 patients with impingement and 12 controls", *Clin.Orthop.Relat Res.*, vol. 448, pp. 22-27.

Happee, R. 1992, "Time optimality in the control of human movements", *Biol.Cybern.*, vol. 66, no. 4, pp. 357-366.

Happee, R. 1994, "Inverse dynamic optimization including muscular dynamics, a new simulation method applied to goal directed movements", *J.Biomech.*, vol. 27, no. 7, pp. 953-960.

Harman, M., Frankle, M., Vasey, M., & Banks, S. 2005, "Initial glenoid component fixation in "reverse" total shoulder arthroplasty: a biomechanical evaluation", *J Shoulder Elbow Surg*, vol. 14, no. 1 Suppl S, pp. 162S-167S.

Hawkins, R.J. and Neer, C.S. 1989, "A functional analysis of shoulder fusions.", Clinical Orthopaedics, vol. 223, pp. 65-76

Hedtmann, A. & Werner, A. 2007, "[Shoulder arthroplasty in rheumatoid arthritis]", *Orthopade*, vol. 36, no. 11, pp. 1050-1061.

Heller, M. O., Bergmann, G., Deuretzbacher, G., Durselen, L., Pohl, M., Claes, L., Haas, N. P., & Duda, G. N. 2001, "Musculo-skeletal loading conditions at the hip during walking and stair climbing", *Journal of Biomechanics*, vol. 34, pp. 883-893.

Hernigou, P., Duparc, F., & Hernigou, A. 2002, "Determining humeral retroversion with computed tomography", *J Bone Joint Surg Am.*, vol. 84-A, no. 10, pp. 1753-1762.

Hogfors C, Peterson B, Sigholm G, Herberts P. 1991, "Biomechanical model of the human shoulder joint--II. The shoulder rhythm",. J Biomech. 1991;24(8):699-709.

Hogfors, C., Karlsson, D., & Peterson, B. 1995, "Structure and internal consistency of a shoulder model", *J.Biomech.*, vol. 28, no. 7, pp. 767-777.

Hopkins, A. R., Hansen, U. N., Amis, A. A., Knight, L., Taylor, M., Levy, O., & Copeland, S. A. 2007, "Wear in the prosthetic shoulder: association with design parameters", *J Biomech.Eng*, vol. 129, no. 2, pp. 223-230.

Inman, V. T., Saunders, J. B. d. M., & Abbott, L. C. 1944, "Observations on the function of the shoulder joint", *Journal of Bone and Joint Surgery*, vol. 26, pp. 1-30.

Jensen, K. L., Williams, G. R., Jr., Russell, I. J., & Rockwood, C. A., Jr. 1999, "Rotator cuff tear arthropathy", *J Bone Joint Surg Am.*, vol. 81, no. 9, pp. 1312-1324.

Jeong, J., Bryan, J., & Iannotti, J. P. 2009, "Effect of a variable prosthetic neck-shaft angle and the surgical technique on replication of normal humeral anatomy", *J Bone Joint Surg Am.*, vol. 91, no. 8, pp. 1932-1941.

Johnson, G. R., Stuart P.R., & Mitchel S. 1993, "A method for the measurement of three dimensional scapular movement", *Clinical Biomechanics*, vol. 8, no. 5, pp. 269-273.

Johnson, G. R., Spalding, D., Nowitzke, A., & Bogduk, N. 1996, "Modelling the muscles of the scapula morphometric and coordinate data and functional implications", *J Biomech.*, vol. 29, no. 8, pp. 1039-1051.

Johnson, M. P., McClure, P. W., & Karduna, A. R. 2001, "New method to assess scapular upward rotation in subjects with shoulder pathology", *J Orthop.Sports Phys.Ther.*, vol. 31, no. 2, pp. 81-89.

Jonsson E., Eqund N., Kelly I, Rdholm U, & Lidgren L 1986, "Cup arthropasty of the rheumatoid shoulder", *Acta Orthopaedica Scandinavica*, vol. 57, no. 6, pp. 542-546.

Kapandji, I. A. 1982, "The shoulder", *Clin.Rheum.Dis.*, vol. 8, no. 3, pp. 595-616.

Karduna, A. R., McClure, P. W., Michener, L. A., & Sennett, B. 2001, "Dynamic measurements of three-dimensional scapular kinematics: a validation study", *J Biomech.Eng*, vol. 123, no. 2, pp. 184-190.

Karlsson, D. & Peterson, B. 1992, "Towards a model for force predictions in the human shoulder", *J Biomech.*, vol. 25, no. 2, pp. 189-199.

Kelly, I. G., Foster, R. S., & Fisher, W. D. 1987, "Neer total shoulder replacement in rheumatoid arthritis", *J Bone Joint Surg Br.*, vol. 69, no. 5, pp. 723-726.

Kelly, I.G., 1993, "The practise of shoulder surgery.", Butterworth-Heinemann Ltd

Kenmore PI, MacCartee C, Vitek B. 1974, "A simple shoulder replacement.", J Biomed Mater Res.vol. 8, no 4 Pt 2, pp. 329-30.

Kessel, L. & Bayley, I. 1979, "Prosthetic replacement of shoulder joint: preliminary communication", *J R.Soc.Med.*, vol. 72, no. 10, pp. 748-752.

Khazzam M. & Fealy S. 2008, "History and Development of Shoudler Arthroplasty," in Complex Issues in the Primary and Revision Setting, Fealy S. et al., eds., Thieme, pp. 1-9.

Kobel R., Rohimann A., & Bergmann G 1983, "Biomechanical considerations in the design of a semi-constrained total shoulder replacement," in Shoulder Surgery, Bayley I & Kessel I, eds., Springer Vertag, New York, pp. 144-152.

Kontaxis A, Banerjee S., Bull MJ A., & Johnson G., 2007, "Kinematics Performance on Activities of Daily Living After Reverse Shoulder Joint Replacement", in *XXI ISB Congress*, Journal of Biomechanics, p. S108.

Kontaxis A. & Johnson G.R. 2009, "Kinematic refinements on the Newcastle Shoulder Model", in *3rd meeting of the UK Shoulder Group*, Cardiff, UK

Kontaxis, A. & Johnson, G. R. 2008, "Adaptation of scapula lateral rotation after reverse anatomy shoulder replacement", *Comput.Methods Biomech.Biomed.Engin.*, vol. 11, no. 1, pp. 73-80.

Kontaxis, A. & Johnson, G. R. 2009, "The biomechanics of reverse anatomy shoulder replacement--a modelling study", *Clin.Biomech.(Bristol., Avon.)*, vol. 24, no. 3, pp. 254-260.

Kontaxis, A., Cutti, A. G., Johnson, G. R., & Veeger, H. E. 2009, "A framework for the definition of standardized protocols for measuring upper-extremity kinematics", *Clin.Biomech.(Bristol., Avon.)*, vol. 24, no. 3, pp. 246-253.

Kreulen, M., Smeulders, M. J., Veeger, H. E., & Hage, J. J. 2007, "Movement patterns of the upper extremity and trunk associated with impaired forearm rotation in patients with hemiplegic cerebral palsy compared to healthy controls", *Gait.Posture.*, vol. 25, no. 3, pp. 485-492.

Krueger JF 1951, "Surgery", *Surgery*, vol. 30, no. 6, pp. 1005-1011.

Labriola, J. E., Lee, T. Q., Debski, R. E., & McMahon, P. J. 2005, "Stability and instability of the glenohumeral joint: the role of shoulder muscles", *J Shoulder Elbow Surg*, vol. 14, no. 1 Suppl S, pp. 32S-38S.

Lee, S. B., Kim, K. J., O'Driscoll, S. W., Morrey, B. F., & An, K. N. 2000, "Dynamic glenohumeral stability provided by the rotator cuff muscles in the mid-range and end-range of motion. A study in cadavera", *J Bone Joint Surg Am.*, vol. 82, no. 6, pp. 849-857.

Lee, S. B. & An, K. N. 2002, "Dynamic glenohumeral stability provided by three heads of the deltoid muscle", *Clin.Orthop.Relat Res.* no. 400, pp. 40-47.

Ludewig, P. M. & Cook, T. M. 2000, "Alterations in shoulder kinematics and associated muscle activity in people with symptoms of shoulder impingement", *Phys.Ther.*, vol. 80, no. 3, pp. 276-291.

Ludewig, P. M., Behrens, S. A., Meyer, S. M., Spoden, S. M., & Wilson, L. A. 2004, "Three-dimensional clavicular motion during arm elevation: reliability and descriptive data", *J Orthop.Sports Phys.Ther.*, vol. 34, no. 3, pp. 140-149.

Lukasiewicz, A. C., McClure, P., Michener, L., Pratt, N., & Sennett, B. 1999, "Comparison of 3-dimensional scapular position and orientation between subjects with and without shoulder impingement", *J Orthop.Sports Phys.Ther.*, vol. 29, no. 10, pp. 574-583.

Marchese S.S & Johnson G.R. "Measuring the kinematics of the clavicle", in *3D Analysis of Human Motion*, pp. 37-40.

Marchese, S. S. 2000, *Sterno-clavicular kinematics - a new measurement system*, Ph.D., University of Newcastle upon Tyne, UK.

Marsden, S. P., Swailes, D. C., & Johnson, G. R. 2008, "Algorithms for exact multi-object muscle wrapping and application to the deltoid muscle wrapping around the humerus", *Proc.Inst.Mech.Eng H.*, vol. 222, no. 7, pp. 1081-1095.

Marsden, S. P. & Swailes, D. C. 2008, "A novel approach to the prediction of musculotendon paths", *Proc.Inst.Mech.Eng H.*, vol. 222, no. 1, pp. 51-61.

Martini (2001) Fundamentals of Anatomy and Physiology, Fifth edition, Published by Prentice-Hall, Inc.

Maxian, T., Brown, T., Pederson, D., & Callaghan, J. 1996, "Adaptive finite element modeling of long-term polyethylene wear in total hip arthroplasty", *Journal of Orthopaedic Research*, vol. 14, pp. 668-675.

McClure, P. W., Bialker, J., Neff, N., Williams, G., & Karduna, A. 2004, "Shoulder function and 3-dimensional kinematics in people with shoulder impingement syndrome before and after a 6-week exercise program", *Phys.Ther.*, vol. 84, no. 9, pp. 832-848.

McClure, P. W., Michener, L. A., & Karduna, A. R. 2006, "Shoulder function and 3-dimensional scapular kinematics in people with and without shoulder impingement syndrome", *Phys.Ther.*, vol. 86, no. 8, pp. 1075-1090.

McMahon, P. J., Dettling, J., Sandusky, M. D., Tibone, J. E., & Lee, T. Q. 1999, "The anterior band of the inferior glenohumeral ligament", *Journal of Bone and Joint Surgery*, vol. 81-B, no. 3, pp. 406-413.

Mell, A. G., LaScalza, S., Guffey, P., Ray, J., Maciejewski, M., Carpenter, J. E., & Hughes, R. E. 2005, "Effect of rotator cuff pathology on shoulder rhythm", *J Shoulder Elbow Surg*, vol. 14, no. 1 Suppl S, pp. 58S-64S.

Meskers, C. G., Vermeulen, H. M., de Groot, J. H., van der Helm, F. C., & Rozing, P. M. 1998, "3D shoulder position measurements using a six-degree-of-freedom electromagnetic tracking device", *Clin.Biomech.(Bristol., Avon.)*, vol. 13, no. 4-5, pp. 280-292.

Meskers, C. G., van de Sande, M. A., & de Groot, J. H. 2007, "Comparison between tripod and skin-fixed recording of scapular motion", *J Biomech.*, vol. 40, no. 4, pp. 941-946.

Moseley HF. (1968) The clavicle: its anatomy and function. Clin Orthop. 1968 May-Jun;58:17-27.

Mollier, S. 1899, *Ueber die statik und mechanik des menslichen schultergurtels unter normalen und pathologische verhaltnissen* Kupffer, Jena.

Morrey, B. F. & Chao, E. Y. S. 1976, "Passive motion of the elbow joint", *Journal of Bone & Joint Surgery*, vol. 58-A, no. 4, pp. 501-508.

Murray, I. A. & Johnson, G. R. 1999, *Upper limb kinematics and dynamics during everyday tasks,* Ph.D., University of Newcastle upon Tyne, UK.

Murray, I. A. 1999, *Determing upper limb kinematics and dynamics during everyday tasks,* PhD, Newcastle University.

Murray, I. A. & Johnson, G. R. 2000, "Definition of marker positions and technical frames for studying the kinematics of the shoulder".

Murray, I. A. & Johnson, G. R. 2004, "A study of the external forces and moments at the shoulder and elbow while performing every day tasks", *Clin.Biomech.(Bristol., Avon.)*, vol. 19, no. 6, pp. 586-594.

Neer, C. S., BROWN, T. H., Jr., & MCLAUGHLIN, H. L. 1953, "Fracture of the neck of the humerus with dislocation of the head fragment", *Am.J Surg*, vol. 85, no. 3, pp. 252-258.

Neer,C.S. II 1955, "Articular replacement for the humeral head.", Journal of Bone and Joint surgery, vol 37-A, pp. 215-228

Neer, C. S. 1974, "Replacement arthroplasty for glenohumeral osteoarthritis", *J Bone Joint Surg Am.*, vol. 56, no. 1, pp. 1-13.

Neer, C. S., Watson, K. C., & Stanton, F. J. 1982, "Recent experience in total shoulder replacement", *J Bone Joint Surg Am.*, vol. 64, no. 3, pp. 319-337.

Nyffeler, R. W., Werner, C. M., Simmen, B. R., & Gerber, C. 2004, "Analysis of a retrieved delta III total shoulder prosthesis", *J Bone Joint Surg Br.*, vol. 86, no. 8, pp. 1187-1191.

Nyffeler, R. W., Werner, C. M., & Gerber, C. 2005, "Biomechanical relevance of glenoid component positioning in the reverse Delta III total shoulder prosthesis", *J Shoulder Elbow Surg*, vol. 14, no. 5, pp. 524-528.

Otis, J. C., Jiang, C. C., Wickiewicz, T. L., Peterson, M. G., Warren, R. F., & Santner, T. J. 1994, "Changes in the moment arms of the rotator cuff and deltoid muscles with abduction and rotation", *J Bone Joint Surg Am.*, vol. 76, no. 5, pp. 667-676.

Packer, T. L., Wyss, U. P., & Costigan, P. 1994, "Elbow kinematics during sit-to-stand-to-sit of subjects with rheumatoid arthritis", *Arch.Phys.Med.Rehabil.*, vol. 75, no. 8, pp. 900-907.

Peterson, B. & Palmerud, G. 1996, "Measurement of upper extremity orientation by video stereometry system", *Med.Biol.Eng Comput.*, vol. 34, no. 2, pp. 149-154.

Petuskey, K., Bagley, A., Abdala, E., James, M. A., & Rab, G. 2007, "Upper extremity kinematics during functional activities: three-dimensional studies in a normal pediatric population", *Gait.Posture.*, vol. 25, no. 4, pp. 573-579.

Piazza, S. J. & Cavanagh, P. R. 2000, "Measurement of the screw-home motion of the knee is sensitive to errors in axis alignment", *J Biomech.*, vol. 33, no. 8, pp. 1029-1034.

Pietrabissa, R., Raimondi, M., & Di, M. E. 1998, "Wear of polyethylene cups in total hip arthroplasty: a parametric mathematical model", *Med.Eng Phys.*, vol. 20, no. 3, pp. 199-210.

Poppen, N. K. & Walker, P. S. 1976, "Normal and abnormal motion of the shoulder", *J Bone Joint Surg Am.*, vol. 58, no. 2, pp. 195-201.

Poppen, N. K. & Walker, P. S. 1978, "Forces at the glenohumeral joint in abduction", *Clinical Orthopaedics and Related Research* , vol. 135, pp. 165-170.

Porcellini, G., Campi, F., Baccarani, G., & Galassi, R. 1999, "Hemiarthroplasty of the shoulder. Clinical experience in 18 cases treated by the Neer monoblock prosthesis", *Chir Organi Mov*, vol. 84, no. 1, pp. 49-57.

Post, M., Haskell, S. S., & Jablon, M. 1980, "Total shoulder replacement with a constrained prosthesis", *J.Bone Joint Surg.Am.*, vol. 62, no. 3, pp. 327-335.

Pronk, G. M. 1989, "A kinematic model of the shoulder girdle: a resume", *J.Med.Eng Technol.*, vol. 13, no. 1-2, pp. 119-123.

Pronk, G. M. & van der Helm, F. C. 1991, "The palpator: an instrument for measuring the positions of bones in three dimensions", *J Med.Eng Technol.*, vol. 15, no. 1, pp. 15-20.

Pronk, G. M. 1991, *The Shoulder Girdle,* Delft University, The Netherlands.

Pronk, G. M., van der Helm, F. C., & Rozendaal, L. A. 1993, "Interaction between the joints in the shoulder mechanism: the function of the costoclavicular, conoid and trapezoid ligaments", *Proc.Inst.Mech.Eng H.*, vol. 207, no. 4, pp. 219-229.

Raimondi, M. T., Sassi, R., & Pietrabissa, R. 2000, "A method for the evaluation of the change in volume of retrieved acetabular cups", *Proc.Inst.Mech.Eng H.*, vol. 214, no. 6, pp. 577-587.

Rasmussen, J., Vondrak, V., Damsgaard, M., de Zee, M., Christensen, S. T., & Dostal, Z., 2002, "The anybody project - computer analysis of the human body", Czech Society for Biomechanics, Cejkovike, Czech Republic.

Rasmussen, J., Zee, M., Torholm, S., & Damsgaard, M., 2007, "Comparison of a musculoskeletal shoulder model with in-vivo joint forces", in *11th Congress of International Society of Biomechanics*, J Biomechanics, p. S67.

Richard, A., Judet, R. and Rene, L. 1952, "Reconstruction prosthetique acrylique de l'extremite superieure de l'humerus specialement au cours de fractures-luxations". Journal de chirurgie, vol 68, pp. 537-547

Rittmeinster M. & Kerschbaumer F. 2001, "Grammont reverse total shoulder arthroplasty in patients with rheumatoid arthritis and nonreconstructible rotator cuff lesions", *Journal of Shoulder and Elbow Surgery* , vol. 10, no. 1, pp. 17-22.

Roberts, S. N., Foley, A. P., Swallow, H. M., Wallace, W. A., & Coughlan, D. P. 1991, "The geometry of the humeral head and the design of prostheses", *J Bone Joint Surg Br.*, vol. 73, no. 4, pp. 647-650.

Rockwood, C. A., Jr. 2007, "The reverse total shoulder prosthesis. The new kid on the block", *J Bone Joint Surg Am.*, vol. 89, no. 2, pp. 233-235.

Rowe CR, Zarins B. 1982, "Chronic unreduced dislocations of the shoulder.", J Bone Joint Surg Am. Vol. 64, no 4, pp.:494-505.

Rowe, C. R., Zarins, B., & Ciullo, J. V. 1984, "Recurrent anterior dislocation of the shoulder after surgical repair. Apparent causes of failure and treatment", *J Bone Joint Surg Am.*, vol. 66, no. 2, pp. 159-168.

Runciman, R. J. & Nicol, A. C. 1994, "Modelling muscle and joint forces at the glenohumeral joint: overview of a current study", *Journal of Engineering in Medicine, Proc.IMechE, Part H*, vol. 208, pp. 97-102.

Saha, A. K. 1973, "Mechanics of elevation of glenohumeral joint. Its application in rehabilitation of flail shoulder in upper brachial plexus injuries and poliomyelitis and in replacement of the upper humerus by prosthesis", *Acta Orthop.Scand.*, vol. 44, no. 6, pp. 668-678.

Schmidt, R., sselhorst-Klug, C., Silny, J., & Rau, G. 1999, "A marker-based measurement procedure for unconstrained wrist and elbow motions", *J Biomech.*, vol. 32, no. 6, pp. 615-621.

Simovitch, R. W., Zumstein, M. A., Lohri, E., Helmy, N., & Gerber, C. 2007, "Predictors of scapular notching in patients managed with the Delta III reverse total shoulder replacement", *J Bone Joint Surg Am.*, vol. 89, no. 3, pp. 588-600.

Sirveaux, F., Favard, L., Oudet, D., Huquet, D., Walch, G., & Mole, D. 2004, "Grammont inverted total shoulder arthroplasty in the treatment of glenohumeral osteoarthritis with massive rupture of the cuff. Results of a multicentre study of 80 shoulders", *J Bone Joint Surg Br.*, vol. 86, no. 3, pp. 388-395.

Soderkvist, I. & Wedin, P. A. 1993, "Determining the movements of the skeleton using well-configured markers", *J Biomech.*, vol. 26, no. 12, pp. 1473-1477.

Spitzer, V., Ackerman, M. J., Scherzinger, A. L., & Whitlock, D. 1996, "The visible human male: a technical report", *J Am.Med.Inform.Assoc.*, vol. 3, no. 2, pp. 118-130.

Spitzer, V. M. & Whitlock, D. G. 1998, "The Visible Human Dataset: the anatomical platform for human simulation", *Anat.Rec.*, vol. 253, no. 2, pp. 49-57.

Steffee AD & Moore RW 1984, "Hemi-resurfacing arthroplasty of the shoulder", *Contemporary Orthopaedics*, vol. 9, pp. 51-59.

Tanner MW, Cofield RH. 1983, "Prosthetic arthroplasty for fractures and fracture-dislocations of the proximal humerus.", Clin Orthop. vol, 179, pp.116-28.

Teran J., Blemker S., Thow Hing V.N., & Fedkiw R., 2009, "Finite Volume Methods for the Simulation of Skeletal Muscle", in *Symposium on Computer Animation*.

Terrier A., Reist A., Merlini F., & Farron A., 2007, "Joint and Muscle Forces in Reverse and Anatomical Shoulder Prosthesis", in *XXI ISB Congress*, Journal of Biomechanics, p. S146.

Terrier, A., Reist, A., Merlini, F., & Farron, A. 2008, "Simulated joint and muscle forces in reversed and anatomic shoulder prostheses", *J Bone Joint Surg Br.*, vol. 90, no. 6, pp. 751-756.

Terrier, A., Merlini, F., Pioletti, D. P., & Farron, A. 2009, "Comparison of polyethylene wear in anatomical and reversed shoulder prostheses", *J Bone Joint Surg Br.*, vol. 91, no. 7, pp. 977-982.

Valenti P, Boutens D, & Nerot C 2001, "DELTA III reversed prosthesis for osteoarthritis with massive rotator cuff tear: long term results (>5 years)," in *2000 shoulder prosthesis...two to ten year follow-up*, Walch G & Mole D, eds., Sauramps Medical, Montpellier, pp. 253-259.

van Andel, C. J., Wolterbeek, N., Doorenbosch, C. A., Veeger, D. H., & Harlaar, J. 2008, "Complete 3D kinematics of upper extremity functional tasks", *Gait.Posture.*, vol. 27, no. 1, pp. 120-127.

Van der Helm F.C. 1998, "The 'reversed' glenohumeral endoprosthesis", *Journal of Biomechanics*, vol. 31, no. Suppl. 1, p. 27.

van der Helm, F. C., Veeger, H. E., Pronk, G. M., Van der Woude, L. H., & Rozendal, R. H. 1992, "Geometry parameters for musculoskeletal modelling of the shoulder system", *J Biomech.*, vol. 25, no. 2, pp. 129-144.

van der Helm, F. C. 1994, "Analysis of the kinematic and dynamic behavior of the shoulder mechanism", *J Biomech.*, vol. 27, no. 5, pp. 527-550.

van der Helm, F. C. & Pronk, G. M. 1995, "Three-dimensional recording and description of motions of the shoulder mechanism", *J Biomech.Eng*, vol. 117, no. 1, pp. 27-40.

van der Helm, F. C., 1996, "A standardised protocol for motion recordings of the shoulder", in *1st Conference of the International Shoulder Group*, Delft, The Netherlands

van der Helm, F. C. & Veeger, H. E. 1996, "Quasi-static analysis of muscle forces in the shoulder mechanism during wheelchair propulsion", *J Biomech.*, vol. 29, no. 1, pp. 39-52.

van der Helm, F. C. T., Pronk, G. M., Veeger, H. E. J., & Van der Woude, L. H. V. 1989, "The rotation centre of the glenohumeral joint", Los Angeles, USA, pp. 676-677.

van der Helm, F. C. T. & Veebaas, R. 1991, "Modelling the mechanical effects of muscles with large attachment sites: application to the shoulder mechanism", *Journal of Biomechanics*, vol. 24, pp. 1151-1163.

van der Helm, F. C. T., Veeger, H. E. J., Pronk, G. M., Van der Woude, L. H. V., & Rozendaal, R. H. 1992, "Geometry parameters for musculoskeletal modelling of the shoulder mechanism", *Journal of Biomechanics*, vol. 25, no. 2, pp. 129-144.

van der Helm, F. C. T. 1994, "A finite element musculoskeletal model of the shoulder mechanism", *Journal of Biomechanics*, vol. 27, no. 5, pp. 551-569.

van der Helm, F. C. T., Heijns, K. P., Veeger, H. E. J., & Rozendaal, L. A., 2000, "The role of the glenoid labrum for reflexive contributions to the stability of the glenohumeral joint", in *2nd Conference of the International Shoulder Group*, Newcastle, UK.

Veeger, H. E., van der Helm, F. C. T., & Rozendal, R. H. 1993, "Orientation of the scapula in a simulated wheelchair push", *Clinical Biomechanics*, vol. 8, no. 2, pp. 59-111.

Veeger, H. E., Yu, B., An, K. N., & Rozendal, R. H. 1997, "Parameters for modeling the upper extremity", *J Biomech.*, vol. 30, no. 6, pp. 647-652.

Veeger, H. E. 2000, "The position of the rotation center of the glenohumeral joint", *J Biomech.*, vol. 33, no. 12, pp. 1711-1715.

Veeger, H. E., Magermans, D. J., Nagels, J., Chadwick, E. K., & van der Helm, F. C. 2006, "A kinematical analysis of the shoulder after arthroplasty during a hair combing task", *Clin.Biomech.(Bristol., Avon.)*, vol. 21 Suppl 1, p. S39-S44.

Veeger, H. E. & van der Helm, F. C. 2007, "Shoulder function: the perfect compromise between mobility and stability", *J.Biomech.*, vol. 40, no. 10, pp. 2119-2129.

Veeger, H. E. J., Yu, B., An, K. N., & Rozendal, R. H. 1997, "Parameters for modelling the upper extremity", *Journal of Biomechanics*, vol. 30, no. 6, pp. 647-652.

Walch, G., Badet, R., Boulahia, A., & Khoury, A. 1999, "Morphologic study of the glenoid in primary glenohumeral osteoarthritis", *J Arthroplasty*, vol. 14, no. 6, pp. 756-760.

Walker, P. S. & Poppen, N. K. 1977, "Biomechanics of the shoulder joint during abduction in the plane of the scapula [proceedings]", *Bull.Hosp.Joint Dis.*, vol. 38, no. 2, pp. 107-111.

Wall B.T. & Walch G. 2008, "Complications and revisions of the reverse prosthesis: A multicentre study of 457 cases", in *19th Annual BESS meeting.*

Ware, J. E., Jr. & Sherbourne, C. D. 1992, "The MOS 36-item short-form health survey (SF-36). I. Conceptual framework and item selection", *Med.Care*, vol. 30, no. 6, pp. 473-483.

Westerhoff, P., Graichen, F., Bender, A., Rohlmann, A., & Bergmann, G. 2009a, "An instrumented implant for in vivo measurement of contact forces and contact moments in the shoulder joint", *Med.Eng Phys.*, vol. 31, no. 2, pp. 207-213.

Westerhoff, P., Graichen, F., Bender, A., Halder, A., Beier, A., Rohlmann, A., & Bergmann, G. 2009b, "In vivo measurement of shoulder joint loads during activities of daily living", *J Biomech.*, vol. 42, no. 12, pp. 1840-1849.

Wheeler, J., Woodward, C., Ucovich, R. L., Perry, J., & Walker, J. M. 1985, "Rising from a chair. Influence of age and chair design", *Phys.Ther.*, vol. 65, no. 1, pp. 22-26.

Wiater, J. M. & Fabing, M. H. 2009, "Shoulder arthroplasty: prosthetic options and indications", *J Am.Acad.Orthop.Surg*, vol. 17, no. 7, pp. 415-425.

Williams, J. R., Leardini, A., & Catini, F., 1996, "The study of upper limb kinematics using a "technical array" marker set, "anatomical callibration" and "technical and anatomical axes"", in the proc. of the *Conference of the British Orthopaedic Research Society*, Oswestry, England.

Woodruff, M. J., Cohen, A. P., & Bradley, J. G. 2003, "Arthroplasty of the shoulder in rheumatoid arthritis with rotator cuff dysfunction", *Int.Orthop.*, vol. 27, no. 1, pp. 7-10.

Wu, G., van der Helm, F. C., Veeger, H. E., Makhsous, M., Van, R. P., Anglin, C., Nagels, J., Karduna, A. R., McQuade, K., Wang, X., Werner, F. W., & Buchholz, B. 2005, "ISB recommendation on definitions of joint coordinate systems of various joints for the reporting of human joint motion--Part II: shoulder, elbow, wrist and hand", *J.Biomech.*, vol. 38, no. 5, pp. 981-992.

Zippel J. 1975, "Dislocation-proof shoulder prosthesis model" BME. Z Orthop Ihre Grenzgeb. Vol 113, no 4, pp. 454-7

Appendix

A1. Clinical Scores

Oxford Shoulder Score

Standard Score – SF36 Version 2

A2. Journal Papers

Kontaxis A. and Johnson G.R. 2009, 'The biomechanics of reverse anatomy shoulder replacement--a modelling study.', Clin Biomech (Bristol, Avon). Mar;24(3):254-60

Kontaxis A. and Johnson G.R. 2008,, 'Adaptation of scapula lateral rotation after reverse anatomy shoulder replacement.', Comput Methods Biomech Biomed Engin. Feb;11(1):73-80. Epub 2007 Oct 15.

Oxford Shoulder Score

1. How would you describe the worst pain you had from your shoulder?

Unbearable Severe Moderate Mild No

2. How would you describe the pain you usually get from your shoulder?

Unbearable Severe Moderate Mild None

3. How much has the pain form your shoulder interfered with your usual work (including housework)?

Totally Greatly Moderately A little bit Not at all

4. Have you been troubled by pain in your shoulder in bed at night?

Every night Most nights Some nights only 1 or 2 No nights

5. Have you had ant trouble dressing yourself because of your shoulder?

Impossible to do Extreme difficulty moderate trouble
Very little trouble No trouble at all

6. Have you had any trouble getting in and out of a car or using public transport because of your shoulder? (Whichever you tend to use)

Impossible to do Extreme difficulty moderate trouble
Very little trouble No trouble at all

7. Have you been able to user a knife and fork at the same time?

No. Impossible With extreme difficulty With moderate difficulty With little difficulty Yes, easily

8. Could you do the household shopping on your own?

No. Impossible With extreme difficulty With moderate difficulty With little difficulty Yes, easily

Oxford Shoulder Score

9. Could you carry a tray containing a plate of food across a room?

No. impossible **With extreme difficulty** **With moderate difficulty** **With little difficulty** **Yes, easily**

10. Could you brush/comb your hair with the affected arm?

No. Impossible **With extreme difficulty** **With moderate difficulty** **With little difficulty** **Yes, easily**

11. Could you hang your clothes up in a wardrobe, using the affected arm?

No. Impossible **With extreme difficulty** **With moderate difficulty** **With little difficulty** **Yes, easily**

12. Have you been able to wash and dry yourself under both arms?

No. Impossible **With extreme difficulty** **with moderate difficulty** **With little difficulty** **Yes, easily**

SF36 VERSION 2

OVERALL HEALTH

The following questions ask for your views about your health and how you feel about life in general. If you are unsure about how to answer any question, try and think about your overall health and give the best answer you can. Do not spend too much time answering, as your immediate response is likely to be the most accurate.

---

1. In general, would you say your health is:

(Please tick **one** box)

- Excellent ☐
- Very good ☐
- Good ☐
- Fair ☐
- Poor ☐

---

2. Compared to 3 months ago, how would you rate your health in general now?

(Please tick **one** box)

- Much better than 3 months ago ☐
- Somewhat better than 3 months ago ☐
- About the same ☐
- Somewhat worse now than 3 months ago ☐
- Much worse now than 3 months ago ☐

3. **The following questions are about activities you might do during a typical day. Does your health limit you in these activities? If so, how much?**

	(Please tick **one** box on each line)	**Yes, limited a lot**	**Yes, limited a little**	**No, not limited at all**
a)	**Vigorous activities,** such as running, lifting heavy objects, participating in strenuous sports	☐	☐	☐
b)	**Moderate activities,** such as moving a table, pushing a vacuum, bowling or playing golf	☐	☐	☐
c)	Lifting or carrying groceries	☐	☐	☐
d)	Climbing **several** flights of stairs	☐	☐	☐
e)	Climbing **one** flight of stairs	☐	☐	☐
f)	Bending kneeling or stooping	☐	☐	☐
g)	Walking **more than a mile**	☐	☐	☐
h)	Walking **half a mile**	☐	☐	☐
i)	Walking **100 yards**	☐	☐	☐
j)	Bathing and dressing yourself	☐	☐	☐

---

4. **During the <u>past 2 weeks</u>, how much time have you had any of the following problems with your work or other regular daily activities <u>as a result of your physical health</u>?**

	(Please tick **one** box) on each line	**All of the time**	**Most of the time**	**Some of the time**	**A little of the time**	**None of the time**
a)	Cut down on the **amount of time** you spent on work or other activities	☐	☐	☐	☐	☐
b)	**Accomplished less** than you would like	☐	☐	☐	☐	☐
c)	Were limited in the **kind** of work or other activities	☐	☐	☐	☐	☐
d)	Had difficulty performing the work or other activities (eg it took more effort)	☐	☐	☐	☐	☐

5. **During the past 2 weeks, how much time have you had any of the following problems with your work or other regular daily activities as a result of any emotional problems (such as feeling depressed or anxious)?**

(Please tick **one** box) on each line		**All of the time**	**Most of the time**	**Some of the time**	**A little of the time**	**None of the time**
a)	Cut down on the **amount of time** you spent on work or other activities	☐	☐	☐	☐	☐
b)	**Accomplished less** than you would like	☐	☐	☐	☐	☐
c)	Didn't do work or other activities as **carefully** as usual	☐	☐	☐	☐	☐

---

6. **During the past 2 weeks, to what extent have your physical health or emotional problems interfered with your normal social activities with family, neighbours or groups?**

(Please tick **one** box)

- Not at all ☐
- Slightly ☐
- Moderately ☐
- Quite a bit ☐
- Extremely ☐

---

7. **How much bodily pain have you had during the past 2 weeks ?**

(Please tick **one** box)

- None ☐
- Very mild ☐
- Mild ☐
- Moderate ☐
- Severe ☐
- Very Severe ☐

8. **During the past 2 weeks, how much did pain interfere with your normal work (including bothoutside the home and housework)?**

(Please tick **one** box)

Not at all	☐
Slightly	☐
Moderately	☐
Quite a bit	☐
Extremely	☐

---

9. **These questions are about how you feel and how things have been with you during the past 2 weeks. For each question please give one answer that comes closest to the way you have been feeling.**

(Please tick **one** box on each line)

	How much time during the last 2 weeks:	All of the time	Most of the time	A good bit of the time	Some of the time	A little of the time	None of the time
a)	Did you feel full of life?	☐	☐	☐	☐	☐	☐
b)	Have you been a very nervous person?	☐	☐	☐	☐	☐	☐
c)	Have you felt so down in the dumps that nothing would cheer you up?	☐	☐	☐	☐	☐	☐
d)	Have you felt calm and peaceful?	☐	☐	☐	☐	☐	☐
e)	Did you have a lot of energy?	☐	☐	☐	☐	☐	☐
f)	Have you felt downhearted and low?	☐	☐	☐	☐	☐	☐
g)	Did you feel worn out?	☐	☐	☐	☐	☐	☐
h)	Have you been a happy person?	☐	☐	☐	☐	☐	☐
i)	Did you feel tired?	☐	☐	☐	☐	☐	☐

10. During the past 2 weeks, how much of the time has your physical health or emotional problems interefered with your social activities (like visiting friends, relatives etc.).

(Please tick **one** box)

- All of the time ☐
- Most of the time ☐
- Some of the time ☐
- A little of the time ☐
- None of the time ☐

---

11. How TRUE or FALSE is each of the following statements for you?

(Please tick **one** box on each line)

		Definitely true	Mostly true	Not sure	Mostly false	Definitely false
a)	I seem to get ill more easily than other people	☐	☐	☐	☐	☐
b)	I am as healthy as anybody I know	☐	☐	☐	☐	☐
c)	I expect my health to get worse	☐	☐	☐	☐	☐
d)	My health is excellent	☐	☐	☐	☐	☐

---

12. During the last 12 months, how many hours on average per day have you spent caring for the person suffering from Parkinson's disease?

_____ **Hours per day**

If you did not have to spend this time caring, what would you otherwise have done withthese hours? *(please tick all those relevant activities and the number of hours which would have been spent on each).*

For example, Paid employment	☑	*4 hours*
Paid employment	☐	___ hours
Leisure activities such as gardening/reading/relaxing	☐	___ hours
Other (e.g. shopping, housework)	☐	___ hours

If other, please specify _____

Completed by: ..... **Date completed:** ..... / ..... / .....

Clinical Biomechanics 24 (2009) 254–260

Contents lists available at ScienceDirect

Clinical Biomechanics

journal homepage: www.elsevier.com/locate/clinbiomech

The biomechanics of reverse anatomy shoulder replacement – A modelling study

A. Kontaxis *, G.R. Johnson

Centre for Rehabilitation and Engineering Studies (CREST), School of Mechanical and Systems Engineering, Newcastle University, Stephenson Building, Newcastle upon Tyne, NE1 7RU, UK

ARTICLE INFO

Article history:
Received 7 April 2008
Accepted 9 December 2008

Keywords:
Reverse prosthesis
Muscle moment arm
Glenoid loading
Impingement
Notches
Shoulder model

ABSTRACT

Background: Reverse anatomy shoulder prostheses, in which a partial sphere is attached to the scapula and a socket to the humerus, have become popular for the treatment of arthritic shoulders with severe rotator cuff arthropathy. While they have been in relatively common use, their biomechanical aspects have not been fully investigated.

Methods: This study uses an adaptation of a 3D biomechanical shoulder model to describe the DELTA® reverse prosthetic shoulder geometry and to investigate its properties. The muscle configuration was modified to represent the pathology and joint contact forces were computed for standardised activities. The model also uses a contact detect algorithm to record the impingement of the prosthesis with the scapula.

Findings: Results showed that the reverse design increases the deltoid function compensating for the dysfunctional rotator cuff muscles by providing sufficient moment arm (increased by 42%) to elevate the arm. It also restores joint stability by reversing the envelope of the joint contact forces and reacting to the increased shear forces. Despite these advantages, the model also confirms impingement and predicts bone notches from the contact of the prosthesis with the scapula border. Results indicate that optimised fixation and design alterations can reduce the problem but is difficult to eliminate it without compromising the joint stability.

Interpretation: The study provides a deep understanding of the function of the reverse designs highlighting their advantages in irreparable rotator cuff arthropathy but also the associated problems that compromise their use. Despite the limitations results indicate that reverse designs can be optimised to provide maximum functionality.

1. Introduction

The normal shoulder is required to have basic mechanical characteristics of range of motion (mobility), stability and strength. However, each of these is commonly compromised in an arthritic or rotator cuff tear shoulder. Arthoplasty is a common solution for immediate pain relief and to restore shoulder functionality (Neer et al., 1982).

Many prostheses are used to address these pathologies and the designs vary in shape and dimensions and in some cases try to address stability issues by fully constraining the joint (Brostrom et al., 1992; Post et al., 1980). Reverse anatomy prostheses are introduced as an alternative solution in challenging pathologies like the arthritic shoulder with massive rotator cuff (RC) tears (Kessel and Bayley, 1979).

The DELTA® prosthesis (produced by DePuy) was first developed by (Grammont et al., 1987), but further modifications were made to the original prosthesis until the Delta® III version (Grammont et al., 1987; Grammont and Baulot, 1993) which has been extensively used in rotator cuff tear arthropathies. There are many clinical reviews reporting stability and good performance of this design (Sirveaux et al., 2004; Woodruff et al., 2003), but also indicating problems of impingement and glenoid loosening after long term use (Nyffeler et al., 2004). There are now a number of competing prostheses in the United Sates (e.g. from Encore, and Zimmer) and in Europe (e.g. Lima, Aston, Tornier, Implants Industries) following the same basic design but with modifications intended to address the above problems.

Despite the longterm use and the popularity of the Grammont type prosthesis, there are only few two dimensional (De Wilde et al., 2004) or three dimensional biomechanical studies (Terrier et al., 2008; Van der Helm, 1998) focusing either on muscle and joint contact analysis or impingement (Nyffeler et al., 2005) without examining how the different aspect of the reverse designs can affect the general joint performance. In this study we try to analyse in more depth the biomechanical properties of the DELTA® (and in general the reverse) design using an interactive biomechanical model of the upper limb (Charlton and Johnson, 2006). The comparison of the results will also lead to a discussion of the relative

* Corresponding author.
E-mail address: Andreas.Kontaxis@ncl.ac.uk (A. Kontaxis).

0268-0033/$ - see front matter © 2008 Elsevier Ltd. All rights reserved.
doi:10.1016/j.clinbiomech.2008.12.004

importance of the implantation and the design features of reverse prostheses and how they can affect the loading, stability and impingement of the prosthetic joint.

The above aim will be achieved by comparing modelling data between the reverse prosthetic and normal anatomy shoulder model on the following aspects:

(a) Lengthening and moment arms of deltoid and RC muscles.
(b) Predicted muscle and joint contact forces during standardised activities.
(c) Range of arm motion in reverse shoulder and prediction of impingement.

2. Materials

2.1. The reverse prosthetic biomechanical model

This modelling study was performed using a modified version of the three dimensional Newcastle upper limb model (Charlton and Johnson, 2006) which in its original state represent a normal anatomy shoulder and elbow. The model consists of six rigid bone segments; the thorax, clavicle, scapula, humerus, radius and ulna. The various bony structures and landmarks were digitised from the Visible Human male dataset (Spitzer and Whitlock, 1998). The segments are connected by three spherical joints (3DoF), the Sternoclavicular (SC), Acromioclavicular (AC) and Glenohumeral (GH), and two single DoF hinge joints at the elbow. Scapula and clavicle kinematics have been described using two sets of regression equations (Barnett et al., 1999; Marchese and Johnson, 2000). The model in its final state includes 31 muscles and three ligaments, works inverse dynamically and predicts muscle and joint contact forces by minimising a physiological cost function (Charlton and Johnson, 2006).

Accurate insertion of the prosthesis was achieved by simulating the standard surgical procedure (DePuy, 2005). A set of virtual instrumentation tools was available in order to define insertion points and resection planes. The humeral resection plane was found to be 1.4 mm under the greater tubercle of the humeral head. The insertion point for the glenoid fixation was defined as the centre of a circle that matches the inferior part of the glenoidal border (surgical guidelines, DePuy, 2005). The glenosphere was fixed after a surface remodelling (reaming) of the glenoid, as is normally required in a normal surgical procedure by the glenoid rasp. The large size sphere (R_{sphere} = 21 mm) was chosen as the primary fixation. For this fixation ('standard fixation') the rim of the sphere was overlapping the inferior reamed glenoid surface. The kinematics constraints of the prosthetic design imply that the centre of the concave cup needs to coincide with the centre of the glenoid sphere in order to slide on its surface and as a result defines the new humeral rotational centre (Fig. 1).

An added feature of the model was a contact detection algorithm that developed to investigate the impingement problems which are reported in a number of clinical reviews (Nyffeler et al., 2004; Simovitch et al., 2007; Sirveaux et al., 2004). The algorithm can detect the site and record the volume of any possible contact between the humeral cup and the scapular border (inferior impingement) or humeral head and acromion or coracoid process of the scapula (superior impingement). The contact detection algorithm works independently from the dynamic solver which calculates loads and muscle forces even if impingement is detected.

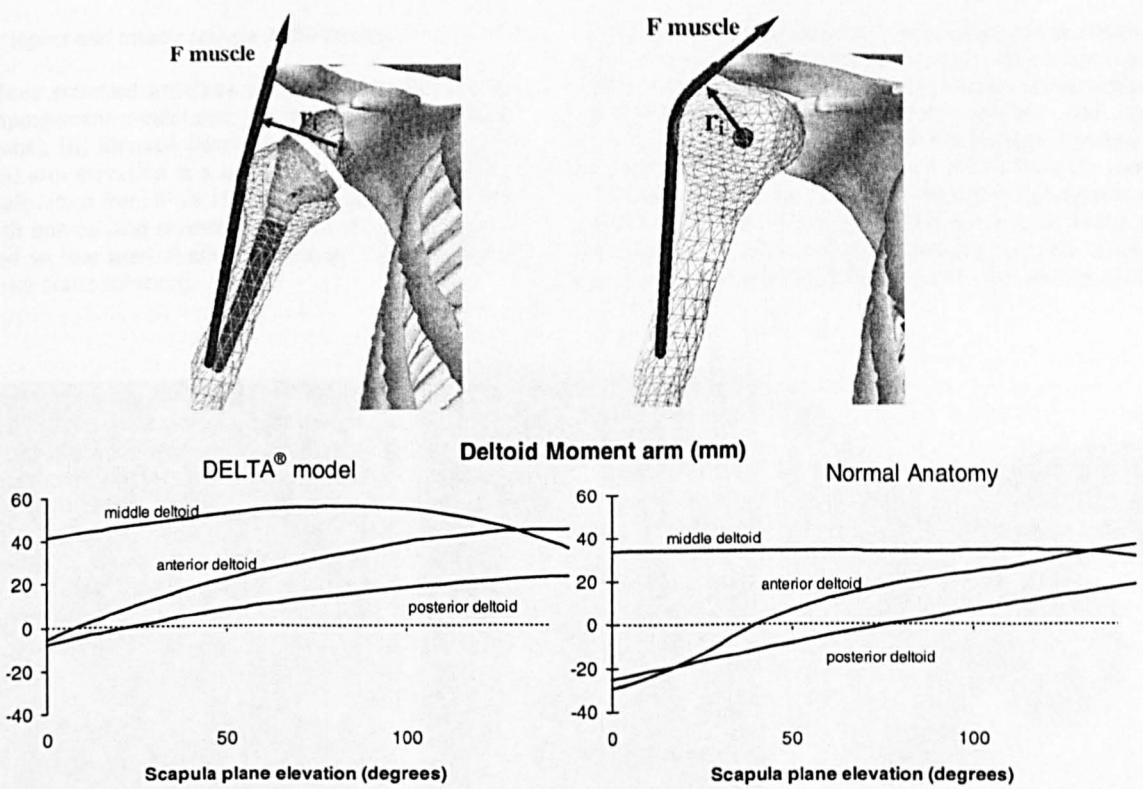

Fig. 1. The DELTA® geometry changes the centre of rotation of the GH joint and affects significantly the deltoid moment arm compared to the normal anatomy (up). In the latter the middle deltoid moment arm has almost constant value, where in the prosthetic geometry it has a much greater fluctuation, which peaks around 90° of abduction, where the arm weight creates its largest adducting moment (down – scapula plane elevation presented here).

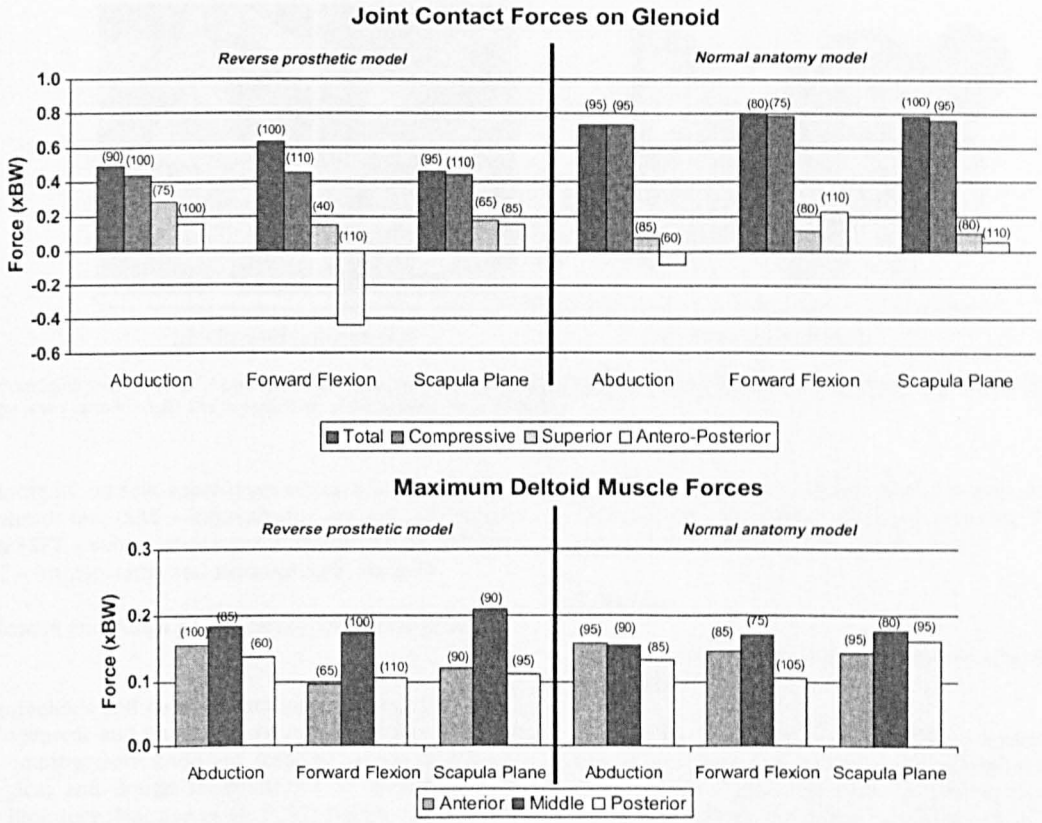

Fig. 2. Maxima of joint contact forces on the glenoid site (up) and deltoid muscle forces (down) during standard activities for reverse prosthetic (FFT model – no RC muscles) and normal anatomy (all muscles) shoulder. In parentheses is the humeral elevating angle that the maxima were observed.

2.2. Kinematic inputs and muscle set-ups of the model

A set of three standard activities were simulated for the dynamic and impingement predictions: (i) abduction (arm elevation in coronal plane), (ii) forward flexion (arm elevation in sagittal plane) and (iii) arm elevation in scapular plane. All the activities describe arm elevation from 0° to 150°. The simulations were performed in both normal and reverse prosthetic anatomy at a low constant speed so that inertial effects could be considered to be negligible (quasi-static solution).

The clinical indication for the use of the reverse prosthesis is a large irreparable RC tear (Boileau et al., 2005; Grammont and Baulot, 1993). In this condition the supraspinatus, infraspinatus and subscapularis muscles are not present (full thickness tear – FTT). In this study the RC tear was simulated by just excluding the corresponding muscle lines of action from the model.

Because information is lacking regarding the natural progression of cuff tears (Ecklund et al., 2007; Jensen et al., 1999), it is possible for the infraspinatus or subscapularis muscle to be present after a reverse joint replacement. In order to investigate the effect

Fig. 3. The predicted scapular notches (right picture) match in shape and volume the notches observed from cadaveric (left image, adapted from Nyffeler et al., 2004) and radiographic studies (middle image, adapted from Simovitch et al., 2007).

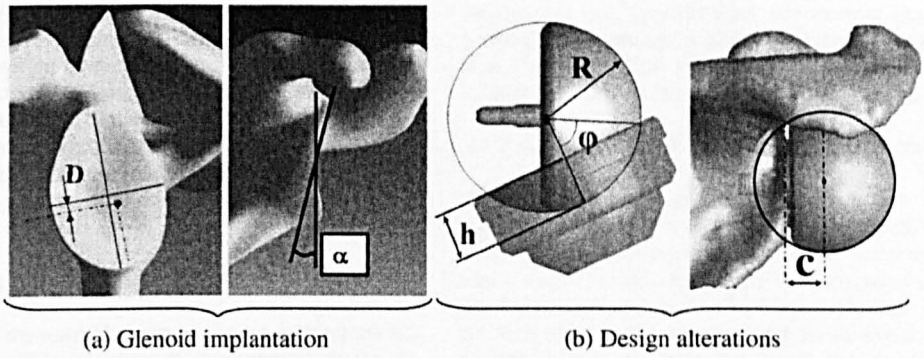

Fig. 4. Different configurations tested on the prosthetic model: (a) glenoid implantation: inferior fixation D (left) and oblique osteotomy α (right), (b) design alterations: cup depth h to sphere size r ratio h/r (left) and lateralisation of the sphere centre c (right).

of any remaining RC muscle, more types of tears were simulated: (i) supero-anterior tear (SAT – infraspinatus present), (ii) supero-posterior tear (SPT – subscapularis present) and (iii) partial superior tear (PST – infraspinatus and subscapularis present).

2.3. Testing fixation and design parameters of the reverse anatomy designs

Surgical guidelines and design alterations try to address problems of impingement and improve survivorship. In this study we present how impingement and joint stability can be affected by different surgical and design modifications as they have been found in the literature (Harman et al., 2005; Nyffeler et al., 2005; Simovitch et al., 2007). The parameters tested are shown in Fig. 4 and involve:

2.3.1. Surgical modifications (glenoid fixations)

2.3.1.1. Glenoid sphere inferior fixation D. Starting from the 'standard fixation' the sphere was fixed inferiorly along the supero-inferior glenoid axis, and in increments of 1 mm.

2.3.1.2. Glenoid reaming angle α. For the standard fixation the instrumentation and the surgical guidelines define a face glenoid reaming (where $\alpha = 0°$, Fig. 4a). By maintaining position of the standard fixation, we investigate the importance of the glenoid preparation by performing an oblique osteotomy in $\alpha = 5°$, 10°, 15° (D = constant). The bone was remodelled accordingly each time.

2.3.2. Design alterations

2.3.2.1. Cup depth to sphere radius ratio (h/R). The depth of the cup (h) for a given sphere radius (R) can influence not only the impingement but also the joint stability, since the ratio h/R influences the maximum shear to compressive force ratio that the prosthetic joint can withstand:

$$\left(\frac{shear}{compressive}\right)_{max} = \frac{\sin\phi \cdot R}{R-h} = \tan\phi$$

where ϕ is the angle that defines the cup width (Fig. 4).

The cup depth of the standard DELTA configuration is $h = 8$ mm and in order to investigate the importance of the h/R ratio sallower cups have been tested ($h = 7$, 6, 5 mm) maintaining the same sphere size ($R = 18$ mm, Fig. 4b).

2.3.2.2. Lateralisation of the centre of the sphere c from the fixation plane. The standard DELTA® III design adopts a half sphere approach for the glenoid design where its centre (which is also the GH rotational centre) is located on the fixation plane ($c = 0$ mm). Alternative designs have introduced a glenoid sphere where its centre is fixed in a more lateral position (Fig. 4b). This study tests glenoid spheres with $c = 1$, 2 and 3 mm.

3. Results

3.1. Muscle lengthening and moment arms after reverse joint replacement

After the DELTA® III replacement, the humerus (and as a result the whole arm) is positioned more medially and inferiorly compared to the normal shoulder, something that can be even observed visually in real subjects (Boileau et al., 2005). As a result the deltoid muscle is stretched giving a passive tension to the GH joint. The predicted lengthening of the middle deltoid was 21.6% compared to normal anatomy (Table 1). It is reported that deltoid extension more than 20%, could damage the axillary nerve (Grant et al., 1999).

The reverse prosthetic geometry medialises the rotational centre of the humerus and as a result moment arms of the muscles crossing the GH joint are greatly affected. One of the most affected muscles is the deltoid where its moment arm peaks an average value of 54.4 ± 0.1 mm (in 90°-middle deltoid) for the three tasks (Table 1). In normal anatomy the middle deltoid moment arm has a smaller almost constant value, where in the prosthetic geometry it has a much greater fluctuation (Fig. 1). Interestingly, the middle deltoid moment arm in the DELTA® III model has a peak at 90° of abduction, where the arm weight creates its largest adducting moment.

Table 1
Summary of peak middle deltoid moment arms and muscle lengthening in literature and in this study.

Study	Motion	Moment arm (mm)		Middle deltoid length increase (%)
		Normal anatomy	Reverse anatomy	Reverse Anatomy
De Wilde et al. (2004)	Scapula plane	40.0	59.3	19.1
Terrier et al. (2007)	Scapula plane	28.0	50.0	-
Van der Helm (1998)	Abduction	35.0	52.0	-
This study	Abduction	34.7	55.1	
	Forward flexion	36.1	52.8	21.6
	Scapula Plane	34.6	55.3	

The moment arms of infraspinatus and subscapularis muscles (when present in the corresponding RC tear prosthetic models) are also affected and have an adducting moment arm throughout the motion (average range −16.8 mm (0° elevation) to −1.5 mm (150° elevation) and −20.2 mm (0° elevation) to 4.5 mm (150° elevation), respectively). In contrast, in the normal anatomy the RC muscles can have an abducting moment arm after 25° of arm elevation (average range −3.6 to 17.9 mm and −4.0 to 15.7 mm, respectively).

3.2. Load sharing: muscle and joint contact forces and GH stability

While simulations of the normal anatomy model with all the RC muscles present were possible, in the model with the full thickness RC tear were not feasible since the high predicted shear contact forces in the GH joint could not be constrained within the glenoid stability area. All the simulations with the reverse prosthetic model converged to stable solutions, independently of the type of the RC tear. In the FTT prosthetic model, the predicted total contact forces were reduced by an average of 31.6% (range 0.463–0.631 times BW) compared with the normal shoulder (all the RC muscles present). The compressive forces reduced by 41.6% on the glenoid site (range 0.435–0.451 times BW) (Fig. 2) with the superior forces being increased in all three activities. The antero-posterior shear forces (glenoid site) changed magnitude and direction depending on the activity (maximum observed in forward flexion where the posterior shear force peaked a high 0.438 times BW – Fig. 2).

Simulations with the different types of RC tears showed small differences. The remaining RC muscles exerted small forces, peaking only 0.06 times BW. In general subscapularis fibres reduced the anterior glenoid shear forces during abduction (0.05 times BW reduction) whereas infraspinatus reduced the posterior shear forces in forward flexion and scapula plane elevation (0.04–0.07 times BW, respectively). The highest difference in the total joint contact force between the FFT and any of the RC tears models was only 0.07 times BW.

Transforming the joint reaction forces into the humeral cup frame, showed that they were well constrained within the stability rim, with the trace of joint contact forces located slightly inferiorly to the centre of the cup. The ratio of shear/compressive peaked only 0.58 (for the FTT model) where in the DELTA® geometry the maximum allowed ratio is 1.86.

The deltoid muscle forces in the prosthetic model during all three activities were close to those of the normal anatomy model, but with the middle part contributing slightly more compared to the anterior and posterior deltoid (Fig. 2).

3.3. Impingement: a compromise on the range of motion

All three simulations of the standard activities with the prosthetic model clearly showed a contact of the humeral cup with the inferior scapular border (inferior impingement) and of the Greater tubercle with the acromion or coracoid process (superior impingement). As it was expected the range of motion (with no impingent) was smaller than the normal shoulder and was restricted to an average of 60° for all three activities (standard fixation, Table 2).. The graphical contact detection predicted also large bone notches on the scapula border (Fig. 3).

3.4. Fixation and design parameters of the reverse anatomy designs

3.4.1. Implantation configurations

3.4.1.1. Glenoid sphere inferior fixation. Results showed that the available range of motion was greatly increased (average 5 deg/mm, Table 2) with a more inferior fixation of the sphere. After an extreme 6 mm of inferior fixation no inferior impingement could be detected, but the fixation screws were well outside the scapula border after 4 mm. Deltoid elongation was also increased significantly (1.2% lengthening increase per mm of inferior fixation) compared to an already large value of 21.6% of the standard fixation. The latter increases even further the risk of damaging the axillary nerve (Grant et al., 1999). Predicted joint contact forces were not affected by the inferior fixation since the muscle lines of actions were almost unaffected.

3.4.1.2. Glenoid reaming angle. Results of an oblique osteotomy (angle α, Fig. 4) of 5°, 10° and 15° showed different outcomes:

(a) For $\alpha = 5°$, the glenoid sphere still overlaps the inferior reamed glenoid surface and the results showed no change for the inferior impingement (Table 2).
(b) When the sphere was fixed in a more aggressive oblique osteotomy, the inferior reamed surface was either flush or exposed under the glenoid sphere (for $\alpha = 10$ and 15°, respectively). The results for this set-up showed a small improvement, but only for the inferior impingement (Table 2).

The above results can be explained by the fact that oblique glenoid reaming can trim away a potential contact of the bone with the cup, but only when inferior glenoid surface is not overlapped by the sphere and the inferior impingement occurs just below the sphere fixation.

The total joint contact and muscle force predictions from the model were not affected by the different glenoid reaming, since fixing the sphere in an oblique orientation had no affect on the joint geometry and to the muscle wrapping around the bones.

3.4.2. Design alterations

3.4.2.1. Cup depth to sphere radius ratio (h/R). Results showed that a reduction of the cup depth h (given R = constant) is a very effective way to reduce inferior impingement (Table 2). A reduction of h by 3 mm ($h = 5$ mm) increased the range of motion by 11.3° in average for the three standard activities. During the dynamic simulations, stability of the joint was not compromised by reducing the cup depth by the same amount ($h/R = 0.38$) since the contact force prediction was well constraint within the centre of the cup.

Table 2
Averaged range of motion results from all three standard activities and the effect of different fixation and design parameters. The numbers present the minimum and maximum humeral elevation (in degrees) as it is constrained by the inferior and superior impingement, respectively.

Impingement	Standard fixation *Configuration:* $D = 0$, $\alpha = 0$, $c = 0$, $h = 11$	Implantation configurations						Design alterations					
		Inferior fixation D (mm) $\alpha = 0$, $c = 0$, $h = 11$			Reaming angle α (degrees) $D = 0$, $c = 0$, $h = 11$			Cup depth h (mm) $D = 0$, $\alpha = 0$, $c = 0$			Lateralised sphere centre c (mm) $D = 0$, $\alpha = 0$, $h = 11$		
		$D = 1$	$D = 2$	$D = 3$	$\alpha = 5$	$\alpha = 10$	$\alpha = 15$	$h = 10$	$h = 9$	$h = 8$	$c = 1$	$c = 2$	$c = 3$
Inferior (°)	33.3	30.1	27.1	24.1	33.3	30.3	28.2	29.4	25.8	22.0	30.8	28.3	26.1
Superior (°)	93.1	95.4	96.4	98.4	93.1	93.1	93.1	93.1	93.1	93.1	92.8	92.6	92.6

3.4.2.2. Lateralisation of the sphere centre c. Simulations of a sphere with a more lateralised centre ($c > 0$, Fig. 4b) showed a great reduction of only inferior impingement (Table 2).

Joint force calculations were slightly affected. The deltoid moment arms were reduced by a small rate when c was increased. The latter caused an slight increased deltoid peak force and increased shear forces (e.g., for $c = 3$, deltoid moment arm decrease by 1.4 mm and average shear force increase by 3.1%).

4. Discussion

4.1. Moment arms, stability and loading

One of the most interesting results of the reverse geometry is how it affects the moment arms (and furthermore the function) of the muscles crossing the GH joint and especially the deltoid. The predicted results for the increased deltoid moment arms of this study agree well with the study of De Wilde et al. (2004) and Van der Helm (1998) where they used the same DELTA® geometry (Table 1). Terrier et al. (2007) using a similar type of prosthesis (Aequalis® Reversed Shoulder Prosthesis, Tornier) reports also a similar peak moment arm of 50.0 mm (Table 1).

The increased moment arm is due to the medialised centre of rotation which is now well offset from the axis of the humeral shaft. By increasing more this offset (e.g., by using either a thicker option cup or larger diameter sphere) the deltoid moment arm can be further increased in the early phase of abduction, but the peak values will be reduced, appear earlier and with a bigger drop after the peak. Geometrical characteristics of the prosthesis define the medialisation of the centre of rotation and its offset from the humeral shaft. In theory a reverse design can medialise the centre of rotation without medialising the humerus (large offset), but such a design can increase dramatically superior impingement.

In a normal shoulder, the RC muscles are arranged all around the superior half of the humeral head and are highly effective in directing the joint reaction force into the glenoid. The prime movers of the shoulder (deltoid, pectoralis major, latissimus dorsi) can also pull the humeral head into the glenoid cavity (Lee et al., 2000; Veeger and Van der Helm, 2007), but the action of these muscles can also result in large antagonistic moments that could lead to dislocating forces (Labriola et al., 2005). It is not surprising then that all the simulations of the normal anatomy with FTT failed to converge to a stable solution. Even if the model did not account for the large translations of the humeral head within the GH joint, which is typical in RC tear pathology (Ecklund et al., 2007), the fact highlights the main problem of instability where humeral migration and superior glenoid erosion are often observed in subjects suffering from chronic irreparable RC tears (Sirveaux et al., 2004). Van der Helm (1998) has also reported similar results for simulation of abduction in a FTT normal anatomy shoulder.

In the normal anatomy the deltoid shares the elevating load mostly with the supraspinatus. In the reverse model the elevating moment is produced by the deltoid action alone. The fact that the predicted deltoid forces are similar to the normal shoulder indicates that the reverse prosthesis provides the necessary moment arm to the deltoid to produce sufficient elevating moment compensating for the lack of the RC muscles. However, the resultant force is in a different direction from that in the normal shoulder since the deltoid pulling action is generating high superior shear forces on the glenoid. The antero-posterior shear forces are also increased, but the direction varies and depends on the plane of the elevation (Fig. 2). The compressive forces are reduced and, as a result, so are the total joint contact forces.

Terrier et al. (2008) predicted 50% total joint contact force reduction when compared a similar reverse prosthesis (in an FTT model) to an anatomical prosthetic shoulder (all RC muscles present) and simulating only scapula plane elevation. This value is close to the current study (40.9%, respectively – Fig. 2). There are differences, however, when comparing results with the PST model (supraspinatus only missing) where Terrier et al. report the impact of the RC muscles to the total joint contact forces. A comparison between the two models is difficult since the latter includes only a limited set of muscles and there is a difference in force prediction methodology. In the current study the large adducting moments of the RC muscles forced a solution where the cost function minimised their activation. This is the reason for the small differences between the results of FFT and the rest of the RC tear models. Different and more complex kinematic inputs can show different results, where the RC muscles can affect more the GH loading.

The results of this study also suggest that DELTA® III geometry restores the joint stability by reversing the envelope of the joint contact forces and by changing the critical articulating surface. The half-spherical glenoid fixation provides a large surface reacting to the increased shear forces. The critical stability region is now the area of the humeral cup where the depth determines the maximum dislocating shear force. The maximum allowable ratio of shear/compressive force in DELTA® is higher than an anatomical shoulder (typical value of 0.6 for the inferior/superior direction (Halder et al., 2001)). In addition, the humeral cup follows the direction of the deltoid force and the high shear forces are well constrained within the cup rim.

4.2. Impingement

Impingement and notching problems have been repeatedly reported for reverse prostheses (Boileau et al., 2006; Grammont and Baulot, 1993) and have been associated with clinical complications (Nyffeler et al., 2004) and glenoid loosening (Valenti et al., 2001). This study supports the concerns of impingement and predicts scapula notches that are very similar in volume and shape with notches that have been observed in cadaveric (Nyffeler et al., 2004) and radiographic studies (Simovitch et al., 2007 – Fig. 3).

The predicted range of motion without impingement agree well with the two dimensional study of De Wilde et al., 2004, where they report 76.3° in scapula plane elevation (80° for the same activity in this study), even if the numbers of inferior and superior impingement are slightly different. In a cadaveric study Nyffeler et al., 2005 reported impingement averaging a range of GH motion of 40.3° for three similar activities. Transforming the kinematics profile and fixation set-up to match the latter study (by excluding the scapulo-humeral rhythm (fixed scapula)), our model showed a close agreement of 41.8°.

Results showed that inferior glenoid fixation can reduce impingement but it is difficult to eliminate it completely, when the sphere was fixed within the reamed glenoid boundaries and without overstretching the deltoid. The absolute lengthening of the deltoid depends also on the physical size of the skeleton, but given the large size male skeleton used in this study deltoid over-stretching can be a potential problem of damaging the axillary nerve. A subject specific pre-operating planning could estimate deltoid lengthening and recommend optimum inferior fixation and prosthesis size.

Oblique glenoid osteotomy did not show great potential compared to the inferior fixation. More significantly, such a glenoid reaming can create a more difficult and narrower fixation surface as shown by Nyffeler et al. (2005) where inferior fixation becomes more difficult and the scapula border can be exposed under the sphere, creating a hinge mechanism for the humeral cup (dislocation concerns). The above clearly suggests that a face glenoid reaming will optimise the inferior fixation and thus reduce the

impingement. The fact has also been supported by Simovitch et al. (2007) who showed reduced notch volumes in scapulae with small progression border angle and face reaming.

Changing the geometry of the prosthesis and creating a very shallow cup is an attractive solution to impingement, but it can also affect the joint stability. A bigger h/R ratio effectively means a deeper cup depth for a given sphere and as a result a bigger shear to compressive ratio (more stable joint). In case of $h = R$ the ratio shear/compressive becomes infinite so that shear forces cannot dislocate the joint (constrained designs (Kessel and Bayley, 1979)). The standard activities simulated in this study can provide a good understanding of the biomechanics of the reverse prosthesis, but they cannot represent the full range of loading during activities of daily living. An optimum cup design should have the minimum possible depth where also providing sufficient stability to a wider range of motion that is expected to be performed by reverse prosthetic subjects (Kontaxis et al., 2007).

Changing the shape of the glenoid sphere by lateralising its centre ($c > 0$) was also a highly efficient way to reduce impingement. Even if this is an attractive solution, there are considerations of excess stresses created by the bending moments of the contact forces. Harman et al., 2005 tested a sphere with a 6 mm lateralised centre fixed on a polyurethane foam to find that the bending moment on the fixation was 69% greater than in the DELTA® III sphere (where $c = 0$) rising fixation strength considerations over long term fatigue.

5. Conclusions – stability over mobility

The results of this study showed the advantages of a reverse prosthesis, where the increased deltoid moment arm helps the muscle to elevate the arm compensating for the dysfunctional RC muscles. The prosthetic design also reverses the envelope of the forces providing a large glenoidal surface and stability to the increased shear forces.

The biomechanical model also confirms the impingement as the main problem on the reverse prosthesis and predicts scapular notches. The results show how the implantation can affect the impingement and suggest an optimum fixation inferiorly placed on a non oblique osteotomy. Anthropometric differences can affect the fixation, which is subjected to limitations of bone stock and maximum deltoid lengthening suggesting that pre-operating planning and guided implantation can help defining the optimum fixation.

The results show also that the impingement and the stability of the joint are antagonistic factors cancelling each other out when changing the prosthetic design parameters. The study has demonstrated how the design can affect the prosthesis function and in general results suggested that less impingement can also mean reduced joint stability or high fixation stresses. A solution to the problem is an optimisation of the design based on an objective function which can be related to the expected kinematics outcome of the joint replacement (e.g., realistic set of activities of daily living).

References

Barnett, N.D., Duncan, R.D.D., Johnson, G.R., 1999. The measurement of three dimensional scapulohumeral kinematics – a study of reliability. Clin. Biomech. 14, 287–290.

Boileau, P., Watkinson, D., Hatzidakis, A.M., Hovorka, I., 2006. Neer Award 2005: the Grammont reverse shoulder prosthesis: results in cuff tear arthritis, fracture sequelae, and revision arthroplasty. J. Shoulder Elbow Surg. 15 (5), 527–540.

Boileau, P., Watkinson, D.J., Hatzidakis, A.M., Balg, F., 2005. Grammont reverse prosthesis: design, rationale, and biomechanics. J. Shoulder Elbow Surg. 14 (1), 147S–161S (Suppl S).

Brostrom, L.A., Wallensten, R., Olsson, E., Anderson, D., 1992. The Kessel prosthesis in total shoulder arthroplasty. A five-year experience. Clin. Orthop. Relat. Res. 277, 155–160.

Charlton, I.W., Johnson, G.R., 2006. A model for the prediction of the forces at the glenohumeral joint. Proc. Inst. Mech. Eng. 220 (8), 801–812.

De Wilde, L.F., Audenaert, E.A., Berghs, B.M., 2004. Shoulder prostheses treating cuff tear arthropathy: a comparative biomechanical study. J. Orthop. Res. 22 (6), 1222–1230.

DePuy. DELTA CTA Reverse Shoulder Prosthesis [9072-78-032], 2005. Ref Type: Catalog.

Ecklund, K.J., Lee, T.Q., Tibone, J., Gupta, R., 2007. Rotator cuff tear arthropathy. J. Am. Acad. Orthop. Surg. 15 (6), 340–349.

Grammont, P.M., Trouilloud, P., Laffay, J.P., Deries, X., 1987. Etude et réalisation d'une nouvelle prosthèse d' épaule. Rhumatologie 39, 407–418.

Grammont, P.M., Baulot, E., 1993. Delta shoulder prosthesis for rotator cuff rupture. Orthopedics 16 (1), 65–68.

Grant, G.A., Goodkin, R., Kliot, M., 1999. Evaluation and surgical management of peripheral nerve problems. Neurosurgery 44 (4), 825–839.

Halder, A.M., Kuhl, S.G., Zobitz, M.E., Larson, D., An, K.N., 2001. Effects of the glenoid labrum and glenohumeral abduction on stability of the shoulder joint through concavity-compression: an in vitro study. J. Bone Joint Surg. Am. 83-A (7), 1062–1069.

Harman, M., Frankle, M., Vasey, M., Banks, S., 2005. Initial glenoid component fixation in "reverse" total shoulder arthroplasty: a biomechanical evaluation. J. Shoulder Elbow Surg. 14 (1), 162S–167S (Suppl. S).

Jensen, K.L., Williams Jr., G.R., Russell, I.J., Rockwood Jr., C.A., 1999. Rotator cuff tear arthropathy. J. Bone Joint Surg. Am. 81 (9), 312–1324.

Kessel, L., Bayley, I., 1979. Prosthetic replacement of shoulder joint: preliminary communication. J. Roy. Soc. Med. 72 (10), 748–752.

Kontaxis, A., Banerjee, S., Bull, M.J.A., Johnson, G., 2007. Kinematics performance on activities of daily living after reverse shoulder joint replacement, in XXI ISB Congress. J. Biomech. 40 (Suppl. 2), S108.

Labriola, J.E., Lee, T.Q., Debski, R.E., McMahon, P.J., 2005. Stability and instability of the glenohumeral joint: the role of shoulder muscles. J. Shoulder Elbow Surg. 14 (1), 32S–38S (Suppl. S).

Lee, S.B., Kim, K.J., O'Driscoll, S.W., Morrey, B.F., An, K.N., 2000. Dynamic glenohumeral stability provided by the rotator cuff muscles in the mid-range and end-range of motion. A study in cadavera. J. Bone Joint Surg. Am. 82 (6), 849–857.

Marchese, S.S., Johnson, G.R., 2000. Measuring the kinematics of the clavicle, in 6th International Symposium of the 3D Analysis of Human motion, Cape Town, pp. 37–40.

Neer, C.S., Watson, K.C., Stanton, F.J., 1982. Recent experience in total shoulder replacement. J. Bone Joint Surg. Am. 64 (3), 319–337.

Nyffeler, R.W., Werner, C.M., Gerber, C., 2005. Biomechanical relevance of glenoid component positioning in the reverse Delta III total shoulder prosthesis. J. Shoulder Elbow Surg. 14 (5), 524–528.

Nyffeler, R.W., Werner, C.M., Simmen, B.R., Gerber, C., 2004. Analysis of a retrieved delta III total shoulder prosthesis. J. Bone Joint Surg. Br. 86 (8), 1187–1191.

Post, M., Haskell, S.S., Jablon, M., 1980. Total shoulder replacement with a constrained prosthesis. J. Bone Joint Surg. Am. 62 (3), 327–335.

Simovitch, R.W., Zumstein, M.A., Lohri, E., Helmy, N., Gerber, C., 2007. Predictors of scapular notching in patients managed with the Delta III reverse total shoulder replacement. J. Bone Joint Surg. Am. 89 (3), 588–600.

Sirveaux, F., Favard, L., Oudet, D., Huquet, D., Walch, G., Mole, D., 2004. Grammont inverted total shoulder arthroplasty in the treatment of glenohumeral osteoarthritis with massive rupture of the cuff. Results of a multicentre study of 80 shoulders. J. Bone Joint Surg. Br. 86 (3), 388–395.

Spitzer, V.M., Whitlock, D.G., 1998. The visible human dataset: the anatomical platform for human simulation. Anat. Rec. 253 (2), 49–57.

Terrier, A., Reist, A., Merlini, F., Farron, A., 2007. Joint and muscle forces in reverse and anatomical shoulder prosthesis, in XXI ISB Congress. J. Biomech. 40 (Suppl. 2), S146.

Terrier, A., Reist, A., Merlini, F., Farron, A., 2008. Simulated joint and muscle forces in reversed and anatomic shoulder prostheses. J. Bone Joint Surg. Br. 90 (6), 751–756.

Valenti, P., Boutens, D., Nerot, C., 2001. DELTA III reversed prosthesis for osteoarthritis with massive rotator cuff tear: long term results (>5 years). In: Walch, G., Mole, D. (Eds.), 2000 Shoulder Prosthesis...2–10 Year Follow-up. Springer, Berlin, pp. 253–259.

Van der Helm, F.C., 1998. The 'reversed' glenohumeral endoprosthesis. J. Biomech. 31 (Suppl. 1), 27.

Veeger, H.E., van der Helm, F.C., 2007. Shoulder function: the perfect compromise between mobility and stability. J. Biomech. 40 (10), 2119–2129.

Woodruff, M.J., Cohen, A.P., Bradley, J.G., 2003. Arthroplasty of the shoulder in rheumatoid arthritis with rotator cuff dysfunction. Int. Orthop. 27 (1), 7–10.

Computer Methods in Biomechanics and Biomedical Engineering,
Vol. 11, No. 1, February 2008, 73–80

Taylor & Francis
Taylor & Francis Group

Adaptation of scapula lateral rotation after reverse anatomy shoulder replacement

ANDREAS KONTAXIS* and GARTH R. JOHNSON

Centre for Rehabilitation and Engineering Studies (CREST), Mechanical and Systems Engineering, Stephenson Building, Newcastle University, Newcastle upon Tyne NE1 7RU, UK

Scapula motion is significant for support of the arm and stability of the shoulder. The effect of the humeral elevation on scapular kinematics has been well investigated for normal subjects, but there are limited published studies investigating adaptations after shoulder arthroplasty.

Scapula kinematics was measured on 10 shoulders (eight subjects) with a reverse total joint replacement. The measurements were performed using an instrumented palpating technique. Every subject performed three simple tasks: abduction, elevation in scapula plane and forward flexion.

Results indicate that, lateral scapula rotation was significantly increased (average of 24.42% over the normal rhythm) but the change was variable. Despite the variability, there is a clear trend correlating humeral performance with increased rotation (R^2 0.829).

There is clearly an adaptation in lateral scapula rotation in patients with shoulder joint replacement. The reason for this is unclear and may be related to joint pathology or to muscle adaptation following arthroplasty.

Keywords: Scapula; Palpating; Reverse joint replacement

1. Introduction

The large range of available motion of the human arm is a result of the combined motion of the humerus, scapula and clavicle. In order to understand the detailed nature of this complex motion of the shoulder mechanism, there have been numerous studies of the scapula motion of normal subjects. The early two-dimensional radiographic studies of scapula plane abduction (Inman *et al.* 1944, Freedman and Munro 1966) identified, largely linear relationships between scapula and humeral abduction angles. In a second study, Poppen and Walker (1976) examined the scapula motion of a further group of normal subjects, together with patients having a variety of shoulder pathologies. For the normal subjects, they found a ratio between total arm abduction and the angle of the scapula of 5:4 (Walker and Poppen 1977); the equivalent ratio of the patient group was widely variable with a tendency for a smaller glenohumeral contribution to arm abduction, thus raising the question as to how scapula motion may be affected by shoulder pathology.

The complex 3D movement of scapula is difficult to measure from two-dimensional studies and de Groot (1999) showed that the range of results reported from radiographic studies could be explained by the variability in radiographic alignment. In order to meet the requirements and to measure the complex scapula motion, palpation techniques were developed. First, Pronk and van der Helm (1991) showed an instrumented three dimensional palpator, which was used to determine the positions of bony landmarks of the arm, trunk and scapula, thus enabling calculation of the scapulothoracic and glenohumeral angles. Johnson *et al.* (1993) proposed the use of a palpation fixture having three palpation points connected to a rigid frame in an attempt to develop a more convenient technique for clinical use. The relative positions of the frame, arm and thorax were measured using an electromagnetic movement measurement system. In a subsequent study, (Barnett *et al.* 1999), the technique was shown to be reliable and repeatable. A similar method has been used by Meskers *et al.* (1998), who further demonstrated its reliability.

Over the last decade, reverse anatomy shoulder replacements have become increasingly popular, particularly for patients with rotator cuff arthropathy. Outcome studies of these patients demonstrate that while there is an impressive

*Corresponding author. Email: andreas.kontaxis@ncl.ac.uk

Computer Methods in Biomechanics and Biomedical Engineering
ISSN 1025-5842 print/ISSN 1476-8259 online © 2008 Taylor & Francis
http://www.tandf.co.uk/journals
DOI: 10.1080/10255840701552069

improvement in function (particularly elevation), complications can arise from inferior impingement between polyethylene and scapula bone leading, in some cases, to loosening of the prosthesis (Sirveaux *et al.* 2004, Kontaxis and Johnson 2005a). A full understanding of the function of these prostheses calls for a combination of biomechanical modelling and functional studies. Therefore, as a contribution to this understanding, particularly impingement, there is a need to measure the accompanying motion of the scapula and the aim of this paper is to investigate and report any changes of the 3D scapula movements of these patients measured by the palpation technique.

2. Materials and methods

2.1 Experimental set-up

Measurements were made, using a published technique (Johnson *et al.* 1993), previously used in a study of scapula kinematics of young healthy shoulders (Barnett *et al.* 1996). The experimental set-up uses the Isotrak II™ (Polhemus Navigation, USA), a six degree of freedom electromagnetic movement sensor, consisting of an electromagnetic source producing low-frequency waves received by a 3-axis sensor; both source and sensor are hardwire connected to an electronics base unit, which can communicate with a computer through a serial connections.

In order to measure scapula movement, a special custom-designed fixture was used together with the electromagnetic device—the Locator. The Locator has legs, specially designed to enable repeatable positioning over the most palpable bony landmarks of the scapula (Johnson *et al.* 1993, figure 1a) as follows: (i) the posterior angle of the acromion, (ii) the root of the scapula spine and (iii) the inferior angle. The palpating legs could be adjusted along slots on the base plate in order to match and have the best possible contact with the bony landmarks. According to this arrangement, the axes of the electromagnetic source of the Isotrak system were aligned with the plane defined by the three contact points of the scapula landmarks.

The spatial position of the Locator was determined by the transmitter of the Isotrak II™ system. One of the receivers was mounted on an adjustable support and taped over the manubrium sterni using a mount, which allowed the sternal receiver to be mounted vertically with respect to the global (laboratory) frame indicated by a bubble level. When direct measurement of arm position was required, a second receiver was fixed to the arm using a moulded polythene arm splint having the elbow fixed at 90° (figure 1c). The purpose of the flexed elbow was to distinguish clearly between forearm prono/supination and humeral internal external rotation. Custom software was developed to determine the position of the arm in the frame of the receiver mounted on the sternum. This was then displayed, as a real time feedback in terms of the azimuth, elevation and roll (or latitude, longitude and bearing) of the humerus.

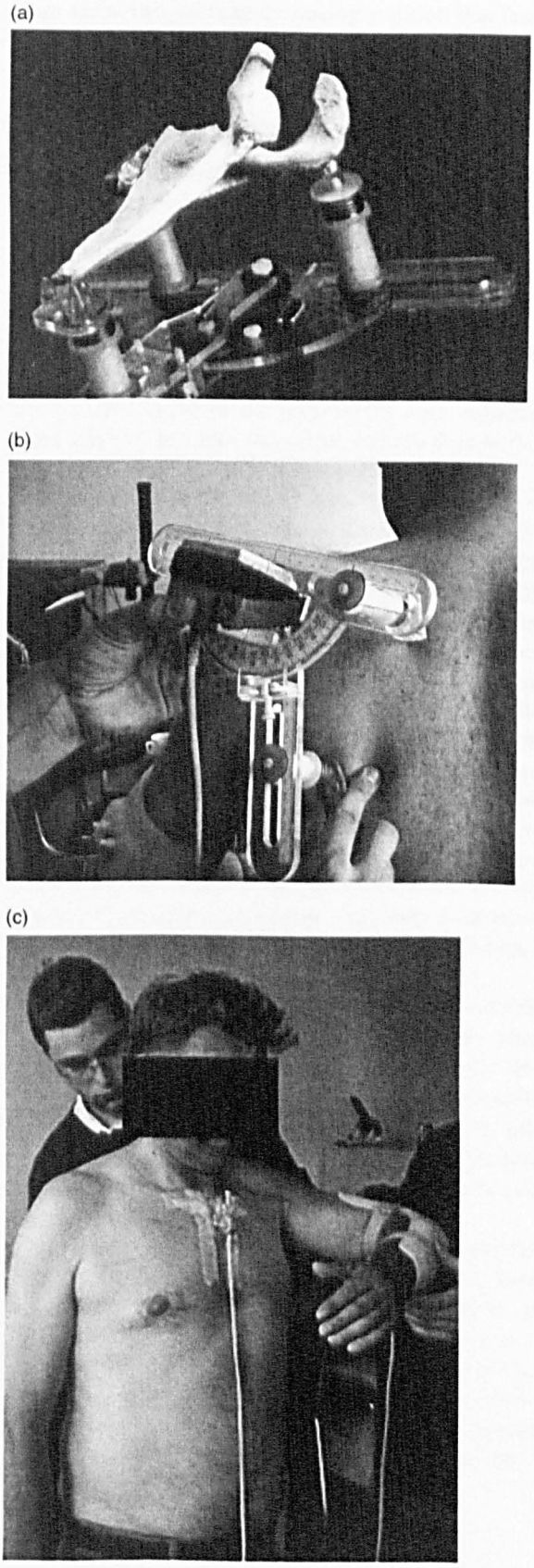

Figure 1. (a) The scapula palpator is adjustable and specially designed in order to locate the most palpable landmarks of scapula. (b) The data can be recorded in static humeral positions and after palpating and locating the position of the scapula anatomical landmarks. (c) An elbow splint was used in order to avoid confusion between humeral rotation and forearm pro/supination.

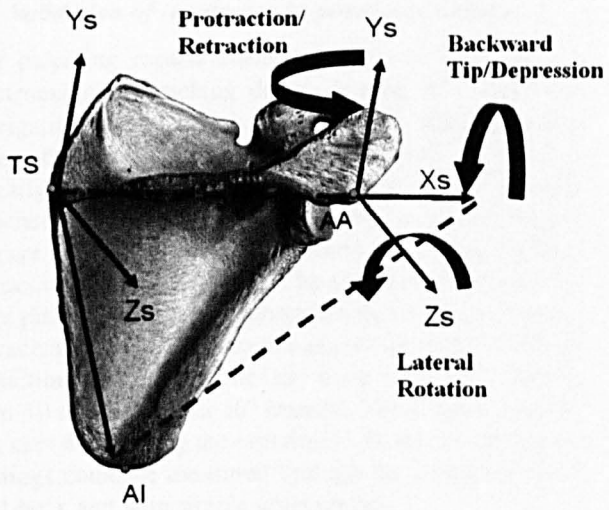

Figure 2. The definition of the scapula frame according to the anatomical landmarks. The scapula rotations are modelled as rotations around the anatomical axis of the embedded anatomical coordinate frame.

2.2 Kinematics and scapula rotation definition, measurement and task protocol

The arbitrary axes of the scapula were defined by the locator and the magnetic tracking device and converted to anatomically appropriate embedded scapula axes (figure 2). In contrast with the studies of De Groot and Karduna, the thoracic and humeral frames were defined with the help of the alignment of the bubble level and the elbow splint (Barnett *et al.* 1996), instead of digitising extra anatomical landmarks.

The directional sine and cosine of the transmitter and the receivers were recorded during the measurements, and standard matrix transformation methods were used to determine the rotation matrix of the humerus and scapula, with respect to the thorax (van der Helm and Pronk 1995). Humeral rotations were represented using a standard Euler angle sequence in which the first rotation defined the plane of elevation (azimuth), the second rotation described the amount of elevation and the last rotation represented the amount of internal/external rotation (table 1, van der Helm 1996). Scapula rotations were represented using an Euler angle sequence of scapula protraction (around *Y*), Lateral Rotation (around *Z*) and Backward tip (around *X*) (figure 2). The scapula rotations were recorded with respect to the thorax, but were post processed and finally analysed in the local scapula co-ordinate system with the arm in the resting position. This is an effective way to minimise the affect of the anthropometric differences between the subjects (Barnett *et al.* 1996) and exclude the large variability of scapula resting position that has been recorded even within the normal population (Pronk 1991).

2.3 Data collection and task protocol

A total of three tasks were studied: (1) Elevation of the arm in the frontal plane, starting from 10° and up to the maximum possible, (2) elevation of the arm in the scapula plane (40° of azimuth) starting again from 10° and up to the maximum possible (3) forward flexion of the arm, starting from 10° and up to the maximum possible. Data were collected at 20° increments from the starting position. As the maximum arm elevation of each subject was variable, more points (every 10°) were collected for some subjects in order to collect enough data within the functional range of the arm movement.

In contrast with the dynamic recording activities of the latest scapula kinematics studies (Karduna *et al.* 2001), due to the nature of the palpating technique, the recordings of the scapula position were taken in discrete static positions. The subject elevated the arm in increments of approximately 20° up to the maximum; the exact position was evaluated each time by the visible feedback of the humeral position on the computer screen. Prior to collecting data for each motion, several practice trials were performed. The investigator could monitor real-time humeral motion, which was displayed on a computer screen, and provided the subject with feedback. The subject was instructed to maintain a forward gaze and not to look either at their arm or the computer screen during the experiment. As with the practice trials, the investigator was able to monitor the humeral motion pattern during the data collection and give feedback for correct humeral position.

Data were collected for eight subjects: 10 shoulders in total. All the subjects had a reverse total shoulder replacement (DELTA® III) for more than 1 year and the average age was 67.7 (SD 13.5). There were four male and four female subjects and 4 out of 10 shoulders suffered from osteoarthritis, two from rheumatoid arthritis and four subjects from tumour in the humeral head. All the subjects were right handed.

The measurements took place in a clinical environment (Ravenscourt Park Hospital, Ravenscourt Park, London) with the presence of an orthopaedic surgeon and a chaperone (when necessary). All the subjects were previously informed of the measurement procedures and agreed to participate on the study, by a formal letter sent prior to them, as it was described in the documentation of the ethical application, which was approved by the local ethical committee.

Table 1. The rotation sequence of the humeral and scapula motion with respect to the thoracic frame and the corresponding clinical terminology.

Segment	Rotation sequence	Rotation terminology (in order specified)		
Scapula	Y, Z', X''	Scapula protraction	Scapula lateral rotation	Scapula backward tip
Humerus	Y, Z', Y''	Humeral azimuth	Humeral elevation	Humeral internal rotation

2.4 Validation of the device in prosthetic subjects

The palpating measurement technique is based on, an electromagnetic tracking device Isotrak II™ (Polhemus Navigation, USA) and is validated for scapulohumeral kinematic measurements in healthy subjects. In order to investigate whether there is an influence of the metallic prosthesis in the joint replacement subjects, a simple plastic linkage of 1 DOF was constructed simulating humeral abduction or forward flexion. The receivers and transmitter were placed in similar position to a subject set-up (defining thoracical, humeral and scapula plane), and simple tasks of abduction and forward flexion were simulated, starting from 10 to 120° with a 10° interval. The scapula palpator was kept fixed during the experiment. Humeral and scapula readings could be measured through the computer visual feed-back and with simple goniometers.

The two tests of abduction and forward flexion, were repeated at five different fixed positions of the palpator and with and without the presence of a real DELTA® III reverse prosthesis attached to the plastic linkage.

3. Results

3.1 Sensitivity test

The sensitivity tests for the influence of the metallic prosthesis in the experimental set-up, showed that, the DELTA® III does not affect the recorded output of the electromagnetic device. The differences in the recorded outputs of humeral and scapula angles, with or without the prosthesis, in all 10 recorded activities (five abductions and five forward flexion with different fixed palpator position) showed that, there was not a significant difference ($p > 0.05$ with $a = 0.95$, original hypothesis H_0: average of differences between models with and without the prosthesis = 0).

3.2 Subject studies

All the subjects were able to complete all three activities, but the maximum arm elevation within the activities, and within the subjects were very variable. The lowest average value was for abduction with 95.81° (SD 8.01°) and the highest for forward flexion with 119.07° (SD 15.2°); the average elevation for scapula plane was 103° (SD 7.14°). All the maximum values of the lateral scapula rotation for each subject and for every activity were greater than, the expected healthy scapula rhythm (Barnett *et al.* 1999) (figure 3). The average maximum lateral rotation was 49.57° (SD 4.92°), 50.57° (SD 2.58°), 52.98° (SD 4.96°) for abduction, scapula plane and forward flexion respectively. The corresponding values for the other two scapula rotations (backward tip and retraction/protraction) were much smaller and even if the averages were different from the normal scapulothoracic rhythm were within the 95% predictive intervals (PI) of the generic model for healthy shoulders. Due to the uncertainty of the results in the above two rotations, this study focuses only on lateral rotation of the scapula.

3.3 Regression analysis

All the data were analysed in the local scapula frame of the resting position. In this way, it was possible to minimise the effect of anthropometric differences and investigate the scapula rotation from its resting position and for a certain arm elevation. Due to the variability of the maximum arm elevation within the subjects and within the three different activities, a comparison of average and maximum scapula rotation values could lead to wrong conclusions. For this reason, the differences of the scapula lateral rotation have been calculated between the collected data and the corresponding predicted value for normal scapulothoracic rhythm (equation (1), Barnett *et al.* 1996):

$$\begin{aligned}\alpha = &-0.0275a + 9.74\times10^{-5}a^2 \\ &+ 0.3866e - 6.48\times10^{-4}e^2 \\ &+ 0.0171r - 1.06\times10^{-4}r^2 - 3.8184 \end{aligned} \quad (1)$$

where α, scapula lateral rotation; a, arm azimuth; e, arm elevation and r, arm rotation.

In order to investigate the differences and define the changes in the scapulohumeral kinematics, a regression analysis was performed in the calculated data. A linear and a quadratic model have both been analysed:

$$\alpha' = \beta e + c \quad (2)$$

$$\alpha' = \beta_1' e - \beta_2' e^2 + c' \quad (3)$$

where, α', difference in lateral rotation; β, β_i', linear and quadratic coefficients and c, c', constants.

The regression analysis showed good correlation for both linear and quadratic models. The average R^2 values for all the subjects and all the activities were 0.989 (SD 0.009) and 0.972 (SD 0.026) for the quadratic and linear models, respectively. Since the correlation factor does not necessarily indicate the accuracy of the model, an analysis of the 95% of the confidence intervals (CI) of the errors (residuals) was also performed. For each activity and each model, the difference of the lateral rotation between normal and prosthetic shoulder was calculated from the recorded arm position. Then, the error calculated between the predicted values (from the linear and quadratic models) and the recorded differences. The 95% CI were calculated from the formula:

$$\mathrm{CI} = c_a \mathrm{SD}_i \sqrt{\frac{1}{n_i}}\bigg|_{a=0.95} \quad (4)$$

where SD_i, standard deviation of the ith sample; n_i, number of the data of the ith sample; c_a, constant for level confidence a ($c = 1.96$ for $a = 0.95$).

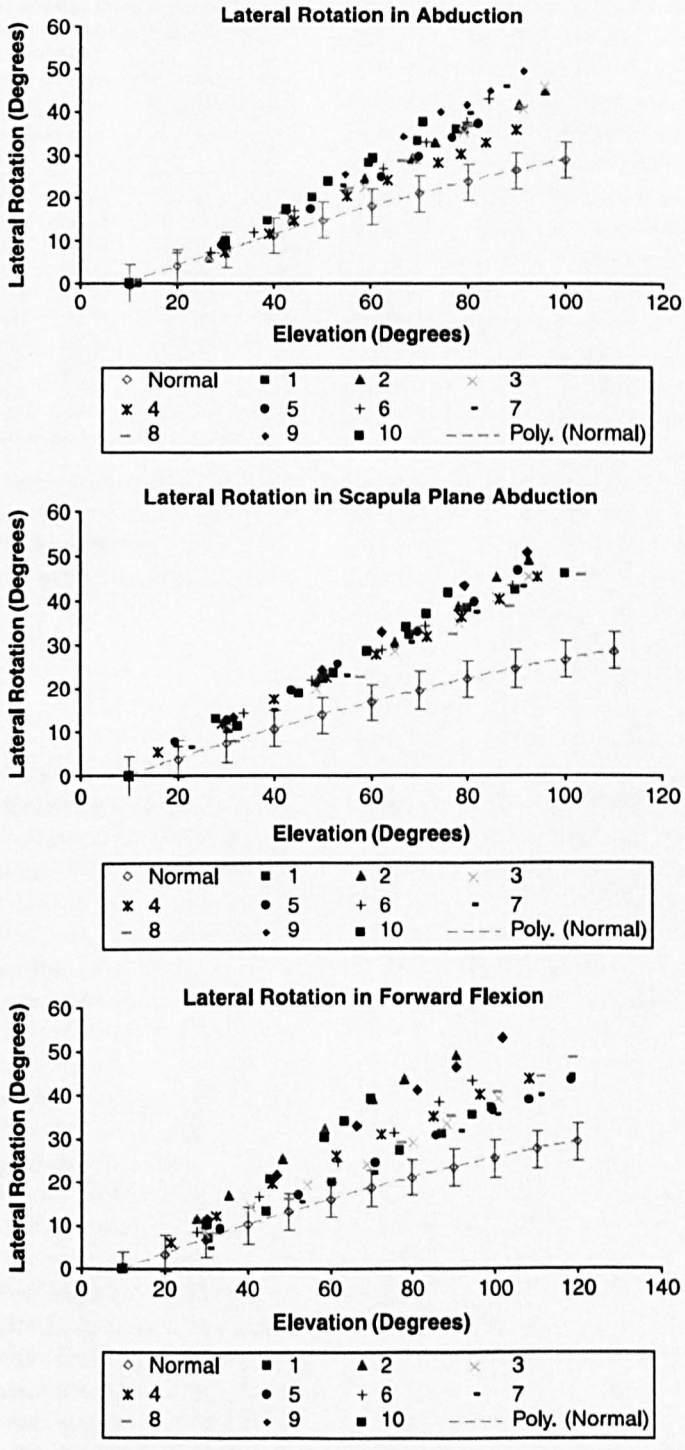

Figure 3. Recorded data of lateral scapula rotation compared with the predicted lateral of a healthy scapula rhythm (Barnett *et al.* 1996) (a) abduction, (b) scapula plane, (c) forward flexion.

All the 95% CI for each subject and for each activity are presented in table 3.

The results show that an increase in the order of the model does not affect the 95% CI for most of the subjects. Only the models of the subjects three and nine showed inconsistencies within the three activities with the 95% CI being significantly smaller in the quadratic models.

The linear coefficients of the linear models in table 2, represent the increase of the scapula lateral rotation in a reverse prosthetic shoulder in comparison to the healthy population. The average values of coefficient for abduction, scapula plane and forward flexion were 0.261 (0.055), 0.257 (0.058), 0.215 (0.111), respectively. The maximum and minimum values were observed within the subjects performing forward flexion, an activity that shows the biggest variability within the linear coefficients (min 0.105, max 0.440). The overall average of all the coefficients was 0.244 but the SD was high (0.079). Four of the subjects showed a similar increase in lateral rotation (SD 0.245) during the three activities, three subjects

Table 2. The constant and the linear coefficient of each subject in every activity of the linear models that describe the increase of lateral rotation in a prosthetic shoulder.

	Abduction		Scapula plane		Forward flexion	
Subjects	*c*	*β*	*c*	*β*	*c*	*β*
1	−4.525	0.251	−0.372	0.206	−2.124	0.165
2	−3.392	0.250	−5.054	0.241	−3.317	0.327
3	−3.580	0.244	−3.290	0.227	−1.879	0.105
4	−0.013	0.189	−0.736	0.209	0.001	0.160
5	−2.348	0.243	−2.326	0.273	−2.504	0.124
6	−3.425	0.273	−1.556	0.233	−2.560	0.209
7	−3.347	0.295	−3.336	0.233	−1.649	0.120
8	−1.197	0.183	−3.298	0.221	−2.601	0.177
9	−3.711	0.330	−1.470	0.368	−0.576	0.322
10	−3.024	0.355	−4.799	0.355	−4.155	0.440

showed a small difference in one of the activities (SD 0.453) and three more subjects, indicated a much larger scapula adaptation within the three activities (SD 0.801). The last group includes the subjects that, the linear model shows large 95% CI.

4. Discussion

With the recent development of sophisticated 3D shoulder models (van der Helm 1994, Charlton and Johnson 2006), accurate description of scapula motion on the thoracic cage is of great importance. Since the scapulothoracic rhythm can affect the stability and loading of the shoulder, customisation of models with patient specific scapula kinematics is necessary when investigating shoulder pathologies.

Evidence exists that adaptation to scapula motion is related to shoulder pathology (Johnson *et al.* 2001). There are studies based mainly on, medical imaging or electromagnetic palpating tracking devices, correlating the change in scapulohumeral kinematics with specific shoulder pathology like impingement or rotator cuff tears (Lukasiewicz *et al.* 1999, Mell *et al.* 2005, Hallstrom and Karrholm 2006). The results always report a statistical significance in the change of the scapula motion, when compared to normal scapula rhythm, but the results also indicate large variability within the pathological shoulders.

In this study, a static palpation method that has been shown to produce reliable measurements was used to record possible changes on the scapula rhythm after reverse total shoulder arthroplasty. A disadvantage of the palpation approach is the near impossibility of making dynamic measurements of the scapula moving beneath the skin. To overcome this limitation, Karduna *et al.* (2001) have made measurements using an electromagnetic sensor attached to the skin overlying the acromion. Since, then several studies replicated this method to investigate scapula kinematics in healthy or pathological shoulders (Mell *et al.* 2005, McClure *et al.* 2006). However, a recent study by Meskers *et al.* (2005) suggests that there is a deviation on the recorded scapula rotations between the dynamic and the static (palpating) techniques, especially during the higher degrees of arm elevation.

The prosthetic shoulders examined in this study were treated with DELTA® III reverse shoulder prosthesis. This specific design is a popular solution for patients suffering from a full thickness Rotator Cuff tear. Using the dynamic measurement technique described by Karduna *et al.* (2001), Meskers *et al.* (2005), have recently published a study, comparing scapula kinematics of a group of healthy shoulders with a series of 14 shoulders suffering from rotator cuff tears. In this study, the subjects had a smaller average humeral elevation (85.6°) but the average lateral scapula rotation was increased by a similar amount (linear coefficient of increased scapula rotation: 0.21–0.16 for phase 1 and 2, respectively). In the same study, the authors also reported that the change in the other two scapula rotations had no statistical significance from the healthy group.

There are limited published data for scapula kinematics in patients after total shoulder replacement. A study, from de Wilde *et al.* (2005), used the palpation method of Johnson *et al.* (1993) to evaluate the functional recovery of prosthetic patients using reverse shoulder prosthesis. The study, is using scapulohumeral data to describe only the lateral rotation of the scapula during scapula plane elevation and calculate muscle moment arms. A group of four patients was reported to show an average increased scapula lateral rotation of 118% compared to healthy shoulders. This value is lower than the average value for scapula plane elevation found in this study (125.7%), but the small number of the sample limits further statistical analysis.

The results of the regression analysis show that the differences calculated from the increased scapula rotation and the normal scapula rhythm can be described with a linear relationship. This is in contrast with the study of Mell *et al.* (2005), who reported a 3-phase scapula rhythm change in patients with rotator cuff tears. The fact can be justified by the difference of the shoulder pathology, but they may also reflect differences between the measurement

Table 3. 95% Confidence intervals of the residuals for the quadratic and linear model.

	1	2	3	4	5	6	7	8	9	10
Quadratic model										
Abduction	0.705	0.200	0.620	0.575	0.481	0.642	0.670	0.818	0.219	0.582
Scapula plane	0.671	1.232	0.532	0.654	0.405	0.364	0.381	0.329	0.426	0.349
Forward flexion	0.321	0.294	1.383	0.282	0.543	0.603	0.400	0.539	0.710	0.711
Linear model										
Abduction	0.851	0.446	1.008	0.429	0.523	0.890	0.894	0.727	0.254	0.573
Scapula plane	0.810	1.507	0.988	0.681	0.455	0.367	0.540	0.637	1.263	0.685
Forward flexion	0.483	0.336	1.200	0.554	0.480	0.847	0.701	0.412	1.189	0.322

techniques followed in the studies (static-palpating and the dynamic). Even if results from Mell show a good correlation with this study in phase-1 (early degrees of arm elevation), they also indicate a smaller increase of scapula rotation during phase-2 and a match to the normal scapula rhythm in the last phase-3 (the higher part of humeral elevation). In contrast, the results of this study indicate a linear increase of scapula rotation throughout the range of humeral elevation. This is in agreement with the findings of Meskers *et al.* (2005), which indicates possible differences of scapula rotation for the dynamic and palpating measurement method, especially during high values of humeral elevation. Also Karduna *et al.* (2001) reports that the dynamic measurements of the scapula with a single sensor attached on the acromion site can be affected by the anthropometric differences and especially the soft tissue and fat concentration around the sensor attachment point.

The results from the residual analysis indicate that a linear fit of the calculated differences provides a good correlation. For most of the subjects, an increase of the order to a quadratic model does not decrease significantly, the 95% CI of the residuals. However, for some subjects, (subjects three and nine) the R^2 values and the 95% CI indicate that, the rotation of the scapula does not have a linear increase compared to the normal rhythm. By analysing further the specific data, it becomes clear that lateral rotation has two phases in which, the rate of lateral rotation is seen to increase above an abduction of 40°. The mechanism for this different change is not clear but it maybe a result of impingement. It is recently reported in clinical reviews that patients with DELTA® III reverse prosthesis may develop notches on the inferior part of the scapula border (Sirveaux *et al.* 2004) and Kontaxis and Johnson (2005a) have shown that this may be related to contact of the polyethylene cup of the prosthesis with the scapula bone (impingement). In the later study, an adapted 3D shoulder model was used (Newcastle shoulder model, Charlton and Johnson (2006)) to simulate impingement of the DELTA® reverse prosthesis during humeral elevation. The study clearly indicates impingement during standard activities and contact of the polyethylene cup can be observed as high as from 50° of abduction and downwards. The impingement mechanism and the contact forces between the polyethylene cup and the scapula border could contribute to the scapula kinematics adaptation.

It is difficult to compare directly the recorded data of the increased scapula lateral rotation within the subjects of the group. The maximum rotation (52.98 ± 2.51°) was observed at 102.98 ± 2.12° of forward flexion, which was not the maximum arm elevation (119.07 ± 2.12°) for that subject. Since the maximum arm elevation for each subject and each activity is different, the linear coefficient of the differences between the recorded values and the expected normal scapula rhythm is a better indication of the adaptation (increase) of the scapula rotation. This coefficient actually shows a decrease in the GH joint rotation indicating joint stiffness after the joint replacement. However, it should be remembered that the values of all the coefficients of this study are highly variable. A second regression analysis with the modelled values was performed in an attempt to create a generic model that describes the increased scapula rotation. The mean coefficient was 0.220 with a poor correlation (R^2 0.633), but an error analysis showed that, the 95% of the predictive intervals for the estimated error are large (9.490°). This means that the margins of the predictive increased rotation include the region of the predictive normal rhythm.

Since there are studies indicating that adaptation to scapula motion is related to shoulder pathologies (Lukasiewicz *et al.* 1999, Johnson *et al.* 2001, Mell *et al.* 2005, Hallstrom and Karrholm 2006) a further analysis of the data was performed to show if there is any correlation of the increased lateral rotation with the sex, age or shoulder pathology of the group. A factorial analysis of the variance of the sample did not reveal any significant trend since, in fact, the size of the sample is rather small ($n = 10$). A similar study, with more subjects could be more conclusive.

Even though, there was a large variability within the results, there was a correlation between maximum arm elevation and the recorded scapula rotation. From the linear correlation of the scapula differences it seems that the lower the maximum achieved elevation the larger the scapula rotation increase (larger coefficient). The graph in figure 4 shows the correlation of the mean "linear coefficient" of each subject (for all three activities) with the corresponding mean "maximum achieved humeral elevation" during the recorded activities. The original correlation factor for all the subjects is not strong (R^2 0.573). Investigating the correlation further, the residuals of each point (to the linear regression) in figure 4 were

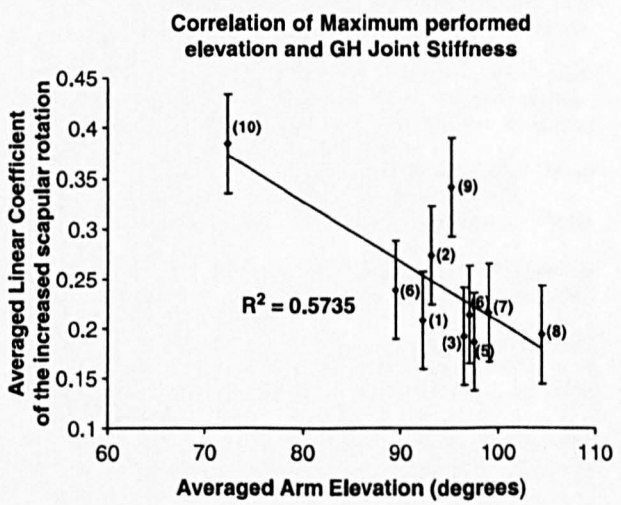

Figure 4. There is a correlation between the averaged maximum performed elevation and the averaged linear coefficient of the increased scapula rotation that represents GH joint stiffness. The correlation is not strong (0.5735) but one of the points (subject nine) has larger residuals from the rest of the points and can be excluded (by applying the Chauvenet's Criterion). By excluding subject no.9 the correlation is increased dramatically to 0.8285 (Numbers in brackets = Number of Subject, error bars = 2 × SD).

calculated. A Kolmogorov–Smirnov normality test showed that, the residual data are normal ($p = 0.150 > 0.05$, H_0: Sample is normal), but one of the residuals of the sample is significantly larger than the mean (subject no. 9). The probability of this residual to be in the normal distribution (mean $x = -0.0016$, SD $= 0.0441$) is very small ($\Phi - 2.37 = 0.0089$) and therefore, by applying the Chauvenet's criterion it can be excluded from the sample. This is not a surprise, if we consider that the linear model of subject nine had the largest 95% CI of the residual errors of the recorded scapula rotations. The re-calculated correlation of figure 4, excluding subject nine, is increased dramatically to 0.829.

5. Conclusions

The results of this study clearly indicate that, there is increased lateral scapula rotation in patients with reverse shoulder arthroplasty compared to healthy shoulders. However, the increase is highly variable within the subjects making it difficult to create a generic model. For this reason, detailed customisation of biomechanical shoulder models with patient specific scapula rhythm should be considered in the case of biomechanical analysis of reverse prosthesis, since the kinematics adaptation can increase the shear contact forces on the glenoid site by 19% (Kontaxis and Johnson 2005b).

It is difficult to explain the reason behind the adaptation, since there is no clear indication, which can correlate the increase of the scapula rotation (e.g. pathology, sex or age) with the recorded data. However, there is a strong trend showing that patients with good recovery and large range of humeral elevation after the surgery have small change in their scapula rhythm whereas those with muscle weakness and small range of movement minimise the glenohumeral rotation and have large scapula rotation. A pre and post operative study of scapula kinematics with a large number of subjects would be required to give a clear indication, whether the adaptation is influenced by the joint replacement and rehabilitation process or is connected only with shoulder pathology (Mell *et al.* 2005).

References

N.D. Barnett, M. Mander, J.C. Peacock, K. Bushby, D. Gardner-Medwin and G.R. Johnson, "Winging of the scapula: the underlying biomechanics and an orthotic solution", *J. Eng. Med. [H]*, 209, pp. 215–223, 1996.

N.D. Barnett, R.D.D. Duncan and G.R. Johnson, "The measurement of three dimensional scapulohumeral kinematics—a study of reliability", *Clin. Biomech.*, 14, pp. 287–290, 1999.

I.W. Charlton and G.R. Johnson, "A model for the prediction of the forces at the glenohumeral joint", *J. Eng. Med. [H]*, 220, pp. 801–812, 2006.

L. Freedman and R.R. Munro, "Abduction of the arm in the scapular plane: scapular and glenohumeral movements", *J. Bone Joint Surg.*, 48-A, pp. 1503–1510, 1966.

J.H. de Groot, "The scapulo-humeral rhythm: effects of 2-D roentgen projection", *Clin. Biomech. (Bristol, Avon)*, 14(1), pp. 63–68, 1999.

E. Hallstrom and J. Karrholm, "Shoulder kinematics in 25 patients with impingement and 12 controls", *Clin. Orthop.*, 448, pp. 22–27, 2006.

F.C.T. van der Helm, "Analysis of the kinematic and dynamic behaviour of the shoulder mechanism", *J. Biomech.*, 27, pp. 527–550, 1994.

F.C.T. van der Helm, "A standardised protocol for motion recordings of the shoulder", *Proceedings of the 1st Conference of The International Shoulder Group*, Delft, The Netherlands: Delft University of Technology, 1996.

F.C.T. van der Helm and G.M. Pronk, "Three-dimensional recording and description of motions of the shoulder mechanism", *J. Biomech. Eng.*, 117, pp. 27–40, 1995.

V.T. Inman, M. Saunders and L.C. Abbott, "Observations on the function of the shoulder joint", *J. Bone Joint Surg.*, 26(1), pp. 1–30, 1944.

G.R. Johnson, P.R. Stuart and S. Mitchell, "A method for the measurement of three dimensional scapula movement", *Clin. Biomech.*, 8, pp. 269–273, 1993.

M.P. Johnson, P.W. McClure and A.R. Karduna, "New method to assess scapular upward rotation in subjects with shoulder pathology", *J. Orthop. Sports Phys. Ther.*, 31(2), pp. 81–89, 2001.

A.R. Karduna, P.W. McClure, L.A. Michener and B. Sennett, "Dynamic measurements of three-dimensional scapular kinematics: a validation study", *J. Biomech. Eng.*, 123(2), pp. 184–190, 2001.

A. Kontaxis and G.R. Johnson, "The biomechanics of reverse anatomy shoulder replacement—a modelling study", *Proceedings of 12th International Conference on Biomedical Engineering*, Singapore, 2005a.

A. Kontaxis and G.R. Johnson, "How scapula adaptation can affect a shoulder prosthetic design", *Proceedings of the 10th Congress of International Society of Biomechanics*, August, Cleveland, USA, 2005b.

A.C. Lukasiewicz, P. McClure, L. Michener, N. Pratt and B. Sennett, "Comparison of 3-dimensional scapular position and orientation between subjects with and without shoulder impingement", *J. Orthop. Sports Phys. Ther.*, 29(10), pp. 574–583, discussion 584-6, 1999.

P.W. McClure, L.A. Michener and A.R. Karduna, "Shoulder function and 3-dimensional scapular kinematics in people with and without shoulder impingement syndrome", *Phys. Ther.*, 86(8), pp. 1075–1090, 2006.

A.G. Mell, S. LaScalza, P. Guffey, J. Ray, M. Maciejewski, J.E. Carpenter and R.E. Hughes, "Effect of rotator cuff pathology on shoulder rhythm", *J. Shoulder Elbow Surg.*, 14(1 Suppl S), pp. 58S–64S, 2005.

C.G.M. Meskers, H.M. Vermeulen, J.H. de Groot, F.C.T. van der Helm and P.M. Rozing, "3D shoulder position measurements using a six-degree-of-freedom electromagnetic tracking device", *Clin. Biomech.*, 13, pp. 280–292, 1998.

C.G.M. Meskers, M.A.J. van der Sande and J.H. de Groot, "Comparison between tripod and skin fixed recording of scapular motion", *Proceedings of the 10th Congress of International Society of Biomechanics*, August, Cleveland, USA, 2005.

N.K. Poppen and P.S. Walker, "Normal and abnormal motion of the shoulder", *J. Bone Joint Surg.*, 58-A(2), pp. 195–201, 1976.

G. Pronk, "The shoulder girdle", PhD Thesis, University of Delft, Netherlands (1991).

G.M. Pronk and F.C. van der Helm, "The palpator: an instrument for measuring the positions of bones in three dimensions", *J. Med. Eng. Technol.*, 15(1), pp. 15–20, 1991.

F. Sirveaux, L. Favard, D. Oudet, D. Huquet, G. Walch and D. Mole, "Grammont inverted total shoulder arthroplasty results of a multicentre study of 80 shoulders", *J. Bone Joint Surg. Br.*, 86(3), pp. 388–395, 2004.

P.S. Walker and N.K. Poppen, "Biomechanics of the shoulder joint during abduction in the plane of the scapula", *Bull. Hosp. Joint Dis.*, 38(2), pp. 107–111, 1977.

L.F. de Wilde, F.S. Plasschaert, E.A. Audenaert and R.C. Verdonk, "Functional recovery after a reverse prosthesis for reconstruction of the proximal humerus in tumor surgery", *Clin. Orthop.*, 430, pp. 156–162, 2005.